

**UCLA**

**UCLA Electronic Theses and Dissertations**

**Title**

Total Synthesis of Lissodendoric Acid A and Chemical Education Initiatives

**Permalink**

<https://escholarship.org/uc/item/91g5q80k>

**Author**

Ippoliti Pfitzer, Francesca Marie

**Publication Date**

2022

Peer reviewed|Thesis/dissertation

UNIVERSITY OF CALIFORNIA

Los Angeles

Total Synthesis of Lissodendoric Acid A and Chemical Education Initiatives

A dissertation submitted in partial satisfaction of the  
requirements for the degree Doctor of Philosophy  
in Chemistry

by

Francesca Marie Ippoliti Pfitzer

2022



© Copyright by

Francesca Marie Ippoliti Pfitzer

2022

## ABSTRACT OF THE DISSERTATION

Total Synthesis of Lissodendoric Acid A and Chemical Education Initiatives

by

Francesca Marie Ippoliti Pfitzer

Doctor of Philosophy in Chemistry

University of California, Los Angeles, 2022

Professor Neil Kamal Garg, Chair

This dissertation describes the total synthesis of a complex natural product, lissodendoric acid A, through the innovative use of a strained cyclic allene intermediate. Strained cyclic allenes have never been previously used in total synthesis, despite being discovered shortly after other strained intermediates, such as benzyne. Cyclic allenes are useful fleeting intermediates as they are highly reactive due to their strain and have the ability to form complex,  $sp^3$ -containing molecules. These benefits, along with the ability to transfer stereochemical information, are leveraged in a key Diels–Alder cycloaddition leading to the enantioenriched azadecalin core of lissodendoric acid A and ultimately the completion of the total synthesis. Additionally, the syntheses of precursors to two other versatile strained intermediates are detailed. The synthesis of

a key biosynthetic precursor to monoterpene indole alkaloids, as well as oxidized derivatives thereof, is also reported. Finally, initiatives toward advancing chemical education on a global scale are detailed.

Chapters one and two describe the first total synthesis of the manzamine natural product lissodendoric acid A. Specifically, chapter one details a concise route to lissodendoric acid A, which proceeds via a key stereospecific Diels–Alder cycloaddition of a transient, strained azacyclic allene intermediate. Model system studies using various cyclic allene precursors are detailed, which informed the synthetic design of the enantioenriched silyl bromide used in the Diels–Alder cycloaddition en route to lissodendoric acid A. Of note, this marks the first use of a strained cyclic allene in a total synthesis. From the cycloadduct, swift late-stage manipulations of the scaffold allow for completion of the natural product. Chapter two discusses the first-generation synthesis of lissodendoric acid A, including a detailed analysis of key challenges encountered. Alterations to the synthetic strategy, which ultimately enable access to the natural product, are described. Specifically, structural modifications to the key Diels–Alder reaction partners, which allow for avoidance of difficult late-stage oxidations, are presented. Additionally, the combination of multiple late-stage reductions into one step to rapidly access the natural product is demonstrated.

Chapter three describes the synthesis of silyl triflate precursors to the strained intermediates cyclohexyne and 1,2-cyclohexadiene. Cyclohexyne and 1,2-cyclohexadiene are versatile building blocks that have been used in a variety of cycloadditions to access complex, polycyclic products. The synthesis described is both concise and divergent, allowing access to precursors to both strained intermediates in an efficient and scalable manner.

Chapters four and five describe the synthesis and evaluation of 8-hydroxygeraniol, a key biosynthetic precursor to all monoterpene indole alkaloids. Specifically, chapter four gives an

account of the optimization of an efficient and highly selective oxidation reaction and subsequent deacetylation to arrive at 8-hydroxygeraniol in good yields and on large scale. Importantly, swift access to 8-hydroxygeraniol through this route enabled investigations into the enzymatic synthesis of downstream monoterpene indole alkaloids, such as those described in chapter five. Chapter five presents the fully enzymatic, one-pot synthesis of nepetalactol, starting from geraniol. 8-hydroxygeraniol and its oxidized derivatives, 8-oxogeraniol and 8-oxogeranial, were all synthesized chemically to confirm their presence in the enzymatic pathway.

Chapters six and seven describe educational projects developed to improve student engagement in chemical education. Chapter six details the development and use of R/S Chemistry, an online game-like resource for students to practice assigning stereocenters. The results of a survey given to hundreds of undergraduate students who used R/S Chemistry to practice stereochemical assignments are detailed, which proved to be overwhelmingly positive. Chapter seven presents a perspective on advancing chemical education through interactive teaching tools. Multiple efforts in the area of chemical education innovation are highlighted, as well as the expansion of these resources to a global scale. These resources include interactive online learning tools, methods to help students visualize structures in 3D, and coloring and activity books for children to expand the reach of these resources to a broader audience.

The dissertation of Francesca Marie Ippoliti Pfitzer is approved.

Kendall N. Houk

Abigail Gutmann Doyle

Yi Tang

Neil Kamal Garg, Committee Chair

University of California, Los Angeles

2022

*For my parents, Tom and Mary, and my husband Josh.*

## TABLE OF CONTENTS

Abstract.....	ii
Committee Page.....	v
Dedication Page.....	vi
Table of Contents.....	vii
List of Figures.....	xii
List of Tables.....	xxii
List of Abbreviations.....	xxiii
Acknowledgements.....	xxix
Biographical Sketch.....	xxxviii

CHAPTER ONE: Total Synthesis of Lissodendoric Acid A via Stereospecific Trapping of a Strained Cyclic Allene.....	1
1.1 Abstract.....	1
1.2 Introduction.....	1
1.3 Results and Discussion.....	5
1.4 Conclusion.....	12
1.5 Experimental Section.....	13
1.5.1 Materials and Methods.....	13
1.5.2 Experimental Procedures.....	15
1.5.2.1 Synthesis of Cyclic Allene Precursors <b>1.12</b> , <b>1.16</b> , and <b>1.18</b> .....	15
1.5.2.2 Synthesis of Pyrone <b>1.13</b> .....	23
1.5.2.3 Diels–Alder Cycloadditions on Model Systems.....	24

1.5.2.4 Synthesis of Pyrone <b>1.22</b> and Silyl Bromide <b>1.27</b> .....	29
1.5.2.5 Key Diels–Alder Cycloaddition and Elaboration to Lissodendoric Acid A ( <b>1.6</b> ) .....	37
1.5.2.6 Verification of enantioenrichment of silyl bromide <b>1.27</b> and cycloadducts <b>1.10</b> , <b>1.15</b> , <b>1.14</b> , <b>1.17</b> , and <b>1.28</b> .....	44
1.6 Spectra Relevant to Chapter One .....	54
1.7 Notes and References .....	78
 CHAPTER TWO: Total Synthesis of Lissodendoric Acid A .....	 83
2.1 Abstract .....	83
2.2 Introduction .....	83
2.3 Model System Studies .....	87
2.4 Synthesis of Cycloadduct and Macrocyclization en Route to Lissodendoric Acid A .....	88
2.5 Revised Route to Lissodendoric Acid A .....	95
2.6 Conclusion .....	99
2.7 Experimental Section .....	100
2.7.1 Materials and Methods .....	100
2.7.2 Experimental Procedures .....	101
2.7.2.1 Model System Diels–Alder Cycloaddition .....	102
2.7.2.2 Synthesis of Silyl Triflate <b>2.33</b> .....	103
2.7.2.3 Diels–Alder Cycloaddition .....	109
2.7.2.4 Synthesis of Macrocyclization Precursor <b>2.41</b> .....	110
2.7.2.5 Macrocyclization and Manipulations of Macrocyclization <b>2.24</b> .....	119



2.7.2.6 Synthesis of Silyl Triflate <b>2.53</b> .....	125
2.7.2.7 Diels–Alder Cycloaddition and Elaboration toward Lissodendoric Acid A ( <b>2.10</b> ) .....	128
2.7.2.8 Verification of Enantioenrichment of Cycloadduct <b>2.23</b> .....	134
2.8 Spectra Relevant to Chapter Two .....	136
2.9 Notes and References.....	163
 CHAPTER THREE: Concise Approach to Cyclohexyne and 1,2-Cyclohexadiene Precursors..	166
3.1 Abstract.....	166
3.2 Introduction.....	166
3.3 Results and Discussion .....	170
3.4 Conclusion .....	172
3.5 Experimental Section.....	173
3.5.1 Materials and Methods.....	173
3.5.2 Experimental Procedures .....	174
3.6 Spectra Relevant to Chapter Three .....	176
3.7 Notes and References.....	179
 CHAPTER FOUR: Synthesis of 8-Hydroxygeraniol .....	185
4.1 Abstract.....	185
4.2 Introduction.....	185
4.3 Previous Approaches and Nomenclature Discussion .....	186
4.4 Synthesis Development.....	188

4.5 Conclusion .....	191
4.6 Experimental Section .....	192
4.6.1 Materials and Methods.....	192
4.6.2 Experimental Procedures .....	193
4.7 Spectra Relevant to Chapter Four .....	196
4.8 Notes and References.....	199
CHAPTER FIVE: Cell-Free Total Biosynthesis of Plant Terpene Natural Products using an Orthogonal Cofactor Regeneration System .....	203
5.1 Abstract.....	203
5.2 Introduction.....	203
5.3 Results and Discussion .....	205
5.4 Conclusion .....	214
5.5 Experimental Section.....	215
5.5.1 Materials and Methods.....	215
5.5.2 Experimental Procedures .....	215
5.5.2.1 Synthesis of 8-Hydroxygeraniol ( <b>5.6</b> ).....	215
5.5.2.2 Synthesis of 8-Oxogeraniol ( <b>5.8</b> ).....	217
5.5.2.3 Synthesis of 8-Oxogeraniol ( <b>5.9</b> ) .....	218
5.5.3 Synthetic Biology Details .....	219
5.6 Notes and References.....	220

CHAPTER SIX: Gaming Stereochemistry .....	227
6.1 Abstract .....	227
6.2 Introduction.....	227
6.3 User Interface and Features of R/S Chemistry .....	228
6.4 Feedback from Students.....	231
6.5 Global Impact and Conclusion.....	232
6.6 References.....	234
CHAPTER SEVEN: Advancing Global Chemical Education Through Interactive Teaching Tools .....	236
7.1 Abstract .....	236
7.2 Introduction.....	236
7.3 Development and Application of Interactive Online Learning Tools .....	238
7.4 Teaching in Three Dimensions .....	241
7.5 Reaching New Audiences .....	246
7.6 Global Impact and Innovation in Education .....	249
7.7 Conclusion .....	250
7.8 Related Links .....	251
7.9 Notes and References.....	252

## LIST OF FIGURES

### CHAPTER ONE

- Figure 1.1 Strained intermediates and overview of current study. a) Seminal strained cyclic intermediates **1.1–1.3** and biorthogonal cyclooctyne reagents **1.4**. b) Geometry-optimized structure of strained azacyclic allene **1.5** ( $\omega$ B97XD/6-31G(d)) and key features. CO<sub>2</sub>Me is omitted from the 3D representations for clarity. c) Our synthetic target, lissodendoric acid A (**1.6**), and our synthetic approach using a [4+2] cycloaddition to access **1.7** from cyclic allene **1.8** and pyrone **1.9** (R'=alkyl group).....5
- Figure 1.2 Regioselectivity and stereospecificity studies using variable cyclic allene precursors and [4+2] cycloaddition partners. a) Use of cyclic allene precursor **1.12** allows for efficient and stereospecific cycloadditions. b) Stereospecificity is modest when employing pseudo-isomeric silyl triflate **1.16**. c) Switching to silyl bromide **1.18** as the cyclic allene precursor allows for regioselective and stereospecific cycloaddition reactions, while providing a plausible entryway to enantioenriched material. Highlights depict the primary differences between cyclic allene precursors **1.12**, **1.16**, and **1.18**. See the Experimental Section 1.5 for reaction conditions. ....7
- Figure 1.3 Assembly of the azadecalin core of lissodendoric acid A (**1.6**) using a strained cyclic allene. a) Synthesis of pyrone **1.22**. b) Enantioselective route to silyl triflate **1.27**. c) Cycloaddition of the strained cyclic allene derived from **1.27** with pyrone **1.22** proceeds with regioselectivity,

	diastereoselectivity, and stereospecificity to deliver enantioenriched adduct <b>1.28</b> with the desired quaternary stereocenter at C8a .....	10
Figure 1.4	Completion of the total synthesis of lissodendoric acid A ( <b>1.6</b> ).....	11
Figure 1.5	SFC trace of racemic <b>1.10</b> .....	47
Figure 1.6	SFC trace of enantioenriched <b>1.10</b> from silyl triflate <b>1.12</b> .....	47
Figure 1.7	SFC trace of enantioenriched <b>1.10</b> from silyl bromide <b>1.18</b> .....	48
Figure 1.8	SFC trace of racemic <b>1.15</b> .....	48
Figure 1.9	SFC trace of enantioenriched <b>1.15</b> .....	49
Figure 1.10	SFC trace of racemic <b>1.14</b> .....	49
Figure 1.11	SFC trace of enantioenriched <b>1.14</b> from silyl triflate <b>1.12</b> .....	50
Figure 1.12	SFC trace of enantioenriched <b>1.14</b> from silyl bromide <b>1.18</b> .....	50
Figure 1.13	SFC trace of racemic <b>1.17</b> .....	51
Figure 1.14	SFC trace of enantioenriched <b>1.17</b> .....	51
Figure 1.15	SFC trace of racemic <b>1.27</b> .....	52
Figure 1.16	SFC trace of enantioenriched <b>1.27</b> .....	52
Figure 1.17	HPLC trace of racemic <b>1.28</b> .....	53
Figure 1.18	HPLC trace of enantioenriched <b>1.28</b> .....	53
Figure 1.19	<sup>1</sup> H NMR (600 MHz, CDCl <sub>3</sub> ) of compound <b>1.33</b> . .....	55
Figure 1.20	<sup>13</sup> C NMR (150 MHz, CDCl <sub>3</sub> ) of compound <b>1.33</b> .....	55
Figure 1.21	<sup>1</sup> H NMR (600 MHz, CDCl <sub>3</sub> ) of compound <b>1.12</b> . .....	56
Figure 1.22	<sup>13</sup> C NMR (125 MHz, CDCl <sub>3</sub> ) of compound <b>1.12</b> .....	56
Figure 1.23	<sup>1</sup> H NMR (600 MHz, CDCl <sub>3</sub> ) of compound <b>1.16</b> . .....	57
Figure 1.24	<sup>13</sup> C NMR (125 MHz, CDCl <sub>3</sub> ) of compound <b>1.16</b> .....	57

Figure 1.25	$^1\text{H}$ NMR (500 MHz, $\text{CDCl}_3$ ) of compound <b>1.36</b> .	58
Figure 1.26	$^{13}\text{C}$ NMR (125 MHz, $\text{CDCl}_3$ ) of compound <b>1.36</b> .	58
Figure 1.27	$^1\text{H}$ NMR (600 MHz, $\text{CDCl}_3$ ) of compound <b>1.18</b> .	59
Figure 1.28	$^{13}\text{C}$ NMR (125 MHz, $\text{CDCl}_3$ ) of compound <b>1.18</b> .	59
Figure 1.29	$^1\text{H}$ NMR (400 MHz, $\text{CDCl}_3$ ) of compound <b>1.38</b> .	60
Figure 1.30	$^{13}\text{C}$ NMR (100 MHz, $\text{CDCl}_3$ ) of compound <b>1.38</b> .	60
Figure 1.31	$^1\text{H}$ NMR (600 MHz, $\text{CDCl}_3$ ) of compound <b>1.13</b> .	61
Figure 1.32	$^{13}\text{C}$ NMR (150 MHz, $\text{CDCl}_3$ ) of compound <b>1.13</b> .	61
Figure 1.33	$^1\text{H}$ NMR (500 MHz, $\text{C}_6\text{D}_6$ ) of compound <b>1.10</b> .	62
Figure 1.34	$^{13}\text{C}$ NMR (125 MHz, $\text{C}_6\text{D}_6$ ) of compound <b>1.10</b> .	62
Figure 1.35	$^1\text{H}$ NMR (500 MHz, $\text{C}_6\text{D}_6$ ) of compound <b>1.15</b> .	63
Figure 1.36	$^{13}\text{C}$ NMR (125 MHz, $\text{C}_6\text{D}_6$ ) of compound <b>1.15</b> .	63
Figure 1.37	$^1\text{H}$ NMR (600 MHz, $\text{CDCl}_3$ ) of compound <b>1.14</b> .	64
Figure 1.38	$^{13}\text{C}$ NMR (125 MHz, $\text{CDCl}_3$ ) of compound <b>1.14</b> .	64
Figure 1.39	$^1\text{H}$ NMR (600 MHz, $\text{CDCl}_3$ ) of compound <b>1.17</b> .	65
Figure 1.40	$^{13}\text{C}$ NMR (125 MHz, $\text{CDCl}_3$ ) of compound <b>1.17</b> .	65
Figure 1.41	$^1\text{H}$ NMR (400 MHz, $\text{CDCl}_3$ ) of compound <b>1.20</b> .	66
Figure 1.42	$^{13}\text{C}$ NMR (100 MHz, $\text{CDCl}_3$ ) of compound <b>1.20</b> .	66
Figure 1.43	$^1\text{H}$ NMR (400 MHz, $\text{CDCl}_3$ ) of compound <b>1.22</b> .	67
Figure 1.44	$^{13}\text{C}$ NMR (100 MHz, $\text{CDCl}_3$ ) of compound <b>1.22</b> .	67
Figure 1.45	$^1\text{H}$ NMR (600 MHz, $\text{CDCl}_3$ ) of compound <b>1.23</b> .	68
Figure 1.46	$^{13}\text{C}$ NMR (125 MHz, $\text{CDCl}_3$ ) of compound <b>1.23</b> .	68
Figure 1.47	$^1\text{H}$ NMR (500 MHz, $\text{CDCl}_3$ ) of compound <b>1.42</b> .	69

Figure 1.48	$^{13}\text{C}$ NMR (125 MHz, $\text{CDCl}_3$ ) of compound <b>1.42</b> .....	69
Figure 1.49	$^1\text{H}$ NMR (600 MHz, $\text{CDCl}_3$ ) of compound <b>1.25</b> . .....	70
Figure 1.50	$^{13}\text{C}$ NMR (125 MHz, $\text{CDCl}_3$ ) of compound <b>1.25</b> .....	70
Figure 1.51	$^1\text{H}$ NMR (600 MHz, $\text{CDCl}_3$ ) of compound <b>1.26</b> . .....	71
Figure 1.52	$^{13}\text{C}$ NMR (125 MHz, $\text{CDCl}_3$ ) of compound <b>1.26</b> .....	71
Figure 1.53	$^1\text{H}$ NMR (500 MHz, $\text{CDCl}_3$ ) of compound <b>1.27</b> . .....	72
Figure 1.54	$^{13}\text{C}$ NMR (125 MHz, $\text{CDCl}_3$ ) of compound <b>1.27</b> .....	72
Figure 1.55	$^1\text{H}$ NMR (500 MHz, $\text{CDCl}_3$ ) of compound <b>1.28</b> . .....	73
Figure 1.56	$^{13}\text{C}$ NMR (125 MHz, $\text{CDCl}_3$ ) of compound <b>1.28</b> .....	73
Figure 1.57	$^1\text{H}$ NMR (500 MHz, $\text{CDCl}_3$ ) of compound <b>1.29</b> . .....	74
Figure 1.58	$^{13}\text{C}$ NMR (125 MHz, $\text{CDCl}_3$ ) of compound <b>1.29</b> .....	74
Figure 1.59	$^1\text{H}$ NMR (600 MHz, $\text{CDCl}_3$ ) of compound <b>1.30</b> . .....	75
Figure 1.60	$^{13}\text{C}$ NMR (125 MHz, $\text{CDCl}_3$ ) of compound <b>1.30</b> .....	75
Figure 1.61	$^1\text{H}$ NMR (500 MHz, $\text{CDCl}_3$ ) of compound <b>1.31</b> . .....	76
Figure 1.62	$^{13}\text{C}$ NMR (125 MHz, $\text{CDCl}_3$ ) of compound <b>1.31</b> .....	76
Figure 1.63	$^1\text{H}$ NMR (500 MHz, $\text{CD}_3\text{OD}$ ) of compound <b>1.6</b> . .....	77

## CHAPTER TWO

Figure 2.1	Select strained intermediates and their use in total synthesis .....	84
Figure 2.2	Envisioned use of an azacyclic allene to construct cores of manzamine alkaloids <b>2.8</b> and <b>2.9</b> (geometry optimized structure using B3LYP/6-31G*) .....	86

Figure 2.3	a) Known cycloaddition of azacyclic allene <b>2.11</b> . b) Envisioned inverse-electron demand Diels–Alder cycloaddition.....	87
Figure 2.4	a) Synthesis of pyrone <b>2.20</b> . b) Diels–Alder reaction on model system....	88
Figure 2.5	Retrosynthetic analysis of lissodendoric acid A ( <b>2.10</b> ) .....	89
Figure 2.6	Synthesis of silyl triflate <b>2.33</b> .....	90
Figure 2.7	Diels–Alder cycloaddition using silyl triflate <b>2.33</b> en route to <b>2.10</b> .....	91
Figure 2.8	Manipulations of cycloadduct <b>2.26</b> to access diene <b>2.25</b> .....	91
Figure 2.9	Elaboration of diene <b>2.25</b> to macrocyclization precursor <b>2.41</b> .....	93
Figure 2.10	a) Macrocyclization and attempted oxidation. b) Synthesis of amide <b>2.45</b> to allow for oxidation to aldehyde <b>2.46</b> .....	94
Figure 2.11	Revision of strategy to pursue cycloadduct <b>2.47</b> .....	95
Figure 2.12	a) Synthesis of ester-containing pyrone <b>2.50</b> . b) Synthesis of silyl triflate <b>2.53</b> .....	96
Figure 2.13	Diels–Alder cycloaddition using revised strategy .....	96
Figure 2.14	Elaboration of cycloadduct <b>2.47</b> to tertiary amine <b>2.59</b> .....	98
Figure 2.15	Optimization of late-stage reductions to access lissodendoric acid A ( <b>2.10</b> ) .....	99
Figure 2.16	SFC trace of racemic <b>2.23</b> .....	135
Figure 2.17	SFC trace of enantioenriched <b>2.23</b> .....	135
Figure 2.18	<sup>1</sup> H NMR (500 MHz, CDCl <sub>3</sub> ) of compound <b>2.23</b> . .....	137
Figure 2.19	<sup>13</sup> C NMR (125 MHz, CDCl <sub>3</sub> ) of compound <b>2.23</b> . .....	137
Figure 2.20	<sup>1</sup> H NMR (500 MHz, CDCl <sub>3</sub> ) of compound <b>2.29</b> . .....	138
Figure 2.21	<sup>13</sup> C NMR (125 MHz, CDCl <sub>3</sub> ) of compound <b>2.29</b> . .....	138



Figure 2.22	$^1\text{H}$ NMR (500 MHz, $\text{CDCl}_3$ ) of compound <b>2.30</b> . .....	139
Figure 2.23	$^{13}\text{C}$ NMR (125 MHz, $\text{CDCl}_3$ ) of compound <b>2.30</b> . .....	139
Figure 2.24	$^1\text{H}$ NMR (500 MHz, $\text{CDCl}_3$ ) of compound <b>2.31</b> . .....	140
Figure 2.25	$^{13}\text{C}$ NMR (125 MHz, $\text{CDCl}_3$ ) of compound <b>2.31</b> . .....	140
Figure 2.26	$^1\text{H}$ NMR (600 MHz, $\text{CDCl}_3$ ) of compound <b>2.32</b> . .....	141
Figure 2.27	$^{13}\text{C}$ NMR (125 MHz, $\text{CDCl}_3$ ) of compound <b>2.32</b> . .....	141
Figure 2.28	$^1\text{H}$ NMR (500 MHz, $\text{CDCl}_3$ ) of compound <b>2.33</b> . .....	142
Figure 2.29	$^{13}\text{C}$ NMR (125 MHz, $\text{CDCl}_3$ ) of compound <b>2.33</b> . .....	142
Figure 2.30	$^1\text{H}$ NMR (600 MHz, $\text{CDCl}_3$ ) of compound <b>2.26</b> . .....	143
Figure 2.31	$^{13}\text{C}$ NMR (150 MHz, $\text{CDCl}_3$ ) of compound <b>2.26</b> . .....	143
Figure 2.32	$^1\text{H}$ NMR (500 MHz, $\text{CDCl}_3$ ) of compound <b>2.34</b> . .....	144
Figure 2.33	$^{13}\text{C}$ NMR (100 MHz, $\text{CDCl}_3$ ) of compound <b>2.34</b> . .....	144
Figure 2.34	$^1\text{H}$ NMR (500 MHz, $\text{CDCl}_3$ ) of compound <b>2.35</b> . .....	145
Figure 2.35	$^{13}\text{C}$ NMR (100 MHz, $\text{CDCl}_3$ ) of compound <b>2.35</b> . .....	145
Figure 2.36	$^1\text{H}$ NMR (500 MHz, $\text{CDCl}_3$ ) of compound <b>2.25</b> . .....	146
Figure 2.37	$^{13}\text{C}$ NMR (100 MHz, $\text{CDCl}_3$ ) of compound <b>2.25</b> . .....	146
Figure 2.38	$^1\text{H}$ NMR (500 MHz, $\text{CDCl}_3$ ) of compound <b>2.37</b> . .....	147
Figure 2.39	$^{13}\text{C}$ NMR (125 MHz, $\text{CDCl}_3$ ) of compound <b>2.37</b> . .....	147
Figure 2.40	$^1\text{H}$ NMR (500 MHz, $\text{CDCl}_3$ ) of compound <b>2.38</b> . .....	148
Figure 2.41	$^1\text{H}$ NMR (500 MHz, $\text{CDCl}_3$ ) of compound <b>2.39</b> . .....	149
Figure 2.42	$^{13}\text{C}$ NMR (125 MHz, $\text{CDCl}_3$ ) of compound <b>2.39</b> . .....	149
Figure 2.43	$^1\text{H}$ NMR (500 MHz, $\text{CDCl}_3$ ) of compound <b>2.41</b> . .....	150
Figure 2.44	$^{13}\text{C}$ NMR (125 MHz, $\text{CDCl}_3$ ) of compound <b>2.41</b> . .....	150

Figure 2.45	$^1\text{H}$ NMR (600 MHz, $\text{CDCl}_3$ ) of compound <b>2.24</b> . .....	151
Figure 2.46	$^{13}\text{C}$ NMR (125 MHz, $\text{CDCl}_3$ ) of compound <b>2.24</b> . .....	151
Figure 2.47	$^1\text{H}$ NMR (500 MHz, $\text{CDCl}_3$ ) of compound <b>2.42</b> . .....	152
Figure 2.48	$^{13}\text{C}$ NMR (125 MHz, $\text{CDCl}_3$ ) of compound <b>2.42</b> . .....	152
Figure 2.49	$^1\text{H}$ NMR (500 MHz, $\text{CDCl}_3$ ) of compound <b>2.43</b> . .....	153
Figure 2.50	$^{13}\text{C}$ NMR (125 MHz, $\text{CDCl}_3$ ) of compound <b>2.43</b> . .....	153
Figure 2.51	$^1\text{H}$ NMR (500 MHz, $\text{CDCl}_3$ ) of compound <b>2.45</b> . .....	154
Figure 2.52	$^{13}\text{C}$ NMR (125 MHz, $\text{CDCl}_3$ ) of compound <b>2.45</b> . .....	154
Figure 2.53	$^1\text{H}$ NMR (500 MHz, $\text{CDCl}_3$ ) of compound <b>2.46</b> . .....	155
Figure 2.54	$^{13}\text{C}$ NMR (125 MHz, $\text{CDCl}_3$ ) of compound <b>2.46</b> . .....	155
Figure 2.55	$^1\text{H}$ NMR (400 MHz, $\text{CDCl}_3$ ) of compound <b>2.51</b> . .....	156
Figure 2.56	$^{13}\text{C}$ NMR (100 MHz, $\text{CDCl}_3$ ) of compound <b>2.51</b> . .....	156
Figure 2.57	$^1\text{H}$ NMR (400 MHz, $\text{CDCl}_3$ ) of compound <b>2.52</b> . .....	157
Figure 2.58	$^{13}\text{C}$ NMR (100 MHz, $\text{CDCl}_3$ ) of compound <b>2.52</b> . .....	157
Figure 2.59	$^1\text{H}$ NMR (400 MHz, $\text{CDCl}_3$ ) of compound <b>2.53</b> . .....	158
Figure 2.60	$^{13}\text{C}$ NMR (100 MHz, $\text{CDCl}_3$ ) of compound <b>2.53</b> . .....	158
Figure 2.61	$^1\text{H}$ NMR (500 MHz, $\text{CDCl}_3$ ) of compound <b>2.56</b> . .....	159
Figure 2.62	$^{13}\text{C}$ NMR (125 MHz, $\text{CDCl}_3$ ) of compound <b>2.56</b> . .....	159
Figure 2.63	$^1\text{H}$ NMR (500 MHz, $\text{CDCl}_3$ ) of compound <b>2.57</b> . .....	160
Figure 2.64	$^{13}\text{C}$ NMR (125 MHz, $\text{CDCl}_3$ ) of compound <b>2.57</b> . .....	160
Figure 2.65	$^1\text{H}$ NMR (500 MHz, $\text{CDCl}_3$ ) of compound <b>2.58</b> . .....	161
Figure 2.66	$^{13}\text{C}$ NMR (125 MHz, $\text{CDCl}_3$ ) of compound <b>2.58</b> . .....	161
Figure 2.67	$^1\text{H}$ NMR (500 MHz, $\text{CDCl}_3$ ) of compound <b>2.59</b> . .....	162

Figure 2.68	$^{13}\text{C}$ NMR (125 MHz, $\text{CDCl}_3$ ) of compound <b>2.59</b> .....	162
 CHAPTER THREE		
Figure 3.1	Strained cyclic alkynes and allenes.....	167
Figure 3.2	Cycloadditions of cyclohexyne ( <b>3.2</b> ) and 1,2-cyclohexadiene ( <b>3.3</b> ) .....	168
Figure 3.3	Synthetic approaches to cyclohexyne precursors <b>3.20a</b> and <b>3.20b</b> and 1,2-cyclohexadiene precursors <b>3.21a</b> and <b>3.21b</b> .....	169
Figure 3.4	Retro-Brook approach to silyl triflates <b>3.20b</b> and <b>3.21b</b> .....	171
Figure 3.5	Examples of Cycloadditions Using Silyl Triflates <b>3.20b</b> and <b>3.21b</b> .....	172
Figure 3.6	$^1\text{H}$ NMR (500 MHz, $\text{CDCl}_3$ ) of compound <b>3.25</b> .....	177
Figure 3.7	$^{13}\text{C}$ NMR (100 MHz, $\text{CDCl}_3$ ) of compound <b>3.25</b> .....	177
Figure 3.8	$^1\text{H}$ NMR (500 MHz, $\text{CDCl}_3$ ) of compound <b>3.20b</b> .....	178
Figure 3.9	$^1\text{H}$ NMR (500 MHz, $\text{CDCl}_3$ ) of compound <b>3.26</b> .....	178
 CHAPTER FOUR		
Figure 4.1	Role of 8-hydroxygeraniol ( <b>4.3</b> ) in the biosynthesis of all monoterpene indole alkaloids, including strychnine ( <b>4.1</b> ) and vinblastine ( <b>4.2</b> ).....	186
Figure 4.2	Various approaches to 8-hydroxygeraniol ( <b>4.3</b> ) .....	187
Figure 4.3	Confusion surrounding the naming of 8-hydroxygeraniol ( <b>4.3</b> ) and its biosynthetic successor 8-oxogeraniol ( <b>4.11</b> ).....	188
Figure 4.4	Preparation of 8-hydroxygeraniol ( <b>4.3</b> ) on 3 mmol scale .....	191
Figure 4.5	$^1\text{H}$ NMR (500 MHz, $\text{CDCl}_3$ ) of compound <b>4.12</b> .....	197
Figure 4.6	$^{13}\text{C}$ NMR (125 MHz, $\text{CDCl}_3$ ) of compound <b>4.12</b> .....	197

Figure 4.7	<sup>1</sup> H NMR (500 MHz, CDCl <sub>3</sub> ) of compound <b>4.3</b> .....198
Figure 4.8	<sup>13</sup> C NMR (125 MHz, CDCl <sub>3</sub> ) of compound <b>4.3</b> .....198

## CHAPTER FIVE

Figure 5.1	<i>Cis-trans</i> nepetalactol ( <b>5.1</b> ) serves as the ten-carbon terpene core of strictosidine ( <b>5.3</b> ), the biosynthetic precursor to vinblastine ( <b>5.2</b> ), ibogaine ( <b>5.4</b> ), and ~3,000 additional monoterpene indole alkaloids.....205
Figure 5.2	Biosynthesis of nepetalactol ( <b>5.1</b> ) and nepetalactone ( <b>5.11</b> ) along with possible shunt products. On pathway intermediates are boxed. Cofactor regeneration enzymes are only shown for main pathway reactions .....207
Figure 5.3	One pot enzymatic synthesis of nepetalactol ( <b>5.1</b> ) and nepetalactone ( <b>5.11</b> ) using an orthogonal cofactor regeneration system. (A) GC-MS chromatograms for 10 mL-scale one-pot conversion of 6 mM geraniol ( <b>5.5</b> ) to nepetalactol ( <b>5.1</b> ) and nepetalactone ( <b>5.11</b> ). Final reaction contained 925.5 mg/L geraniol ( <b>5.5</b> ), 5 μM TfG8H, 10 μM FpR, 10 μM YkuN, 10 μM GOR, 0.5 μM ISY, 5 μM MLPL, 1 μM FumC, 10 μM MaeB, 100 μM NADPH, 100 μM NAD <sup>+</sup> and 18 mM fumarate in BTP buffer (pH 9.0) unless otherwise specified. (i) starting material, 2 mM <b>5.5</b> , (ii) 1.5-hour reaction with TfG8H, (iii) additional 1.5-hour reaction with TfG8H and an additional aliquot of 2 mM <b>5.5</b> added, (iv) additional 1.5-hour reaction with TfG8H and an additional aliquot of 2 mM <b>5.5</b> added, (v) 2-hour reaction after GOR was added to (iv), (vi) 2-hour reaction after ISY and MLPL were added to (v), (vii) 2-hour reaction after ISY/MLPL and NEPS1 were added to (v).

Peak identities were deduced from GC-MS and by comparison to authentic standards (see Supporting Information). **(B)** Substrate (**5.5**, blue circle) and products' (**5.6**, orange star; **5.9**, green diamond; **5.1**, purple cross) concentrations measured over time, with timing of added enzymes indicated with arrows atop. The reaction condition is as specified above with starting **5.5** concentration of 957 mg/L (6.2 mM) .....212

## CHAPTER SIX

Figure 6.1 The R/S Chemistry user interface. a) Step 1 prompts users to assign substituent priorities around a stereocenter. b) In 'Learn' mode, Step 2 displays a Newman projection for the user to help determine stereochemical assignment. c) A detailed explanation of the correct stereochemical assignment is given after the user submits an answer.....230

## CHAPTER SEVEN

Figure 7.1 A selected example from BACON (Biology and Chemistry Online Notes), an online set of tutorials that connect organic chemistry to human health and popular culture .....239

Figure 7.2 Backside Attack, a smartphone game that challenges students to master the  $S_N2$  reaction, an important reaction in undergraduate organic chemistry coursework.....241

Figure 7.3 QR Chem, a site that allows students, instructors, and researchers to create QR codes that link to interactive 3D structures. In this example, two

	potential scenarios for the classic Diels–Alder reaction are depicted, each leading to different isomeric outcomes.....	243
Figure 7.4	R/S Chemistry, a resource for students to practice assigning stereocenters in a game-like environment .....	245
Figure 7.5	<i>The Organic Coloring Book</i> series and <i>The O-Chem (Re)Activity Book</i> are designed to connect organic chemistry to the everyday lives of both children and adults .....	247
Figure 7.6	ChemMatch, an online matching game that serves as an educational resource for children, students, and adults.....	249
Figure 7.7	Map of combined users of QR Chem, R/S Chemistry, and ChemMatch worldwide (data from Google Analytics) .....	250

## LIST OF TABLES

### CHAPTER FOUR

Table 4.1	Optimization of SeO <sub>2</sub> -promoted oxidation of <b>4.10</b> .....	190
-----------	---	-----

## LIST OF ABBREVIATIONS

$\alpha$	alpha
$\beta$	beta
$\gamma$	gamma
$\lambda$	wavelength
$\mu$	micro
$\pi$	pi
$\delta$	chemical shift
$\Delta$	heat
(Het)	hetero
[H]	reduction
[O]	oxidation
$[\alpha]_D$	specific rotation at wavelength of sodium D line
$^{\circ}\text{C}$	degrees Celsius
$\text{\AA}$	angstrom
AcOH	acetic acid
$\text{AlCl}_3$	aluminum trichloride
Alk	alkyl
APCI	atmospheric-pressure chemical ionization
app.	apparent
aq.	aqueous
Ar	aryl
Au	gold
B(pin)	pinacol borane
Benz-ICy $\cdot$ HCl	1,3-dicyclohexylbenzimidazolium chloride
$\text{BF}_3\cdot\text{Et}_2\text{O}$	boron trifluoride diethyl etherate
Bn	benzyl
$\text{BnNH}_2$	benzylamine
Boc	<i>tert</i> -butoxycarbonyl
$\text{Boc}_2\text{O}$	di- <i>tert</i> -butyl dicarbonate
Bu	butyl
Bz	benzoyl
c	centi

<i>c</i>	concentration for specific rotation measurements
C	carbon
C <sub>6</sub> D <sub>6</sub>	deuterated benzene
C <sub>6</sub> H <sub>6</sub>	benzene
CaH <sub>2</sub>	calcium hydride
cal	calorie
calcd	calculated
cat.	catalytic or catalyst
CD <sub>3</sub> CN	deuterated acetonitrile
CDCl <sub>3</sub>	deuterated chloroform
CF <sub>3</sub>	trifluoromethyl
CH <sub>2</sub> Cl <sub>2</sub>	dichloromethane
CH <sub>3</sub>	methyl
CH <sub>3</sub> CN	acetonitrile
CHCl <sub>3</sub>	chloroform
CO <sub>2</sub>	carbon dioxide
cod	1,5-cyclooctadiene
d	doublet
DART	direct analysis in real time
DMAP	4-dimethylaminopyridine
DMF	<i>N,N</i> -dimethylformamide
DMSO	dimethyl sulfoxide
dppf	1,1'-bis(diphenylphosphino)ferrocene
EDC	1-ethyl-3-(3-dimethylaminopropyl)carbodiimide
EDC•HCl	1-ethyl-3-(3-dimethylaminopropyl)carbodiimide hydrochloride
eds.	editors
EDTA	ethylenediaminetetraacetic acid
ee	enantiomeric excess
equiv	equivalent
ESI	electrospray ionization
Et	ethyl
Et <sub>2</sub> O	diethyl ether
Et <sub>3</sub> N	triethylamine
EtOAc	ethyl acetate



FAQ	frequently asked questions
FT	Fourier transform
g	gram(s)
GC-MS	gas chromatography mass spectrometry(er)
h	hour(s)
H	proton
$h\nu$	light
HCl	hydrochloric acid
Hf	hafnium
HMB	hexamethylbenzene
HOBt	hydroxybenzotriazole
HPLC	high-performance liquid chromatography
HRMS	high resolution mass spectroscopy
Hz	hertz
<i>i</i> -Bu	isobutyl
<i>i</i> -Pr	<i>iso</i> -propyl
<i>i</i> -PrNH <sub>2</sub>	<i>iso</i> -propyl amine
<i>i</i> -PrOAc	<i>iso</i> -propyl acetate
<i>i</i> -PrOH	<i>iso</i> -propyl alcohol
I <sub>2</sub>	iodine
ICy•HCl	1,3-dicyclohexylimidazolium chloride
IPr	1,3-Bis(2,6-diisopropylphenyl)-imidazol-2-ylidene
IR	infrared (spectroscopy)
<i>J</i>	coupling constant
K <sub>3</sub> PO <sub>4</sub>	potassium phosphate tribasic
KOt-Bu	potassium <i>tert</i> -butoxide
KRED	ketoreductase
L	liter
LDA	lithium diisopropylamide
LiAlH <sub>4</sub>	lithium aluminum hydride
LiCl	lithium chloride
LiHMDS	lithium bis(trimethylsilyl)amide
m	multiplet or milli or meter
M	molecular mass, molar, or metal
<i>m</i> -	meta

$m/z$	mass to charge ratio
Me	methyl
MgSO <sub>4</sub>	magnesium sulfate
MHz	megahertz
min	minute(s)
Mo	molybdenum
mol	mole(s)
mp	melting point
MS	molecular sieves
N	normal
<i>n</i> -Bu	butyl (linear)
<i>n</i> -BuLi	butyl (linear) lithium
N <sub>2</sub>	nitrogen gas
Na <sup>0</sup>	sodium metal
Na <sub>2</sub> S <sub>2</sub> O <sub>3</sub>	sodium thiosulfate
Na <sub>2</sub> SO <sub>4</sub>	sodium sulfate
NADP	nicotinamide adenine dinucleotide phosphate
NaH	sodium hydride
NaHCO <sub>3</sub>	sodium bicarbonate
NaOH	sodium hydroxide
NaO <i>t</i> -Bu	sodium <i>tert</i> -butoxide
NH <sub>4</sub> Cl	ammonium chloride
NHC	<i>N</i> -heterocyclic carbene
Ni	nickel
nM	nanomolar
NMR	nuclear magnetic resonance
NOESY	nuclear overhauser effect spectroscopy
<i>o</i> -	ortho
OMe	methoxy
<i>p</i> -	para
Pd	palladium
PDB	protein data bank
Ph	phenyl
PhCOCF <sub>3</sub>	2,2,2-trifluoroacetophenone
PhH	benzene

PhMe	toluene
Piv	pivaloyl
PPh <sub>3</sub>	triphenylphosphine
ppm	parts per million
Pr	Propyl
Pt	platinum
PTFE	polytetrafluoroethylene
q	quartet
quint.	quintet
rac	racemic
R <sub>f</sub>	retention factor
rpm/RPM	revolutions per minute
Ru	ruthenium
s	singlet or second
sat.	saturated
sext.	sextet
SFC	supercritical fluid chromatography
SiPr	1,3-Bis(2,6-diisopropylphenyl)-1,3-dihydro-2 <i>H</i> -imidazol-2-ylidene
SiPr•HCl	1,3-Bis(2,6-diisopropylphenyl)-1,3-dihydro-2 <i>H</i> -imidazol-2-ylidene hydrochloride
SmI <sub>2</sub>	samarium diiodide
t	triplet
<i>t</i> -Bu	<i>tert</i> -butyl
<i>t</i> -BuNH <sub>2</sub>	<i>tert</i> -butyl amine
<i>t</i> -BuOH	<i>tert</i> -butyl alcohol
TA	teaching assistant
TBDPS	<i>tert</i> -butyldiphenylsilyl
TBDPSCl	<i>tert</i> -butyldiphenylchlorosilane
TCI	Tokyo Chemical Industry Co.
temp	temperature
THF	tetrahydrofuran
Ti	titanium
TLC	thin layer chromatography
TMB	1,3,5-trimethoxybenzene

TMSCl	chlorotrimethylsilane
t <sub>R</sub>	retention time
Trit	trityl
Ts	tosyl
UATR	universal attenuated total reflectance
UHP	ultra-high purity
UV	ultraviolet
WT	wild-type
ZnEt <sub>2</sub>	diethyl zinc
Zr	zirconium

## ACKNOWLEDGEMENTS

There are many people that have helped me along my path to graduate school and during graduate school and I am grateful for all of them.

I first have to thank Professor Neil Garg. Neil, you have been an incredible advisor. I truly couldn't have asked for a better mentor in grad school. Your knowledge of chemistry and natural product synthesis has always amazed me, and I couldn't have gotten through late-stage lisso without your advice! You have helped me grow into the scientist I am today by motivating me to keep pushing forward and have taught me many life lessons beyond just chemistry. Thank you for everything you have done to support me throughout graduate school!

I would like to thank the members of my committee, Professors Ken Houk, Yi Tang, and Abigail Doyle. I have appreciated all of your advice and guidance you have provided me during my time at UCLA.

A major contributing factor to going to graduate school was my undergraduate research experience in the lab of Professor Lisa Prevette. Thank you Dr. Prevette for giving me an incredible experience as an undergraduate student and for being a wonderful mentor and role model. I learned so much about scientific research while working with you and I will always be grateful for the time I spent under your guidance.

The people who I have spent the most time with during these last five years are my fellow labmates, who have all made graduate school such an enjoyable experience for me. As I started grad school as a first-year student, I remember how welcoming everyone in the Garg Lab was. After I joined the Garg Lab, I knew I had made the right decision in choosing to pursue my PhD studies at UCLA. I have learned so much from everyone in the lab and I am grateful to have gone through this experience with them.

Drs. Emma Baker-Tripp, Elias Picazo, and Junyong Kim were 5<sup>th</sup> years when I joined graduate school, and all were awesome chemists. Emma was in 5235 with me and she was an awesome example of an all-star chemist and always very helpful in answering my questions. It was clear that Elias would become an amazing professor and now he has! Junyong always brought a fun energy to the lab. Thank you to all three of you for being great role models for me as a young grad student.

Drs. Joyann Barber, Lucas Morrill, and Bryan Simmons were 4<sup>th</sup> years when I joined the lab. Joyann continually had a bright and optimistic presence in the lab, which was a quality I admired. Thank you Joyann for welcoming me into the lab as my mentor and helping me to learn the “Garg Lab ways.” You were a wonderful project partner on both lisso and 8-hydroxygeraniol, as well as an incredible mentor. I also hope I have lived up to your legacy as typo-check queen! Lucas, thank you for keeping things lively in lab, whether that was putting on the Lido Shuffle or singing “Squirrels Like You.” He also took his role as a fifth year in the room very seriously with supplying treats on Apple Fritter Friday weekly. Additionally, some of my favorite memories of fifth-year Lucas include checking the air quality on Purple Air or perusing houses on Zillow. Bryan and I were able to connect about our Italian heritage, and I have fond memories of our Italian food night, Oktoberfest, and visiting you in San Diego.

The next class, which included Drs. Michael Yamano, Jordan Dotson, Jacob Dander, and Robert Susick, always brought a lively quality to lab. Michael and I became good friends in 5235, even though he did play some practical jokes on me every once in a while (sorry for stealing your desk). Even during the pandemic, he made our Zoom mechanism of the day meetings more enjoyable by making them into a Jeopardy game. Beyond being an expert chemist, he was also an expert on Vegas, which proved useful especially while drinking Fat Tuesdays. Thank you,

Michael, for being a great friend and for making lab a fun place to be! Jordan is a phenomenal chemist and also such a nice person. Jordan was also my TA for Phys. Org. and he was exceptional at explaining concepts in an easy-to-understand way. Jordan, thank you for being a patient teacher and being so helpful with all of my chemistry questions, especially during my candidacy exam. Jacob, thank you for being the life of the party! You always had interesting stories to tell that really captivated the audience. I also appreciated our bond over some of our Midwestern commonalities. I'll always remember the good times we all spent at Jacob and Rob's place, aka Los Leones. Rob was our lab's trusty safety officer, the duties of which he eventually passed on to me. Thank you for being a levelheaded member of the lab who was always willing to help.

The class above me who I spent many years with included Drs. Sarah Anthony, Melissa Ramirez, and Timothy Boit. Sarah has become one of my best friends during graduate school and I don't know how I could have gone through it without her. With her singing in the lab, we bonded over our love of musicals and she made the lab a fun place to be. Thank you for always being there for me for real-time chemistry advice or just a good chat! Beyond the lab, our wine and game nights as well as weekend trips around southern California have created many amazing memories. I know you tried your hardest to get me to go to San Diego for my postdoc, but I know we'll visit each other anyway! I'm so thankful to have you as a friend. Tim is an exceptionally smart chemist. Tim, being in lab with you was always fun, and I hope the music of the ladies of 5235 didn't annoy you too much! Thank you for always being willing to give advice or talk through any chemistry problems. Melissa is such a kind-hearted person and is extremely supportive of her younger labmates. She never fails to check in and see how I'm doing and is always able to give supportive advice. Thank you, Melissa, for being a supportive labmate, mentor, and friend!

Melinda Nguyen was an undergraduate student in the Garg Lab and we were able to work together on educational projects. While creating R/S Chemistry, we spent a lot of time thinking about how to teach stereochemical assignments. Your passion for education is evident and I know you have found your calling in being an educator.

The postdocs in the lab have all been excellent chemists and were all great to work with. When I first joined the lab, the postdocs were Drs. Sophie Racine, Maude Giroud, and Evan Darzi. Although Sophie and I only overlapped for a short amount of time, I enjoyed her fun energy, and her shoes as a parting gift. Maude was always a kind person, but definitely showed her competitive side during laser tag. Evan, thank you for being a great project partner. You were instrumental in guiding me through the early stages of lisso. Thank you for also providing good advice to me in terms of both chemistry and life on our drives home to Palms.

Later in my time in the Garg lab, two other postdocs, Drs. Veronica Tona and Logan Bachman joined the lab. Veronica, your bold and fun personality really made the lab a vibrant place. Thank you for connecting over our shared Italian heritage, even though you are the true Italian. Although we weren't able to visit Vegas while you were here, hopefully in the future we can visit together! Logan, you are an awesome person, beyond being an incredible chemist and very helpful in the lab. I always appreciated your great advice, and my back appreciated your Thera Cane.

Finally, Drs. Nathan Adamson and Daniel Nasrallah joined the lab as postdocs during my last few years of graduate school. Nathan, thank you for being a great project partner. You always think about reactions carefully and your contributions helped finish lisso. Dan, thank you for being such a great desk buddy! You have given me so much useful advice and are always willing to help, especially when I needed to send an important email to help get the wording just right. You are an



amazing postdoc and teacher; I aspire to have the qualities you do when I'm a postdoc and in my future career.

In my own cohort, Jason Chari and Rachel Knapp have really made our past five years in graduate school a great experience. As Frachelson, we are the class that always does everything together and in a specific order (thanks for letting me always go first). It has been amazing getting to become such good friends with both of you. Our year stepped up the level of classiness as well, which surprised some older lab members when we went to an art show our first year! Jason, whether it was talking about new chemistry ideas or last week's episode of the Bachelor, you are always there for good conversation. You are a remarkably caring and thoughtful person, and you have been an incredible friend. You are a creative chemist and Pfizer is lucky to have you! Rachel, thank you for being a wonderful friend! Our bond of both being Minnesotans instantly connected us and I'm so glad we've grown so close. I'm always impressed by the expansive breadth of research you've accomplished in the Garg Lab. You are an exceptional chemist and I know you'll do great things at Eli Lilly. We've gone through it all together and I'll miss you both!

When the next class came in, Andrew Kelleghan, Katie Spence, and Milauni Mehta, it was exciting to not be the youngest in the lab anymore! Andrew, you are one of the smartest chemists I know, and I have always admired your ability to analyze every aspect of a reaction. You always have a calming and laid-back presence in the lab, while accomplishing an incredible amount of research. I also have to thank you for being patient and always helping me at the SFC! Katie, you are so fun and energetic, and it has been awesome being in 5234 with you this past year. I'll always remember you dancing whenever a banger comes on, whether that be on a boat or in the lab. Your confidence and ability to take charge will get you far! Milauni, thank you for being such an amazing friend! Our morning chats were always a highlight of my day. Josh and I have loved being

“parents” to you and our dinners together were wonderful. It has also been amazing to see you grow as a chemist over the past few years with your transition from methods to total synthesis, and I’m excited to see you continue to excel in the future with kermit! I’m confident that the three of you will be amazing leaders of the lab as 5<sup>th</sup> years!

The current 3<sup>rd</sup> years, Matthew McVeigh, Ana Bulger, and Laura Wonilowicz, are some of the kindest people I have ever met, and I have been lucky to get to know all three of them over the past few years. Matt, thank you for being such an awesome hood mate and desk mate, I always enjoy our conversations! You have already accomplished an impressive amount of research in the Garg Lab, while being an all-around good person. I know you’ll do great at your internship this summer! Laura, thank you for being the best mentee that I could ask for! I am so thankful that you are both my project partner and friend. You have developed into an independent chemist and I’m excited to see what you’ll accomplish during the rest of your graduate school career. Ana, I am so glad we became friends over the past few years. I have also enjoyed seeing your confidence as a chemist grow and see you rise to be a leader in the lab. Game nights with you and Nathaniel are always awesome and I look forward to more in the future! I know all three of you will continue to make incredible progress in your last couple of years of grad school!

The next class are the current 2<sup>nd</sup> year students, Dominick Witkowski, Arismel Tena-Meza, and Luca Catena McDermott. Dominick, I’m so glad we have gotten to know each other in 5234 and been able to bond over plant care. You are always so prepared for things and working on everything in advance, I’m amazed at how calm, cool, and collected you are. I’ll always remember you chuckling in the corner and rolling around in the chairs. Ari, you are so fun and sweet, and an amazing boat captain! It has been awesome getting to know you these past couple of years. I know I can always count on you to get a hot chocolate with me in education subgroup. I’ll miss you but

I hope “we are not concerned” about staying in touch! Luca, you are such an intelligent and optimistic chemist, I know you’ll go far. Your love and enthusiasm for chemistry are admirable qualities, and your lab polls on how your reaction will proceed really create a sense of community in the lab. I will miss your daily updates on chemistry! Good luck to all three of you on candidacy!

Finally, our newest members of the Garg Lab are Georgia Scherer and Jordan Gonzalez. Georgia, you are an amazing person and I’m so glad that we have gotten to know each other this past year. I’ll miss our daily Wordle comparisons and chatting with you in lab. Jordan, you are such a thoughtful person, and I’ll miss seeing your creative daily coffee announcements. Thank you for inspiring the 5<sup>th</sup> years to start a new Garg Lab tradition (you know what I’m talking about). You are both such sweet and kind people and I know you’ll do amazing things in the Garg Lab!

My friends in Minnesota have been so supportive of me during my time in graduate school, even though we are halfway across the country. I want to especially thank Marissa, Sarah, Jackie, and Stephanie; thank you all for being wonderful friends. Our chats on the phone and your visits out to California have helped make the years fly by a bit faster.

Finally, my family has been so supportive of me during my time in graduate school. I have so many amazing people who care about me and I’m so lucky to have all of them in my life.

The two people who I have to thank the most are my parents, Mary and Tom. Thank you, Mom and Dad, for being the most supportive and wonderful parents. You have always helped me to be my best and I couldn’t have gotten where I am without the two of you. Your constant reminders of how proud you are of me, mean so much to me. You both help to keep me motivated to pursue my goals. Mom, thank you for always being there to talk and encourage me, and being willing to help in any way I needed! Dad, you inspired me to become a chemist as a little girl and I’m glad we can talk about chemistry together now. I love you both so much!

Thank you to my little sister, Christina, who has continually believed in me. Thank you for always being a phone call away, especially with those late nights due to the time difference! You are the sweetest and most caring person I know, and I am truly inspired by how you want to tackle big problems and change the world. I know you'll do great things! I love you so much!

I also want to thank my grandparents, Marie and Don, for being such caring grandparents and supporting me on my path toward becoming a chemist!

Dawn and Perry, thank you for being great in-laws! I'm so glad to have married into such a kind family.

Josh I couldn't have done it without you! I am so grateful to have you as my partner in life. You are the most supportive husband in all aspects of life, whether that's having dinner ready after I come home from a long day in lab or helping me relax with a board game and a glass of wine. It was also clear how supportive you were when you were willing to drop your life in Minnesota and drive out to California together so that I could pursue my graduate studies. Thank you for everything you have done to help me succeed in graduate school. I am so excited for our future together back in the Midwest. I love you so much!

Chapter 1 is unpublished material.

Chapter 2 is unpublished material.

Chapter 3 is a version of Chari, J. V.<sup>†</sup>; Ippoliti, F. M.<sup>†</sup>; Garg, N. K. Concise Approach to Cyclohexyne and 1,2-Cyclohexadiene Precursors. *J. Org. Chem.* **2019**, *84*, 3652–2655. Chari and Ippoliti were responsible for experimental studies.

Chapter 4 is a version of Ippoliti, F. M.<sup>†</sup>; Barber, J. S.<sup>†</sup>; Tang, Y.; Garg, N. K. Synthesis of 8-Hydroxygeraniol. *J. Org. Chem.* **2018**, *83*, 11323–11326. Ippoliti and Barber were responsible for experimental studies.

Chapter 5 is a version of Bat-Erdene, U.; Billingsley, J. M.; Turner, W. C.; Lichman, B. R.; Ippoliti, F. M.; Garg, N. K.; O'Connor, S. E.; Tang, Y. Cell-Free Total Biosynthesis of Plant Terpene Natural Products Using an Orthogonal Cofactor Regeneration System. *ACS Catal.* **2021**, *11*, 9898–9903. Bat-Erdene, Billingsley, and Turner were responsible for the enzymology. Ippoliti was responsible for the experimental synthetic chemistry.

Chapter 6 is a version of Ippoliti, F. M.; Nguyen, M. M.; Reilly, A. J.; Garg, N. K. Gaming Stereochemistry. *Nat. Rev. Chem.* Accepted Article. DOI: 10.1038/s41570-022-00395-5.

Chapter 7 is a version of Ippoliti, F. M.<sup>†</sup>; Chari, J. V.<sup>†</sup>; Garg, N. K. Advancing Global Education Through Interactive Teaching Tools. *Chem. Sci.* **2022**, *13*, 5790–5796.

## BIOGRAPHICAL SKETCH

### Education:

#### University of California, Los Angeles, CA

- Ph.D. in Organic Chemistry, anticipated Spring 2022
- Current GPA: 3.74/4.00

#### University of St. Thomas, St. Paul, MN

- B.S. in Chemistry - May 2017
- Minor in Materials Science & Engineering
- *Summa Cum Laude*; Cumulative GPA: 3.91/4.00

### Professional and Academic Experience:

#### Graduate Research Assistant: University of California, Los Angeles, CA

- September 2017 – present; Advisor: Prof. Neil K. Garg.
- Established a robust synthesis of key pyrone and azacyclic allene fragments and developed an inverse-electron demand azacyclic allene Diels–Alder cycloaddition that builds the azadecalin core of lissodendoric acid A.
- Devised and explored late-stage strategies, including a Negishi cross-coupling and macrocyclization, to complete the first total synthesis of the bioactive natural product lissodendoric acid A.
- Developed a concise synthesis of cyclohexyne and 1,2-cyclohexadiene precursors.
- Optimized an efficient and scalable synthesis of 8-hydroxygeraniol.

#### Graduate Teaching Assistant: University of California, Los Angeles, CA

- Undergraduate organic chemistry laboratory sections (Fall 2017 – Summer 2018, Fall 2020): Taught students organic laboratory techniques for synthesizing small molecules and polymers.
- Undergraduate organic chemistry discussion section (Winter 2019): Led students through problem sets to learn organic reactions, retrosynthetic analysis, and spectroscopy.

#### Undergraduate Research Assistant: University of St. Thomas, St. Paul, MN

- June 2014 – May 2017; Advisor: Prof. Lisa E. Prevette.
- Developed micelle-forming, orthoester-containing polymers for delivery of anti-cancer drugs and characterized the properties of the micelles.
- Performed synthetic modifications of chitosan and evaluated the potential of the resulting derivatives as gene delivery agents.

#### Undergraduate Teaching Assistant: University of St. Thomas, St. Paul, MN

- Undergraduate accelerated general chemistry, general chemistry for engineers, and materials science laboratory sections (Fall 2016 – Spring 2017): Taught students general chemistry laboratory techniques and how to analyze various materials.

## Honors and Awards:

### Graduate Honors and Awards:

- Graduate Research Fellowship, National Science Foundation, 2019 – 2022
- Saul and Sylvia Winstein Dissertation Award, UCLA, 2022
- Horizon Prize for Education, Royal Society of Chemistry, 2021
- Ralph and Charlene Bauer Award, UCLA, 2021
- Hanson–Dow Excellence in Teaching Award, UCLA, 2019
- Christopher Foote Fellowship, UCLA, 2017 – 2018
- Graduate Dean’s Scholar Award, UCLA, 2017 – 2019

### Select Undergraduate Honors and Awards:

- American Institute of Chemists Outstanding Senior Award, University of St. Thomas, Spring 2017
- Undergraduate Award in Organic Chemistry, University of St. Thomas, Spring 2017
- Barry Goldwater Scholarship, Spring 2016
- William D. Larson Scholarship, Spring 2016

## Publications:

1. **Total Synthesis of Lissodendoric Acid A via Stereospecific Trapping of a Strained Cyclic Allene.** Francesca M. Ippoliti, Nathan J. Adamson, Laura G. Wonilowicz, Evan R. Darzi, Joyann S. Donaldson, and Neil K. Garg. *Manuscript in Preparation*.
2. **Total Synthesis of Lissodendoric Acid A.** Francesca M. Ippoliti, Nathan J. Adamson, Laura G. Wonilowicz, Evan R. Darzi, Joyann S. Donaldson, and Neil K. Garg. *Manuscript in Preparation*.
3. **Advancing Global Chemical Education Through Interactive Teaching Tools.** Francesca M. Ippoliti<sup>†</sup>, Jason V. Chari<sup>†</sup>, and Neil K. Garg. *Chem. Sci.* **2022**, *13*, 5790–5796.
4. **Gaming Stereochemistry.** Francesca M. Ippoliti, Melinda M. Nguyen, Amber J. Reilly, and Neil K. Garg. *Nat. Rev. Chem.* Accepted Article. DOI: 10.1038/s41570-022-00395-5.
5. **Cell-Free Total Biosynthesis of Plant Terpene Natural Products Using an Orthogonal Cofactor Regeneration System.** Undramaa Bat-Erdene, John M. Billingsley, William C. Turner, Benjamin R. Lichman, Francesca M. Ippoliti, Neil K. Garg, Sarah E. O’Connor, and Yi Tang. *ACS Catal.* **2021**, *11*, 9898–9903.
6. **Synthesis of 8-Hydroxygeraniol.** Francesca M. Ippoliti, Joyann S. Barber, and Neil K. Garg. *Org. Synth.* **2019**, *96*, 586–598.
7. **Concise Approach to Cyclohexyne and 1,2-Cyclohexadiene Precursors.** Jason V. Chari<sup>†</sup>, Francesca M. Ippoliti<sup>†</sup>, and Neil K. Garg. *J. Org. Chem.* **2019**, *84*, 3652–2655.
8. **Synthesis of 8-Hydroxygeraniol.** Francesca M. Ippoliti<sup>†</sup>, Joyann S. Barber<sup>†</sup>, Yi Tang, and Neil K. Garg. *J. Org. Chem.* **2018**, *83*, 11323–11326.
9. **Shining a Light on Amine Synthesis.** Joyann S. Barber, Francesca M. Ippoliti, and Neil K. Garg. *Nat. Catal.* **2018**, *1*, 97–98.

## CHAPTER ONE

### **Total Synthesis of Lissodendoric Acid A via Stereospecific Trapping of a Strained Cyclic Allene**

Francesca M. Ippoliti, Nathan J. Adamson, Laura G. Wonilowicz,  
Evan R. Darzi, Joyann S. Donaldson, and Neil K. Garg.

*Manuscript in Preparation.*

#### **1.1 Abstract**

Small rings containing allenes are unconventional compounds that have been known since the 1960s. Despite being discovered around the age of benzyne chemistry and having a number of attractive features, strained cyclic allenes have seen relatively little use in chemical synthesis and have never been employed in the synthesis of natural products. We report a concise total synthesis of the manzamine alkaloid lissodendoric acid A, which hinges on the development of a regioselective, diastereoselective, and stereospecific trapping of a fleeting cyclic allene intermediate. This key step swiftly assembles the cis-azadecalin framework of the natural product and allows for a concise synthetic endgame. These studies show that strained cyclic allenes, despite being unusual and relatively understudied since their discovery in the 1960s, are versatile building blocks in chemical synthesis.

#### **1.2 Introduction**

Strained intermediates have fascinated the scientific community for well over a century. Small rings that contain triple bonds have been particularly well-studied since the early 1900s,



ultimately leading to the validation of benzyne (**1.1**) in the 1950s (Figure 1.1a). These seminal studies, pioneered by the laboratories of Roberts<sup>1</sup> and Wittig,<sup>2,3</sup> prompted numerous experimental and theoretical efforts.<sup>4,5,6,7,8</sup> Cyclohexyne (**1.2**) was validated in 1957,<sup>9</sup> followed by 1,2-cyclohexadiene (**1.3**) in both 1964<sup>10</sup> and 1966.<sup>11</sup> Intermediates **1.1–1.3** exhibit significant strain energies (~30–50 kcal/mol),<sup>12,13</sup> leading to short lifetimes<sup>14,15</sup> and high reactivity. Although high strain could be viewed as problematic, chemists have recently sought to leverage the strain present in **1.1–1.3** and their derivatives in chemical synthesis and biological applications. Aromatic and non-aromatic cyclic alkynes are most well-used and have been used to synthesize heterocycles, ligands for catalysis (e.g, XPhos), natural products, agrochemicals, organic materials, and medicinal compounds.<sup>8</sup> Moreover, strained alkynes **1.4** have become mainstream tools in bioorthogonal chemistry.<sup>16</sup>

Strained cyclic allenes are much less well-studied intermediates compared to strained cyclic alkynes, but have a number of attractive attributes that warrant their further investigation. The geometry-optimized structure of azacyclic allene **1.5** is depicted to illustrate such benefits (Figure 1.1b). As shown, the allene C=C bonds are each 1.32 Å, whereas the central allene carbon bears an internal angle of 133°. Additionally, the allene C–H and C–CH<sub>3</sub> bonds are twisted out of the allene C=C=C plane by 39° and 36°, respectively. Several features result from this unique structure, including the high reactivity of cyclic allenes due to strain, their ability to undergo cycloaddition or metal-catalyzed reactions, and the formation of two new bonds in a single transformation, with introduction of a C(sp<sup>3</sup>) stereocenter. As such, strained cyclic allenes have recently been used to prepare highly substituted, sp<sup>3</sup>-rich compounds<sup>8,17,18,19,20,21,22,23,24</sup> and have even been used to access DNA-encoded libraries.<sup>25</sup> Further underscoring their attractiveness is the fact that cyclic allenes are axially chiral and could serve as unconventional,

yet valuable building blocks for stereoselective synthesis. Moreover, from a practical perspective, strained cyclic allenes may possess heteroatoms and can be accessed under mild conditions (e.g., fluoride-based conditions, ambient temperatures). Lastly, because of the relatively scarce body of synthetic literature surrounding strained cyclic allenes, there exist many opportunities for discovery, particularly in considering regioselectivity and stereospecificity trends, in addition to efforts in complex molecule synthesis. Strained cyclic allenes have never been used previously in natural product synthesis, which is notable given that their close relatives, strained cyclic alkynes, have been employed extensively in such studies.<sup>5,6</sup>

With the aim of developing the chemistry of strained cyclic allenes and evaluating their utility in total synthesis, we considered lissodendoric acid A (**1.6**), a structurally complex member of the manzamine family of alkaloids (Figure 1.1c).<sup>26</sup> This natural product was isolated in 2017 from the marine sponge *Lissodendoryx florida* and has been shown to reduce reactive oxygen species (ROS) in a Parkinson's disease model consisting of Neuro 2a cells treated with 6-hydroxydopamine (~50% reduction in ROS levels at concentrations of 0.1 and 10  $\mu$ M).<sup>27</sup> The natural product possesses a daunting structure that we suspected would help push the limits of strained cyclic allene chemistry. The central core of lissodendoric acid A (**1.6**) is an azadecalin scaffold bearing a conjugated diene, a carboxylic acid substituent, and two stereogenic centers, one of which is quaternary at C8a. In addition, the natural product bears a 14-membered macrocycle tethered beneath the C8 aminodecane substituent. A total synthesis of lissodendoric acid A (**1.6**) has not been reported.

We questioned if the azadecalin core, with the C8a quaternary stereocenter intact (e.g., **1.7**), could be made using a [4+2] cycloaddition between strained cyclic allene **1.8** and pyrone **1.9** (Figure 1.1c). It should be noted that controlling the absolute stereochemistry of **1.8** could

enable an enantioselective total synthesis and the use of pyrone **1.9** could enable control of regioselectivity via an inverse electron-demand Diels–Alder process. The use of pyrones in cyclic allene Diels–Alder reactions was unknown, but if successful, would also provide access to a [2.2.2]-bicyclic product (i.e., **1.7**), which in turn, would function as a masked diene needed for the total synthesis via the later expulsion of CO<sub>2</sub>.

In this Chapter, we disclose the first total synthesis of lissodendoric acid A (**1.6**), which is enabled by the development of a regioselective, diastereoselective, and stereospecific trapping of a fleeting cyclic allene intermediate. The total synthesis is concise owing to significant structural complexity being generated in the key cyclic allene trapping step. These studies show that strained cyclic allenes, despite being unusual and relatively understudied, are powerful building blocks in chemical synthesis.

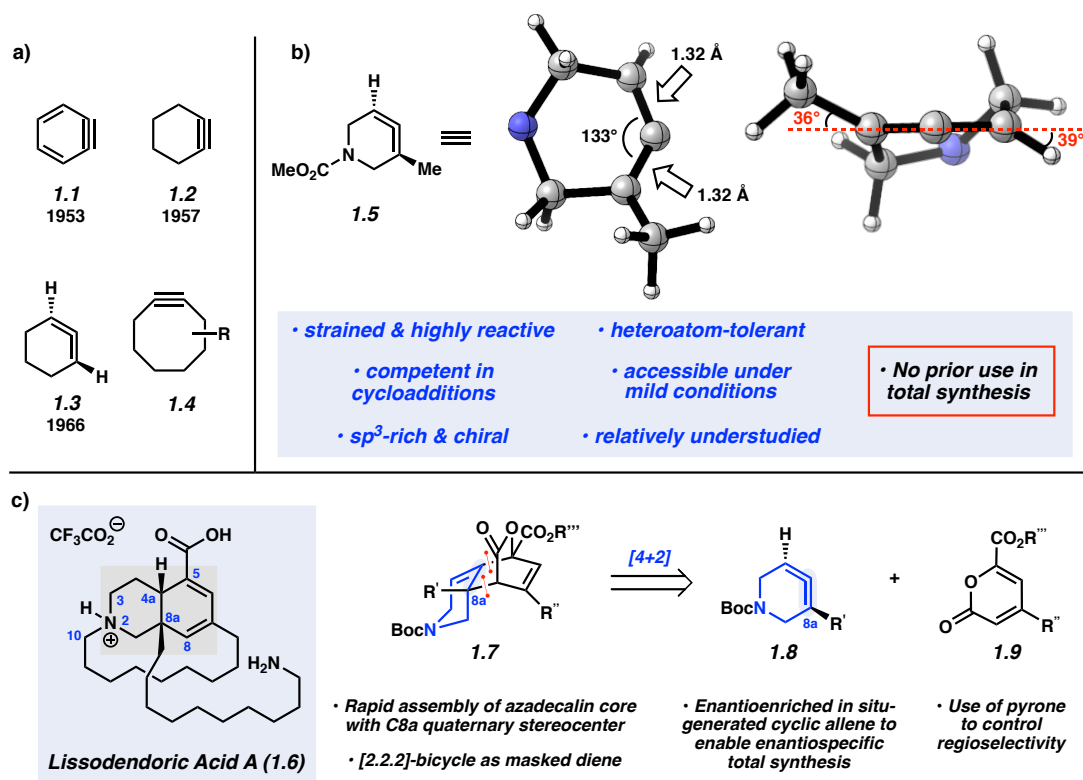


**Figure 1.1.** Strained intermediates and overview of current study. **a)** Seminal strained cyclic intermediates **1.1–1.3** and biorthogonal cyclooctyne reagents **1.4**. **b)** Geometry-optimized structure of strained azacyclic allene **1.5** ( $\omega$ B97XD/6-31G(d)) and key features. CO<sub>2</sub>Me is omitted from the 3D representations for clarity. **c)** Our synthetic target, lissodendoric acid A (**1.6**), and our synthetic approach using a [4+2] cycloaddition to access **1.7** from cyclic allene **1.8** and pyrone **1.9** (R'=alkyl group).

### 1.3 Results and Discussion

The success of our approach would hinge on the ability to control the regioselectivity and absolute stereochemistry in the key [4+2] cycloaddition step. As such, we performed the studies shown in Figure 1.2 where furan (**1.11**) and pyrone **1.13** were employed as cyclic allene trapping partners. The syntheses of **1.12**, **1.16**, and **1.18**, which function as precursors to cyclic allene **1.8**

(see Figure 1c), are provided in the Experimental Section 1.5, and utilize chiral separation technology to access enantioenriched material. Treatment of silyl triflate **1.12** with furan (**1.11**) and CsF in acetonitrile at 23 °C delivered the undesired cycloadduct **1.10**, consistent with prior experiments using the N-Cbz derivative of **1.12**.<sup>18</sup> In a crucial result, we found that treatment of **1.12** with readily available pyrone **1.13**<sup>28</sup> gave cycloadduct **1.14**, which possesses the desired connectivity and the necessary C8a quaternary center, without significant loss of stereochemical information. These results demonstrate for the first time that regioselectivity in cyclic allene [4+2] cycloadditions can be modulated by judicious selection of the trapping agent.

Our excitement for the results shown in Figure 1.2a was somewhat dampened by the inability to access compounds such as **1.12** in high ee without the use of chiral separation technologies. As such, we evaluated alternative cyclic allene precursors **1.16** and **1.18** in the corresponding cycloaddition reactions, where the silicon substituent would be placed on a less-substituted carbon. As shown in Figure 1.2b, the use of pseudo-isomeric silyl triflate **1.16** (albeit with Et in place of Me due to substrate synthesis logistics), furnished the expected cycloadducts **1.15** and **1.17**. However, regardless of trapping agent, modest stereoretention was observed. Lastly, we examined silyl bromide **1.18**, analogous to an approach to cyclic allene generation reported by West and co-workers (Figure 1.2c).<sup>22</sup> Although yields were modest in these initial studies, significant stereoretention was observed in the formation of cycloadducts **1.10** and **1.14**. It should be noted that silyl bromide precursors to cyclic allenes had not been synthesized previously in enantioenriched fashion, but we were optimistic that derivatives of **1.18** could be prepared without the need for chiral separations. Before describing the translation of these studies to the total synthesis of lissodendoric acid A (**1.6**), we also highlight several key features of cyclic allene chemistry that are reflected in the results shown in Figure 1.2. More specifically,

all reactions proceed under mild conditions, lead to the formation of two C–C bonds, occur with high diastereoselectivity (endo-selectivity<sup>29</sup>), and provide access to complex heterocyclic products that contains three stereocenters, with one of them being quaternary in the cases of the pyrone cycloadducts.

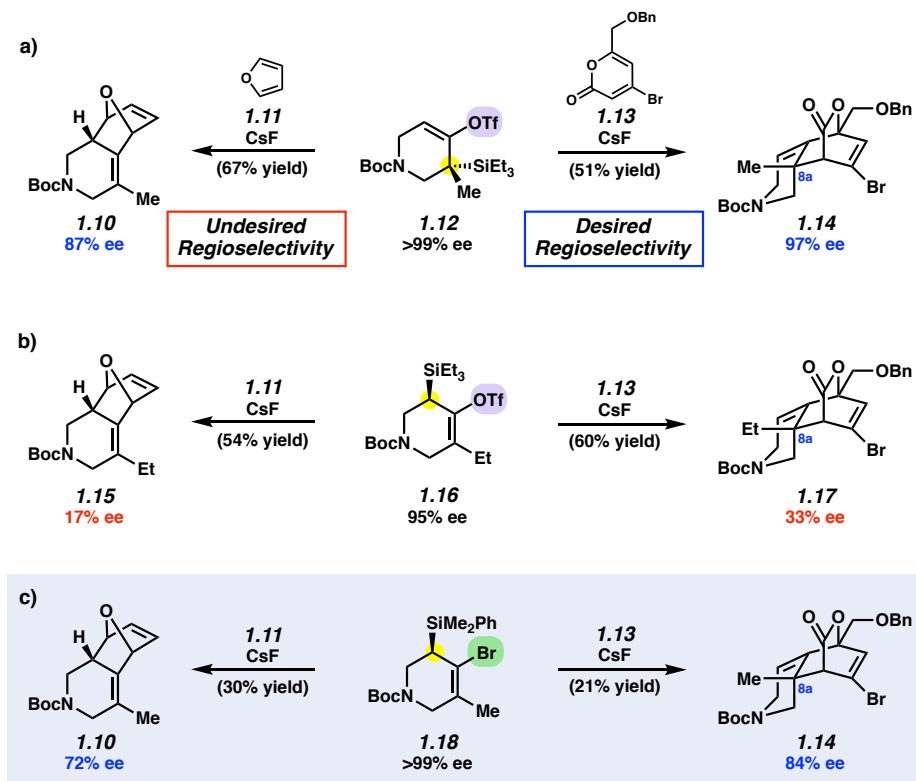


**Figure 1.2.** Regioselectivity and stereospecificity studies using variable cyclic allene precursors and [4+2] cycloaddition partners. **a)** Use of cyclic allene precursor **1.12** allows for efficient and stereospecific cycloadditions. **b)** Stereospecificity is modest when employing pseudo-isomeric silyl triflate **1.16**. **c)** Switching to silyl bromide **1.18** as the cyclic allene precursor allows for regioselective and stereospecific cycloaddition reactions, while providing a plausible entryway to enantioenriched material. Highlights depict the primary differences between cyclic allene precursors **1.12**, **1.16**, and **1.18**. See the Experimental Section 1.5 for reaction conditions.

Having established the feasibility of the key cyclic allene trapping step, we sought to perform analogous studies on a more elaborate substrate. Pursuing this endeavor could allow us to push the limits of strained cyclic allene chemistry, while enabling a concise total synthesis of lissodendoric acid A (**1.6**). The pyrone fragment, **1.22**, was prepared in two steps from commercially available carboxylic acid **1.19** (Figure 1.3a). Double tosylation, followed by addition of *t*-BuOH, furnished tosylate **1.20**, bearing a *t*-butyl ester substituent. Subsequent Negishi coupling with organozinc reagent **1.21** provided substrate **1.22**, which contains a terminal alkene necessary for eventual installation of the macrocycle using ring-closing metathesis. The desired cyclic allene precursor, silyl bromide **1.27**, was prepared from bromotriflate **1.23**, which was obtained commercially (Figure 1.3b). Treatment of **1.23** with alkylzirconium reagent **1.24** gave ketone **1.25** via 1,4-addition and ejection of the triflate leaving group.<sup>30</sup> CBS reduction,<sup>31</sup> followed by treatment with ethylchloroformate, gave **1.26** in 90% ee. Displacement of the carbonate with a silyl cuprate nucleophile<sup>22,32,33</sup> delivered cyclic allene precursor **1.27** without loss in ee. Of note, the conversion of bromoketone **1.25** to silyl bromide **1.27** parallels a general racemic strategy pioneered by West,<sup>22</sup> but the enantioselective reduction and stereoselective displacement of the carbonate had not been demonstrated previously.

With pyrone **1.22** and cyclic allene precursor **1.27** in hand, we evaluated the key [4+2] cycloaddition as shown in Figure 1.3c. Simply treating these reactants with CsF in acetonitrile at 23 °C delivered cycloadduct **1.28** in 54% isolated yield, presumably via the depicted transition structure. Several aspects of this complexity-generating step should be noted: a) With regard to regioselectivity of the cyclic allene, the more substituted olefin reacts with the electron-deficient pyrone. b) The diene in pyrone **1.22** aligns with the cyclic allene to promote bond formation between C8a and C8. The pyrone carbonyl, which is conjugated to the diene in **1.22**, is thought

to provide a dominant electronic effect that leads to this selectivity. c) The reaction is thought to proceed in an endo fashion, with orbital overlap between the diene and non-reactive olefin of the cyclic allene, giving rise to **1.28** in >20:1 dr. This reactivity has been proposed previously in Diels–Alder reactions of cyclic allenes with furan.<sup>29</sup> d) Cycloadduct **1.28**, which forms under fairly mild reaction conditions, bears considerable structural complexity and functionality.

The topics of absolute stereochemistry and optical yield also deserves special attention. Cyclic allene precursor **1.27** bears a single stereocenter (marked \*). Upon generation of the cyclic allene intermediate, point chirality in **1.27** is transmitted to axial chirality in the cyclic allene intermediate. Then, cycloaddition re-introduces point chirality, with the introduction of two tertiary stereocenters and the C8a quaternary stereocenter, but with ablation of the sole stereocenter present in reactant **1.27**. It is also notable that the optical yield in forming **1.28** is 70%, indicative that strain-driven cycloaddition between two highly substituted reactants is favorable over facile racemization of the strained cyclic allene.



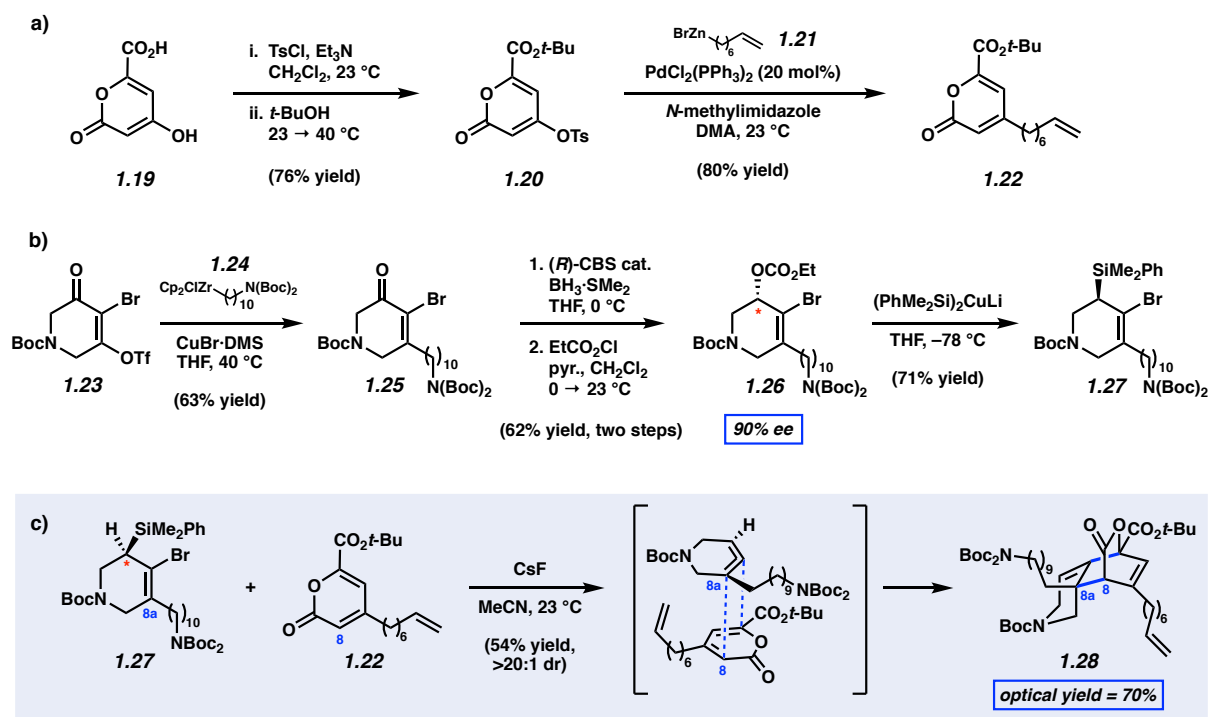


**Figure 1.3.** Assembly of the azadecalin core of lissodendoric acid A (**1.6**) using a strained cyclic allene. **a)** Synthesis of pyrone **1.22**. **b)** Enantioselective route to silyl triflate **1.27**. **c)** Cycloaddition of the strained cyclic allene derived from **1.27** with pyrone **1.22** proceeds with regioselectivity, diastereoselectivity, and stereospecificity to deliver enantioenriched adduct **1.28** with the desired quaternary stereocenter at C8a.

To complete the total synthesis of lissodendoric acid A (**1.6**), we developed the concise late-stage sequence shown in Figure 1.4. The route has been performed on racemic material thus far, but enantioenriched material will soon be employed as well. The first challenge was to introduce the C4a hydrogen substituent, without reduction of the terminal olefin. We achieved this by first oxidizing C3 with PDC and then treating the resulting intermediate with a copper hydride source<sup>34</sup> to effect diastereoselective 1,4-reduction and furnish *cis*-azadecalin **1.29**. Next, we arrived at tetraene **1.30** via a sequence involving thermal extrusion of CO<sub>2</sub>,<sup>35</sup> copper triflate-promoted removal of two of the three Boc groups,<sup>36</sup> and amidation of N2 with acryloyl chloride.

Access to **1.30** set the stage for macrocyclization, which was achieved using ring-closing metathesis promoted by the robust Grubbs' 2<sup>nd</sup> Generation catalyst.<sup>37</sup> The intended macrocycle **1.31** was obtained in 83% yield and as an inconsequential 7:2 mixture of *E:Z* olefin isomers. All that remained to complete the total synthesis was to perform global reduction and deprotection. The former was achieved using a reduction protocol reported by Beller,<sup>38</sup> which led to saturation of the C3 amide and the C10  $\alpha,\beta$ -unsaturated amide selectively without reduction of the ester or diene functionalities. Finally, treatment of the reduced intermediate with TFA furnished lissodendoric acid A (**1.6**).

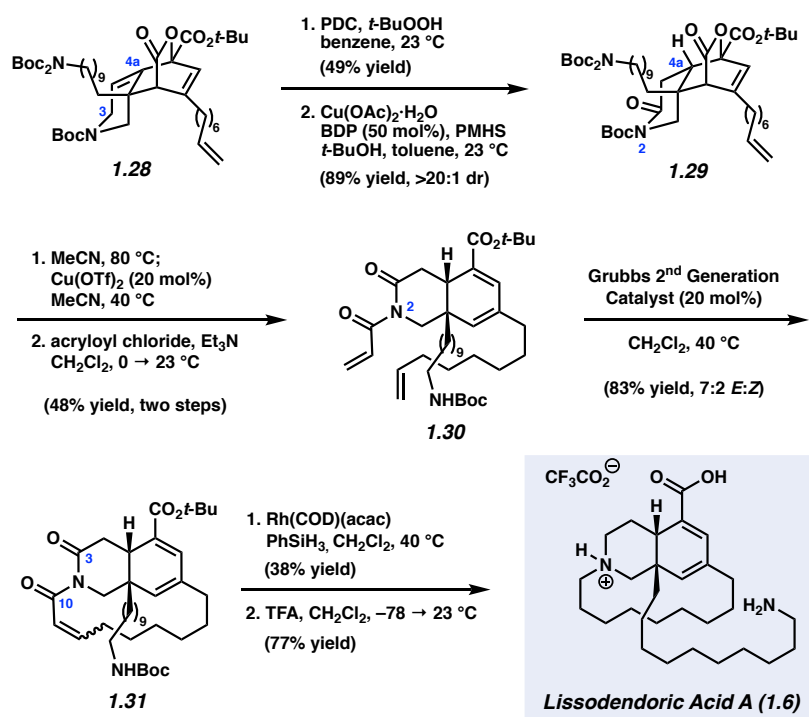


**Figure 1.4.** Completion of the total synthesis of lissodendoric acid A (**1.6**).

## 1.4 Conclusion

In contrast to strained alkynes, strained cyclic allenes have seen relatively little use in chemical synthesis and have never been employed in total synthesis. This is notable because strained cyclic allenes were discovered in the 1960s, in the dawn of strained alkyne chemistry, and have a number of attractive attributes. Fueled by the development of a regioselective, diastereoselective, and stereospecific trapping of a fleeting cyclic allene intermediate, we have completed a concise total synthesis of the manzamine alkaloid lissodendoric acid A (**1.6**). The key step is an inverse electron-demand Diels–Alder reaction between two highly functionalized substrates that gives rise to cycloadduct **1.28** via the formation of two C–C bonds, the ablation of a single stereocenter present in a substrate, and the creation of three new stereocenters, including the C8a quaternary center. With rapid access to the carbon skeleton of lissodendoric acid A (**1.6**), a concise late-stage sequence was executed to deliver the natural product. These studies demonstrate that cyclic allenes are powerful tools for complex molecule synthesis and should prompt the further investigation and application of these long-overlooked and unusual compounds.

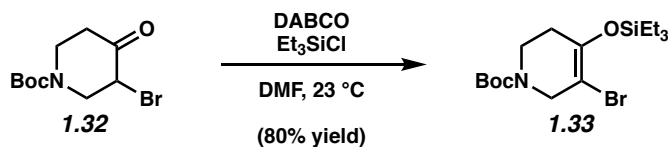
## 1.5 Experimental Section

**1.5.1 Materials and Methods.** Unless stated otherwise, reactions were conducted in flame-dried glassware under an atmosphere of nitrogen using anhydrous solvents (either freshly distilled or passed through activated alumina columns). All commercially obtained reagents were used as received unless otherwise specified. 1,4-Diazabicyclo[2.2.2]octane (DABCO),  $\text{CeCl}_3 \cdot 7\text{H}_2\text{O}$ , and  $\text{CuBr} \cdot \text{DMS}$  were purchased from Acros Organics.  $\text{AgOTf}$ , NBS, *n*-Butyllithium 2.5 M solution in hexanes (*n*-BuLi), allyl chloroformate, *n*-Bu<sub>4</sub>NBr<sub>3</sub>, NaBH<sub>4</sub>, ethyl chloroformate, alkynyl trifluoroborate **1.35**, anhydrous *t*-BuOH, AIBN, NaH, Grubbs' 2<sup>nd</sup> generation catalyst, KHMDS, PDC, *t*-BuOOH 70 wt% in H<sub>2</sub>O, *N*-methylimidazole, LiAlH<sub>4</sub> 2.0 M solution in THF, acryloyl chloride, PhSiH<sub>3</sub>, and TsCl were obtained from Sigma-Aldrich. AgNO<sub>3</sub>, *N*-Phenyl-bis(trifluoromethanesulfonimide) (PhNTf<sub>2</sub>), triethylsilyl chloride (Et<sub>3</sub>SiCl), PPh<sub>3</sub>, azetidinone **1.34**, DMAP, Tf<sub>2</sub>O, Cs<sub>2</sub>CO<sub>3</sub>, and trifluoroacetic acid (TFA) were purchased from Oakwood Chemical. CsF, (PPh<sub>3</sub>)AuCl, Pd(PPh<sub>3</sub>)<sub>4</sub>, Cl<sub>2</sub>Pd(PPh<sub>3</sub>)<sub>2</sub>, Cu(OTf)<sub>2</sub>, Rh(COD)(acac), Ni(cod)<sub>2</sub>, zirconocene hydrochloride, and 1,2-bis(diphenylphosphino)benzene (BDP) were purchased from Strem Chemicals. Copper(II) acetate monohydrate (Cu(OAc)<sub>2</sub>·H<sub>2</sub>O) and 10-bromodec-1-ene (**1.41**) were purchased from TCI chemicals. Poly(methylhydrosiloxane) (PMHS), triethylamine, diisopropylamine, and BH<sub>3</sub>·SMe<sub>2</sub> were purchased from Alfa-Aesar. *t*-BuOH was purchased from Fisher Scientific.  $\alpha$ -Bromo ketone **1.32**, Comins' reagent, diketone **1.40**, and (*R*)-CBS catalyst were purchased from Combi-Blocks. Di-*tert*-butyl iminodicarbonate (NH(Boc)<sub>2</sub>) was purchased from Ambeed. Et<sub>3</sub>SiCl, allyl chloroformate, pyridine, diisopropylamine, and acryloyl chloride were distilled over CaH<sub>2</sub> prior to use. PMHS and *t*-BuOH were sparged with N<sub>2</sub> prior to use. NBS was recrystallized from H<sub>2</sub>O prior to use. Unless stated otherwise, reactions were performed at 23 °C. Thin-layer chromatography (TLC) was conducted with EMD gel 60 F254

pre-coated plates (0.25 mm) and visualized using anisaldehyde or potassium permanganate staining. Silicycle Siliaflash P60 (particle size 0.040–0.063 mm) was used for flash column chromatography.  $^1\text{H-NMR}$  spectra were recorded on Bruker spectrometers (at 400, 500, or 600 MHz) and are reported relative to the residual solvent signal. Data for  $^1\text{H-NMR}$  spectra are reported as follows: chemical shift ( $\delta$  ppm), multiplicity, coupling constant (Hz) and integration.  $^{13}\text{C-NMR}$  spectra were recorded on Bruker spectrometers (at 100, 125 or 150 MHz) and are reported relative to the residual solvent signal. Data for  $^{13}\text{C-NMR}$  spectra are reported in terms of chemical shift ( $\delta$  ppm). IR spectra were obtained on a Perkin-Elmer UATR Two FT-IR spectrometer and are reported in terms of frequency of absorption ( $\text{cm}^{-1}$ ). DART-MS spectra were collected on a Thermo Exactive Plus MSD (Thermo Scientific) equipped with an ID-CUBE ion source, a Vapor Interface (IonSense Inc.), and an Orbitrap mass analyzer. Both the source and MSD were controlled by Excalibur software v. 3.0. The analyte was spotted onto OpenSpot sampling cards (IonSense Inc.) using  $\text{CDCl}_3$  as the solvent. Ionization was accomplished using UHP He (Airgas Inc.) plasma with no additional ionization agents. The mass calibration was carried out using Pierce LTQ Velos ESI (+) and (–) Ion calibration solutions (Thermo Fisher Scientific). Determination of enantiopurity was carried out on a JASCO SFC (supercritical fluid chromatography) using Daicel ChiralPak IA and IB columns and an Agilent 1200 series HPLC using a Daicel ChiralPak ID column.

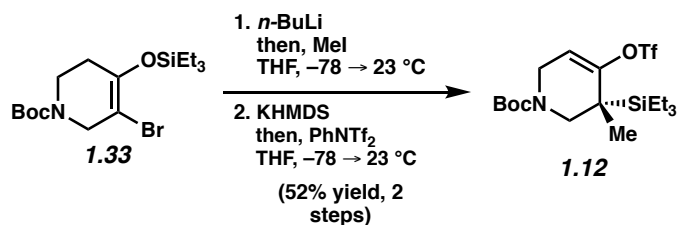
## 1.5.2 Experimental Procedures

### 1.5.2.1 Synthesis of Cyclic Allene Precursors 1.12, 1.16, and 1.18



**Bromo silyl enol ether 1.33.** To a solution of  $\alpha$ -bromo ketone **1.32** (4.51 g, 16.2 mmol, 1.00 equiv) dissolved in DMF (14.7 mL, 1.10 M) using sonication, was added triethylsilyl chloride (4.40 mL, 25.9 mmol, 1.60 equiv) and DABCO (4.18 g, 37.3 mmol, 2.30 equiv). Then, the reaction was allowed to stir for 23.5 h at 23 °C before being quenched with a saturated aqueous solution of NaHCO<sub>3</sub> (10 mL). The reaction mixture was then transferred to a separatory funnel and diluted with water (20 mL). The layers were separated and the aqueous layer was extracted with EtOAc (3 x 20 mL). The combined organic layers were sequentially washed with water (2 x 20 mL) and brine (1 x 20 mL), dried with MgSO<sub>4</sub>, filtered, and concentrated under reduced pressure to provide the crude residue. The crude residue was purified via flash chromatography (100% hexanes  $\rightarrow$  39:1 hexanes:EtOAc) to obtain bromo silyl enol ether **1.33** (5.07 g, 80% yield) as a colorless oil. Bromo silyl enol ether **1.33**:  $R_f$  0.67 (5:1 hexanes:EtOAc); <sup>1</sup>H NMR (600 MHz, CDCl<sub>3</sub>):  $\delta$  4.07 (br s, 2H), 3.57 (br s, 2H), 2.28 (br s, 2H), 1.46 (s, 9H), 1.00 (t,  $J = 7.9$ , 9H), 0.71 (q,  $J = 7.9$ , 6H); <sup>13</sup>C NMR (150 MHz, CDCl<sub>3</sub>):  $\delta$  154.3, 146.0, 97.5, 96.9, 80.3, 49.0, 48.4, 41.7, 40.4, 31.5, 28.5, 6.8, 5.7; IR (film): 2957, 2877, 1700, 1412, 1226, 1166 cm<sup>-1</sup>; HRMS-APCI ( $m/z$ ) [M + H]<sup>+</sup> calcd for C<sub>16</sub>H<sub>31</sub>BrNO<sub>3</sub>Si<sup>+</sup>, 392.1251; found 392.1243.

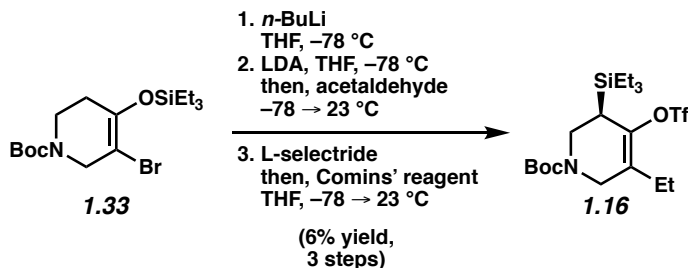
*Note: 1.33 was obtained as a mixture of rotamers. These data represent empirically observed chemical shifts from the <sup>1</sup>H and <sup>13</sup>C NMR spectra.*



**Silyl Triflate 1.12.** A solution of silyl enol ether **1.33** (3.00 g, 7.65 mmol, 1.00 equiv) in THF (76.5 mL, 0.10 M) was cooled to  $-78$  °C. Then, *n*-BuLi (3.53 mL, 2.38 M solution in hexanes, 8.41 mmol, 1.10 equiv) was added dropwise over 40 min, then the reaction was allowed to stir at  $-78$  °C for 3 h. MeI (4.78 mL, 76.5 mmol, 10.0 equiv) was added as a neat liquid dropwise over 5 min, and the reaction was allowed to stir at  $-78$  °C for 20 min before warming to 23 °C and stirring for an additional 14 h. The reaction was then quenched with water (30 mL) and transferred to a separatory funnel. The layers were separated and the aqueous layer was extracted with EtOAc (3 x 30 mL). The combined organic layers were then dried with sodium sulfate, filtered, and concentrated under reduced pressure. The crude residue was purified via flash chromatography (4:1 hexanes:EtOAc) to afford the  $\alpha$ -silyl ketone. The  $\alpha$ -silyl ketone enantiomers were separated by chiral SFC by Lotus Separations (enantiopurity of the  $\alpha$ -silyl ketone was determined to be >99% ee by Lotus Separations). To a flask in the glovebox was added KHMDS (110 mg, 0.551 mmol, 1.21 equiv) and the flask was then removed from the glovebox. The powder was then dissolved in THF (1.5 mL) and cooled to  $-78$  °C for 20 min. To the solution was added a solution of the  $\alpha$ -silyl ketone (150 mg, 0.457 mmol, 1.00 equiv, >99% ee) in THF (1.5 mL) dropwise over 5 min and the subsequent mixture was stirred at  $-78$  °C for an additional 1 h. To the reaction mixture was added a solution of Comins' reagent (215 mg, 0.548 mmol, 1.20 equiv) in THF (1.5 mL) dropwise over 5 min. The cold bath was then removed and the reaction was allowed to warm to 23 °C. After stirring for 1 h, the reaction was quenched with saturated aq. NaHCO<sub>3</sub> (20 mL) and was extracted with ether (3 x 30 mL). The organic

layers were combined, dried over magnesium sulfate, filtered, and concentrated under reduced pressure. The crude residue was purified via flash chromatography (1:1 hexanes:benzene → 99:1 benzene:EtOAc) to afford silyl triflate (**1.12**, 121 mg, 52% yield over two steps, >99% ee) as a colorless oil. Silyl triflate **1.12**:  $R_f$  0.51 (9:1 hexanes:EtOAc);  $^1\text{H}$  NMR (600 MHz,  $\text{CDCl}_3$ ):  $\delta$  5.61 (d,  $J = 29.5$ , 1H), 4.07 (t,  $J = 16.8$ , 1H), 4.00–3.89 (m, 1H), 3.68 (d,  $J = 12.9$ , 1H), 3.35 (dd,  $J = 36.1, 12.3$ , 1H), 1.47 (s, 9H), 1.17 (s, 3H), 0.99 (t,  $J = 7.9$ , 9H), 0.74–0.65 (m, 6H);  $^{13}\text{C}$  NMR (125 MHz,  $\text{CDCl}_3$ ):  $\delta$  155.1, 154.7, 154.5, 154.3, 118.4 (q,  $J = 322.4$ ), 110.5, 109.9, 80.5, 50.5, 49.5, 42.7, 42.1, 31.4, 28.51, 28.48, 18.6, 7.9, 2.5; IR (film): 2960, 2882, 1702, 1417, 1246, 1214  $\text{cm}^{-1}$ ; HRMS-APCI ( $m/z$ )  $[\text{M} + \text{H}]^+$  calcd for  $\text{C}_{18}\text{H}_{33}\text{F}_3\text{NO}_5\text{SSi}^+$ , 460.17953; found 460.18305.

*Note: 1.12 was obtained as a mixture of rotamers. These data represent empirically observed chemical shifts from the  $^1\text{H}$  and  $^{13}\text{C}$  NMR spectra.*



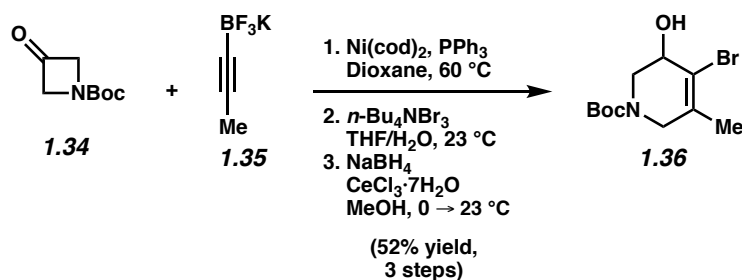
**Silyl Triflate 1.16.** A solution of silyl enol ether **1.33** (2.80 g, 7.14 mmol, 1.00 equiv) in THF (60 mL, 0.12 M) was cooled to  $-78\text{ }^\circ\text{C}$  and stirred for 5 min. To this solution was added  $n$ -butyllithium (4.9 mL, 11 mmol, 2.2 M in hexanes, 1.5 equiv) dropwise over 2 min and then the solution was allowed to stir at  $-78\text{ }^\circ\text{C}$  for 2.5 h. The reaction was quenched by the addition of saturated aq.  $\text{NaHCO}_3$  (20 mL) and then the reaction mixture was allowed to warm to  $23\text{ }^\circ\text{C}$ . The reaction was diluted with  $\text{H}_2\text{O}$  (50 mL) and the aqueous layer was extracted with  $\text{Et}_2\text{O}$  (3 x 30 mL). The combined organic layers were then dried over  $\text{MgSO}_4$ , filtered, and concentrated under



reduced pressure. The crude residue purified via flash chromatography (20:1 hexanes:EtOAc → 5:1 hexanes:EtOAc) to afford the silyl ketone. A solution of diisopropylamine (0.34 mL, 2.4 mmol, 1.5 equiv) and in THF (7 mL) was cooled to  $-78\text{ }^{\circ}\text{C}$  for 10 min. To this solution was added *n*-butyllithium (1.10 mL, 2.20 M in hexanes, 2.42 mmol, 1.52 equiv) dropwise over 5 min. The resulting LDA solution was allowed to stir at  $-78\text{ }^{\circ}\text{C}$  for 30 min and then allowed to warm to  $23\text{ }^{\circ}\text{C}$  and stirred for 10 min. The solution was then cooled to  $-78\text{ }^{\circ}\text{C}$  and a solution of the silyl ketone (500 mg, 1.59 mmol, 1.00 equiv) in THF (7 mL) was added dropwise over 5 min. The resulting mixture was allowed to stir at  $-78\text{ }^{\circ}\text{C}$  for 1 h. After this time, acetaldehyde (892  $\mu\text{L}$ , 15.9 mmol, 10.0 equiv) was added to the solution. The reaction mixture was allowed to stir at  $-78\text{ }^{\circ}\text{C}$  for 15 min and then allowed to warm to  $23\text{ }^{\circ}\text{C}$  and stir for 1 h. After this time, the reaction mixture was quenched with saturated aq.  $\text{NaHCO}_3$  (20 mL) and then diluted with  $\text{Et}_2\text{O}$  (20 mL). The layers were separated and the aqueous layer was extracted with  $\text{Et}_2\text{O}$  (2 x 20 mL). The organic layers were combined, dried over  $\text{MgSO}_4$ , filtered, and concentrated under reduced pressure. The crude residue was purified via flash chromatography (19:1 hexanes:EtOAc → 9:1 hexanes:EtOAc) to afford the enone. The enone enantiomers were separated by chiral SFC by Lotus Separations (enantiopurity of the enone was determined to be 95% ee by Lotus Separations). A solution of the enone (155 mg, 0.456 mmol, 1.00 equiv, 95% ee) in THF (2.0 mL, 0.23 M) and was cooled to  $-78\text{ }^{\circ}\text{C}$ . To this solution was added L-selectride (0.50 mL, 1.0 M in THF, 0.50 mmol, 1.1 equiv) dropwise over 2 min and the resulting solution was allowed to stir at  $-78\text{ }^{\circ}\text{C}$  for 1 h. To the reaction mixture was then added a solution of Comins' reagent (199 mg, 0.506 mmol, 1.1 equiv) in THF (2 mL) dropwise over 5 min and then the reaction was allowed to warm to  $23\text{ }^{\circ}\text{C}$  and stir for 20 h. After this time, the reaction was quenched with saturated aq.  $\text{NaHCO}_3$  (20 mL) and diluted with  $\text{Et}_2\text{O}$  (20 mL). The layers were separated and

the aqueous layer was extracted with Et<sub>2</sub>O (2 x 20 mL). The organic layers were combined, dried over MgSO<sub>4</sub>, filtered, and concentrated under reduced pressure. The crude residue was purified via flash chromatography (1:1 benzene:hexanes → 99:1 benzene:EtOAc) to afford silyl triflate **1.16** (35.0 mg, 6% yield over three steps, 95% ee) as a colorless oil. Silyl triflate **1.16**: *R<sub>f</sub>* 0.40 (9:1 hexanes:EtOAc); <sup>1</sup>H NMR (600 MHz, CDCl<sub>3</sub>): δ 4.28–2.15 (m, 1H), 4.15–4.02 (m, 1H), 3.77–3.64 (m, 1H), 3.35–3.18 (m, 1H), 2.38–2.24 (m, 1H), 2.12–2.03 (m, 1H), 1.98 (bs, 1H), 1.48 (s, 9H), 1.05 (t, *J* = 7.6, 3H), 0.97–0.88 (m, 9H), 0.64 (q, *J* = 8.0, 6H); <sup>13</sup>C NMR (125 MHz, CDCl<sub>3</sub>): δ 154.4, 143.6, 142.9, 125.5, 125.2, 118.4 (q, *J* = 318.8), 80.6, 80.5, 45.4, 45.1, 43.3, 42.2, 28.5, 21.9, 12.2, 7.2, 2.8; IR (film): 2959, 2880, 1705, 1412, 1212, 1142 cm<sup>-1</sup>; HRMS-APCI (m/z) [M + H]<sup>+</sup> calcd for C<sub>19</sub>H<sub>35</sub>F<sub>3</sub>NO<sub>5</sub>SSi<sup>+</sup>, 474.19518; found 474.19987.

*Note: 1.16 was obtained as a mixture of rotamers. These data represent empirically observed chemical shifts from the <sup>1</sup>H and <sup>13</sup>C NMR spectra.*

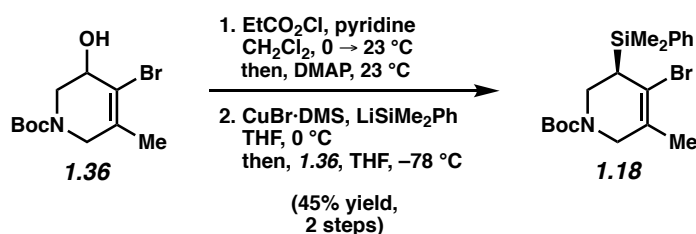


**Alcohol 1.36.** Three vials containing triphenylphosphine (162 mg, 617 μmol, 37.0 mol%), azetidinone **1.34** (493 mg, 2.88 mmol, 1.73 equiv), and alkynyl trifluoroborate **1.35** (243 mg, 1.67 mmol, 1.00 equiv), respectively, were brought into the glovebox. Inside the glovebox, Ni(cod)<sub>2</sub> (56.5 mg, 206 μmol, 12.3 mol%) and dioxane (1.7 mL, 0.12 M) were added to the vial containing triphenylphosphine. The mixture was allowed to stir inside the glovebox for 10 min. Next, azetidinone **1.34**, alkynyl trifluoroborate **1.35**, and dioxane (5.1 mL, 0.40 M) were added

to the catalyst solution. The vial was capped with a Teflon-coated cap and brought out of the glovebox. The reaction mixture was then warmed to 60 °C and stirred for 18 h. After 18 h, the reaction was allowed to cool to 23 °C, then diluted with acetonitrile (15 mL) and concentrated under reduced pressure. Next, acetone (10 mL) and Et<sub>2</sub>O (80 mL) were added to the reaction mixture to induce precipitation. The solution was filtered through a sintered Buchner funnel, rinsing with Et<sub>2</sub>O (30 mL). The solid was collected from the filter and dried under vacuum. The product was triturated with Et<sub>2</sub>O (3 x 5 mL) to provide the enone trifluoroborate potassium salt. To a solution of the enone trifluoroborate potassium salt (764 mg, 2.41 mmol, 1.00 equiv) in THF (12.0 mL) and water (12.0 mL) was added tetra-*n*-butylammonium tribromide (1.16 g, 2.41 mmol, 1.00 equiv) in one portion. The mixture was stirred at 23 °C for 1.5 h. After 1.5 h, the reaction was diluted with Et<sub>2</sub>O (15 mL) and transferred to a separatory funnel. The layers were separated, and the aqueous layer was extracted with Et<sub>2</sub>O (3 x 10 mL). The combined organic layers were dried over MgSO<sub>4</sub>, filtered, and concentrated. The crude residue was purified via flash chromatography (4:1 hexanes:EtOAc) to provide the bromoenone. To a solution of the bromoenone (80 mg, 0.28 mmol, 1.0 equiv) in methanol (0.70 mL) was added cerium(iii)chloride heptahydrate (0.11 g, 29 μL, 0.30 mmol, 1.1 equiv). The solution was cooled to 0 °C and sodium borohydride (13 mg, 1.2 Eq, 0.33 mmol, 1.2 equiv) was added in 3 portions over 5 min. The reaction was stirred at 0 °C for 1 h, then allowed to warm to 23 °C and stirred for an additional 1 h. The reaction was cooled to 0 °C and quenched with the addition of 1 M HCl (1 mL) added dropwise over 1 min. The mixture was transferred to a separatory funnel with Et<sub>2</sub>O, the layers were separated, and the aqueous layer was extracted with Et<sub>2</sub>O (3 x 6 mL). The organic layers were combined, dried over MgSO<sub>4</sub>, filtered, and concentrated. The crude residue was purified via flash chromatography (3:1 hexanes:EtOAc) to afford alcohol **1.36** (68.0 mg,

52% yield over three steps) as a white sticky foam. Alcohol **1.36**:  $R_f$  0.28 (3:1 hexanes:EtOAc);  $^1\text{H}$  NMR (500 MHz,  $\text{CDCl}_3$ ):  $\delta$  4.22 (bs, 1H), 4.06 (bs, 1H), 3.84 (bs, 1H), 3.72 (d,  $J = 17.8$ , 1H), 3.49 (dd,  $J = 13.5, 2.9$ , 1H), 2.16 (bs, 1H), 1.83 (d,  $J = 0.8$ , 3H), 1.47 (s, 9H);  $^{13}\text{C}$  NMR (125 MHz,  $\text{CDCl}_3$ ):  $\delta$  154.8, 134.8, 120.0, 80.7, 69.9, 48.5, 47.8, 28.4, 20.3; IR (film): 3406, 2920, 2850, 1681, 1423, 1244, 1146  $\text{cm}^{-1}$ ; HRMS-APCI ( $m/z$ )  $[\text{M} + \text{H}]^+$  calcd for  $\text{C}_{11}\text{H}_{19}\text{BrNO}_3$ , 292.05428; found 292.05255.

*Note: 1.36 was obtained as a mixture of rotamers. These data represent empirically observed chemical shifts from the  $^1\text{H}$  and  $^{13}\text{C}$  NMR spectra.*

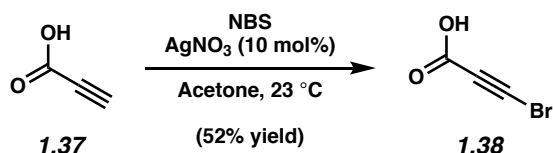


**Silyl bromide 1.18.** A solution of alcohol **1.36** (414 mg, 1.42 mmol, 1.00 equiv) in  $\text{CH}_2\text{Cl}_2$  (14.2 mL, 0.100 M) was cooled to  $0^\circ\text{C}$ . To the solution was added pyridine (172  $\mu\text{L}$ , 2.13 mmol, 1.50 equiv) dropwise over 1 minute. Next, ethyl chloroformate (163  $\mu\text{L}$ , 1.70 mmol, 1.20 equiv) was added to the solution dropwise over 1 minute. The reaction was stirred at  $0^\circ\text{C}$  for 5 min and then allowed to warm to  $23^\circ\text{C}$  and stirred for 1.25 h. DMAP (52.0 mg, 426  $\mu\text{mol}$ , 30.0 mol%) was added to the reaction in one portion and the reaction mixture was stirred for an additional 1 h at  $23^\circ\text{C}$ . The reaction mixture was then cooled to  $0^\circ\text{C}$  and quenched by the addition of 1 M HCl (5 mL) and water (10 mL). The reaction mixture was warmed to  $23^\circ\text{C}$ , the layers were separated, and the aqueous layer was extracted with  $\text{Et}_2\text{O}$  (3 x 10 mL). The organic layers were combined, dried over  $\text{MgSO}_4$ , filtered, and concentrated under reduced pressure. The crude residue was purified via flash chromatography (9:1 hexanes:EtOAc  $\rightarrow$  5:1 hexanes:EtOAc) to afford the

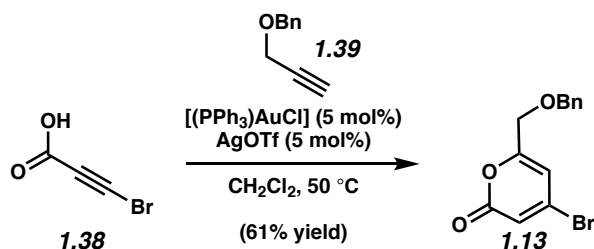
carbonate. A solution of bromocopper methylsulfanylmethane (50.2 mg, 244  $\mu\text{mol}$ , 1.30 equiv) in THF (1.6 mL) was cooled to 0  $^{\circ}\text{C}$ . To the solution was added (dimethyl(phenyl)silyl)lithium<sup>19</sup> (2.12 mL, 0.23 M, 488  $\mu\text{mol}$ , 2.60 equiv) dropwise over 3 min and the mixture was stirred at 0  $^{\circ}\text{C}$  for 40 min. The reaction mixture was cooled to  $-78$   $^{\circ}\text{C}$  and to the solution was added the carbonate (68.4 mg, 188  $\mu\text{mol}$ , 1.00 equiv) in THF (0.45 mL) dropwise over 2 minutes. The reaction mixture was allowed to stir at  $-78$   $^{\circ}\text{C}$  for 3 h. After this time, the reaction was diluted with Et<sub>2</sub>O (2 mL) and quenched with water (2 mL) at  $-78$   $^{\circ}\text{C}$ , then allowed to warm to 23  $^{\circ}\text{C}$ . The reaction mixture was then transferred to a separatory funnel containing Et<sub>2</sub>O (5 mL) and water (5 mL). The layers were separated and the aqueous layer was extracted with Et<sub>2</sub>O (2 x 5 mL). The combined organic layers were dried over MgSO<sub>4</sub>, filtered, and concentrated under reduced pressure. The crude residue was purified via flash chromatography (50:1  $\rightarrow$  9:1 hexanes:EtOAc) to afford silyl bromide **1.18** (42.0 mg, 45% yield over two steps) as a colorless oil. The silyl bromide enantiomers were separated by chiral SFC by Lotus Separations (enantiopurity of the silyl bromide was determined to be >99% ee by Lotus Separations). Silyl bromide **1.18**:  $R_f$  0.61 (5:1 hexanes:EtOAc); <sup>1</sup>H NMR (500 MHz, CDCl<sub>3</sub>):  $\delta$  7.49 (d,  $J$  = 6.6, 2H), 7.41–7.28 (m, 3H), 4.25–3.88 (m, 1H), 3.64–3.26 (m, 2H), 3.26–3.04 (m, 1H), 2.24 (s, 1H), 1.70 (d,  $J$  = 26.6, 3H), 1.44 (s, 9H), 0.54–0.33 (m, 6H); <sup>13</sup>C NMR (125 MHz, CDCl<sub>3</sub>):  $\delta$  154.2, 137.4, 133.8, 129.1, 127.8, 127.6, 127.5, 79.9, 48.8, 48.6, 44.2, 43.1, 38.0, 28.5, 28.4, 20.4,  $-2.4$ ,  $-2.7$ ,  $-3.1$ ,  $-3.5$ ; IR (film): 2979, 1698, 1407, 1256, 1148, 818  $\text{cm}^{-1}$ ; HRMS-APCI ( $m/z$ ) [ $M + H$ ]<sup>+</sup> calcd for C<sub>19</sub>H<sub>29</sub>BrNO<sub>2</sub>Si<sup>+</sup>, 410.11454; found 410.11383.

*Note: 1.18 was obtained as a mixture of rotamers. These data represent empirically observed chemical shifts from the <sup>1</sup>H and <sup>13</sup>C NMR spectra.*

### 1.5.2.2 Synthesis of Pyrone 1.13



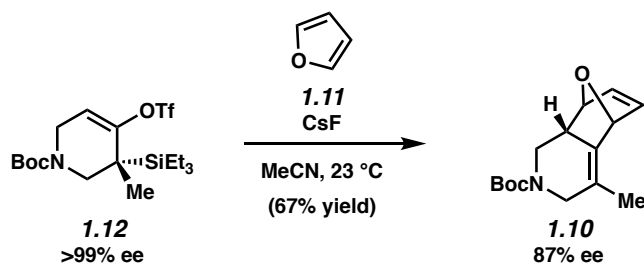
**3-Bromopropiolic acid (1.38).** To a solution of propiolic acid (**1.37**, 0.890 mL, 14.0 mmol, 1.00 equiv) in acetone (27 mL, 0.50 M) was added silver nitrate (0.24 g, 1.4 mmol, 10 mol%). The solution was allowed to stir for 5 min before NBS (3.1 g, 17 mmol, 1.2 equiv) was added in one portion. The reaction mixture was allowed to stir at 23 °C for 20 h. After this time, the reaction mixture was filtered through a pad of celite (3 x 5 cm) rinsing with acetone (50 mL) and the filtrate was concentrated under reduced pressure. The crude residue was purified via flash chromatography (7:3 hexanes:EtOAc) to afford 3-bromopropiolic acid (**1.38**, 1.11 g, 52% yield) as a white solid. 3-Bromopropiolic acid (**1.38**): *R<sub>f</sub>* 0.17 (98:2 EtOAc:AcOH); <sup>1</sup>H NMR (400 MHz, CDCl<sub>3</sub>): δ 10.46 (br s, 1H); <sup>13</sup>C NMR (100 MHz, CDCl<sub>3</sub>): δ 156.8, 72.1, 56.2; spectral data match those previously reported.<sup>28</sup>



**Pyrone 1.13.** To a solution of 3-bromopropiolic acid (**1.38**, 991 mg, 6.65 mmol, 1.00 equiv), benzyl propargyl alcohol<sup>39</sup> (**1.39**, 4.86 g, 33.3 mmol, 5.00 equiv), and (PPh<sub>3</sub>)AuCl (165 mg, 0.333 mmol, 5.00 mol%) in CH<sub>2</sub>Cl<sub>2</sub> (34 mL, 0.20 M) was added AgOTf (85.5 mg, 0.333 mmol, 5.00 mol%). Then, the flask was equipped with a reflux condenser and the reaction mixture was

heated to 50 °C and allowed to stir for 14.5 h. After 14.5 h, the reaction was allowed to cool to 23 °C, filtered over celite (1 cm) with CH<sub>2</sub>Cl<sub>2</sub> (~20 mL) to remove the black precipitate, and concentrated under reduced pressure to afford a crude oil. The crude oil was purified by flash chromatography (19:1 → 9:1 hexanes:EtOAc) to obtain pyrone **1.13** (1.21 g, 61% yield) as an orange oil. Pyrone **1.13**: *R<sub>f</sub>* 0.31 (9:1 hexanes:EtOAc); <sup>1</sup>H NMR (600 MHz, CDCl<sub>3</sub>): δ 7.39–7.31 (m, 5H), 6.50–6.49 (m, 2H), 4.62 (s, 2H), 4.28 (t, *J* = 7.9, 2H); <sup>13</sup>C NMR (150 MHz, CDCl<sub>3</sub>): δ 161.4, 159.7, 141.1, 136.7, 128.6, 128.3, 127.9, 116.0, 107.4, 73.5, 67.2; IR (film): 3090, 3031, 2863, 1732, 1622, 1549, 1107 cm<sup>-1</sup>; HRMS-APCI (*m/z*) [M + H]<sup>+</sup> calcd for C<sub>13</sub>H<sub>12</sub>BrO<sub>3</sub><sup>+</sup>, 294.9964; found 294.9964.

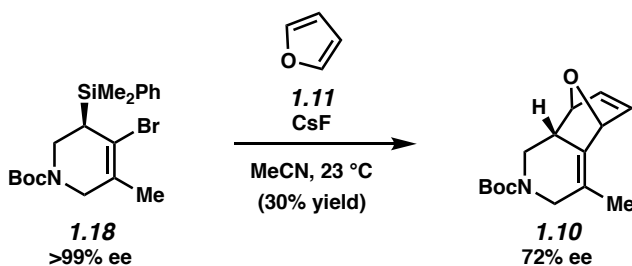
### 1.5.2.3 Diels–Alder Cycloadditions on Model Systems



**Methyl-Substituted Furan Cycloadduct 1.10.** From silyl triflate **1.12**: To a solution of silyl triflate **1.12** (20.9 mg, 45.5 μmol, 1.00 equiv) in acetonitrile (0.45 mL, 0.10 M) was added furan (**1.11**, 16.5 μL, 227 μmol, 5.00 equiv). Then, cesium fluoride (34.5 mg, 227 μmol, 5.00 equiv) was added to the solution, the vial was capped with a Teflon-lined screw cap, and the reaction was allowed to stir for 16.5 h at 23 °C. After 16.5 h, the reaction was filtered over a 2.5 cm plug of silica gel (monster pipette) with EtOAc (10 mL) and concentrated to a crude oil. The crude residue was purified via preparative TLC (4:1 hexanes:EtOAc) to obtain cycloadduct **1.10** (8.0 mg, 67% yield, 87% ee) as a colorless oil. Cycloadduct **1.10**: *R<sub>f</sub>* 0.26 (4:1 hexanes:EtOAc); <sup>1</sup>H

NMR (500 MHz, C<sub>6</sub>D<sub>6</sub>):  $\delta$  5.97–5.85 (m, 1H), 5.56–5.45 (m, 1H), 4.99 (s, 1H), 4.66–4.26 (m, 2H), 4.22–3.98 (m, 1H), 3.29–3.10 (m, 1H), 2.47–2.37 (m, 1H), 1.50 (s, 9H), 1.27–1.17 (m, 3H); <sup>13</sup>C NMR (125 MHz, C<sub>6</sub>D<sub>6</sub>):  $\delta$  154.9, 154.6, 135.4, 134.8, 133.2, 132.3, 129.7, 129.3, 128.6, 127.5, 121.2, 120.2, 80.2, 80.1, 79.2, 78.6, 47.7, 47.5, 46.0, 45.0, 40.2, 40.1, 28.6, 27.93, 27.88, 16.5; IR (film): 2976, 2927, 2858, 1691, 1395, 1159 cm<sup>-1</sup>; HRMS-APCI (m/z) [M + H]<sup>+</sup> calcd for C<sub>15</sub>H<sub>22</sub>NO<sub>3</sub><sup>+</sup>, 264.15942; found 264.16156.

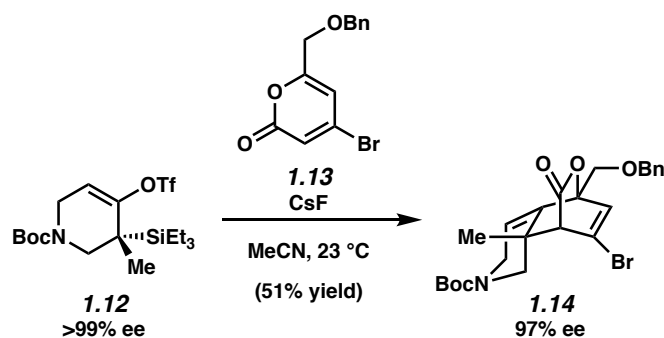
*Note: 1.10 was obtained as a mixture of rotamers. These data represent empirically observed chemical shifts from the <sup>1</sup>H and <sup>13</sup>C NMR spectra.*



**Methyl-Substituted Furan Cycloadduct 1.10.** From silyl bromide **1.18**: To a solution of silyl bromide **1.18** (3.2 mg, 7.8  $\mu$ mol, 1.0 equiv) in acetonitrile (0.20 mL, 0.10 M) was added furan (**1.11**, 23  $\mu$ L, 39  $\mu$ mol, 5.0 equiv). Then, cesium fluoride (5.9 mg, 39  $\mu$ mol, 5.0 equiv) was added to the solution, the vial was capped with a Teflon-lined screw cap, and the reaction was allowed to stir for 16 h at 23 °C. After 16 h, the reaction was filtered over a 2.5 cm plug of silica gel (monster pipette) with EtOAc (10 mL) and concentrated to afford a crude oil. The crude residue was purified via preparative TLC (4:1 hexanes:EtOAc) to obtain cycloadduct **1.10** (0.7 mg, 30% yield, 72% ee) as a colorless oil. Spectral data matched those provided above.

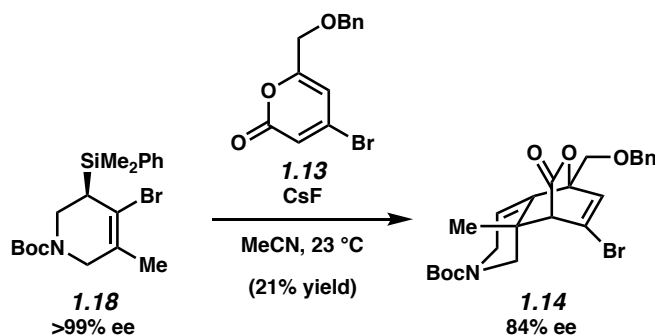




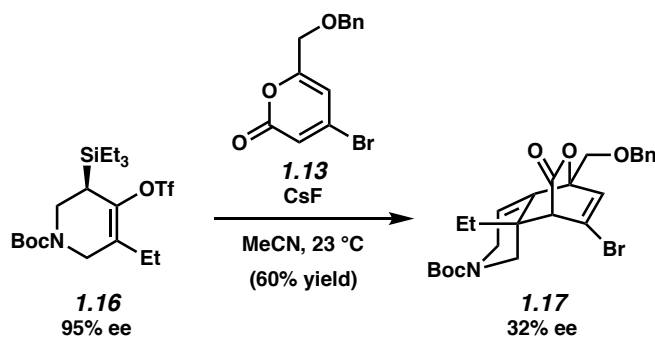


**Methyl-Substituted Pyrone Cycloadduct 1.14.** From silyl triflate **1.12**: To a solution of silyl triflate **1.12** (14.4 mg, 31.3  $\mu\text{mol}$ , 1.00 equiv) and pyrone **1.13** (46.0 mg, 156  $\mu\text{mol}$ , 5.00 equiv) in acetonitrile (0.31 mL, 0.10 M) was added cesium fluoride (23.8 mg, 157  $\mu\text{mol}$ , 5.00 equiv). The vial was capped with a Teflon-lined screw cap and the reaction was allowed to stir for 16.5 h at 23 °C. After 16.5 h, the reaction was filtered over a 3 cm plug of silica gel (monster pipette) with EtOAc (10 mL) and concentrated to afford a crude oil. The crude residue was purified via preparative TLC (4:1 hexanes:EtOAc) to obtain cycloadduct **1.14** (7.8 mg, 51% yield, 97% ee). Cycloadduct **1.14**:  $R_f$  0.27 (4:1 hexanes:EtOAc);  $^1\text{H}$  NMR (500 MHz,  $\text{CDCl}_3$ ):  $\delta$  7.40–7.33 (m, 5H), 6.54 (dd,  $J = 21.4, 2.4$ , 1H), 5.77–5.67 (m, 1H), 4.67 (s, 2H), 4.30–4.11 (m, 1H), 4.11–4.02 (m, 2H), 3.95–3.87 (m, 2H), 3.72–3.60 (m, 1H), 3.55–3.50 (m, 1H), 2.46 (dd,  $J = 33.5, 11.6$ , 1H), 1.78–1.74 (m, 1H), 1.50–1.41 (m, 13H), 1.16–1.11 (m, 3H);  $^{13}\text{C}$  NMR (125 MHz,  $\text{CDCl}_3$ ):  $\delta$  169.33, 169.30, 155.5, 155.2, 137.7, 137.3, 137.23, 137.21, 133.1, 132.7, 128.8, 128.6, 128.31, 128.29, 128.14, 128.11, 128.0, 119.3, 118.9, 117.9, 117.5, 85.2, 85.1, 80.7, 80.5, 74.2, 67.9, 67.8, 60.5, 60.4, 50.0, 48.9, 43.0, 42.5, 37.5, 37.4, 36.0, 35.6, 29.9, 28.6, 28.5, 28.4, 28.3, 22.8, 22.1, 22.0, 21.9, 14.3; IR (film): 2976, 2929, 1763, 1697, 1394, 1145  $\text{cm}^{-1}$ ; HRMS-APCI ( $m/z$ ) [ $\text{M} + \text{H}$ ] $^+$  calcd for  $\text{C}_{24}\text{H}_{29}\text{BrNO}_5^+$ , 490.12236; found 490.12632.

*Note: 1.14 was obtained as a mixture of rotamers. These data represent empirically observed chemical shifts from the  $^1\text{H}$  and  $^{13}\text{C}$  NMR spectra.*



**Methyl-Substituted Pyrone Cycloadduct 1.14.** From silyl bromide **1.18**: To a solution of silyl bromide **1.18** (4.4 mg, 11  $\mu\text{mol}$ , 1.0 equiv) and pyrone **1.13** (16 mg, 54  $\mu\text{mol}$ , 5.0 equiv) in acetonitrile (0.20 mL, 0.10 M) was added cesium fluoride (8.1 mg, 54  $\mu\text{mol}$ , 5.0 equiv). The vial was capped with a Teflon-lined screw cap and the reaction was allowed to stir for 15 h at 23 °C. After 15 h, the reaction was filtered over a 2.5 cm plug of silica gel (monster pipette) with EtOAc (10 mL) and concentrated to afford a crude oil. The crude residue was purified via preparative TLC (4:1 hexanes:EtOAc) to obtain cycloadduct **1.14** (1.1 mg, 21% yield, 84% ee). Spectral data matched those provided above.

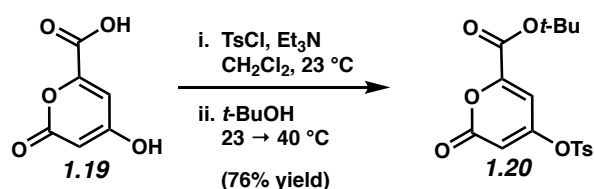


**Ethyl-Substituted Pyrone Cycloadduct 1.17.** To a solution of silyl triflate **1.16** (0.80 mg, 1.7  $\mu\text{mol}$ , 1.0 equiv) and pyrone **1.13** (2.5 mg, 8.4  $\mu\text{mol}$ , 5.0 equiv) in acetonitrile (0.20 mL, 0.020 M) was added cesium fluoride (2.6 mg, 17  $\mu\text{mol}$ , 10 equiv). The vial was capped with a Teflon-lined screw cap and the reaction was allowed to stir for 18 h at 23 °C. After 18h the reaction was

filtered over a 2.5 cm plug of silica gel (monster pipette) with EtOAc (10 mL) and concentrated to afford a crude oil. The crude residue was purified via preparative TLC (4:1 hexanes:EtOAc) to obtain cycloadduct **1.17** (0.5 mg, 60% yield, 32% ee). Cycloadduct **1.17**:  $R_f$  0.28 (4:1 hexanes:EtOAc);  $^1\text{H}$  NMR (500 MHz,  $\text{CDCl}_3$ ):  $\delta$  7.41–7.33 (m, 5H), 6.55 (dd,  $J = 22.6, 2.3$ , 1H), 5.73–5.64 (m, 1H), 4.67 (s, 2H), 4.39–4.08 (m, 2H), 4.07–4.01 (m, 1H), 3.96–3.90 (m, 1H), 3.72–3.54 (m, 2H), 2.38–2.26 (m, 1H), 1.50–1.45 (m, 11H), 1.25 (s, 4H), 0.97 (t,  $J = 7.6$ , 3H);  $^{13}\text{C}$  NMR (125 MHz,  $\text{CDCl}_3$ ):  $\delta$  169.21, 169.17, 155.2, 155.0, 138.8, 138.3, 137.3, 137.2, 133.6, 133.1, 128.8, 128.29, 128.27, 128.13, 128.10, 119.2, 118.8, 117.6, 117.3, 85.2, 85.1, 80.7, 80.4, 74.2, 67.9, 67.8, 57.0, 56.9, 45.1, 44.3, 43.0, 42.5, 41.04, 40.95, 33.2, 32.1, 29.9, 29.7, 29.6, 29.5, 29.4, 29.2, 28.6, 28.5, 28.2, 27.3, 27.1, 24.9, 22.8, 14.3, 8.0, 7.9; IR (film): 2974, 2926, 1763, 1697, 1401, 1139  $\text{cm}^{-1}$ ; HRMS-APCI ( $m/z$ )  $[\text{M} + \text{H}]^+$  calcd for  $\text{C}_{25}\text{H}_{31}\text{BrNO}_5^+$ , 504.13801; found 504.14232.

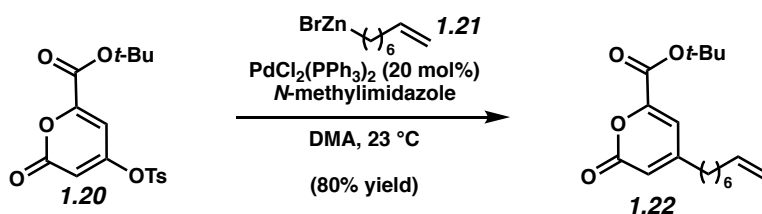
*Note: 1.17 was obtained as a mixture of rotamers. These data represent empirically observed chemical shifts from the  $^1\text{H}$  and  $^{13}\text{C}$  NMR spectra.*

#### 1.5.2.4 Synthesis of Pyrone 1.22 and Silyl Bromide 1.27



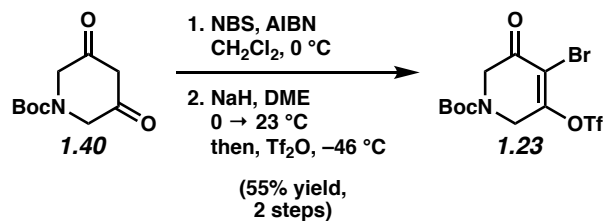
**Vinyl tosylate 1.20.** To a solution of pyrone **1.19** (544 mg, 3.48 mmol, 1.00 equiv) in  $\text{CH}_2\text{Cl}_2$  (23 mL, 0.15 M) was added triethylamine (1.90 mL, 13.6 mmol, 3.91 equiv) dropwise over 5 min. The reaction mixture was allowed to stir at 23  $^\circ\text{C}$  until homogenous (~5 min) and then p-toluenesulfonyl chloride (1.46 g, 2.20 equiv, 7.67 mmol) was added as a solution in  $\text{CH}_2\text{Cl}_2$  (18

mL) via cannula transfer over 5 min. The reaction mixture was allowed to stir at 23 °C for 21.5 h. After this time, anhydrous *tert*-butanol (2.56 g, 3.30 mL, 9.91 equiv, 34.5 mmol) was added in one portion and the reaction mixture was allowed to stir at 23 °C for 30 min. The flask was then fitted with a reflux condenser and heated to 40 °C for 4 h. After this time, the reaction mixture was quenched with saturated aq. NaHCO<sub>3</sub> (50 mL) and diluted with CH<sub>2</sub>Cl<sub>2</sub> (50 mL). The aqueous layer was separated from the organics and washed with CH<sub>2</sub>Cl<sub>2</sub> (2 x 50 mL). The combined organic fractions were dried over MgSO<sub>4</sub>, filtered, and concentrated under reduced pressure. The crude residue was purified via flash chromatography (4:1 hexanes:EtOAc → 7:3 hexanes:EtOAc) to afford vinyl tosylate **1.20** (971 mg, 76% yield) as a white solid. Vinyl tosylate **1.20**: R<sub>f</sub> 0.37 (4:1 Hexanes:EtOAc); <sup>1</sup>H NMR (400 MHz, CDCl<sub>3</sub>): δ 7.83 (d, *J* = 8.4, 2H), 7.41 (d, *J* = 8.2, 2H), 6.88 (d, *J* = 2.2, 1H), 6.18 (d, *J* = 2.2, 1H), 2.48 (s, 3H), 1.55 (s, 9H); <sup>13</sup>C NMR (100 MHz, CDCl<sub>3</sub>): δ 160.51, 160.46, 157.3, 151.5, 147.1, 131.3, 130.5, 128.5, 106.9, 106.7, 84.8, 27.9, 21.9; IR (film): 3107, 2982, 1743, 1334, 1175 cm<sup>-1</sup>; HRMS-APCI (*m/z*) [M + H]<sup>+</sup> calcd for C<sub>17</sub>H<sub>19</sub>O<sub>7</sub>S<sup>+</sup>, 367.08460; found 367.08067.



**Pyrone 1.22.** To a vial containing vinyl tosylate **1.20** (503 mg, 1.00 equiv, 1.37 mmol) was added bis(triphenylphosphine)palladium(II) chloride (192 mg, 20.0 mol%, 274 μmol), 1-methylimidazole (0.34 g, 0.33 mL, 3.0 equiv, 4.1 mmol), and a solution of alkylzinc bromide<sup>40</sup> **1.21** in DMA (1.1 g, 5.8 mL, 0.71 M, 3.0 equiv, 4.1 mmol). The reaction mixture was stirred at 23 °C for 21.5 h. After this time, the reaction was quenched with saturated aq. NH<sub>4</sub>Cl (30 mL)

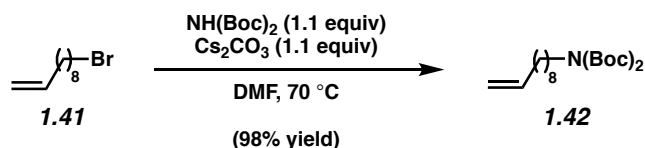
and diluted with Et<sub>2</sub>O (30 mL). The layers were separated and the aqueous layer was extracted with Et<sub>2</sub>O (2 x 30 mL). The combined organic fractions were washed with water (3 x 30 mL) and brine (10 mL), dried over MgSO<sub>4</sub>, filtered, and concentrated under reduced pressure. The crude residue was purified via flash chromatography (9:1 pentane:EtOAc) to afford pyrone **1.22** (336 mg, 80% yield) as a pale yellow oil. Pyrone **1.22**: R<sub>f</sub> 0.55 (4:1 Hexanes:EtOAc); <sup>1</sup>H NMR (400 MHz, CDCl<sub>3</sub>): δ 6.89 (d, *J* = 1.6, 1H), 6.26 (d, *J* = 1.5, 1H) 5.80 (ddt, *J* = 17.1, 10.2, 6.7, 1H), 5.03–4.90 (m, 2H), 2.45 (t, *J* = 7.7, 2H), 2.04 (q, *J* = 7.1, 2H), 1.57 (s, 9H), 1.51–1.40 (m, 2H), 1.39–1.30 (6H); <sup>13</sup>C NMR (125 MHz, CDCl<sub>3</sub>): δ 161.0, 158.67, 158.65, 149.7, 116.6, 114.5, 111.5, 84.0, 35.2, 33.7, 28.9, 28.8, 28.7, 28.1, 28.0; IR (film): 3082, 2981, 2929, 1732, 1117 cm<sup>-1</sup>; HRMS-APCI (m/z) [M + H]<sup>+</sup> calcd for C<sub>18</sub>H<sub>27</sub>O<sub>4</sub><sup>+</sup>, 307.19039; found 307.18763.



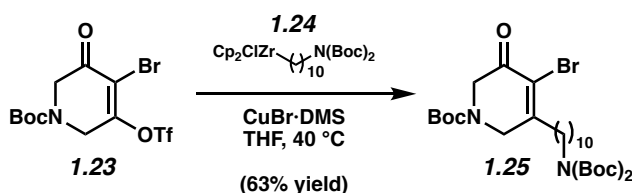
**Bromotriflate 1.23.** This compound was obtained from commercial sources, but could also be prepared in two steps as follows. A solution of diketone **1.40** (2.00 g, 9.38 mmol, 1.00 equiv) in CH<sub>2</sub>Cl<sub>2</sub> (40 mL, 0.23 M) was cooled to 0 °C. To the solution was added NBS (1.67 g, 9.38 mmol, 1.00 equiv) in one portion and AIBN (108 mg, 657 μmol, 7.00 mol%) in one portion. The reaction mixture was allowed to stir at 0 °C for 3.5 h. Then, the reaction mixture was diluted with CH<sub>2</sub>Cl<sub>2</sub> (30 mL) and water (100 mL) and allowed to warm to 23 °C. The solution was transferred to a separatory funnel and the layers were separated. The aqueous layer was extracted with CH<sub>2</sub>Cl<sub>2</sub> (2 x 30 mL). The combined organic layers were washed with water (3 x 50 ml) and then dried over MgSO<sub>4</sub>, filtered, and concentrated under reduced pressure. The crude residue

purified via flash chromatography (1:1 hexanes:EtOAc) to afford the bromide. A solution of sodium hydride (0.58 g, 60% Wt, 14 mmol, 1.2 equiv) in DME (70 mL) was cooled to 0 °C. To this solution was added the bromide (3.40 g, 11.6 mmol, 1.00 equiv) as a solid in portions over 15 min. The solution was allowed to stir at 0 °C for 15 min and then allowed to warm to 23 °C and stir for 1 h. After this time, the reaction mixture was cooled to -46 °C and trifluoromethanesulfonic anhydride (1.87 mL, 11.1 mmol, 0.950 equiv) was added dropwise over 15 min. The reaction mixture was allowed to stir at -46 °C for 1 h. After this time, the reaction mixture was quenched with Et<sub>2</sub>O (5 mL) and water (5 mL) and allowed to warm to 23 °C. The reaction mixture was transferred to a separatory funnel with Et<sub>2</sub>O (100 mL) and water (100 mL). The layers were separated and the aqueous layer was extracted with Et<sub>2</sub>O (2 x 50 mL). The combined organic fractions were dried over MgSO<sub>4</sub>, filtered, and concentrated under reduced pressure. The crude residue was purified via flash chromatography (4:1 hexanes:EtOAc) to afford bromotriflate **1.23** (3.38 g, 55% yield over two steps) as a pale yellow solid. Bromotriflate **1.23**: R<sub>f</sub> 0.55 (4:1 hexanes:EtOAc); <sup>1</sup>H NMR (500 MHz, CDCl<sub>3</sub>): δ 4.56 (s, 2H), 4.33 (s, 2H), 1.49 (s, 9H); <sup>13</sup>C NMR (125 MHz, CDCl<sub>3</sub>): δ 185.9, 153.4, 118.4 (q, *J* = 322.2), 116.8, 83.2, 52.0, 45.9, 28.5; IR (film): 2981, 1704, 1432, 1214, 1131 cm<sup>-1</sup>; HRMS-APCI (m/z) [M + H]<sup>+</sup> calcd for C<sub>11</sub>H<sub>13</sub>BrF<sub>3</sub>NO<sub>6</sub>SK<sup>+</sup>, 461.92306; found 461.92398.

*Note: 1.23 was obtained as a mixture of rotamers. These data represent empirically observed chemical shifts from the <sup>1</sup>H and <sup>13</sup>C NMR spectra.*



**Alkene 1.42** To a solution of 10-bromodec-1-ene (**1.41**, 1.99 g, 9.11 mmol, 1.00 equiv) in DMF (45 mL, 0.20 M) was added di-*tert*-butyl iminodicarbonate (2.18 g, 10.0 mmol, 1.10 equiv) and cesium carbonate (3.26 g, 10.0 mmol, 1.10 equiv). The flask was equipped with a reflux condenser and the reaction mixture was heated to 70 °C for 2.5 h. After this time, the mixture was allowed to cool to room temperature and then was transferred to a separatory funnel with water (50 mL) and Et<sub>2</sub>O (50 mL). The layers were separated and the aqueous layer was extracted with Et<sub>2</sub>O (3 x 30 mL). The combined organic layers were dried over MgSO<sub>4</sub>, filtered, and concentrated under reduced pressure. The crude residue was purified via flash chromatography (19:1 hexanes:EtOAc) to afford alkene **1.42** (3.18 g, 98% yield) as a colorless oil. Alkene **1.42**: *R<sub>f</sub>* 0.60 (9:1 hexanes:EtOAc); <sup>1</sup>H NMR (600 MHz, CDCl<sub>3</sub>): δ 5.80 (ddt, *J* = 17.2, 10.2, 6.7, 1H), 4.98 (ddt, *J* = 17.2, 1.9, 1.7, 1H), 4.95–4.89 (m, 1H), 3.59–3.50 (m, 2H), 2.08–2.00 (m, 2H), 1.58–1.52 (m, 2H), 1.50 (s, 18H), 1.40–1.33 (m, 2H), 1.31–1.24 (m, 8H); <sup>13</sup>C NMR (125 MHz, CDCl<sub>3</sub>): δ 152.9, 139.3, 114.3, 82.1, 46.6, 33.9, 29.6, 29.4, 29.2, 29.0, 28.2, 26.9; <sup>19</sup>F NMR (376 MHz, CDCl<sub>3</sub>): δ –73.3; IR (film): 2979, 2927, 2856, 1697, 1367, 1126 cm<sup>-1</sup>; HRMS-APCI (*m/z*) [M + H]<sup>+</sup> calcd for C<sub>20</sub>H<sub>38</sub>NO<sub>4</sub><sup>+</sup>, 356.27954; found 356.28069.

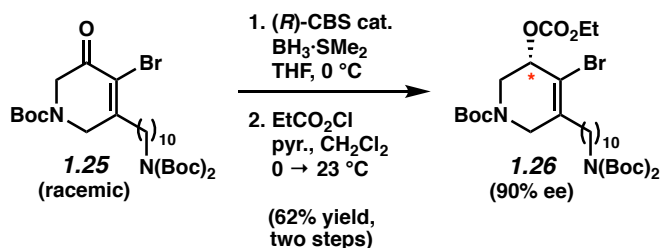


**Bromoenone 1.25.** A flask was brought into the glovebox where zirconocene hydrochloride (Schwartz's reagent) (678 mg, 2.63 mmol, 3.00 equiv) was added. The flask was removed from



the glovebox and a solution of alkene **1.42** (941 mg, 2.65 mmol, 3.00 equiv) in THF (3.8 mL) was added via rapid cannula transfer. The flask was equipped with a reflux condenser and the suspension was heated to 40 °C for 30 min during which time the solution became homogenous. After this time, the reaction mixture was allowed to cool to 23 °C. To a separate solution of vinyl tosylate **1.23** (374 mg, 883 μmol, 1.00 equiv) in THF (1.9 mL) was added the solution of freshly prepared alkylzirconium **1.24** rapidly via cannula transfer. After 3 min, a solution of CuBr·DMS (541 mg, 2.63 mmol, 3.00 equiv) in THF (4 mL) was added rapidly via syringe. The resulting reaction mixture was allowed to stir at 40 °C for 3 min, after which the reaction was immediately removed from heat and diluted with Et<sub>2</sub>O (3 mL) and water (5 mL). The mixture was transferred to a separatory funnel, washing the reaction vial with additional Et<sub>2</sub>O (15 mL) and water (15 mL). The layers were separated and the aqueous layer was extracted with Et<sub>2</sub>O (2 x 20 mL). The combined organic fractions were dried over MgSO<sub>4</sub>, filtered, and concentrated under reduced pressure. The crude residue was purified via flash chromatography (9:1 hexanes:EtOAc to 85:15 hexanes:EtOAc) to afford bromoenone **1.25** (349 mg, 63% yield) as a pale yellow oil. Bromoenone **1.25**: R<sub>f</sub> 0.37 (4:1 hexanes:EtOAc); <sup>1</sup>H NMR (600 MHz, CDCl<sub>3</sub>): δ 4.35–4.20 (m, 4H), 3.59–3.50 (m, 2H), 2.52–2.41 (m, 2H), 1.63–1.52 (m, 5H), 1.52–1.44 (m, 27H), 1.42–1.35 (m, 2H), 1.35–1.22 (m, 11H); <sup>13</sup>C NMR (125 MHz, CDCl<sub>3</sub>): δ 186.0, 161.7, 153.7, 152.8, 129.0, 128.2, 125.3, 120.3, 82.0, 81.5, 51.8, 47.6, 46.5, 36.4, 29.6, 29.5, 29.4, 29.29, 29.25, 29.0, 28.3, 28.1, 26.9, 26.8; IR (film): 2978, 2929, 1694, 1367, 1127 cm<sup>-1</sup>; HRMS-APCI (m/z) [M + H]<sup>+</sup> calcd for C<sub>30</sub>H<sub>51</sub>BrN<sub>2</sub>O<sub>7</sub>Na<sup>+</sup>, 653.2777; found 653.2845.

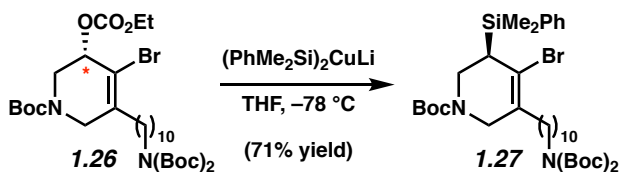
*Note: 1.25 was obtained as a mixture of rotamers. These data represent empirically observed chemical shifts from the <sup>1</sup>H and <sup>13</sup>C NMR spectra.*



**Carbonate 1.26.** To a vial in the glovebox was added (*R*)-CBS catalyst (19.3 mg, 69.7  $\mu$ mol, 20.0 mol%). The vial was brought out of the glovebox and the CBS catalyst was dissolved in THF (1 mL). To a solution of bromoenone **1.25** (220 mg, 358  $\mu$ mol, 1.00 equiv) in THF (1 mL) was added the CBS catalyst solution. The reaction mixture was cooled to 0 °C and to this mixture was added borane-methyl sulfide complex (261  $\mu$ L, 2.00 M, 522  $\mu$ mol, 1.50 equiv) dropwise over 5 min at 0 °C. The mixture was allowed to stir at 0 °C for 1 h. After this time, the reaction was quenched with methanol (1 mL) and warmed to 23 °C. The mixture was then transferred to a separatory funnel with Et<sub>2</sub>O (20 mL) and water (20 mL). The layers were separated and the aqueous layer was extracted with Et<sub>2</sub>O (2 x 20 mL). The combined organic layers were then dried over MgSO<sub>4</sub>, filtered, and concentrated under reduced pressure. The crude residue was purified via flash chromatography (4:1 hexanes:EtOAc) to afford the enantioenriched alcohol (90% ee) as a pale yellow oil. A solution of the alcohol (181 mg, 271  $\mu$ mol, 1.00 equiv) in CH<sub>2</sub>Cl<sub>2</sub> (2.5 mL, 0.11 M) was cooled to 0 °C. To the solution was added pyridine (32.9  $\mu$ L, 407  $\mu$ mol, 1.50 equiv) dropwise over 1 min and ethyl carbonochloridate (31.0  $\mu$ L, 326  $\mu$ mol, 1.20 equiv) dropwise over 1 minute. The reaction was stirred for at 0 °C for 5 min and then allowed to warm to 23 °C and stirred for 1.5 h. After this time, the reaction mixture was diluted with Et<sub>2</sub>O (20 mL) quenched with saturated aq. NaHCO<sub>3</sub> (20 mL). The layers were separated and the aqueous layer was extracted with Et<sub>2</sub>O (2 x 20 mL). The combined organic layers were dried over magnesium sulfate, filtered, and concentrated under reduced pressure. The crude residue was purified via flash chromatography (85:15 hexanes:EtOAc) to afford

carbonate **1.26** (157 mg, 62% yield over two steps, 90% ee) as a colorless oil. Carbonate **1.26**:  $R_f$  0.47 (4:1 hexanes:EtOAc);  $^1\text{H}$  NMR (600 MHz,  $\text{CDCl}_3$ ):  $\delta$  5.28–5.07 (m, 1H), 4.44 (app. d,  $J = 17.6$ , 1H), 4.30 (dd,  $J = 14.5$ , 2.1, 1H), 4.24 (q,  $J = 7.1$ , 2H), 3.69–3.50 (m, 3H), 3.25 (dd,  $J = 14.5$ , 2.8, 1H), 2.26–2.11 (m, 2H), 1.58–1.52 (m, 2H), 1.50 (s, 18H), 1.48–1.41 (m, 9H), 1.36–1.24 (m, 17H);  $^{13}\text{C}$  NMR (125 MHz,  $\text{CDCl}_3$ ):  $\delta$  154.7, 154.4, 152.9, 143.2, 128.5, 112.8, 82.1, 80.5, 75.8, 68.1, 66.0, 64.5, 47.9, 47.1, 46.7, 46.3, 45.3, 34.5, 30.5, 29.7, 29.6, 29.4, 29.2, 28.4, 28.2, 27.2, 27.0, 25.8, 15.4, 14.4; IR (film): 2978, 2929, 1744, 1698, 1256  $\text{cm}^{-1}$ ; HRMS-APCI (m/z)  $[\text{M} + \text{H}]^+$  calcd for  $\text{C}_{33}\text{H}_{58}\text{BrN}_2\text{O}_9^+$ , 705.33202; found 705.33299.

*Note: 1.26 was obtained as a mixture of rotamers. These data represent empirically observed chemical shifts from the  $^1\text{H}$  and  $^{13}\text{C}$  NMR spectra.*

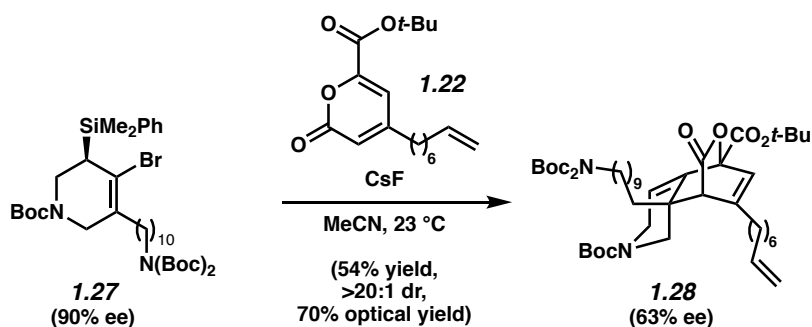


**Silyl Bromide 1.27.** A solution of bromocopper methylsulfanylmethane (7.5 mg, 36  $\mu\text{mol}$ , 1.4 equiv) in THF (0.5 mL) was cooled to  $0\text{ }^\circ\text{C}$ . Then, (dimethyl(phenyl)silyl)lithium<sup>19</sup> (0.27 mL, 0.26 M, 70  $\mu\text{mol}$ , 2.6 equiv) was added dropwise over 3 min and then the mixture was stirred at  $0\text{ }^\circ\text{C}$  for 30 min. The reaction mixture was cooled to  $-78\text{ }^\circ\text{C}$  and a solution of carbonate **1.26** (20.0 mg, 26.9  $\mu\text{mol}$ , 1.00 equiv) in THF (0.3 mL) was added dropwise over 2 minutes. The reaction was allowed to stir at  $-78\text{ }^\circ\text{C}$  for 1 h. After this time, the reaction was diluted with  $\text{Et}_2\text{O}$  (1 mL), quenched with water (1 mL), and allowed to warm to  $23\text{ }^\circ\text{C}$ . The reaction mixture was then transferred to a separatory funnel containing  $\text{Et}_2\text{O}$  (5 mL) and water (5 mL). The layers were separated and the aqueous layer was extracted with  $\text{Et}_2\text{O}$  (2 x 5 mL). The combined organic layers were dried over  $\text{MgSO}_4$ , filtered, and concentrated under reduced pressure. The crude

residue was purified via preparative TLC (4:1 hexanes:EtOAc) to afford silyl bromide **1.27** (14.4 mg, 71% yield) as a colorless oil. Silyl bromide **1.27**:  $R_f$  0.69 (4:1 hexanes:EtOAc);  $^1\text{H}$  NMR (500 MHz,  $\text{CDCl}_3$ ):  $\delta$  7.53–7.47 (m, 2H), 7.36–7.29 (m, 3H), 4.20–3.93 (m, 1H), 3.76–3.60 (m, 1H), 3.58–3.43 (m, 3H), 3.15 (bs, 1H), 2.27–2.04 (m, 2H), 1.97 (bs, 1H), 1.58–1.53 (m, 2H), 1.50 (s, 16H), 1.44 (bs, 9H), 1.34–1.18 (m, 14H), 0.49–0.36 (m, 6H);  $^{13}\text{C}$  NMR (125 MHz,  $\text{CDCl}_3$ ):  $\delta$  154.3, 152.7, 137.3, 134.2, 133.9, 133.6, 130.6, 130.1, 129.3, 129.1, 128.3, 127.9, 127.8, 127.6, 118.5, 117.6, 82.0, 80.0, 47.7, 47.5, 46.5, 44.1, 43.2, 37.9, 34.7, 29.6, 29.5, 29.4, 29.3, 29.1, 28.4, 28.1, 27.6, 26.9, –2.4, –2.5, –3.1, –3.2, –3.3; IR (film): 2979, 2929, 1748, 1698, 1366, 1131  $\text{cm}^{-1}$ ; HRMS-APCI ( $m/z$ )  $[\text{M} + \text{H}]^+$  calcd for  $\text{C}_{38}\text{H}_{64}\text{BrN}_2\text{O}_6\text{Si}^+$ , 751.3717; found 751.3689.

*Note: 1.27 was obtained as a mixture of rotamers. These data represent empirically observed chemical shifts from the  $^1\text{H}$  and  $^{13}\text{C}$  NMR spectra.*

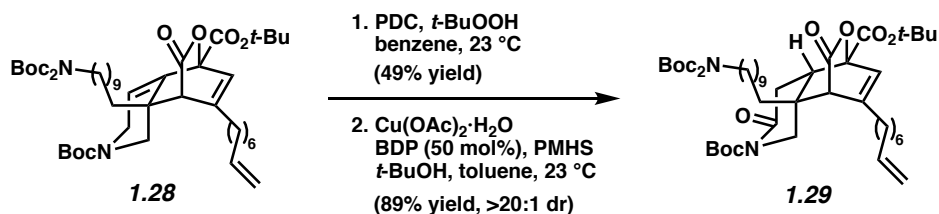
### 1.5.2.5 Key Diels–Alder Cycloaddition and Elaboration to Lissodendoric Acid A (1.6)



**Cycloadduct 1.28.** A vial containing silyl bromide **1.27** (5.0 mg, 6.6  $\mu\text{mol}$ , 1.0 equiv, 90% ee) and pyrone **1.22** (10 mg, 33  $\mu\text{mol}$ , 5.0 equiv) was brought into the glovebox. To this vial was added CsF (7.1 mg, 47  $\mu\text{mol}$ , 7.0 equiv) and MeCN (0.2 mL, 0.03 M). The vial was sealed with a Teflon-coated cap and the vial was removed from the glovebox. The reaction mixture was

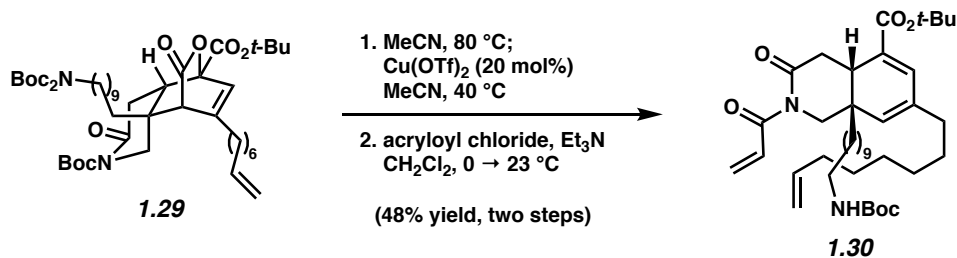
allowed to stir vigorously at 23 °C for 15.5 h. After this time, the reaction mixture was diluted with EtOAc (1 mL) and filtered through a 1 cm plug of silica gel eluting with 1:1:1 hexanes:CH<sub>2</sub>Cl<sub>2</sub>:Et<sub>2</sub>O (8 mL) and the concentrated under reduced pressure. The crude residue was purified via preparative TLC (8:1:1 hexanes:CH<sub>2</sub>Cl<sub>2</sub>:Et<sub>2</sub>O → 3:1:1 hexanes:CH<sub>2</sub>Cl<sub>2</sub>:Et<sub>2</sub>O) to afford the cycloadduct **1.28** (3.0 mg, 54% yield, 63% ee, 70% optical yield) as yellow foam. Cycloadduct **1.28**: R<sub>f</sub> 0.31 (5:1:1 Hexanes:CH<sub>2</sub>Cl<sub>2</sub>:Et<sub>2</sub>O); <sup>1</sup>H NMR (500 MHz, CDCl<sub>3</sub>): δ 6.35–6.25 (m, 1H), 5.79 (ddt, *J* = 17.2, 10.2, 6.7, 1H), 5.58–5.46 (m, 1H), 4.98 (dq, *J* = 17.1, 1.8, 1H), 4.93 (d, *J* = 10.2, 1H), 4.32–4.08 (m, 2H), 3.67–3.49 (m, 3H), 3.38 (d, *J* = 13.2, 1H), 2.26–2.08 (m, 3H), 2.06–1.99 (m, 2H), 1.61–1.58 (m, 2H), 1.58–1.55 (m, 8H), 1.54–1.51 (m, 2H), 1.50 (s, 9H), 1.48–1.45 (m, 9H), 1.41–1.10 (m, 22H); <sup>13</sup>C NMR (125 MHz, CDCl<sub>3</sub>): δ 165.0, 155.2, 154.9, 152.9, 142.2, 139.11, 139.08, 126.2, 115.5, 115.2, 114.49, 114.47, 84.1, 84.0, 83.9, 83.8, 82.09, 82.08, 80.4, 80.3, 52.28, 52.26, 46.7, 46.4, 42.9, 42.5, 38.8, 38.7, 34.7, 34.6, 34.3, 34.2, 33.8, 30.1, 30.0, 29.84, 29.78, 29.73, 29.69, 29.5, 29.4, 29.2, 29.10, 29.08, 28.91, 28.88, 28.8, 28.6, 28.5, 28.23, 28.16, 27.14, 27.10, 27.00, 26.99, 23.8, 23.6; IR (film): 2979, 2924, 1736, 1698, 1367, 1033 cm<sup>-1</sup>; HRMS-APCI (*m/z*) [M + H]<sup>+</sup> calcd for C<sub>48</sub>H<sub>79</sub>N<sub>2</sub>O<sub>10</sub><sup>+</sup>, 843.57292; found 843.56626.

*Note: 1.28 was obtained as a mixture of rotamers. These data represent empirically observed chemical shifts from the <sup>1</sup>H and <sup>13</sup>C NMR spectra.*



**Amide 1.29.** To a solution of cycloadduct **1.28** (30.0 mg, 33.8  $\mu\text{mol}$ , 1.00 equiv) in benzene (3.3 mL, 0.01 M) was added PDC (38.1 mg, 101  $\mu\text{mol}$ , 3.00 equiv). The suspension was stirred rapidly (1000 rpm) and then tert-butyl hydroperoxide in water (13.1 mg, 14  $\mu\text{L}$ , 70 wt%, 101  $\mu\text{mol}$ , 3.00 equiv). The reaction mixture was stirred at 23 °C for 17 h. After this time, celite (50 mg) was added to the reaction and was stirred for 30 min at which point it was filtered through a celite plug (1 cm), rinsed with EtOAc (20 mL), and diluted with saturated aq. sodium thiosulfate (20 mL) to quench any remaining peroxides. The layers were separated and the aqueous layer was extracted with EtOAc (2 x 20 mL). The combined organic fractions were dried over MgSO<sub>4</sub>, filtered, and the solvent was removed under reduced pressure. The crude residue was purified via flash chromatography (9:1 hexanes:EtOAc  $\rightarrow$  4:1 hexanes:EtOAc) to afford the enamide. To a flask was added copper(II)acetate monohydrate (80.2 mg, 402  $\mu\text{mol}$ , 0.990 equiv) and 1,2-bis(diphenylphosphaneyl)benzene (BDP) (88.5 mg, 198  $\mu\text{mol}$ , 50.0 mol%). These were dissolved in sparged *t*BuOH (602 mg, 0.77 mL, 8.12 mmol, 20.0 equiv) and toluene (5 mL) and the reaction was stirred for 20 minutes to give a blue solution. At this point PMHS (2.30 mL, 1.22 mmol, 3.00 equiv) was added dropwise over 3 min and the solution gradually turned from blue to a yellow/green color (30 min). A separate vial was charged with the enamide (355 mg, 406  $\mu\text{mol}$ , 1.00 equiv) and toluene (5 mL). The enamide solution was then added to the Strykers reagent dropwise over 3 min. The reaction was stirred at 23 °C for 21.5 h. After this time, the reaction mixture was filtered through a plug of silica gel (1.5 x 5 cm silica) eluting with 1:1 hexanes:EtOAc (100 mL). The crude residue was purified via flash chromatography (9:1

hexanes:EtOAc → 6:1 hexanes:EtOAc → 4:1 hexanes:EtOAc) to afford amide **1.29** (388 mg, 44% yield over 2 steps) as a colorless oil. Amide **1.29**:  $R_f$  0.38 (4:1 Hexanes:EtOAc);  $^1\text{H}$  NMR (500 MHz,  $\text{CDCl}_3$ ):  $\delta$  6.38–6.34 (m, 1H), 5.79 (ddt,  $J = 17.1, 10.3, 6.7$ , 1H), 4.99 (ddt,  $J = 17.1, 3.9, 1.6$ , 1H), 4.96–4.91 (m, 1H), 4.16 (d,  $J = 13.7$ , 1H), 3.56–3.50 (m, 2H), 3.29–3.25 (m, 2H), 2.90 (d,  $J = 13.8$ , 1H), 2.44 (dd,  $J = 14.5, 5.7$ , 1H), 2.31 (dd,  $J = 11.7, 5.6$ , 1H), 2.23–2.17 (m, 1H), 2.13–2.07 (m, 1H), 2.07–2.01 (m, 2H), 1.68–1.61 (m, 2H), 1.53 (s, 9H), 1.52 (s, 9H), 1.50 (s, 18H), 1.41–1.18 (m, 24H);  $^{13}\text{C}$  NMR (125 MHz,  $\text{CDCl}_3$ ):  $\delta$  170.8, 168.9, 165.8, 152.9, 151.5, 146.0, 139.0, 122.8, 114.5, 84.36, 84.35, 84.0, 82.1, 51.6, 47.0, 46.7, 46.2, 41.8, 38.7, 37.7, 34.9, 33.8, 30.0, 29.74, 29.69, 29.52, 29.49, 29.4, 29.2, 29.1, 28.9, 28.8, 28.2, 28.08, 28.06, 27.0, 26.9, 23.4; IR (film): 2978, 2930, 1770, 1731, 1368, 1152  $\text{cm}^{-1}$ ; HRMS-APCI ( $m/z$ )  $[\text{M} + \text{H}]^+$  calcd for  $\text{C}_{48}\text{H}_{79}\text{N}_2\text{O}_{11}^+$ , 859.56784; found 859.56714.

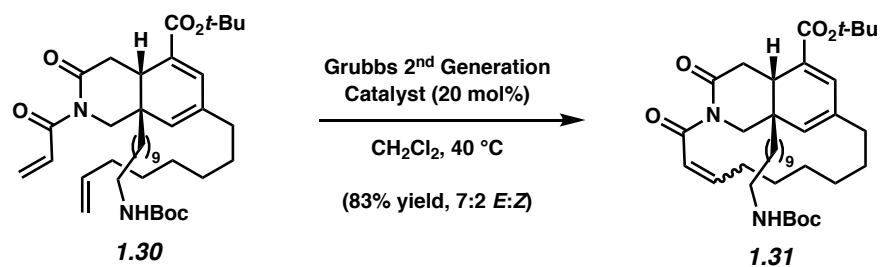


**Imide 1.30.** A vial containing a solution of amide **1.29** (10.0 mg, 11.6  $\mu\text{mol}$ , 1.00 equiv) in acetonitrile (0.39 mL, 0.30 M) was sealed with a Teflon-lined cap and heated to 80 °C for 14.25 h. The solution was then cooled to 23 °C and to the solution was added copper(II) triflate (0.8 mg, 2.3  $\mu\text{mol}$ , 20 mol%) in one portion and the vial was resealed with a Teflon-lined cap. The vial was heated to 40 °C for 1.5 h. The reaction mixture was then allowed to cool to 23 °C and filtered through a short plug of silica gel (0.9 x 2.5 cm silica) eluting with EtOAc (10 mL) and then concentrated under reduced pressure. The crude residue was purified via preparative TLC

(1:1 hexanes:EtOAc) to afford the diene. A solution of the diene (55.0 mg, 1.00 equiv, 89.4  $\mu\text{mol}$ ) in  $\text{CH}_2\text{Cl}_2$  (0.90 mL, 0.10 M) was cooled to 0  $^\circ\text{C}$ . To this solution was added triethylamine (37.4  $\mu\text{L}$ , 268  $\mu\text{mol}$ , 3.00 equiv) followed by acryloyl chloride (21.9  $\mu\text{L}$ , 268  $\mu\text{mol}$ , 3.00 equiv) dropwise over 1 min. The reaction was allowed to warm to 23  $^\circ\text{C}$  and stir for 15 h. The reaction mixture was quenched with water (1 mL) and saturated aq.  $\text{NaHCO}_3$  (1 mL) and diluted with  $\text{Et}_2\text{O}$  (2 mL). The layers were separated and the aqueous layer was washed with  $\text{Et}_2\text{O}$  (3 x 1 mL). The combined organic layers were dried over  $\text{MgSO}_4$ , filtered, and concentrated under reduced pressure. The crude residue was purified by flash chromatography (5:1 hexanes:EtOAc) to afford imide **1.30** (42.5 mg, 48% yield over two steps) as a colorless oil.

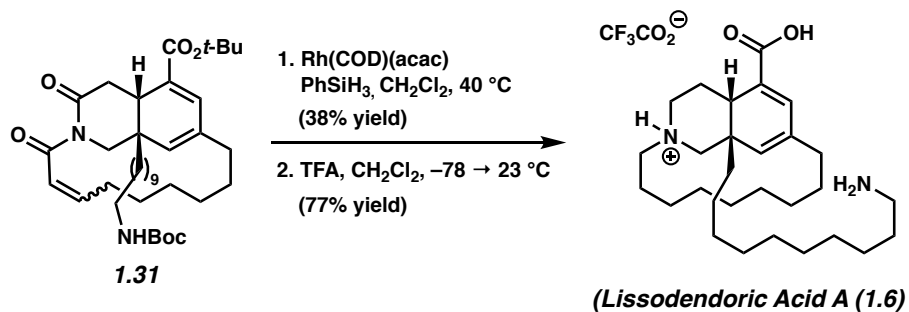
Imide **1.30**:  $R_f$  0.64 (2:1 Hexanes:EtOAc);  $^1\text{H}$  NMR (600 MHz,  $\text{CDCl}_3$ ):  $\delta$  7.1 (dd,  $J = 16.9$ , 10.3, 1H), 6.76 (s, 1H), 6.38 (dd,  $J = 16.9$ , 1.7, 1H), 5.83–5.74 (m, 2H), 5.23 (s, 1H), 4.98 (dq,  $J = 17.1$ , 1.7, 1H), 4.96–4.90 (m, 1H), 4.50 (br s, 1H), 4.03 (d,  $J = 13.6$ , 1H), 3.61 (d,  $J = 13.6$ , 1H), 3.15–3.04 (m, 2H), 2.93 (t,  $J = 7.7$ , 1H), 2.74 (dd,  $J = 16.1$ , 7.9, 1H), 2.33 (dd,  $J = 16.1$ , 7.0, 1H), 2.10–2.05 (m, 2H), 2.05–2.00 (m, 2H), 1.51 (s, 9H), 1.43 (s, 9H), 1.39–1.32 (m, 4H), 1.32–1.15 (m, 22H);  $^{13}\text{C}$  NMR (125 MHz,  $\text{CDCl}_3$ ):  $\delta$  174.1, 168.2, 165.9, 156.1, 139.2, 136.11, 134.17, 131.4, 130.8, 130.7, 129.5, 114.4, 81.2, 79.2, 50.0, 40.8, 40.7, 39.8, 38.5, 35.6, 35.1, 33.9, 30.3, 30.2, 29.6, 29.5, 29.42, 29.37, 29.00, 28.95, 28.8, 28.6, 28.4, 28.3, 26.9, 23.7; IR (film): 2925, 2854, 1713, 1463, 1366, 1163  $\text{cm}^{-1}$ ; HRMS-APCI ( $m/z$ )  $[\text{M} + \text{H}]^+$  calcd for  $\text{C}_{40}\text{H}_{65}\text{N}_2\text{O}_6^+$ , 669.48371; found 669.48489.





**Macrocycle 1.31.** To a flask in the glovebox was added the Grubbs' 2<sup>nd</sup> generation catalyst (2.4 mg, 2.9  $\mu\text{mol}$ , 20 mol%). The flask was then removed from the glovebox and imide **1.30** (9.6 mg, 14  $\mu\text{mol}$ , 1.0 equiv) dissolved in  $\text{CH}_2\text{Cl}_2$  (14.0 mL, 0.00100 M) was added to the flask containing Grubbs' catalyst. The flask was equipped with a reflux condenser and heated to 40 °C for 16 h. After 16 h, the reaction was cooled to 23 °C and the solvent evaporated under reduced pressure. The crude residue was purified via preparative TLC (3:1 hexanes:EtOAc) to afford macrocycle **1.31** (7.6 mg, 83%) as an colorless oil. Macrocycle **1.31**:  $R_f$  0.28 (4:1 Hexanes:EtOAc);  $^1\text{H}$  NMR (500 MHz,  $\text{CDCl}_3$ ):  $\delta$  7.21 (d,  $J = 15.3$ , 2H), 6.95 (ddd,  $J = 15.4$ , 10.8, 4.3, 2H), 6.70 (s, 2H), 6.66 (s, 1H), 6.60 (dd,  $J = 11.6$ , 2.2, 1H), 5.90 (td,  $J = 12.0$ , 4.1, 1H), 5.13 (s, 1H), 4.99 (s, 2H), 4.70 (d,  $J = 13.5$ , 1H), 4.49 (br s, 2H), 4.42 (d,  $J = 13.5$ , 2H), 3.21–3.14 (m, 3H), 3.13–3.04 (m, 8H), 3.01–2.92 (m, 1H), 2.86–2.76 (m, 3H), 2.46–2.35 (m, 4H), 2.27 (d,  $J = 15.0$ , 1H), 2.23–2.09 (m, 6H), 1.94–1.80 (m, 3H), 1.76–1.67 (m, 2H), 1.52–1.48 (m, 29H), 1.43 (s, 30H), 1.39–1.10 (m, 59H), 1.03–0.66 (m, 5H);  $^{13}\text{C}$  NMR (125 MHz,  $\text{CDCl}_3$ ):  $\delta$  174.3, 173.3, 168.8, 167.4, 166.0, 165.9, 151.6, 143.2, 136.0, 135.7, 135.5, 134.0, 131.9, 130.6, 130.4, 126.6, 125.3, 81.1, 81.0, 50.9, 49.3, 43.2, 43.0, 41.2, 40.9, 40.8, 40.0, 39.4, 35.5, 35.1, 34.8, 34.1, 33.2, 30.30, 30.26, 30.24, 30.19, 29.6, 29.51, 29.46, 29.39, 29.36, 28.7, 28.6, 28.3, 28.2, 27.9, 27.54, 27.51, 27.2, 26.9, 26.6, 26.3, 26.2, 23.34, 23.28; IR (film): 3385, 2927, 2854, 1699, 1251, 1160  $\text{cm}^{-1}$ ; HRMS-APCI ( $m/z$ )  $[\text{M} + \text{H}]^+$  calcd for  $\text{C}_{38}\text{H}_{61}\text{N}_2\text{O}_6^+$ , 641.45241; found 641.45533.

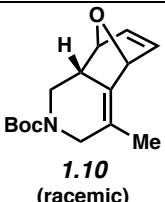
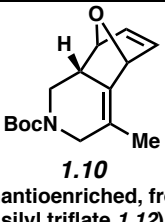
Note: **1.31** was obtained as a mixture of *E* and *Z* isomers. These data represent empirically observed chemical shifts from the  $^1\text{H}$  and  $^{13}\text{C}$  NMR spectra.

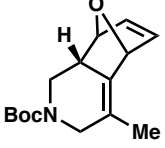
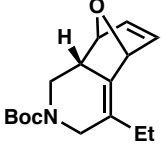
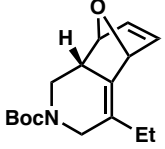
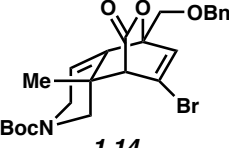
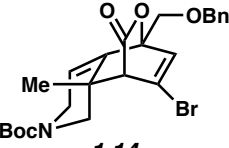
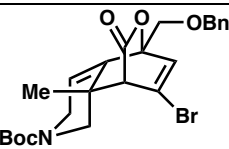
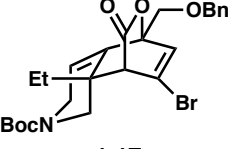


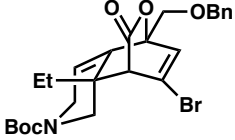
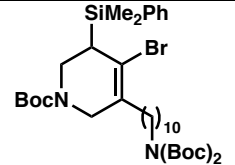
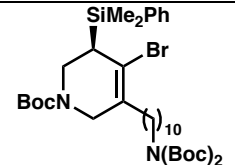
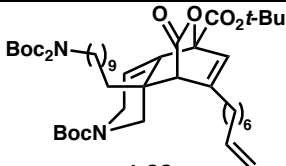
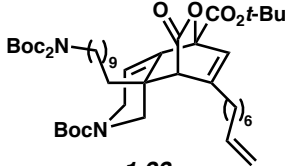
**Lissodendoric Acid A (1.6).** A vial containing macrocycle **1.31** (4.4 mg, 6.9  $\mu\text{mol}$ , 1.00 equiv) was brought into the glovebox and  $\text{Rh}(\text{COD})(\text{acac})$  (1.1 mg, 3.4  $\mu\text{mol}$ , 50 mol%) was added. The vial was then removed from the glovebox and the mixture was dissolved in  $\text{CH}_2\text{Cl}_2$  (0.3 mL) and to this solution was added phenylsilane (8.5  $\mu\text{L}$ , 69  $\mu\text{mol}$ , 10 equiv). The vial was sealed with a Teflon-coated cap and the reaction mixture was heated to  $40\text{ }^\circ\text{C}$  and stirred for 15 h. After this time, the reaction mixture allowed to cool to  $23\text{ }^\circ\text{C}$  and was then quenched slowly with saturated aq. ammonium fluoride (0.5 mL). The reaction mixture was allowed to stir for 3 h at  $23\text{ }^\circ\text{C}$  and then diluted with  $\text{Et}_2\text{O}$  (1 mL), water (1 mL) and 1 M aq NaOH (1 mL). The layers were separated and the aqueous layer was washed with  $\text{Et}_2\text{O}$  (3 x 1 mL). The combined organic layers were dried over  $\text{MgSO}_4$ , filtered, and concentrated under reduced pressure. The crude residue was purified via preparative TLC (4:1 hexanes:EtOAc with 2% triethylamine) to afford the tertiary amine. A vial containing a solution of the tertiary amine (2.1 mg, 3.4  $\mu\text{mol}$ , 1.00 equiv) in  $\text{CH}_2\text{Cl}_2$  (0.20 mL, 0.017 M) was cooled to  $-78\text{ }^\circ\text{C}$ . To the vial was added trifluoroacetic acid (0.10 mL, 0.034 M) dropwise over 2 min. The reaction was subsequently stirred at  $-78\text{ }^\circ\text{C}$  for 1 min and then warmed to  $23\text{ }^\circ\text{C}$  and stirred for 2.75 h. At this point, a nitrogen inlet and vent needle were added to the septum and the reaction mixture was concentrated.  $\text{CH}_2\text{Cl}_2$  (0.5 mL)

was added to resuspended the crude material and was subsequently evaporated off with a nitrogen inlet and vent needle. This was repeated twice more. The crude residue was purified via reversed-phase filtration through a Sep-Pak reverse phase C18 cartridge (6 cc, 500 mg): column flushed with 100% MeCN, then the crude residue was loaded with 20% MeCN in H<sub>2</sub>O, then filtered with 20% MeCN in H<sub>2</sub>O containing 0.1% TFA → 100% MeCN containing 0.1% TFA (**1.6** collected in 35% MeCN in H<sub>2</sub>O containing 0.1% TFA) to afford lissodendoric acid A (**1.6**, 1.5 mg, 29% yield over two steps). Lissodendoric Acid A (**1.6**): *R<sub>f</sub>* 0.47 (1:1 CH<sub>2</sub>Cl<sub>2</sub>:MeOH); <sup>1</sup>H NMR (500 MHz, CD<sub>3</sub>OD): δ 6.98–6.92 (m, 1H), 5.89 (s, 1H), 3.56 (d, *J* = 13.5, 1H), 3.47–3.38 (m, 3H), 2.90 (t, *J* = 7.7, 2H), 2.82 (dd, *J* = 12.3, 4.2, 1H), 2.45–2.36 (m, 1H), 2.30–2.1 (m, 1H), 1.97–1.83 (m, 2H), 1.80–1.12 (42H); HRMS-APCI (*m/z*) [*M* + *H*]<sup>+</sup> calcd for C<sub>29</sub>H<sub>51</sub>N<sub>2</sub>O<sub>2</sub><sup>+</sup>, 459.39451; found 459.39411; spectral data match those previously reported.<sup>27</sup>

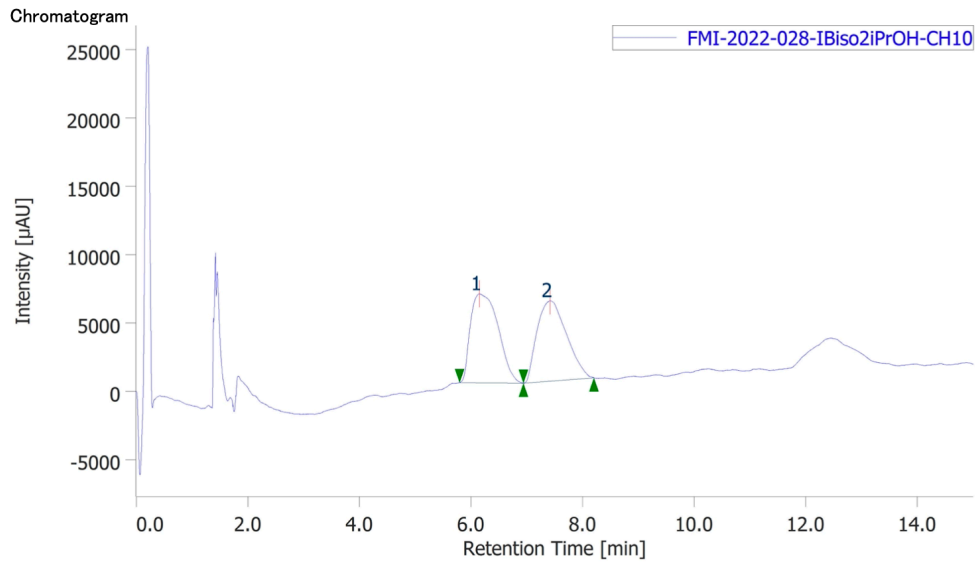
### 1.5.2.6 Verification of enantioenrichment of silyl bromide **1.27** and cycloadducts **1.10**, **1.15**, **1.14**, **1.17**, and **1.28**:

Compound	Method Column/Temp.	Solvent	Method Flow Rate	Retention Times (min)	Enantiomeric Ratio (er)
 <p><b>1.10</b> (racemic)</p>	Diacel ChiralPak IB / 30 °C	2% isopropanol in CO <sub>2</sub>	4 mL/min	6.15/7.42	~51.1:48.9
 <p><b>1.10</b> (enantioenriched, from silyl triflate <b>1.12</b>)</p>	Diacel ChiralPak IB / 30 °C	2% isopropanol in CO <sub>2</sub>	4 mL/min	6.16/7.32	~6.3:93.7

 <b>1.10</b> (enantioenriched, from silyl bromide <b>1.18</b> )	Diacel ChiralPak IB / 30 °C	2% isopropanol in CO <sub>2</sub>	4 mL/min	6.38/7.46	~14.2:85.8
 <b>1.15</b> (racemic)	Diacel ChiralPak IB / 30 °C	2% isopropanol in CO <sub>2</sub>	10 mL/min	12.0/15.0	~49.8:50.2
 <b>1.15</b> (enantioenriched)	Diacel ChiralPak IB / 30 °C	2% isopropanol in CO <sub>2</sub>	10 mL/min	12.0/15.0	~41.6:58.4
 <b>1.14</b> (racemic)	Diacel ChiralPak IA / 30 °C	5%–40% isopropanol in CO <sub>2</sub>	4 mL/min	5.49/5.88	~50.0:50.0
 <b>1.14</b> (enantioenriched, from silyl triflate <b>1.12</b> )	Diacel ChiralPak IA / 30 °C	5%–40% isopropanol in CO <sub>2</sub>	4 mL/min	4.94/5.48	~1.5:98.5
 <b>1.14</b> (enantioenriched, from silyl bromide <b>1.18</b> )	Diacel ChiralPak IA / 30 °C	5%–40% isopropanol in CO <sub>2</sub>	4 mL/min	5.50/5.89	~92.1:7.9
 <b>1.17</b> (racemic)	Diacel ChiralPak IA / 30 °C	10% isopropanol in CO <sub>2</sub>	10 mL/min	10.76/12.34	~50.4:49.6

 <p><b>1.17</b> (enantioenriched)</p>	Diacel ChiralPak IA / 30 °C	10% isopropanol in CO <sub>2</sub>	10 mL/min	10.82/12.43	~66.6:33.4
 <p><b>1.27</b> (racemic)</p>	Diacel ChiralPak IA / 30 °C	5% isopropanol in CO <sub>2</sub>	4 mL/min	7.90/9.09	~50.0:50.0
 <p><b>1.27</b> (enantioenriched)</p>	Diacel ChiralPak IA / 30 °C	5% isopropanol in CO <sub>2</sub>	4 mL/min	7.76/8.88	~5.1:94.9
 <p><b>1.28</b> (racemic)</p>	Diacel ChiralPak ID / 23 °C	10% isopropanol in hexanes	1 mL/min	7.86/8.44	~46.8:53.2
 <p><b>1.28</b> (enantioenriched)</p>	Diacel ChiralPak ID / 23 °C	10% isopropanol in hexanes	1 mL/min	7.92/8.47	~18.6:81.4

FMI-2022-028-029\_IBiso2iPrOH FMI-2022-028-IBiso2iPrOH 2/25/2022 9:03:41 AM

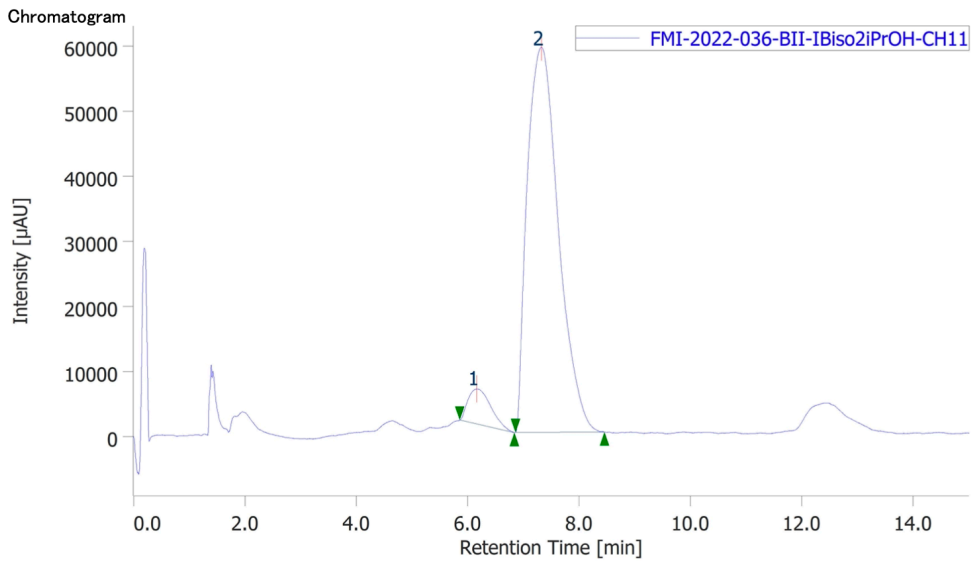


**Peak Information**

#	Peak Name	CH	tR [min]	Area [µV·sec]	Height [µV]	Area%	Height%	Quantity	NTP	Resolution	Symmetry Factor	Warning
1	Unknown	10	6.147	224793	6485	51.128	52.522	N/A	617	1.259	1.640	
2	Unknown	10	7.417	214872	5862	48.872	47.478	N/A	824	N/A	1.322	

**Figure 1.5.** SFC trace of racemic **1.10**.

FMI-2022-036-BII FMI-2022-036-BII-IBiso2iPrOH 4/13/2022 5:33:15 PM

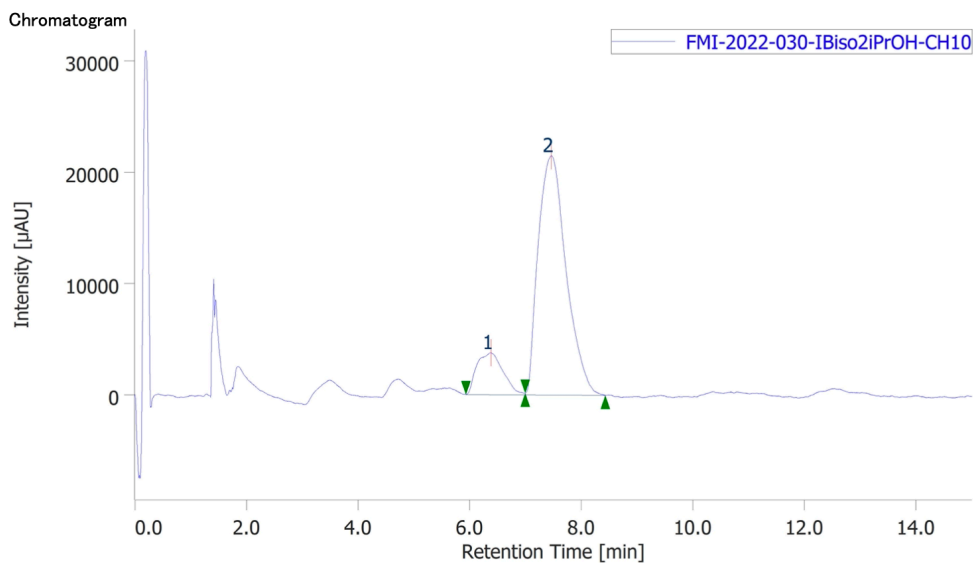


**Peak Information**

#	Peak Name	CH	tR [min]	Area [µV·sec]	Height [µV]	Area%	Height%	Quantity	NTP	Resolution	Symmetry Factor	Warning
1	Unknown	11	6.160	155390	5383	6.333	8.341	N/A	940	1.255	1.507	
2	Unknown	11	7.323	2298110	59151	93.667	91.659	N/A	772	N/A	1.424	

**Figure 1.6.** SFC trace of enantioenriched **1.10** from silyl triflate **1.12**.

FMI-2022-030-IBiso2iPrOH FMI-2022-030-IBiso2iPrOH 2/25/2022 1:14:27 PM

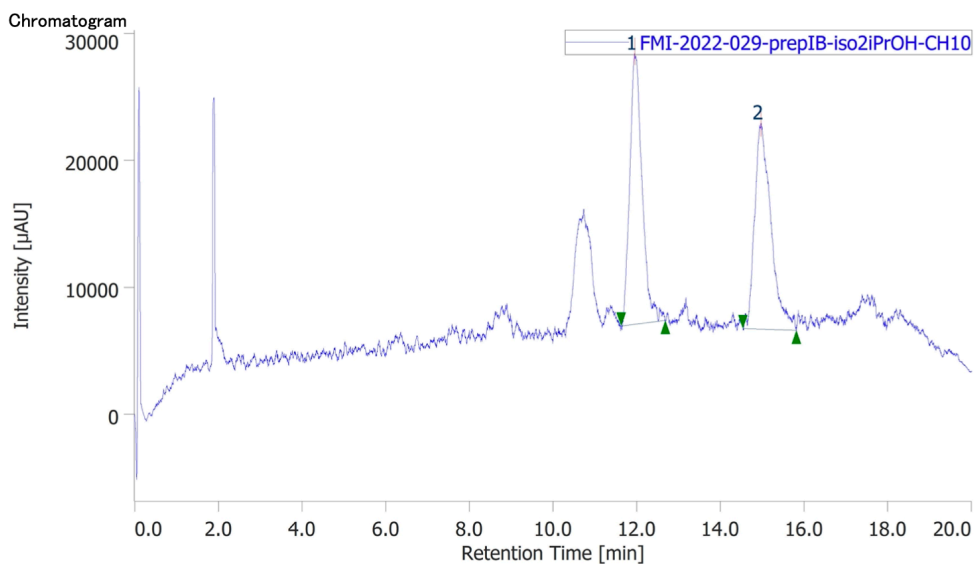


**Peak Information**

#	Peak Name	CH	tR [min]	Area [μV·sec]	Height [μV]	Area%	Height%	Quantity	NTP	Resolution	Symmetry Factor	Warning
1	Unknown	10	6.380	122997	3759	14.158	14.899	N/A	745	1.163	1.209	
2	Unknown	10	7.463	745738	21472	85.842	85.101	N/A	1022	N/A	1.329	

**Figure 1.7.** SFC trace of enantioenriched **1.10** from silyl bromide **1.18**.

MI-2022-029- r d-pr pl 20 MI-2022-029-pr pl -i 2iPrOH 4/21/2022 :01:2 PM

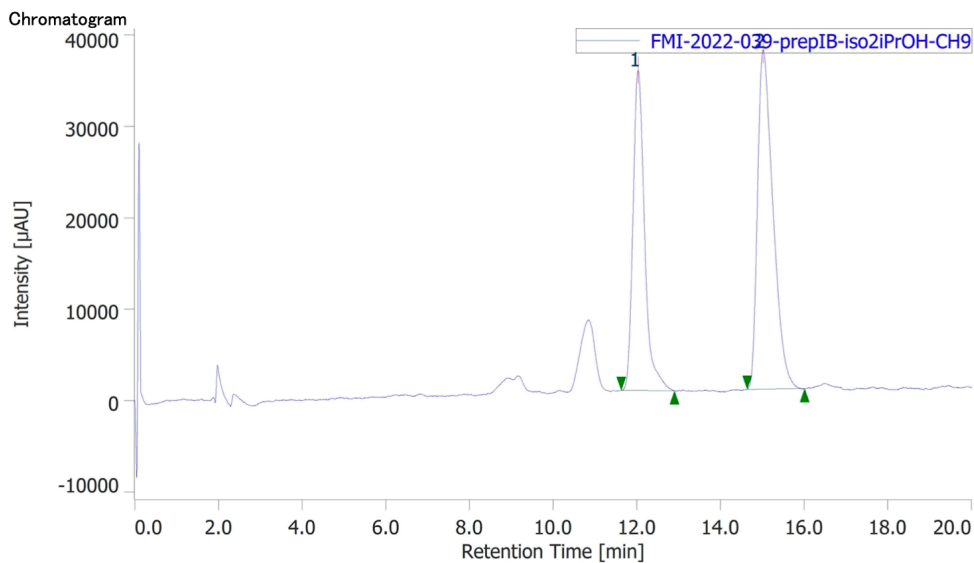


**Peak Information**

#	Peak Name	CH	tR [min]	Area [μV·sec]	Height [μV]	Area%	Height%	Quantity	NTP	Resolution	Symmetry Factor	Warning
1	Unknown	10	11.950	437352	21484	49.845	56.970	N/A	8533	4.874	1.625	
2	Unknown	10	14.963	440079	16227	50.155	43.030	N/A	6864	N/A	1.526	

**Figure 1.8.** SFC trace of racemic **1.15**.

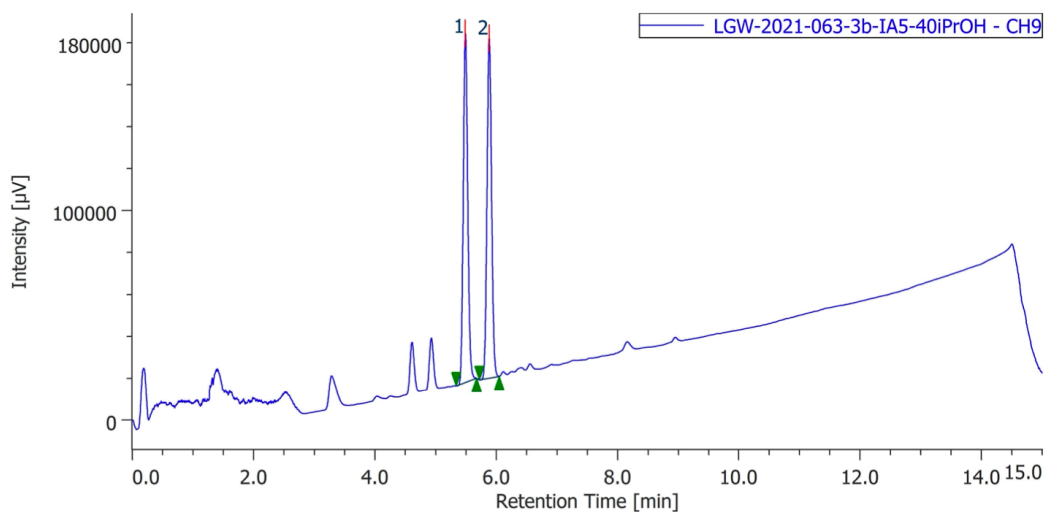
-2022-13 137- -2021-054 r -FMI-2022-02 -039-040 FMI-2022-039- r I -i 2iPrOH 4/20/2022 9:00:0 AM



Peak Information

#	Peak Name	CH	tR [min]	Area [μV·sec]	Height [μV]	Area%	Height%	Quantity	NTP	Resolution	Symmetry Factor	Warning
1	Unknown	9	12.030	677407	35006	41.607	48.556	N/A	9851	5.150	1.432	
2	Unknown	9	15.010	950687	37088	58.393	51.444	N/A	7897	N/A	1.599	

Figure 1.9. SFC trace of enantioenriched **1.15**.

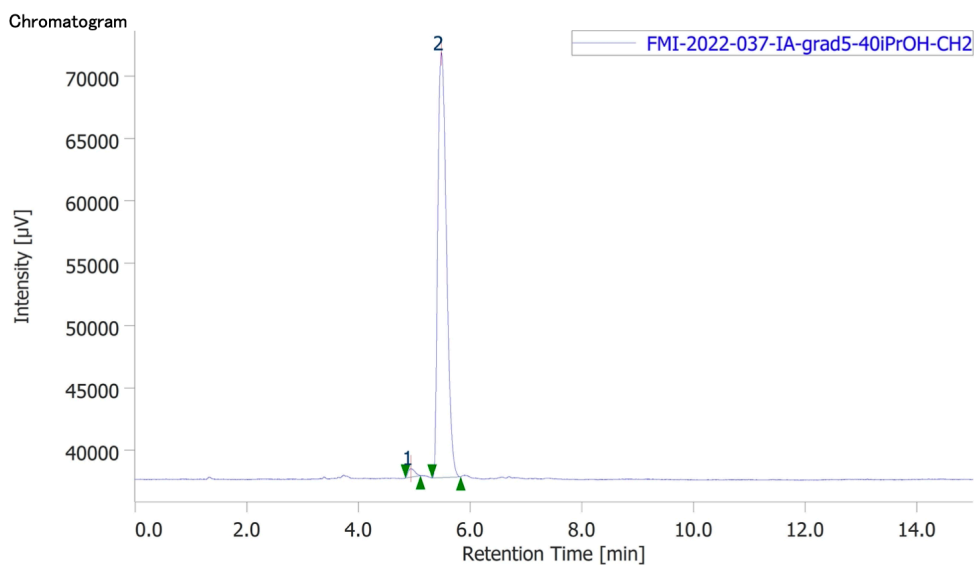


#	Peak Name	CH	tR [min]	Area [μV·sec]	Height [μV]	Area%	Height%	Quantity	NTP	Resolution	Symmetry Factor	Warning
1	Unknown	9	5.487	851401	166444	50.042	50.681	N/A	26876	2.899	1.123	
2	Unknown	9	5.880	849977	161975	49.958	49.319	N/A	28968	N/A	1.067	

Figure 1.10. SFC trace of racemic **1.14**.



FMI-2022-036-037-N2 FMI-2022-037-IA-grad5-40iPrOH 4/11/2022 6:43:10 PM

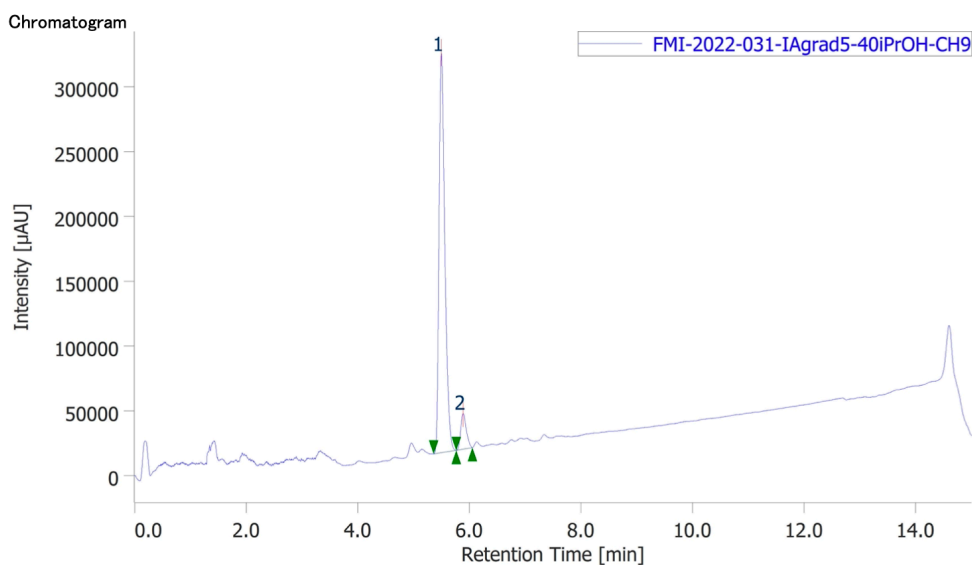


**Peak Information**

#	Peak Name	CH	tR [min]	Area [µV·sec]	Height [µV]	Area%	Height%	Quantity	NTP	Resolution	Symmetry Factor	Warning
1	Unknown	2	4.938	5694	680	1.524	1.955	N/A	7284	2.078	1.341	
2	Unknown	2	5.483	367858	34102	98.476	98.045	N/A	5548	N/A	1.411	

**Figure 1.11.** SFC trace of enantioenriched **1.14** from silyl triflate **1.12**.

DJN-2022-019column-screen-5%iPrOH FMI-2022-031-IAgrad5-40iPrOH 2/24/2022 6:00:55 PM

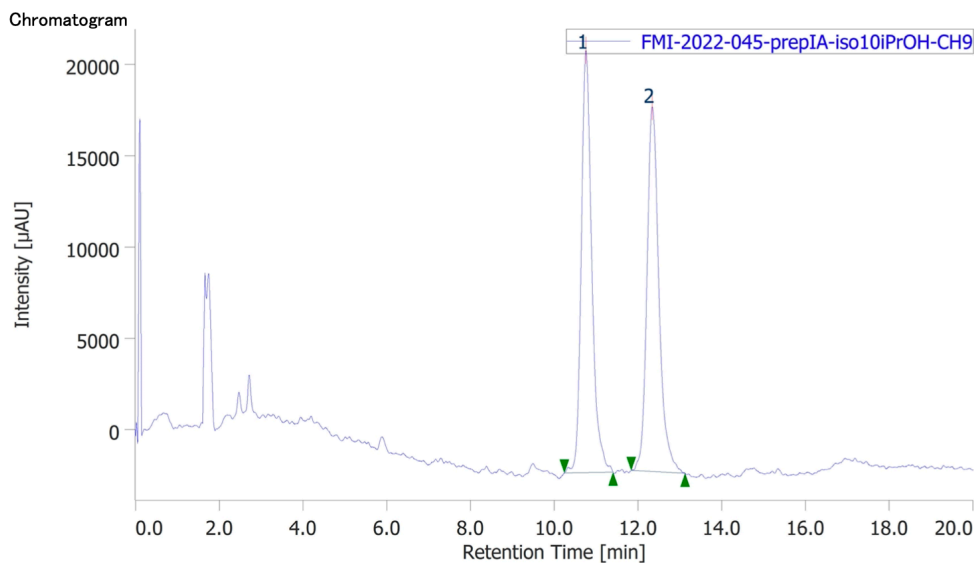


**Peak Information**

#	Peak Name	CH	tR [min]	Area [µV·sec]	Height [µV]	Area%	Height%	Quantity	NTP	Resolution	Symmetry Factor	Warning
1	Unknown	9	5.497	2225945	308233	92.147	91.815	N/A	13948	2.120	1.411	
2	Unknown	9	5.887	189703	27478	7.853	8.185	N/A	16593	N/A	1.277	

**Figure 1.12.** SFC trace of enantioenriched **1.14** from silyl bromide **1.18**.

FMI-2022-045 FMI-2022-045-prepIA-iso10iPrOH 4/24/2022 2:44:43 PM

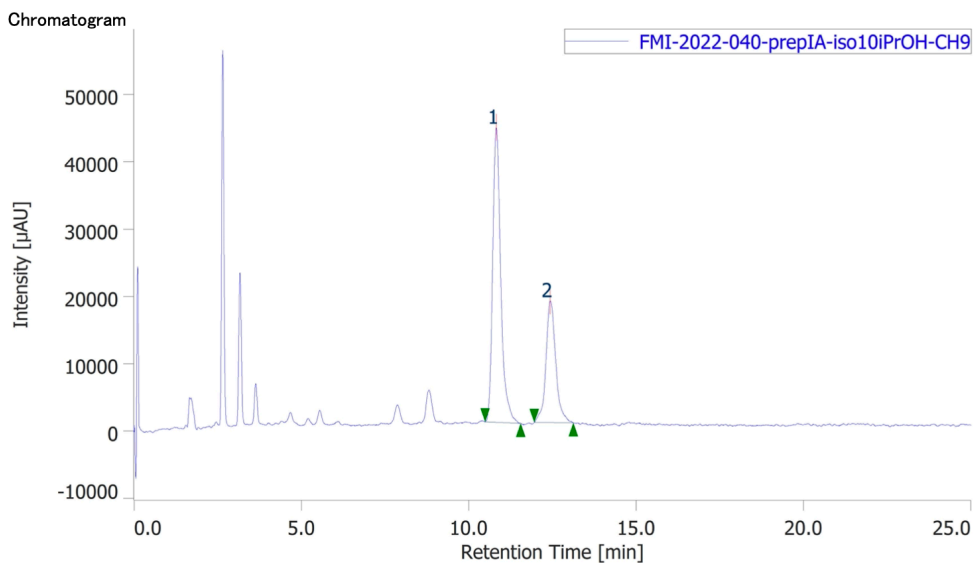


Peak Information

#	Peak Name	CH	tR [min]	Area [µV·sec]	Height [µV]	Area%	Height%	Quantity	NTP	Resolution	Symmetry Factor	Warning
1	Unknown	9	10.757	403689	23110	50.392	53.642	N/A	9816	3.409	1.320	
2	Unknown	9	12.337	397406	19971	49.608	46.358	N/A	9934	N/A	1.283	

Figure 1.13. SFC trace of racemic 1.17.

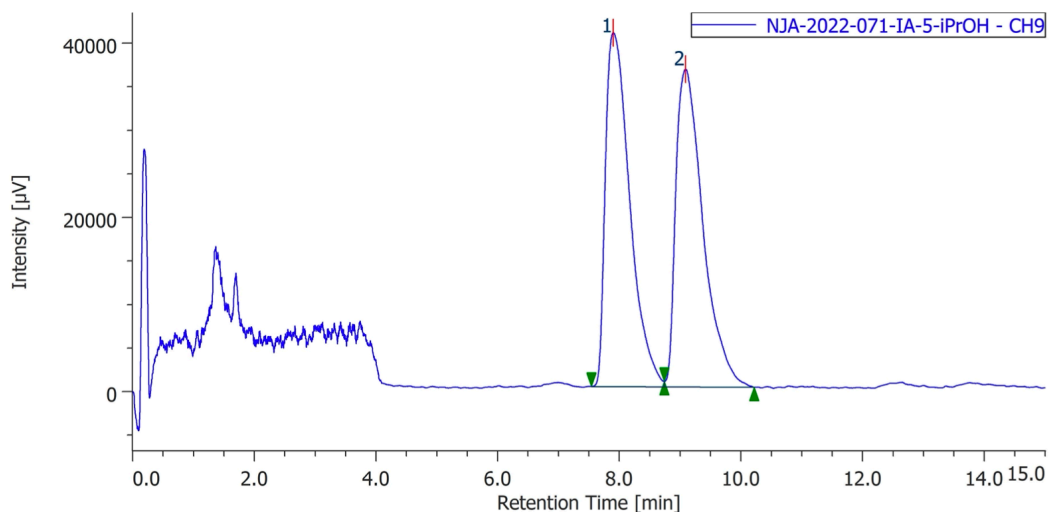
-2022-13 137- -2021-054 r -FMI-2022-02 -039-040 FMI-2022-040- r IA-i 10iPrOH 4/20/2022 9:03:0 AM



Peak Information

#	Peak Name	CH	tR [min]	Area [µV·sec]	Height [µV]	Area%	Height%	Quantity	NTP	Resolution	Symmetry Factor	Warning
1	Unknown	9	10.823	734376	43765	66.608	70.786	N/A	10618	3.490	1.357	
2	Unknown	9	12.430	368164	18062	33.392	29.214	N/A	9765	N/A	1.122	

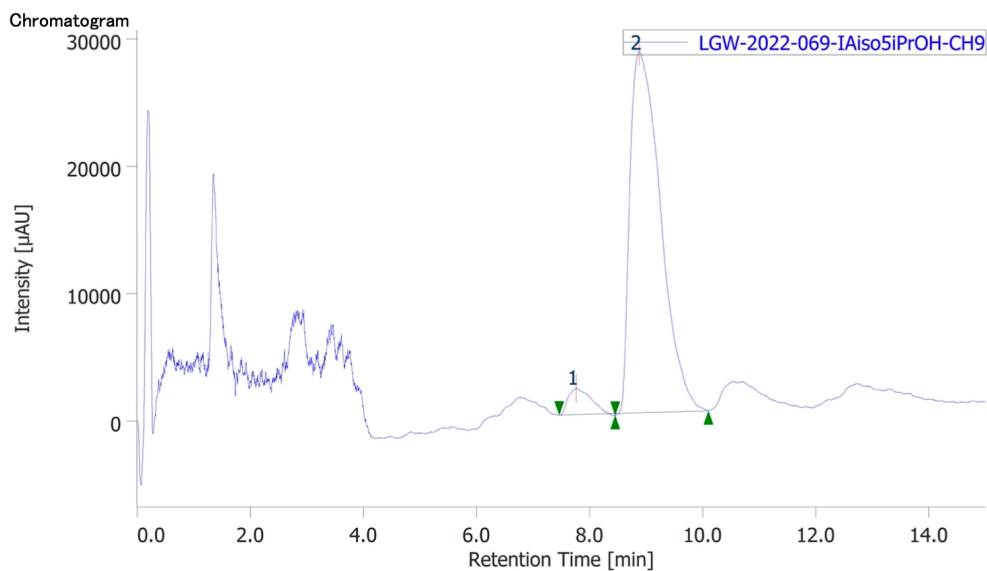
Figure 1.14. SFC trace of enantioenriched 1.17.



#	Peak Name	CH	tR [min]	Area [µV·sec]	Height [µV]	Area%	Height%	Quantity	NTP	Resolution	Symmetry Factor	Warning
1	Unknown	9	7.900	1129612	40602	49.980	52.696	N/A	1879	1.557		1.958
2	Unknown	9	9.087	1130514	36448	50.020	47.304	N/A	2069	N/A		1.855

**Figure 1.15.** SFC trace of racemic **1.27**.

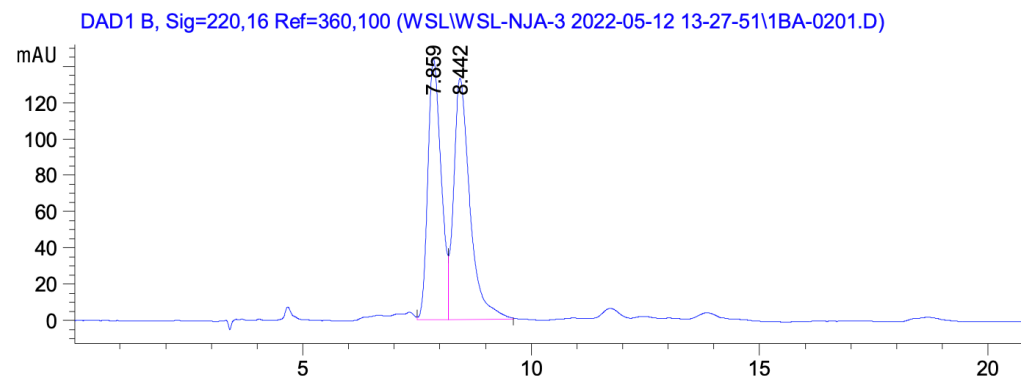
LGW-2022-069-FMI-2022-028-039-040 LGW-2022-069-IAiso5iPrOH 4/26/2022 6:22:35 PM



**Peak Information**

#	Peak Name	CH	tR [min]	Area [µV·sec]	Height [µV]	Area%	Height%	Quantity	NTP	Resolution	Symmetry Factor	Warning
1	Unknown	9	7.763	57096	2049	5.091	6.738	N/A	1528	1.233		1.584
2	Unknown	9	8.877	1064505	28362	94.909	93.262	N/A	1219	N/A		2.004

**Figure 1.16.** SFC trace of enantioenriched **1.27**.

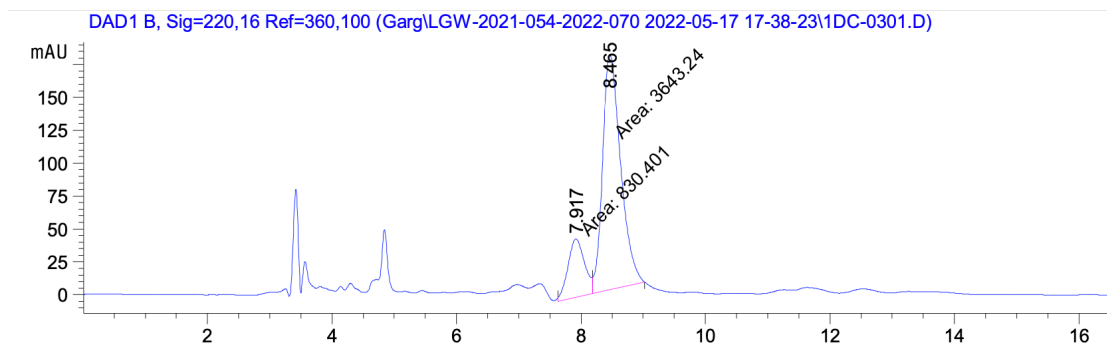


Signal 2: DAD1 B, Sig=220,16 Ref=360,100

Peak #	RetTime [min]	Type	Width [min]	Area [mAU*s]	Height [mAU]	Area %
1	7.859	VV	0.3067	2903.66821	144.33865	46.8102
2	8.442	VB	0.3677	3299.40405	132.85863	53.1898

Totals : 6203.07227 277.19728

**Figure 1.17.** HPLC trace of racemic **1.28**.



Signal 2: DAD1 B, Sig=220,16 Ref=360,100

Peak #	RetTime [min]	Type	Width [min]	Area [mAU*s]	Height [mAU]	Area %
1	7.917	MF	0.3114	830.40106	44.44971	18.5621
2	8.465	FM	0.3389	3643.23975	179.19023	81.4379

Totals : 4473.64081 223.63994

**Figure 1.18.** HPLC trace of enantioenriched **1.28**.

## **1.6 Spectra Relevant to Chapter One:**

### **Total Synthesis of Lissodendoric Acid A via Stereospecific Trapping of a Strained Cyclic Allene**

Francesca M. Ippoliti, Nathan J. Adamson, Laura G. Wonilowicz,

Evan R. Darzi, Joyann S. Donaldson, and Neil K. Garg.

*Manuscript in Preparation.*

Purified Product, <sup>1</sup>H NMR

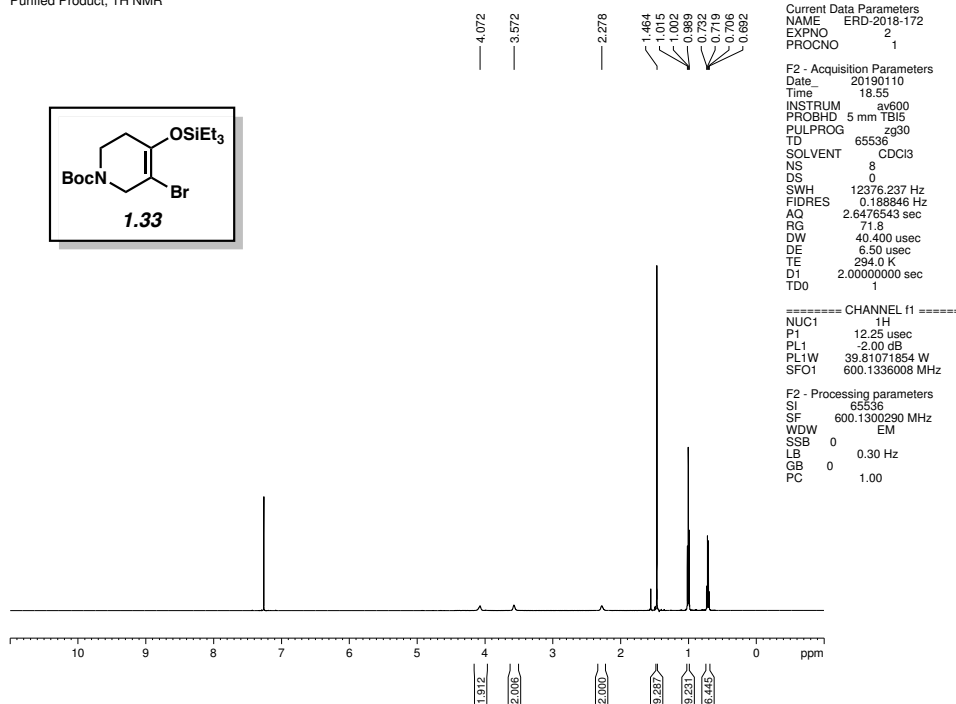


**Figure 1.19.** <sup>1</sup>H NMR (600 MHz, CDCl<sub>3</sub>) of compound **1.33**.

Purified Product, <sup>13</sup>C NMR

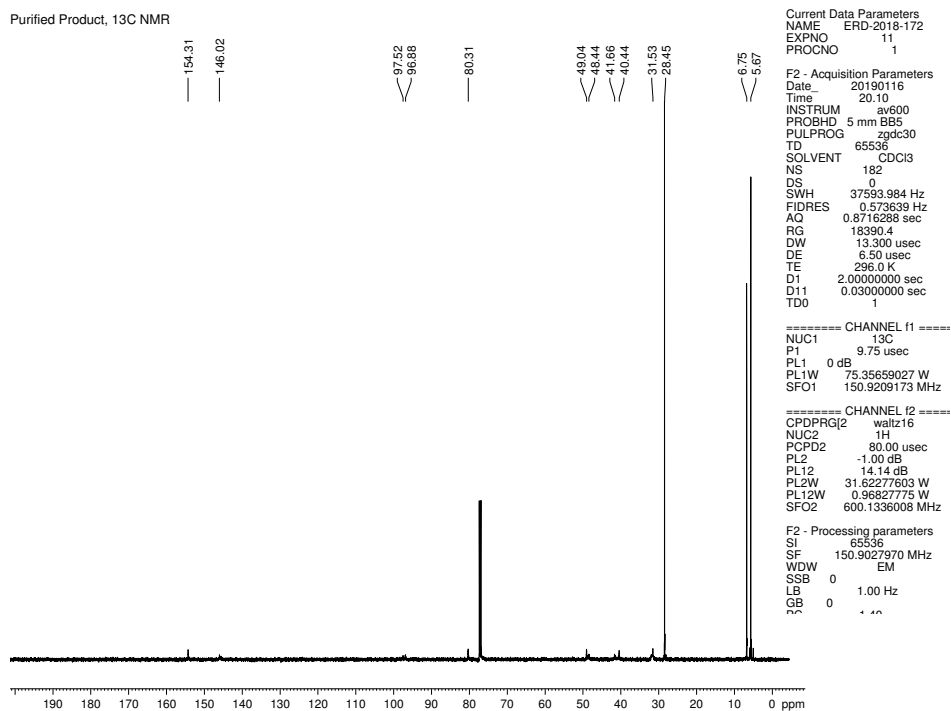


**Figure 1.20.** <sup>13</sup>C NMR (150 MHz, CDCl<sub>3</sub>) of compound **1.33**.

Purified Product, <sup>1</sup>H NMR

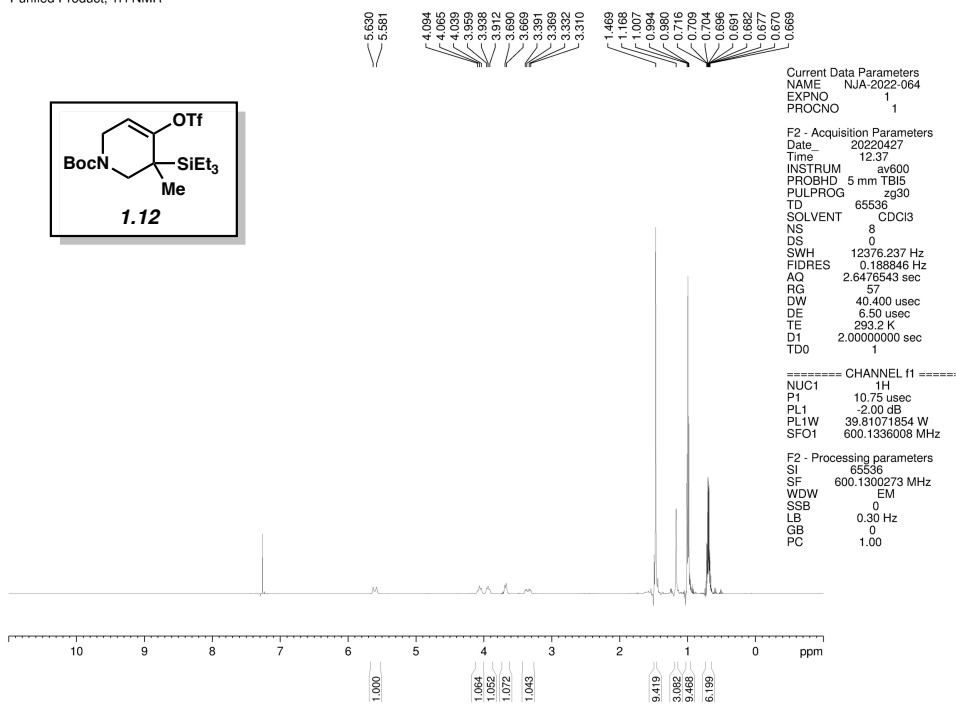


Figure 1.21. <sup>1</sup>H NMR (600 MHz, CDCl<sub>3</sub>) of compound 1.12.

Purified Product, <sup>13</sup>C NMR

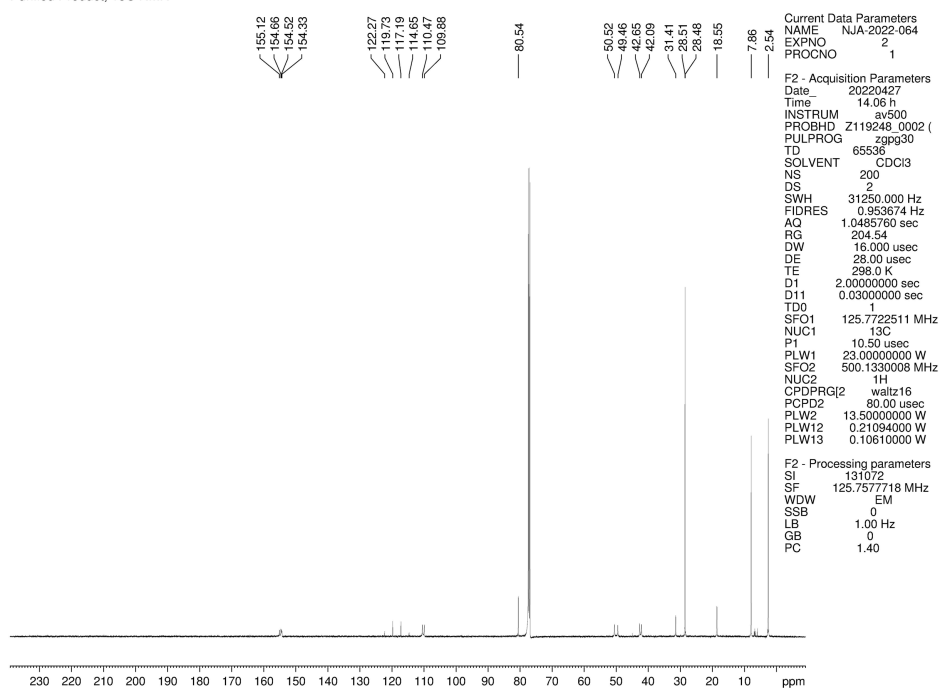


Figure 1.22. <sup>13</sup>C NMR (125 MHz, CDCl<sub>3</sub>) of compound 1.12.





Purified Product, 1H NMR

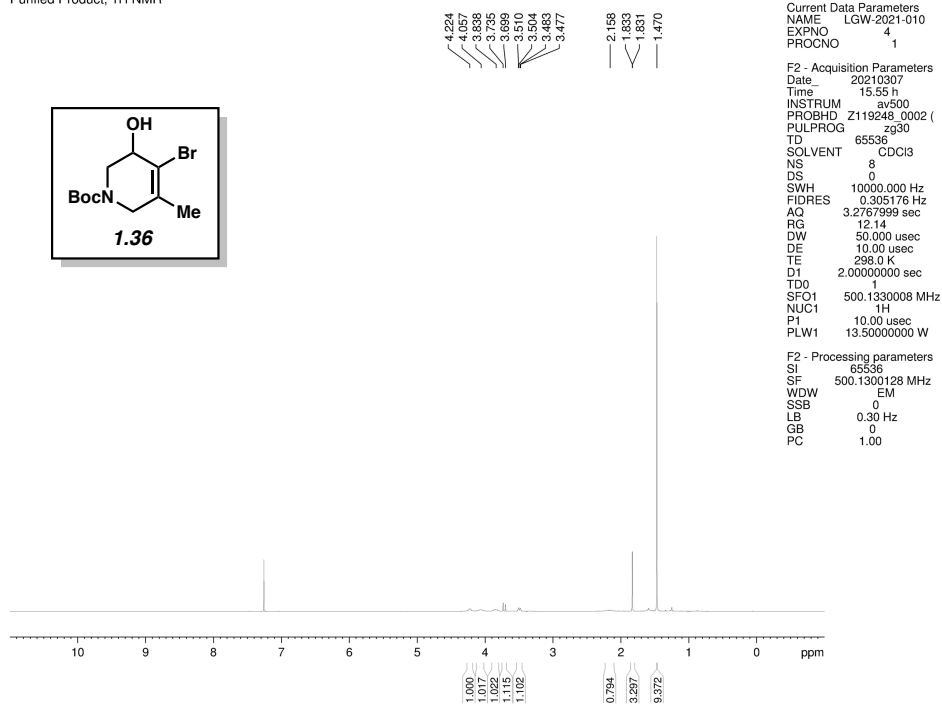


Figure 1.25.  $^1\text{H}$  NMR (500 MHz,  $\text{CDCl}_3$ ) of compound **1.36**.

Purified Product,  $^{13}\text{C}$  NMR

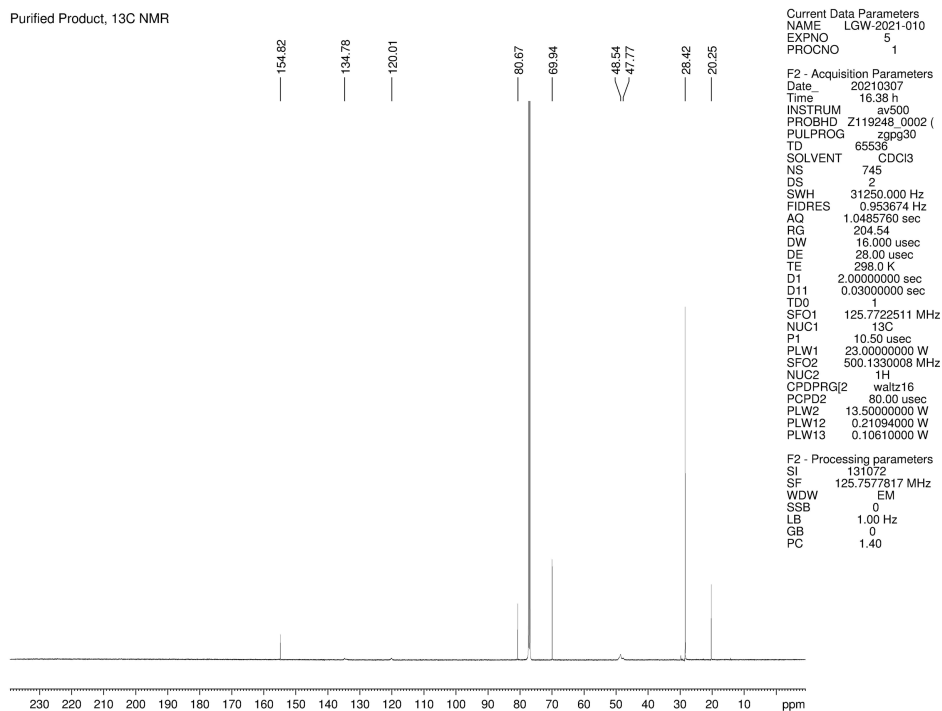


Figure 1.26.  $^{13}\text{C}$  NMR (125 MHz,  $\text{CDCl}_3$ ) of compound **1.36**.

Purified Product, <sup>1</sup>H NMR

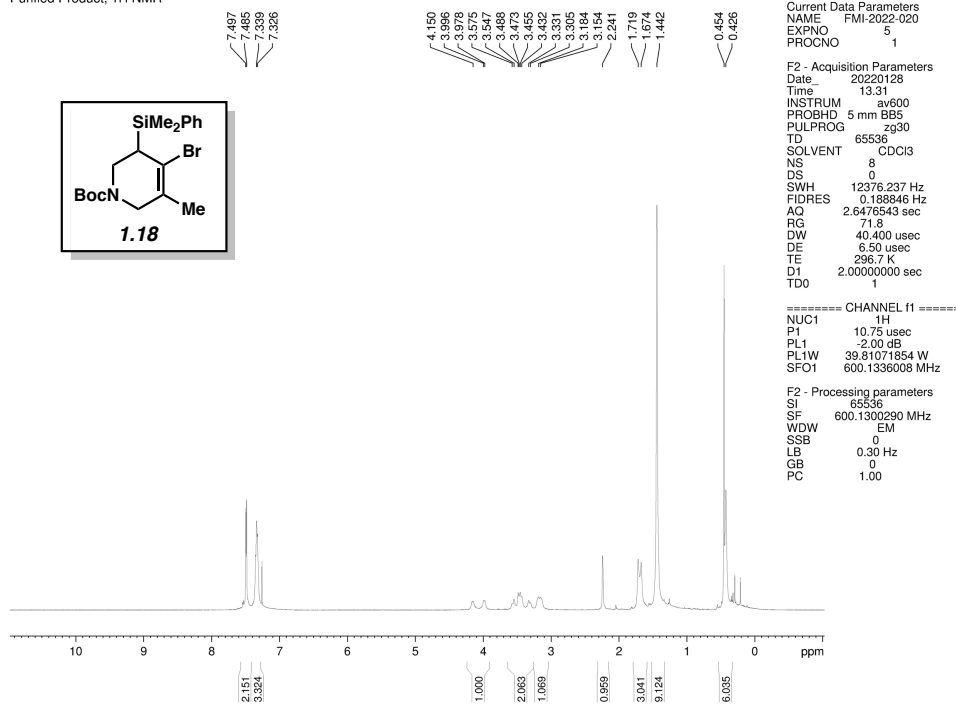


Figure 1.27. <sup>1</sup>H NMR (600 MHz, CDCl<sub>3</sub>) of compound **1.18**.

Purified Product, <sup>13</sup>C NMR

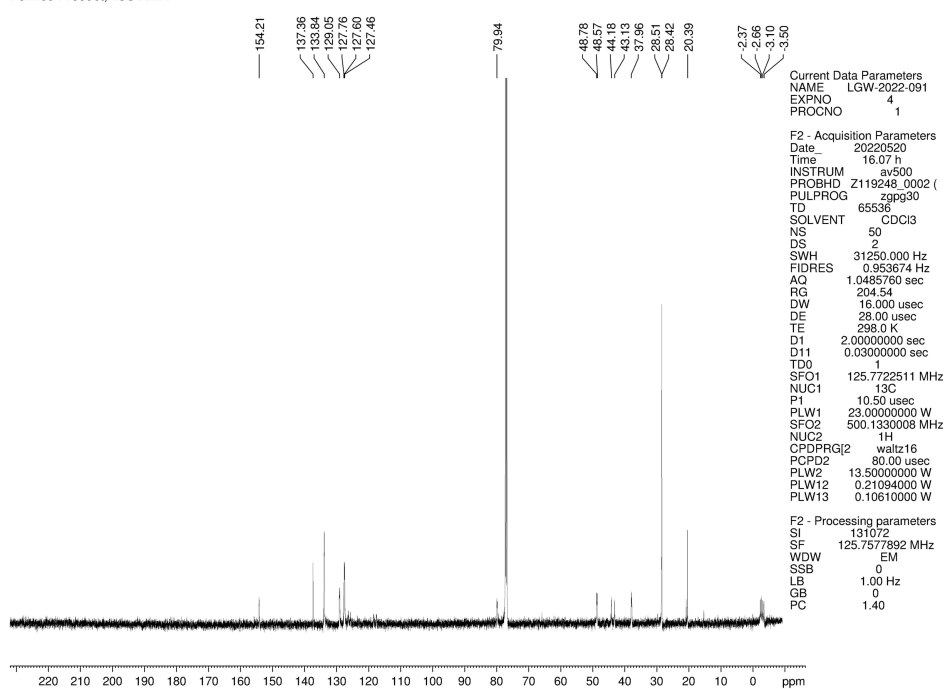
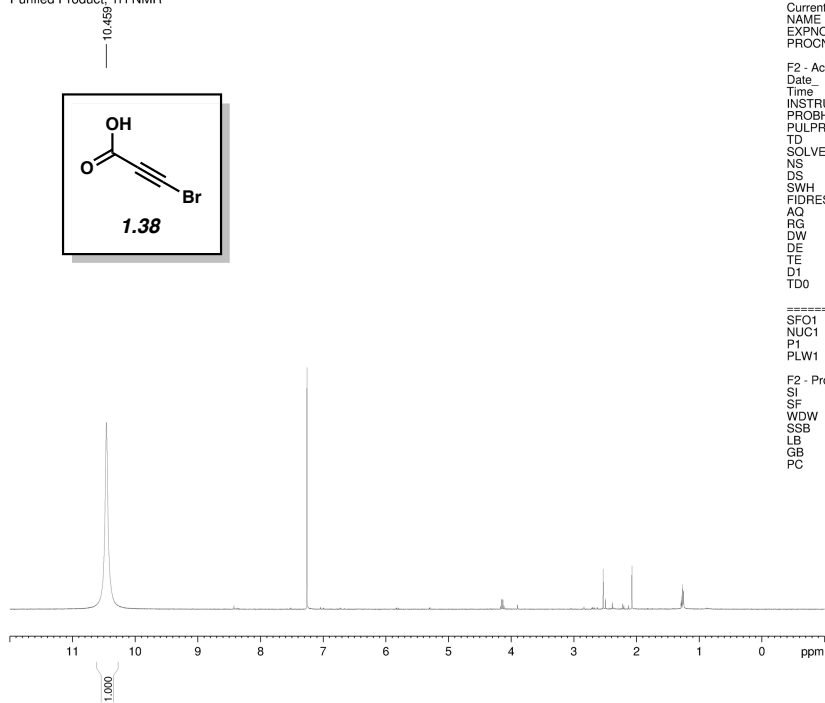


Figure 1.28. <sup>13</sup>C NMR (125 MHz, CDCl<sub>3</sub>) of compound **1.18**.

Purified Product, 1H NMR



Current Data Parameters  
NAME NJA-2021-182\_1H fla  
EXPNO 90  
PROCNO 1

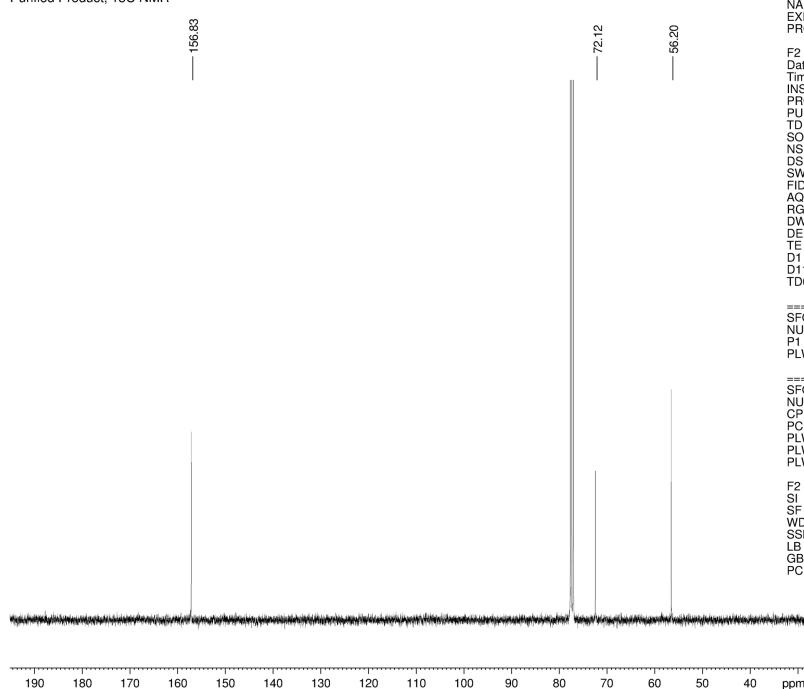
F2 - Acquisition Parameters  
Date\_ 20210813  
Time 21.41  
INSTRUM av400  
PROBHD 5 mm PABBO BB/  
PULPROG zg30  
TD 52882  
SOLVENT CDCl3  
NS 8  
DS 0  
SWH 8012.820 Hz  
FIDRES 0.151523 Hz  
AQ 3.2998369 sec  
RG 189.85  
DW 62.400 usec  
DE 6.50 usec  
TE 297.2 K  
D1 2.00000000 sec  
TD0 1

=====  
CHANNEL f1 =====  
SFO1 400.1324008 MHz  
NUC1 1H  
P1 15.00 usec  
PLW1 13.00000000 W

F2 - Processing parameters  
SI 65536  
SF 400.1300176 MHz  
WDW EM  
SSB 0  
LB 0.30 Hz  
GB 0  
PC 1.00

Figure 1.29. <sup>1</sup>H NMR (400 MHz, CDCl<sub>3</sub>) of compound 1.38.

Purified Product, 13C NMR



Current Data Parameters  
NAME NJA-2021-182\_13C\_  
EXPNO 91  
PROCNO 1

F2 - Acquisition Parameters  
Date\_ 20210813  
Time 22.05  
INSTRUM av400  
PROBHD 5 mm PABBO BB/  
PULPROG zgpg30  
TD 65536  
SOLVENT CDCl3  
NS 400  
DS 0  
SWH 25252.625 Hz  
FIDRES 0.385323 Hz  
AQ 1.2976128 sec  
RG 189.85  
DW 19.800 usec  
DE 6.50 usec  
TE 298.0 K  
D1 2.00000000 sec  
D11 0.03000000 sec  
TD0 1

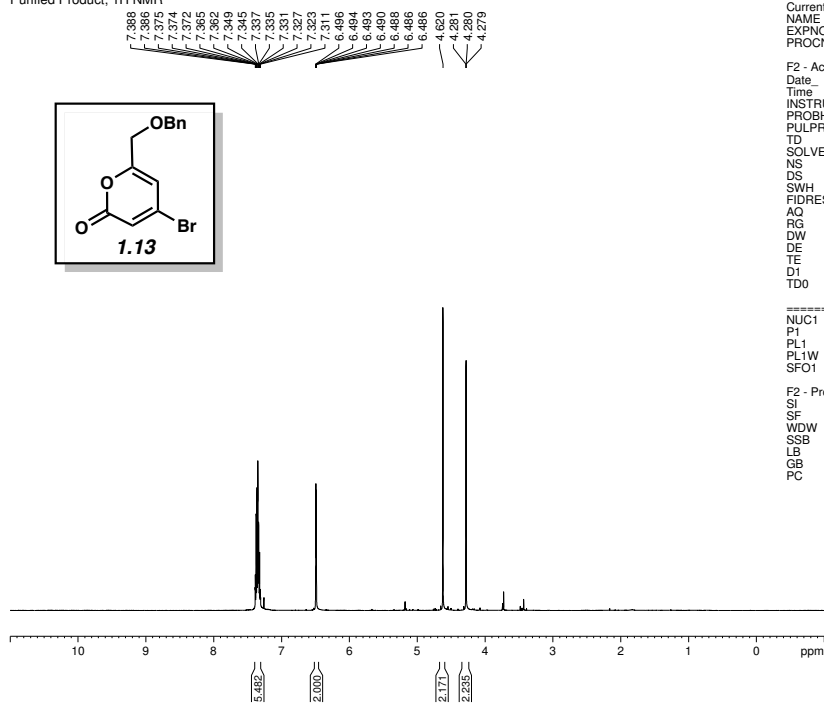
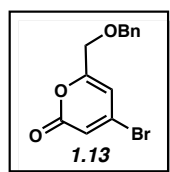
=====  
CHANNEL f1 =====  
SFO1 100.6243395 MHz  
NUC1 13C  
P1 10.00 usec  
PLW1 52.00000000 W

=====  
CHANNEL f2 =====  
SFO2 400.1324008 MHz  
NUC2 1H  
CPDPRG[2] waltz16  
PCPD2 90.00 usec  
PLW2 13.00000000 W  
PLW12 0.35111000 W  
PLW13 0.29249999 W

F2 - Processing parameters  
SI 65536  
SF 100.6127363 MHz  
WDW EM  
SSB 0  
LB 1.00 Hz  
GB 0  
PC 1.40

Figure 1.30. <sup>13</sup>C NMR (100 MHz, CDCl<sub>3</sub>) of compound 1.38.

Purified Product, <sup>1</sup>H NMR



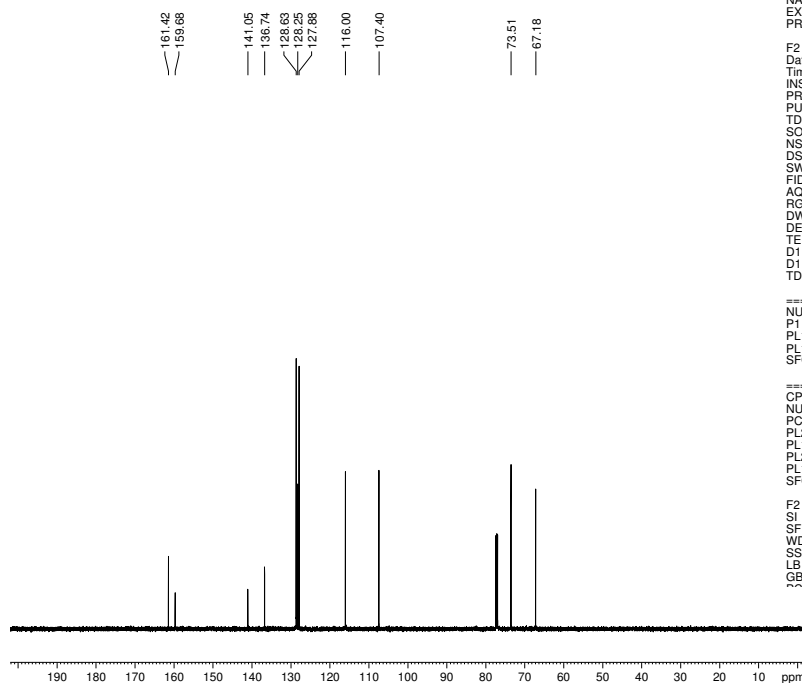
Current Data Parameters  
NAME FMI-2018-123  
EXPNO 10  
PROCNO 1

F2 - Acquisition Parameters  
Date\_ 20190117  
Time 18.10  
INSTRUM av600  
PROBHD 5 mm BB5  
PULPROG zg30  
TD 65536  
SOLVENT CDCl3  
NS 8  
DS 0  
SWH 12376.237 Hz  
FIDRES 0.188846 Hz  
AQ 2.6476543 sec  
RG 45.3  
DW 40.400 usec  
DE 6.50 usec  
TE 295.3 K  
D1 2.0000000 sec  
TDO 1

===== CHANNEL f1 =====  
NUC1 <sup>1</sup>H  
P1 18.25 usec  
PL1 -1.00 dB  
PL1W 31.62277603 W  
SFO1 600.1336008 MHz  
F2 - Processing parameters  
SI 65536  
SF 600.1300280 MHz  
WDW EM  
SSB 0  
LB 0.30 Hz  
GB 0  
PC 1.00

**Figure 1.31.** <sup>1</sup>H NMR (600 MHz, CDCl<sub>3</sub>) of compound **1.13**.

Purified Product, <sup>13</sup>C NMR



Current Data Parameters  
NAME FMI-2018-123  
EXPNO 11  
PROCNO 1

F2 - Acquisition Parameters  
Date\_ 20190117  
Time 18.13  
INSTRUM av600  
PROBHD 5 mm BB5  
PULPROG zgdc30  
TD 65536  
SOLVENT CDCl3  
NS 25  
DS 0  
SWH 37593.984 Hz  
FIDRES 0.573639 Hz  
AQ 0.8716288 sec  
RG 18390.4  
DW 13.300 usec  
DE 6.50 usec  
TE 295.5 K  
D1 2.0000000 sec  
D11 0.0300000 sec  
TDO 1

===== CHANNEL f1 =====  
NUC1 <sup>13</sup>C  
P1 9.75 usec  
PL1 0 dB  
PL1W 75.35659027 W  
SFO1 150.9209173 MHz  
===== CHANNEL f2 =====  
CPDPRG2 waltz16  
NUC2 <sup>1</sup>H  
PCPD2 80.00 usec  
PL2 -1.00 dB  
PL12 14.14 dB  
PL2W 31.62277603 W  
PL12W 0.96827775 W  
SFO2 600.1336008 MHz

F2 - Processing parameters  
SI 65536  
SF 150.9028181 MHz  
WDW EM  
SSB 0  
LB 1.00 Hz  
GB 0

**Figure 1.32.** <sup>13</sup>C NMR (150 MHz, CDCl<sub>3</sub>) of compound **1.13**.

Purified Product, <sup>1</sup>H NMR

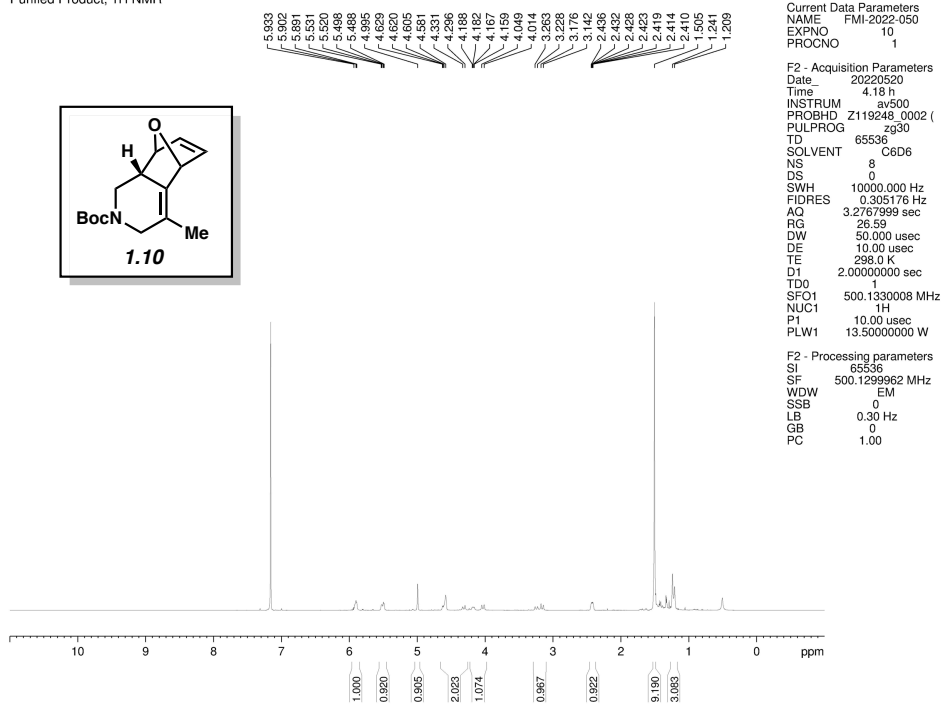
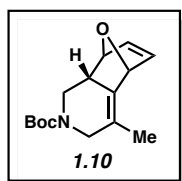


**Figure 1.33.** <sup>1</sup>H NMR (500 MHz, C<sub>6</sub>D<sub>6</sub>) of compound **1.10**.

Purified Product, <sup>13</sup>C NMR

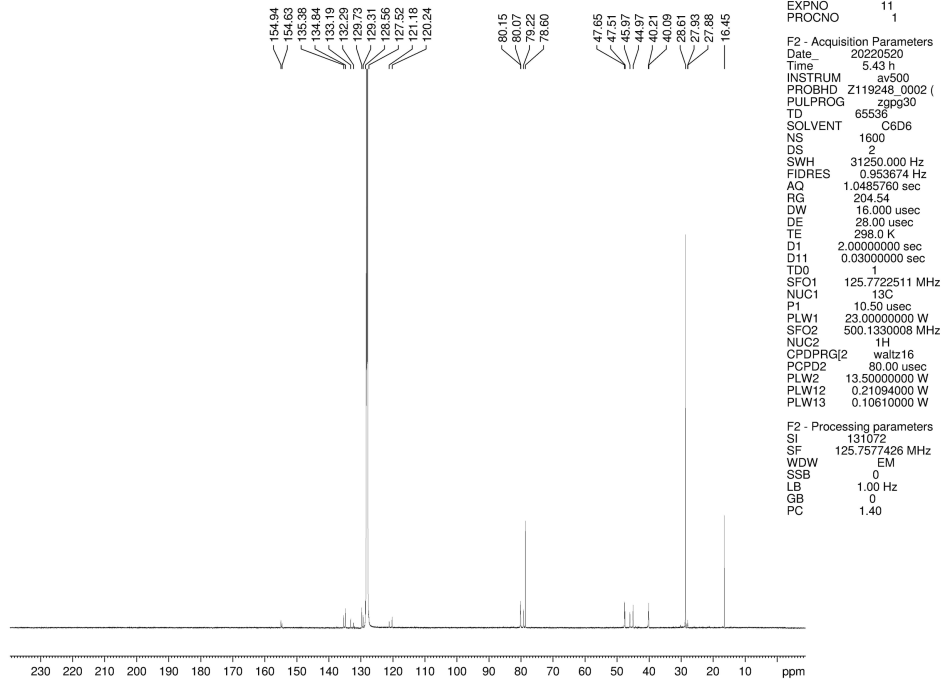


**Figure 1.34.** <sup>13</sup>C NMR (125 MHz, C<sub>6</sub>D<sub>6</sub>) of compound **1.10**.

Purified Product, <sup>1</sup>H NMR

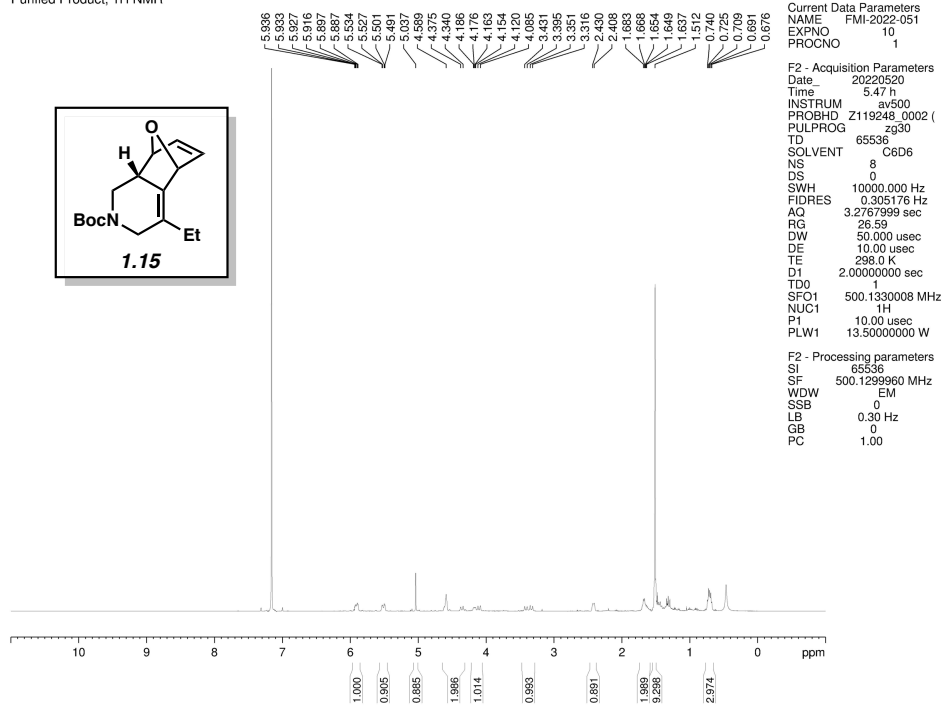


Figure 1.35. <sup>1</sup>H NMR (500 MHz, C<sub>6</sub>D<sub>6</sub>) of compound 1.15.

Purified Product, <sup>13</sup>C NMR

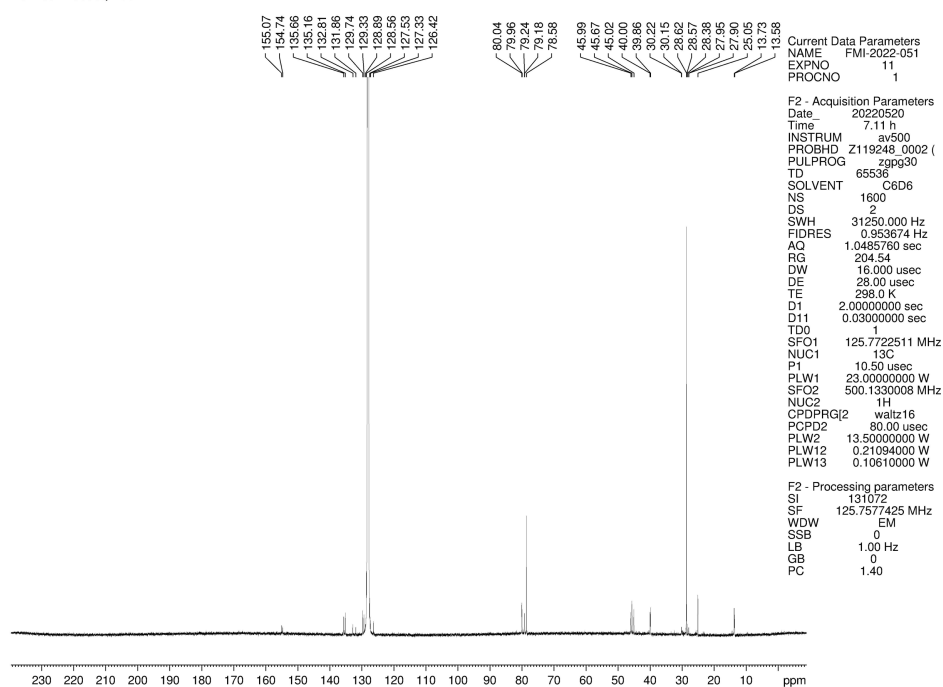


Figure 1.36. <sup>13</sup>C NMR (125 MHz, C<sub>6</sub>D<sub>6</sub>) of compound 1.15.

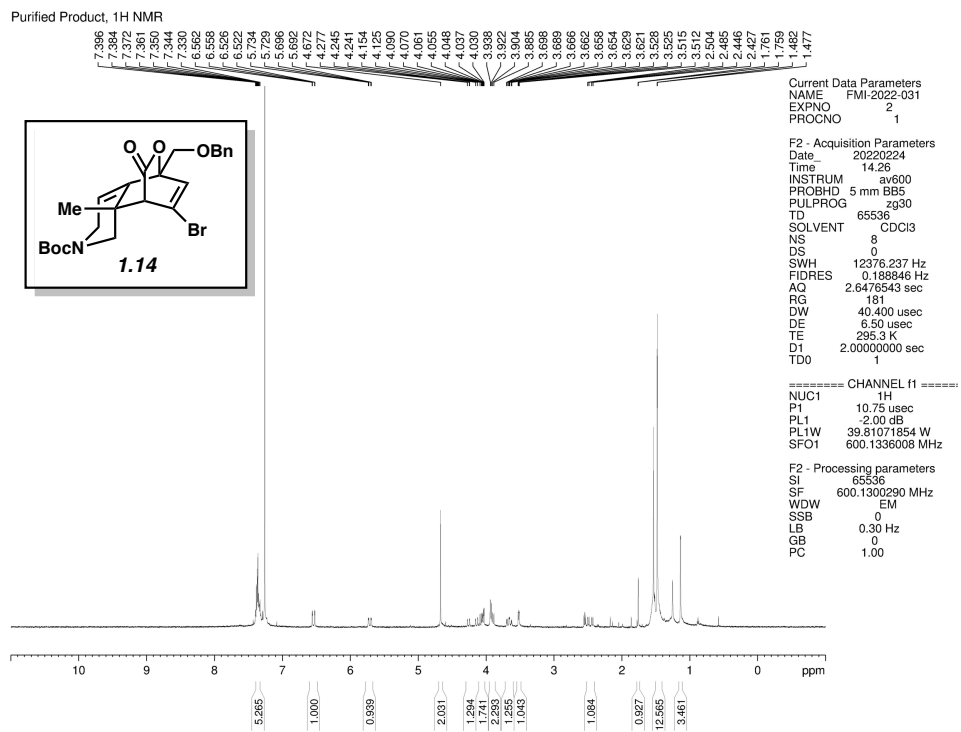


Figure 1.37. <sup>1</sup>H NMR (600 MHz, CDCl<sub>3</sub>) of compound **1.14**.

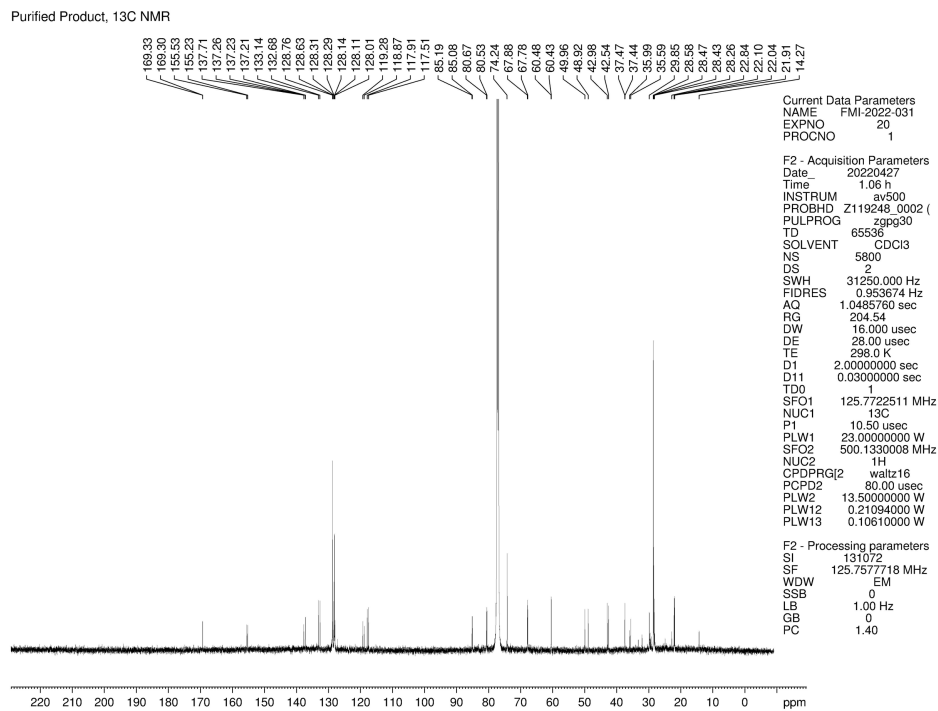


Figure 1.38. <sup>13</sup>C NMR (125 MHz, CDCl<sub>3</sub>) of compound **1.14**.

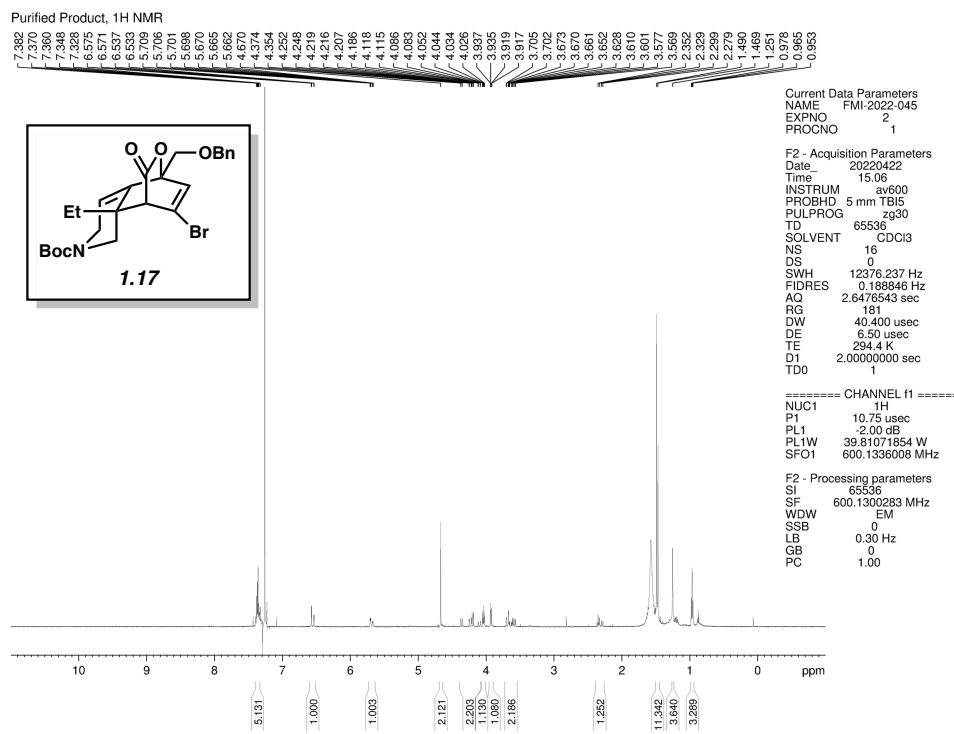


Figure 1.39. <sup>1</sup>H NMR (600 MHz, CDCl<sub>3</sub>) of compound 1.17.

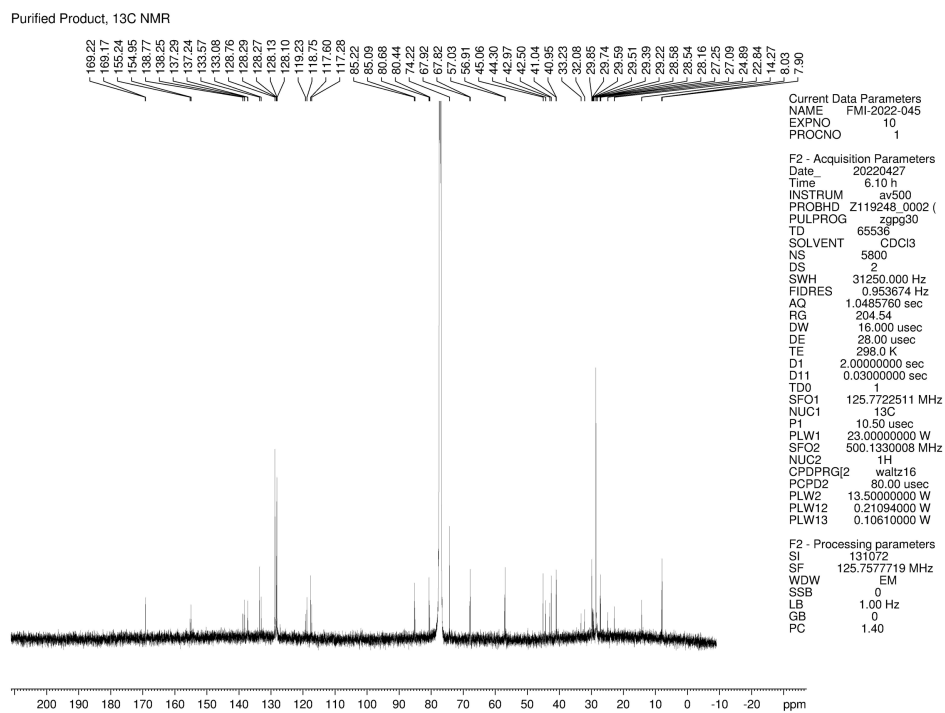


Figure 1.40. <sup>13</sup>C NMR (125 MHz, CDCl<sub>3</sub>) of compound 1.17.



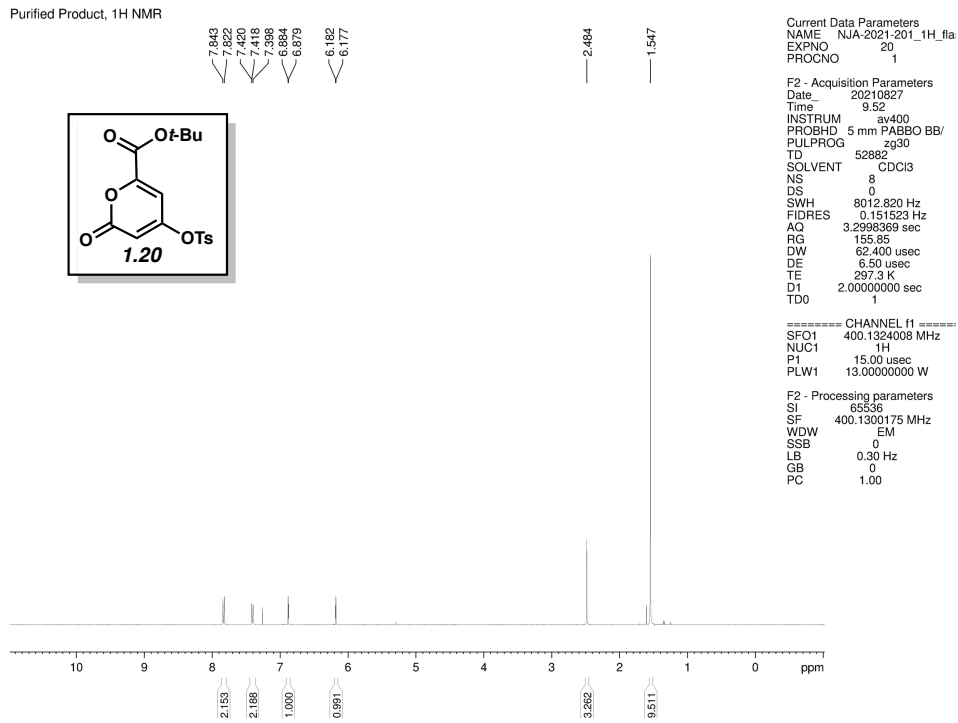


Figure 1.41. <sup>1</sup>H NMR (400 MHz, CDCl<sub>3</sub>) of compound 1.20.

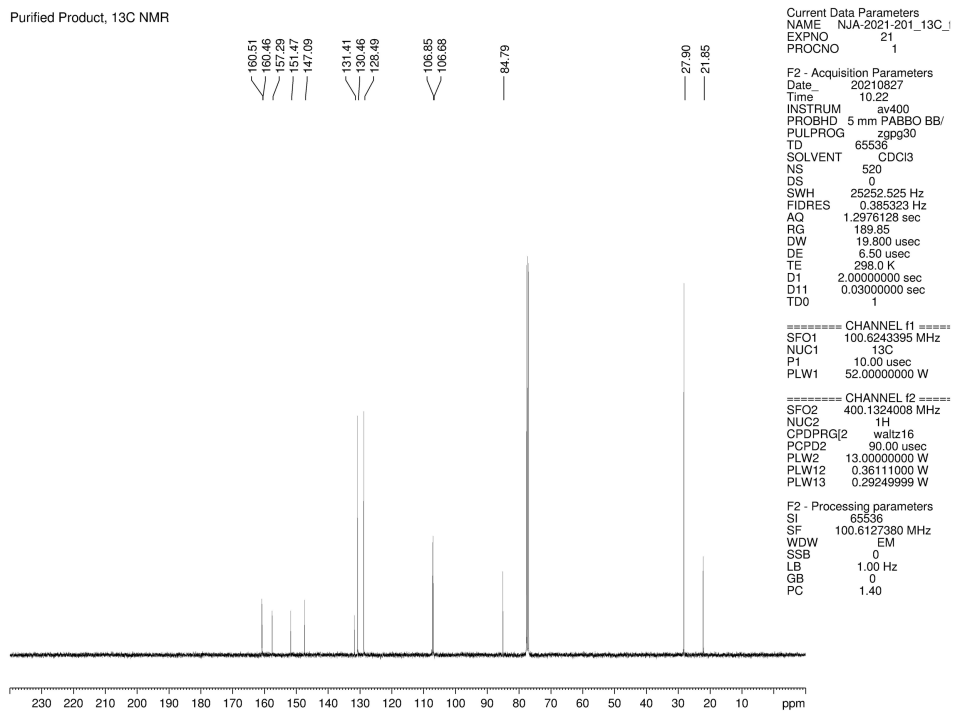


Figure 1.42. <sup>13</sup>C NMR (100 MHz, CDCl<sub>3</sub>) of compound 1.20.

Purified Product, 1H NMR

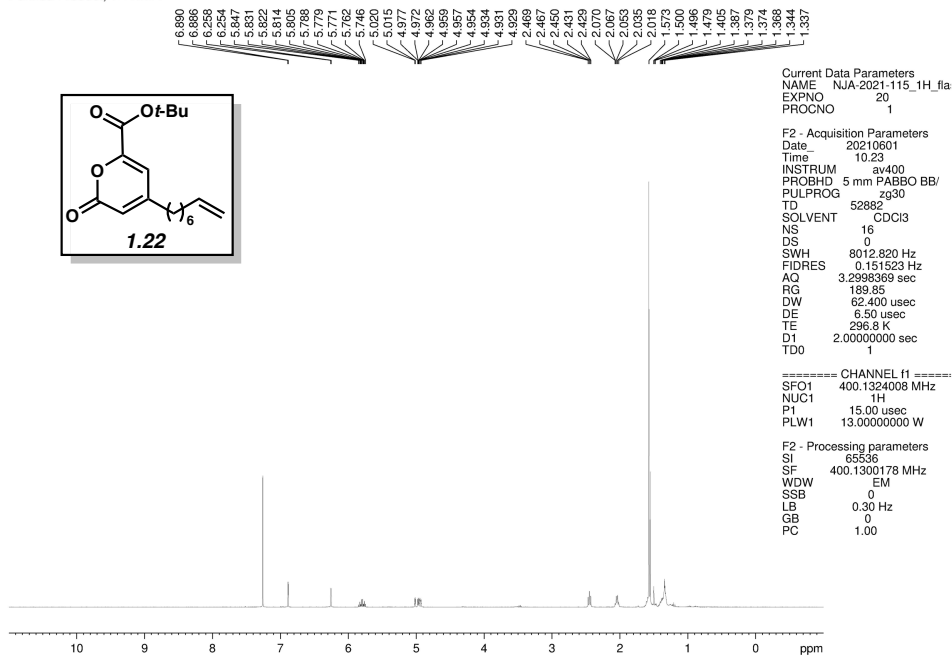


Figure 1.43. <sup>1</sup>H NMR (400 MHz, CDCl<sub>3</sub>) of compound 1.22.

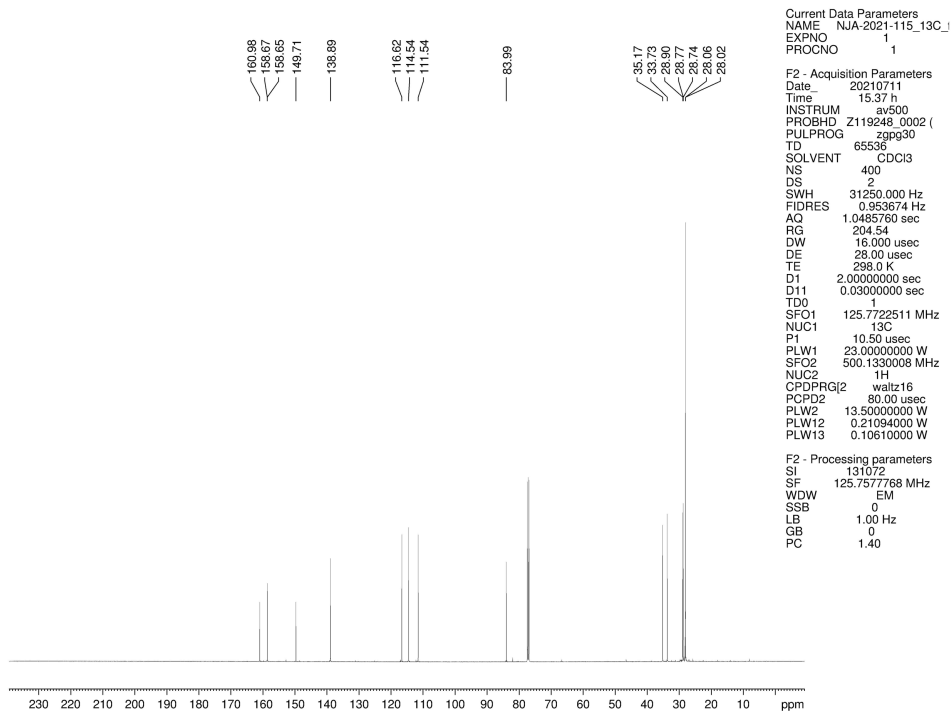
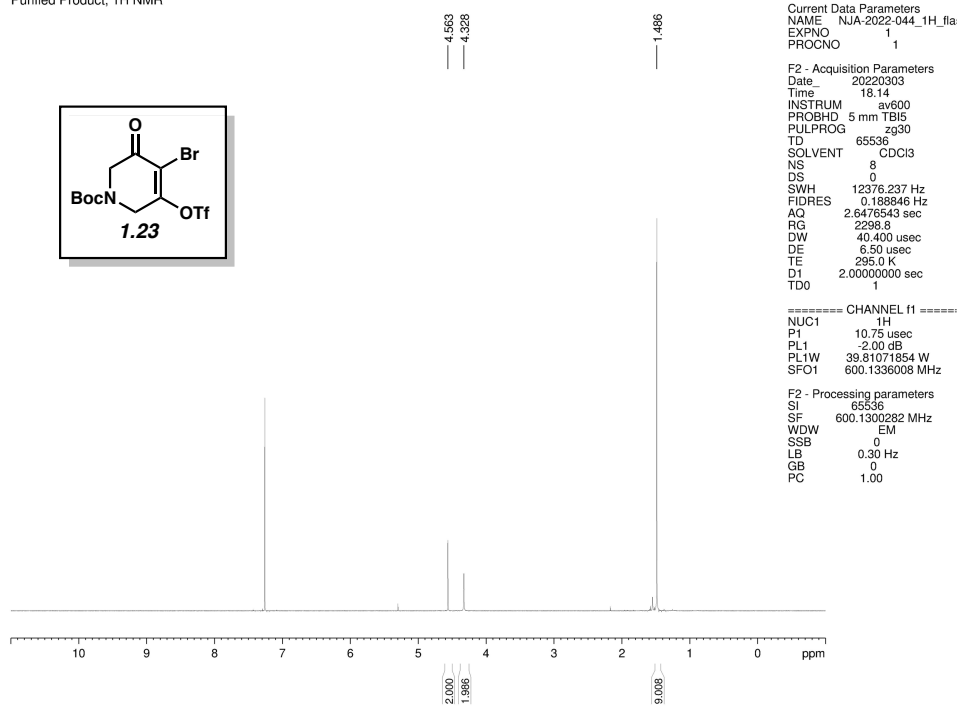


Figure 1.44. <sup>13</sup>C NMR (100 MHz, CDCl<sub>3</sub>) of compound 1.22.

Purified Product, <sup>1</sup>H NMR



**Figure 1.45.** <sup>1</sup>H NMR (600 MHz, CDCl<sub>3</sub>) of compound **1.23**.

Purified Product, <sup>13</sup>C NMR

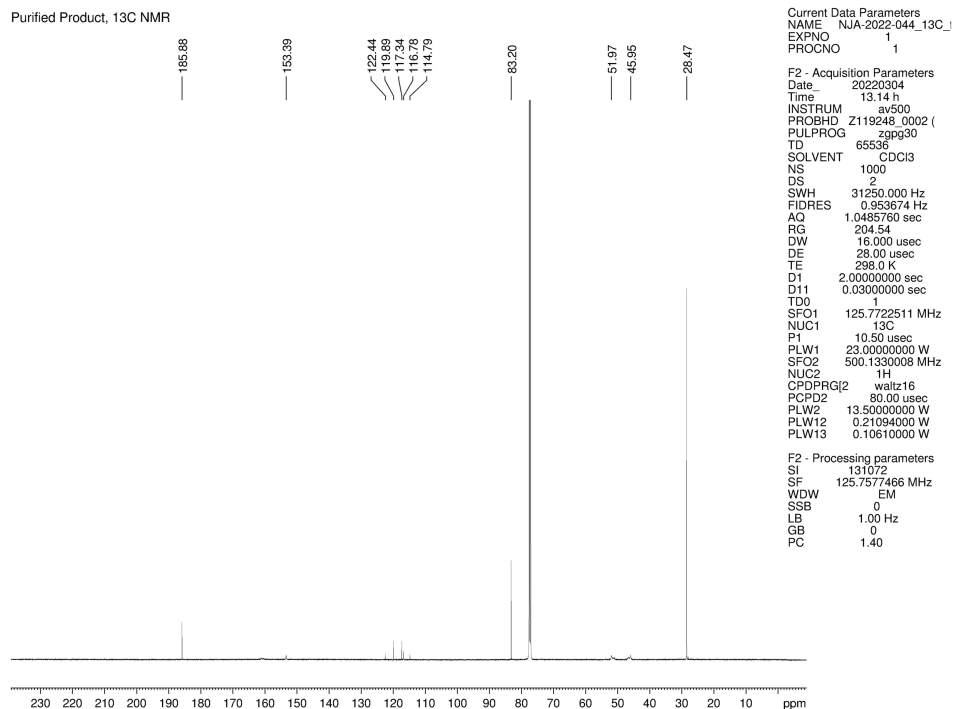


**Figure 1.46.** <sup>13</sup>C NMR (125 MHz, CDCl<sub>3</sub>) of compound **1.23**.

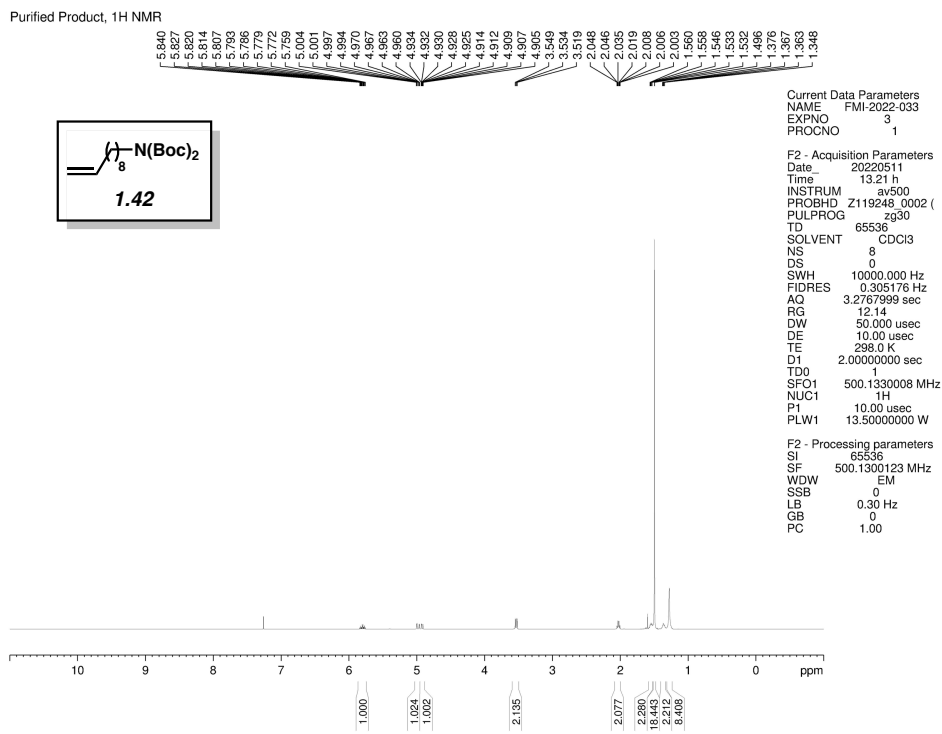


**Figure 1.47.** <sup>1</sup>H NMR (500 MHz, CDCl<sub>3</sub>) of compound **1.42**.

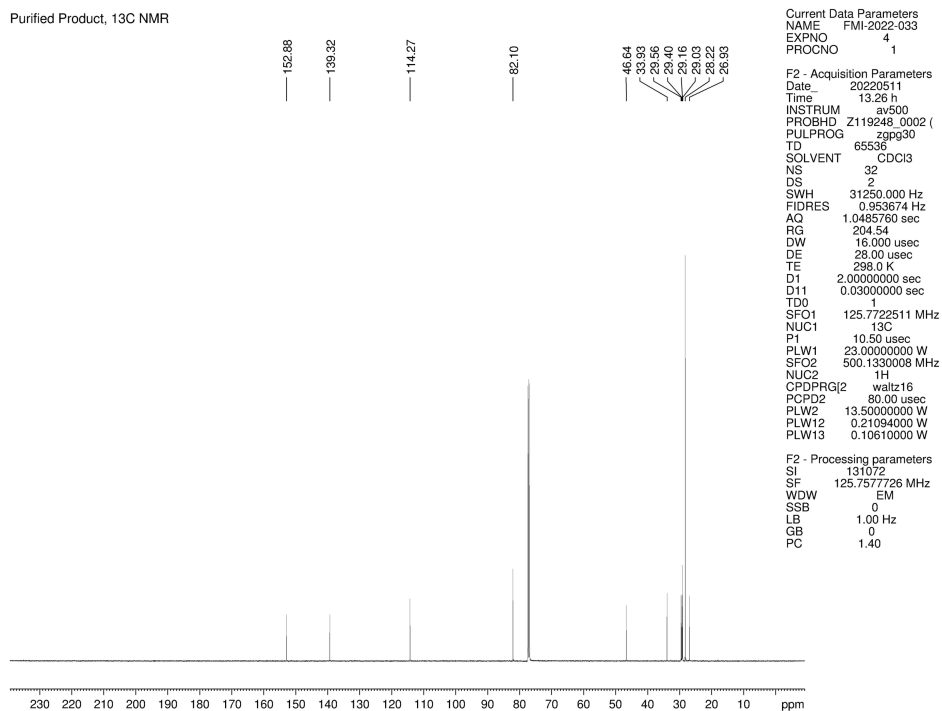


**Figure 1.48.** <sup>13</sup>C NMR (125 MHz, CDCl<sub>3</sub>) of compound **1.42**.

Purified Product, <sup>1</sup>H NMR

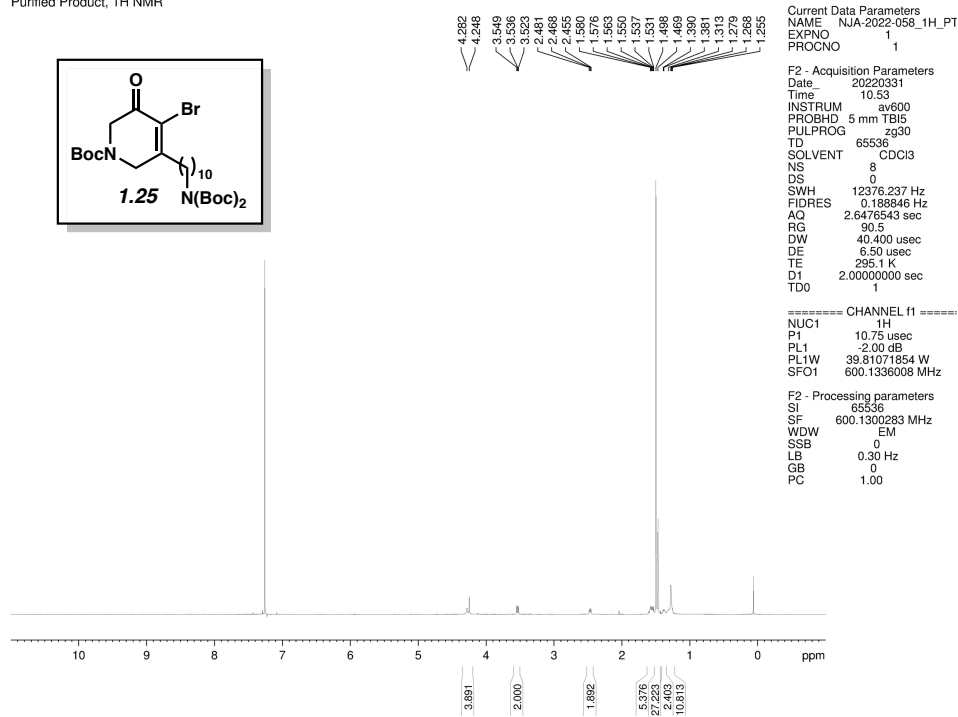


Figure 1.49. <sup>1</sup>H NMR (600 MHz, CDCl<sub>3</sub>) of compound 1.25.

Purified Product, <sup>13</sup>C NMR

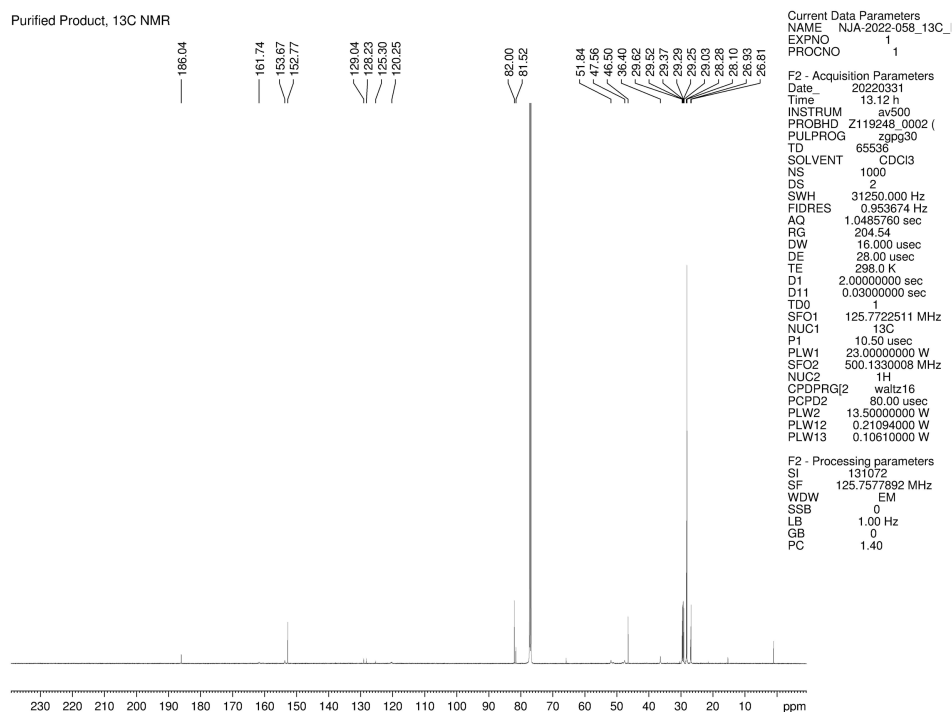


Figure 1.50. <sup>13</sup>C NMR (125 MHz, CDCl<sub>3</sub>) of compound 1.25.

Purified Product, <sup>1</sup>H NMR

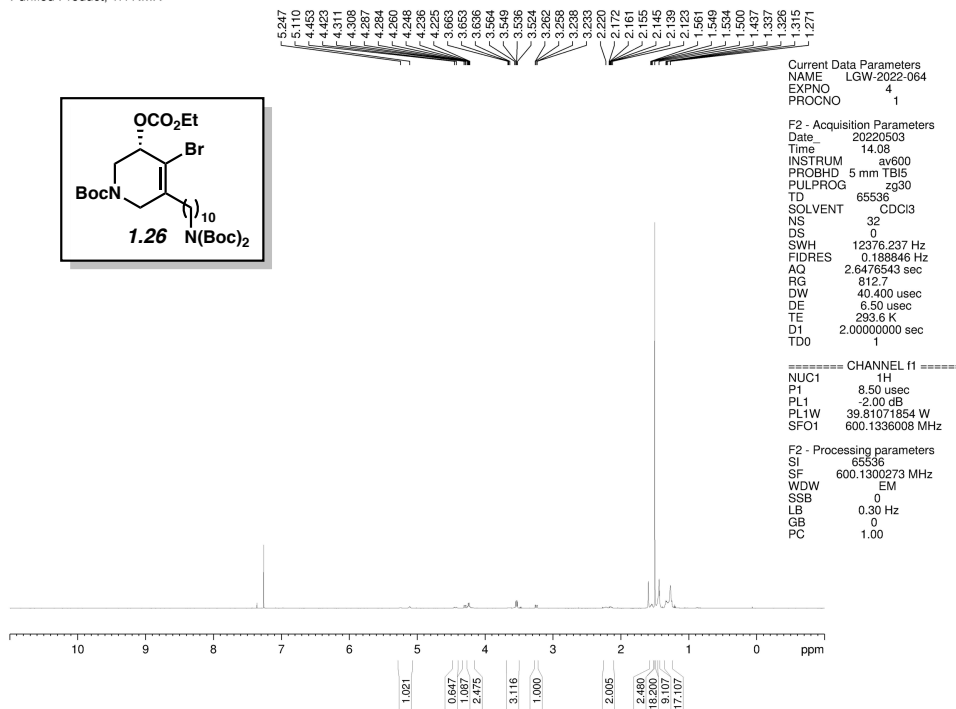


Figure 1.51. <sup>1</sup>H NMR (600 MHz, CDCl<sub>3</sub>) of compound 1.26.

Purified Product, <sup>13</sup>C NMR

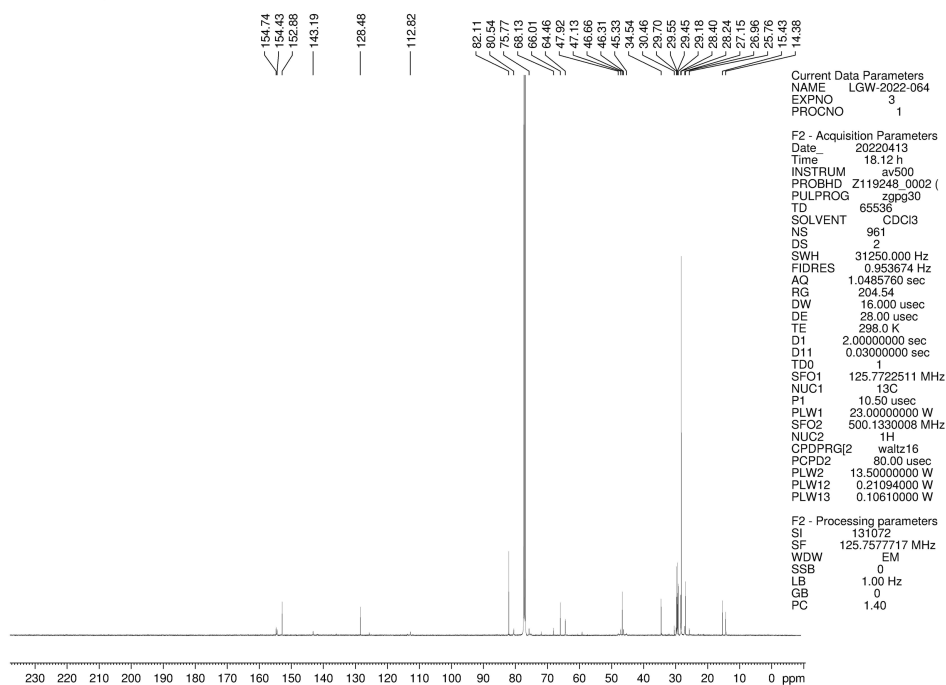
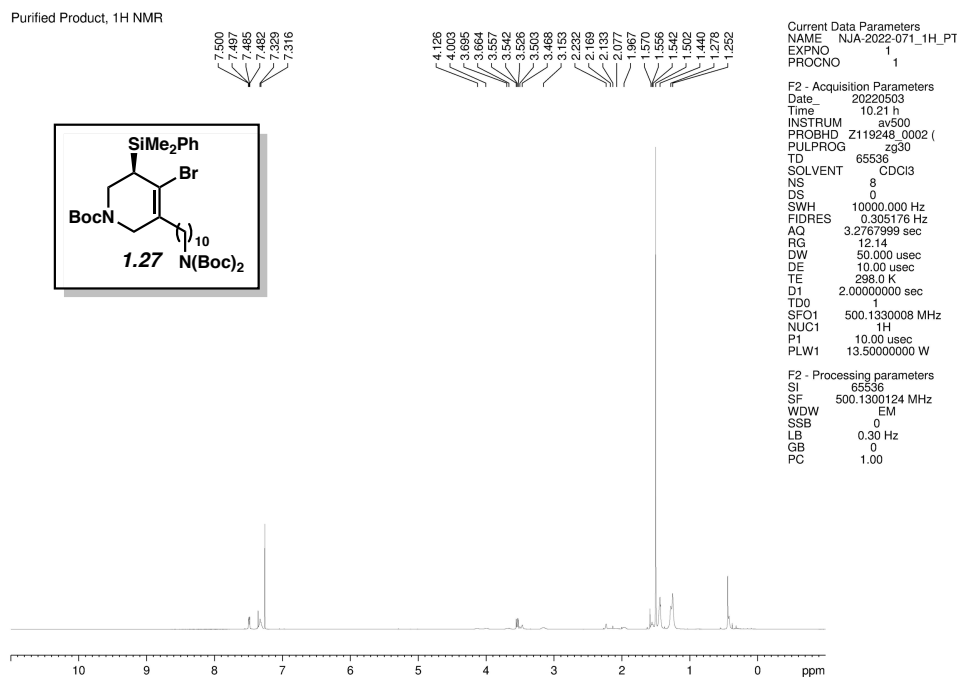
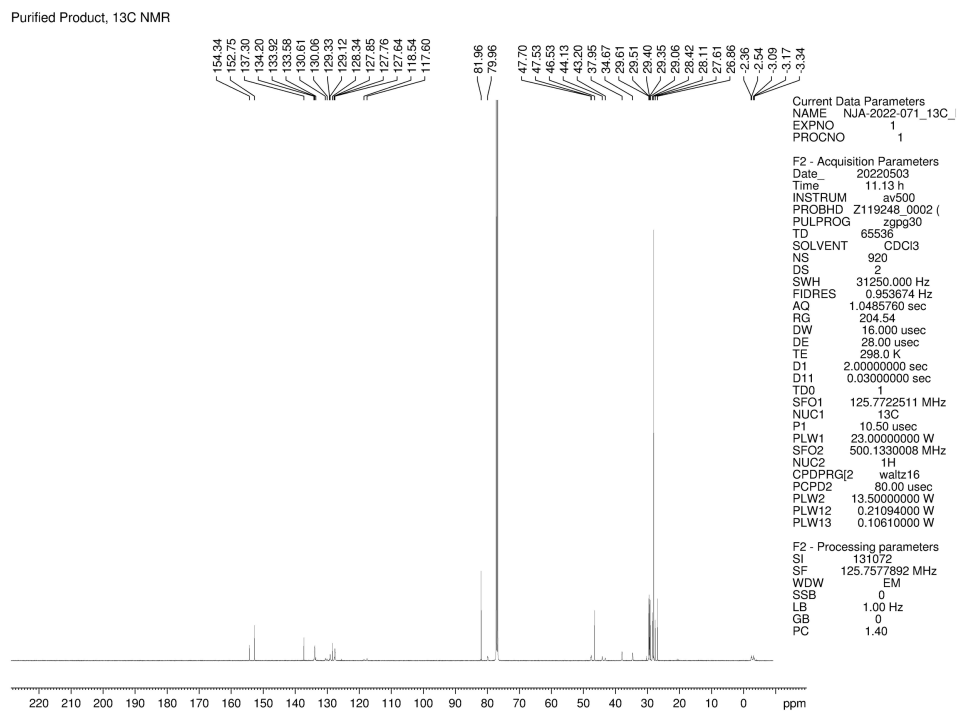


Figure 1.52. <sup>13</sup>C NMR (125 MHz, CDCl<sub>3</sub>) of compound 1.26.



**Figure 1.53.** <sup>1</sup>H NMR (500 MHz, CDCl<sub>3</sub>) of compound **1.27**.



**Figure 1.54.** <sup>13</sup>C NMR (125 MHz, CDCl<sub>3</sub>) of compound **1.27**.

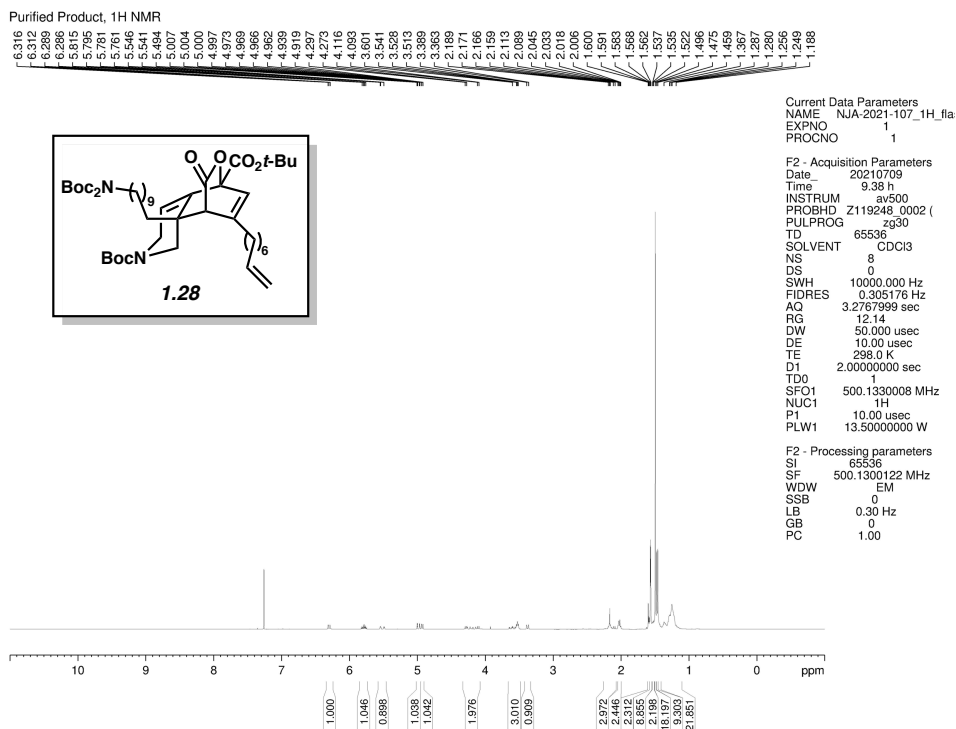


Figure 1.55. <sup>1</sup>H NMR (500 MHz, CDCl<sub>3</sub>) of compound 1.28.

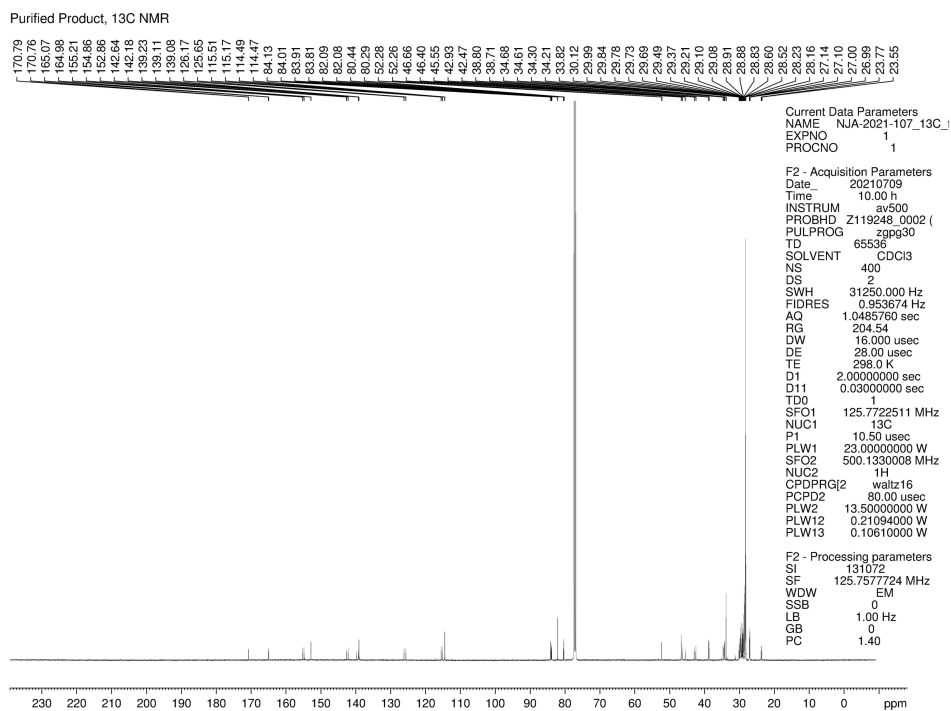


Figure 1.56. <sup>13</sup>C NMR (125 MHz, CDCl<sub>3</sub>) of compound 1.28.



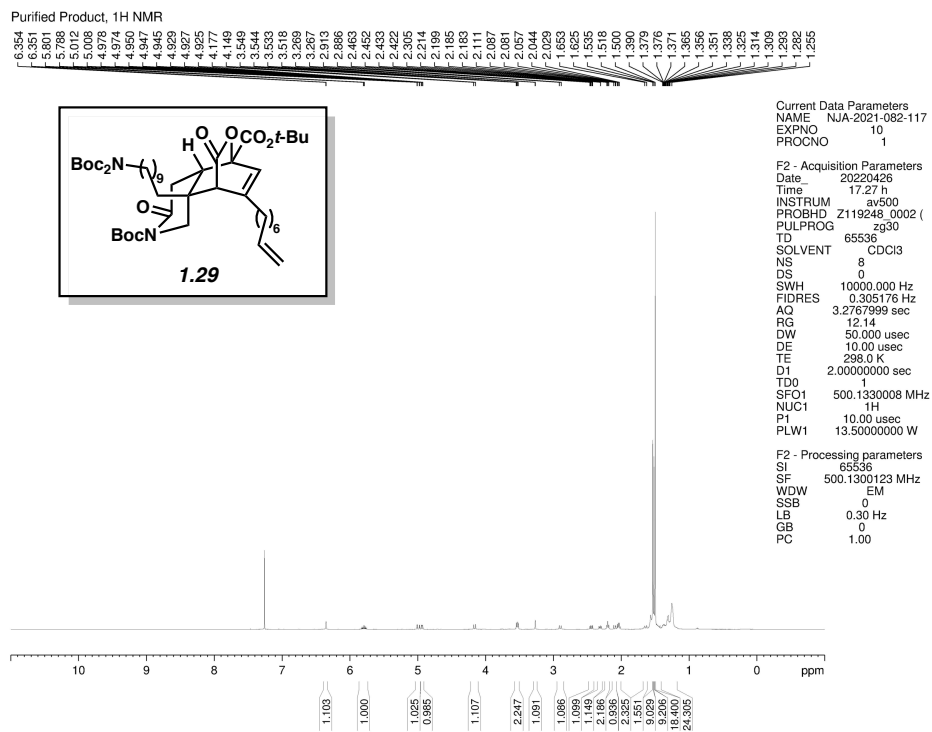


Figure 1.57. <sup>1</sup>H NMR (500 MHz, CDCl<sub>3</sub>) of compound 1.29.

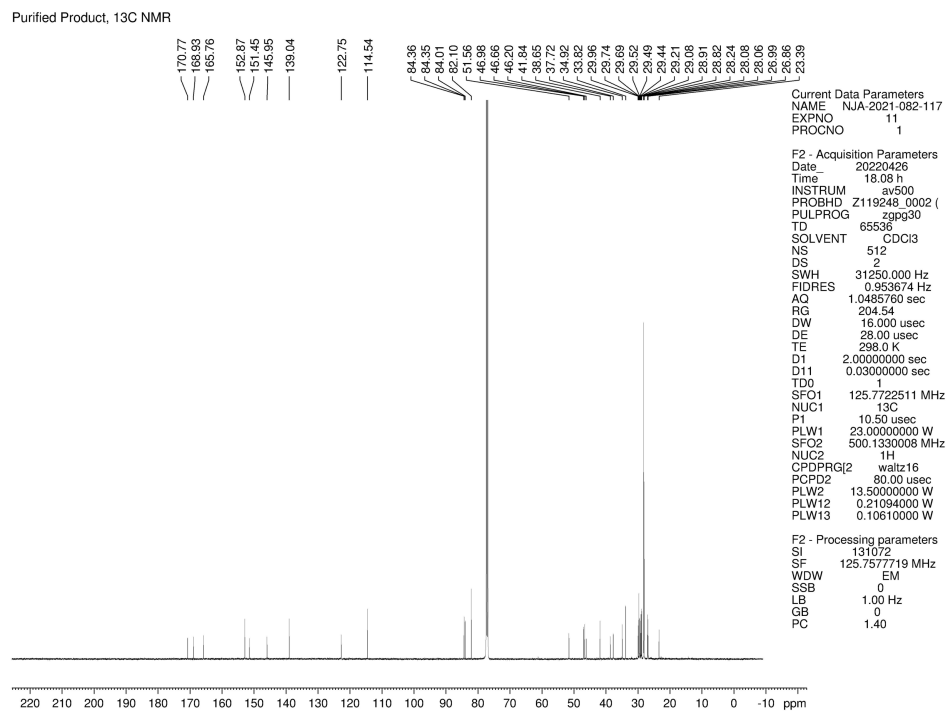


Figure 1.58. <sup>13</sup>C NMR (125 MHz, CDCl<sub>3</sub>) of compound 1.29.

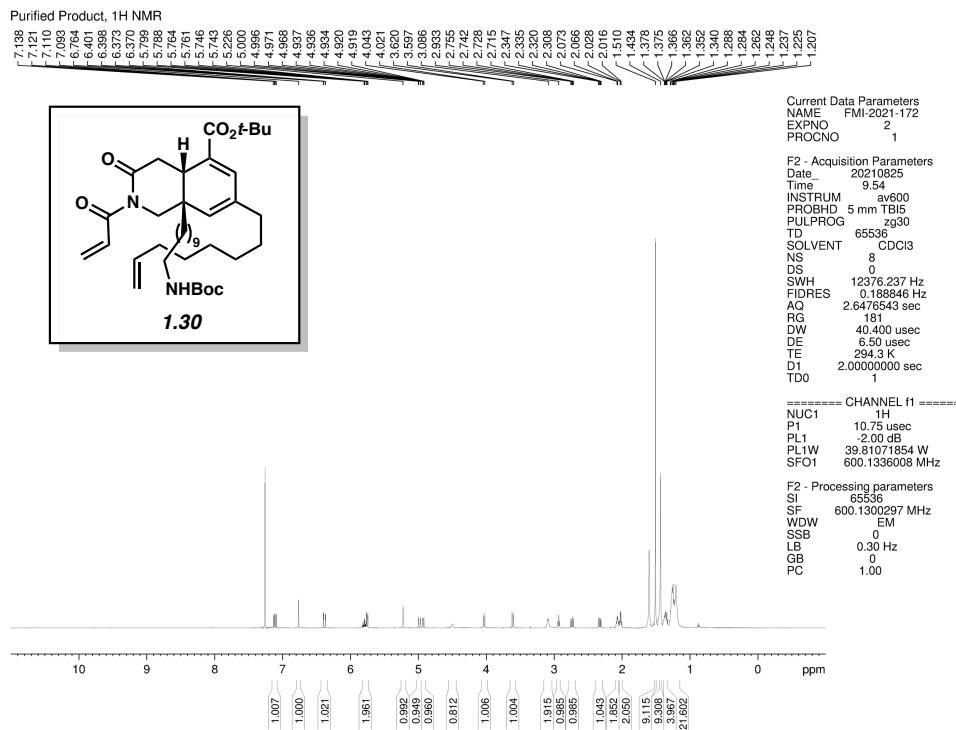


Figure 1.59. <sup>1</sup>H NMR (600 MHz, CDCl<sub>3</sub>) of compound 1.30.

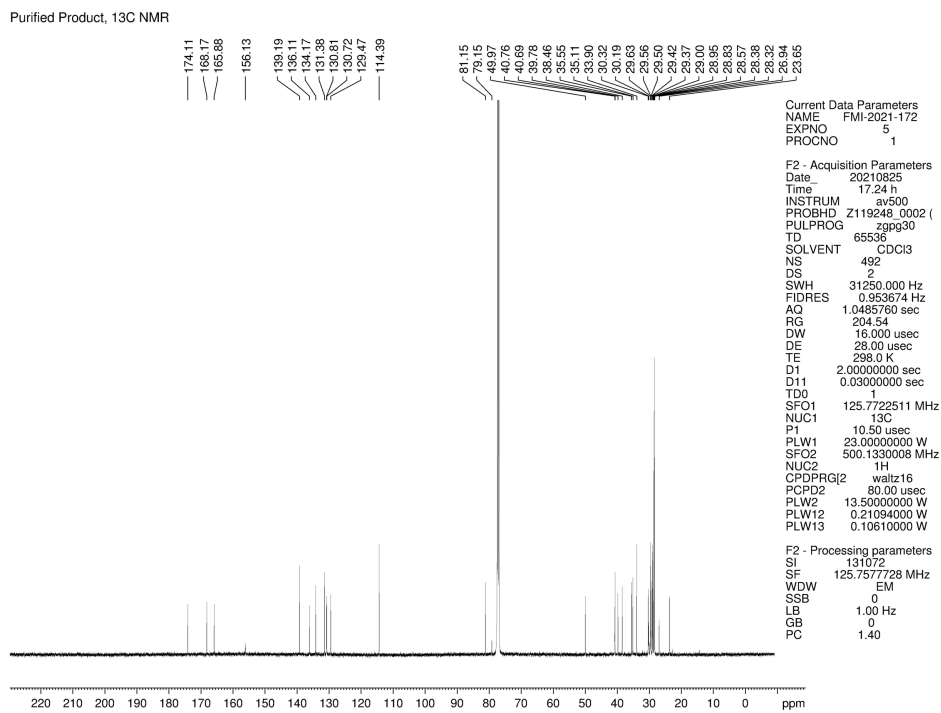


Figure 1.60. <sup>13</sup>C NMR (125 MHz, CDCl<sub>3</sub>) of compound 1.30.

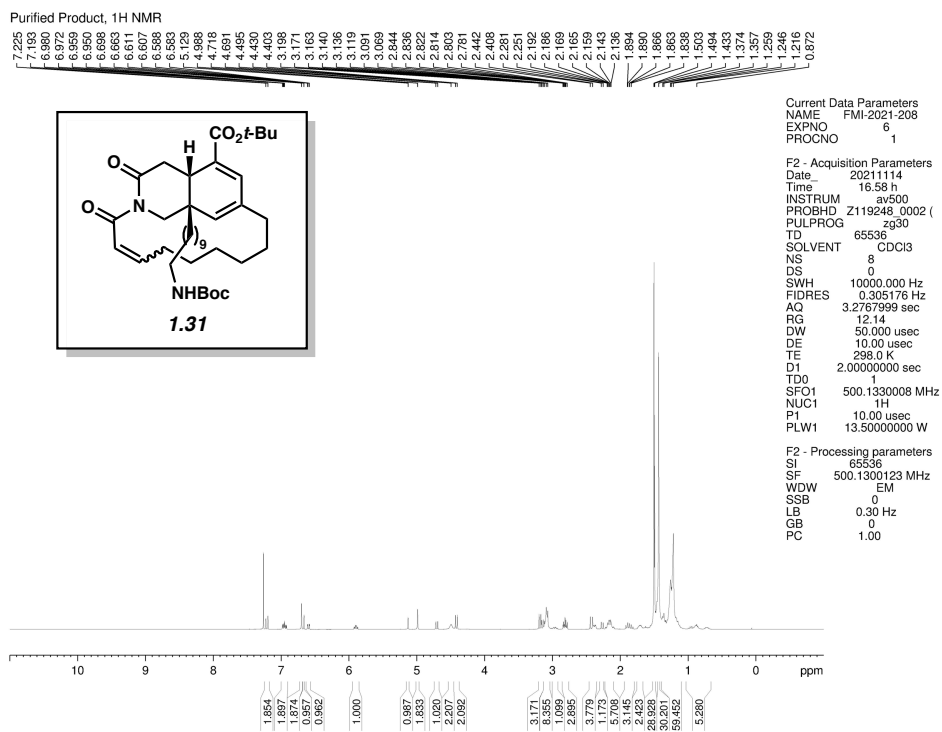


Figure 1.61. <sup>1</sup>H NMR (500 MHz, CDCl<sub>3</sub>) of compound **1.31**.

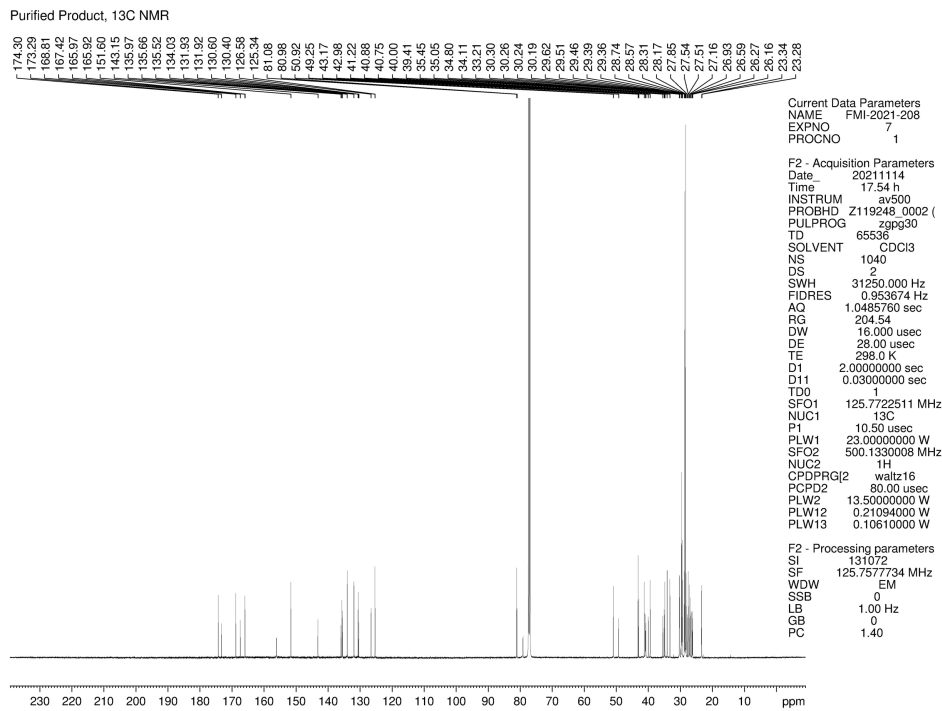


Figure 1.62. <sup>13</sup>C NMR (125 MHz, CDCl<sub>3</sub>) of compound **1.31**.

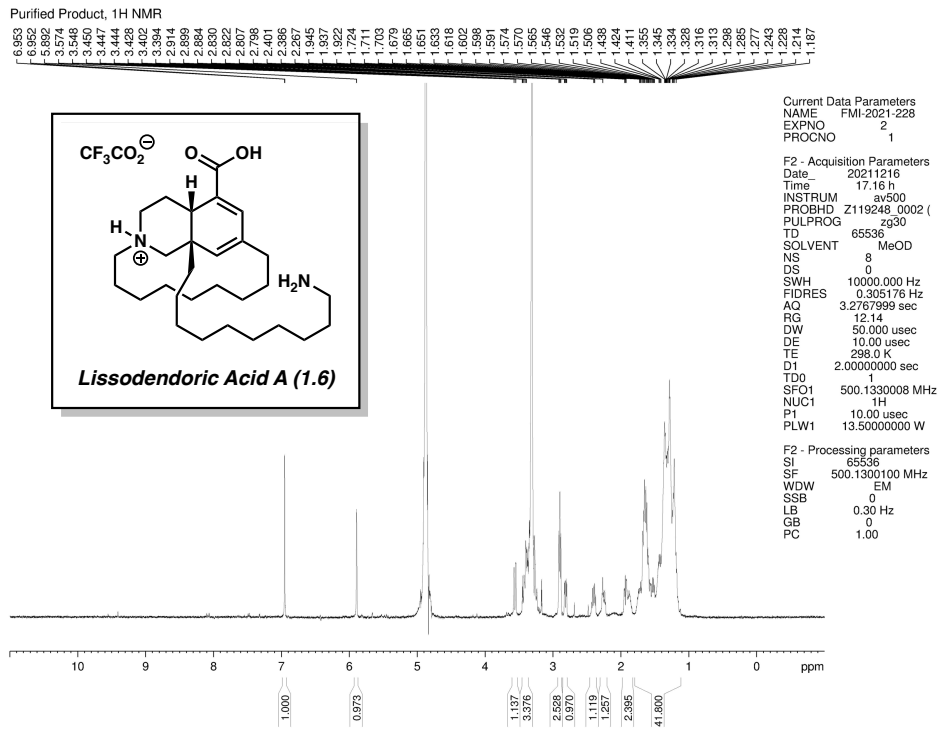


Figure 1.63. <sup>1</sup>H NMR (500 MHz, CD<sub>3</sub>OD) of compound 1.6.

## 1.7 Notes and References

- (1) Roberts, J. D.; Simmons, H. E.; Carlsmith, L. A.; Vaughn, C. W. Rearrangement in the Reaction of Chlorobenzene-1-C<sup>14</sup> with Potassium Amide. *J. Am. Chem. Soc.* **1953**, *75*, 3290–3291.
- (2) Wittig, G. Phenyl-lithium, der Schlüssel zu einer neuen Chemie metallorganischer Verbindungen. *Naturwissenschaften* **1942**, *30*, 696–703.
- (3) Wittig, G.; Pohmer, L. Intermediäre Bildung von Dehydrobenzol (Cyclohexa-dienin). *Angew. Chem.* **1955**, *67*, 348.
- (4) Wenk, H. H.; Winkler, M.; Sander, W. One Century of Aryne Chemistry. *Angew. Chem., Int. Ed.* **2003**, *42*, 502–528.
- (5) Tadross, P. M.; Stoltz, B. M. A Comprehensive History of Arynes in Natural Product Total Synthesis. *Chem. Rev.* **2012**, *112*, 3550–3577.
- (6) Gampe, C. M.; Carreira, E. M. Arynes and Cyclohexyne in Natural Product Synthesis. *Angew. Chem., Int. Ed.* **2012**, *51*, 3766–3778.
- (7) Takikawa, H.; Nishii, A.; Sakai, T.; Suzuki, K. Aryne-Based Strategy in the Total Synthesis of Naturally Occurring Polycyclic Compounds. *Chem. Soc. Rev.* **2018**, *47*, 8030–8056.
- (8) Anthony, S. M.; Wonilowicz, L. G.; McVeigh, M. S.; Garg, N. K. Leveraging Fleeting Strained Intermediates to Access Complex Scaffolds. *JACS Au* **2021**, *1*, 897–912.
- (9) Scardiglia, F.; Roberts, J. D. Evidence for Cyclohexyne as an Intermediate in the Coupling of Phenyllithium with 1-Chlorocyclohexene. *Tetrahedron* **1957**, *1*, 343–344.

- (10) Moser, W. M. The Reactions of gem-Dihalocyclopropanes with Organometallic Reagents. Ph. D. Thesis. Massachusetts Institute of Technology, Cambridge, MA, 1964.
- (11) Wittig, G.; Fritze, P. On the Intermediate Occurrence of 1,2-Cyclohexadiene. *Angew. Chem., Int. Ed. Engl.* **1966**, *5*, 846.
- (12) Liebman, J. F.; Greenberg, A. A Survey of Strained Organic Molecules. *Chem. Rev.* **1976**, *76*, 311–365.
- (13) Angus Jr., R. O.; Schmidt, M. W.; Johnson, R. P. Small-Ring Cyclic Cumulenes: Theoretical Studies of the Structure and Barrier to Inversion of Cyclic Allenes. *J. Am. Chem. Soc.* **1985**, *107*, 532–537.
- (14) Berry, R. S.; Clardy, J.; Schafer, M. E.; Benzyne. *J. Am. Chem. Soc.* **1964**, *86*, 2738–2739.
- (15) Diau, E. W.-G.; Casanova, J.; Roberts, J. D.; Zewail, A. H. Femtosecond Observation of Benzyne Intermediates in a Molecular Beam: Bergman Rearrangement in the Isolated Molecule. *Proc. Acad. Nat. Sci.* **2000**, *97*, 1376–1379.
- (16) Sletten, E. M.; Bertozzi, C. R. Bioorthogonal Chemistry: Fishing for Selectivity in a Sea of Functionality. *Angew. Chem., Int. Ed.* **2009**, *48*, 6974–6998.
- (17) Quitana, I.; Peña, D.; Pérez, D.; Guitián, E. Generation and Reactivity of 1,2-Cyclohexadiene Under Mild Reaction Conditions. *Eur. J. Org. Chem.* **2009**, 5519–5524.
- (18) Barber, J. S.; Yamano, M. M.; Ramirez, M.; Darzi, E. R.; Knapp, R. R.; Liu, F.; Houk, K. N.; Garg, N. K. Diels–Alder Cycloadditions of Strained Azacyclic Allenes. *Nat. Chem.* **2018**, *10*, 953–960.

- (19) Lofstrand, V. A.; West, F. G. Efficient Trapping of 1,2-Cyclohexadienes with 1,3-Dipoles. *Chem. Eur. J.* **2016**, *22*, 10763–10767.
- (20) Barber, J. S.; Styduhar, E. D.; Pham, H. V.; McMahon, T. C.; Houk, K. N.; Garg, N. K. Nitrono Cycloadditions of 1,2-Cyclohexadiene. *J. Am. Chem. Soc.* **2016**, *138*, 2512–2515.
- (21) Yamano, M. M.; Knapp, R. R.; Ngamnithiporn, A.; Ramirez, M.; Houk, K. N.; Stoltz, B. M.; Garg, N. K. Cycloadditions of Oxacyclic Allenes and a Catalytic Asymmetric Entryway to Enantioenriched Cyclic Allenes. *Angew. Chem., Int. Ed.* **2019**, *58*, 5653–5657.
- (22) Lofstrand, V. A.; McIntosh, K. C.; Almeahadi, Y. A.; West, F. G. Strain-Activated Diels–Alder Trapping of 1,2-Cyclohexadienes: Intramolecular Capture by Pendent Furans. *Org. Lett.* **2019**, *21*, 6231–6234.
- (23) Yamano, M. M.; Kelleghan, A. V.; Shao, Q.; Giroud, M.; Simmons, B. J.; Li, B.; Chen, S.; Houk, K. N.; Garg, N. K. Intercepting Fleeting Cyclic Allenes with Asymmetric Nickel Catalysis. *Nature* **2020**, *586*, 242–247.
- (24) Kelleghan, A. V.; Witkowski, D. C.; McVeigh, M. S.; Garg, N. K. Palladium-Catalyzed Annulations of Strained Cyclic Allenes. *J. Am. Chem. Soc.* **2021**, *143*, 9338–9342.
- (25) Westphal, M. V.; Hudson, L.; Mason, J. W.; Pradeilles, J. A.; Zécri, F.; J.; Briner, K.; Schreiber, S. L. Water-Compatible Cycloadditions of Oligonucleotide-Conjugated Strained Allenes for DNA-Encoded Library Synthesis. *J. Am. Chem. Soc.* **2020**, *142*, 7776–7782.

- (26) Radwan, M.; Hanora, A.; Khalifa, S.; Abou-El-Ela, S. H. Manzamines. *Cell Cycle* **2012**, *11*, 1765–1772.
- (27) Lyakhova, E. G.; Kolesnikova, S. A.; Kalinovsky, A. I.; Berdyshev, D. V.; Pislyagin, E. A.; Kuzmich, A. S.; Popov, R. S.; Dmitrenok, P. S.; Makarieva, T. N.; Stonik, V. A. Lissodendoric Acids A and B, Manzamine-Related Alkaloids from the Far Eastern Sponge *Lissodendoryx florida*. *Org. Lett.* **2017**, *19*, 5320–5323.
- (28) Luo, T.; Dai, M.; Zheng, S.-L.; Schreiber, S. L. Syntheses of  $\alpha$ -Pyrone Using Gold-Catalyzed Coupling Reactions. *Org. Lett.* **2011**, *13*, 2834–2836.
- (29) Ramirez, M.; Svatunek, D.; Liu, F.; Garg, N. K.; Houk, K. N. Origins of *Endo* Selectivity in Diels–Alder Reactions of Cyclic Allene Dienophiles. *Angew. Chem., Int. Ed.* **2021**, *60*, 14989–14997.
- (30) Wipf, P.; Smitrovich, J. H. Transmetalation Reactions of Alkylzirconocenes: Copper-Catalyzed Conjugate Addition to Enones. *J. Org. Chem.* **1991**, *56*, 6494–6496.
- (31) Corey, E. J.; Helal, C. J. Reduction of Carbonyl Compounds with Chiral Oxazaborolidine Catalysts: A New Paradigm for Enantioselective Catalysis and a Powerful New Synthetic Method. *Angew. Chem., Int. Ed.* **1998**, *37*, 1986–2012.
- (32) Ito, H.; Horita, Y.; Sawamura, M. Copper(I)-Catalyzed Allylic Substitution of Silyl Nucleophiles through Si–Si Bond Activation. *Adv. Synth. Catal.* **2012**, *354*, 813–817.
- (33) Weickgenannt, A.; Oestreich, M. Silicon- and Tin-Based Cuprates: Now Catalytic in Copper! *Chem. Eur. J.* **2010**, *16*, 402–412.
- (34) Baker, B. A.; Bošković, Z. V.; Lipshutz, B. H. (BDP)CuH: A “Hot” Stryker’s Reagent for Use in Achiral Conjugate Reductions. *Org. Lett.* **2008**, *10*, 289–292.



- (35) Abdullahi, M. H.; Thompson, L. M.; Bearpark, M. J.; Vinader, V.; Afarinkia, K. The Role of Substituents in Retro Diels–Alder Extrusion of CO<sub>2</sub> from 2(*H*)-Pyrone Cycloadducts. *Tetrahedron* **2016**, *72*, 6021–6024.
- (36) Evans, V.; Mahon, M. F.; Webster, R. L. A Mild, Copper-Catalysed Amide Deprotection Strategy: Use of *tert*-Butyl as a Protecting Group. *Tetrahedron* **2014**, *70*, 7593–7597.
- (37) a) Chatterjee, A. K.; Morgan, J. P.; Scholl, M.; Grubbs, R. H. Synthesis of Functionalized Olefins by Cross and Ring-Closing Metathesis. *J. Am. Chem. Soc.* **2000**, *122*, 3783–3784;  
b) Chatterjee, A. K.; Choi, T.-L.; Sanders, D. P.; Grubbs, R. H. A General Model for Selectivity in Olefin Cross Metathesis. *J. Am. Chem. Soc.* **2003**, *125*, 11360–11370.
- (38) Das, S.; Li, Y.; Lu, L.-Q.; Junge, K.; Beller, M. A General and Selective Rhodium-Catalyzed Reduction of Amides, *N*-Acyl Amino Esters, and Dipeptides Using Phenylsilane. *Chem. Eur. J.* **2016**, *22*, 7050–7053.
- (39) Ishikawa, T.; Mizuta, T.; Hagiwara, K.; Aikawa, T.; Kudo, T.; Saito, S. Catalytic Alkynylation of Ketones and Aldehydes Using Quaternary Ammonium Hydroxide Base. *J. Org. Chem.* **2003**, *68*, 3702–3705.
- (40) Huo, S. Highly Efficient, General Procedure for the Preparation of Alkylzinc Reagents from Unactivated Alkyl Bromides and Chlorides. *Org. Lett.* **2003**, *5*, 423–425.

## CHAPTER TWO

### Total Synthesis of Lissodendoric Acid A

Francesca M. Ippoliti, Nathan J. Adamson, Laura G. Wonilowicz,

Evan R. Darzi, Joyann S. Donaldson, and Neil K. Garg.

*Manuscript in Preparation.*

#### 2.1 Abstract

Lissodendoric acid A is a member of the manzamine family of alkaloids and was first isolated in 2017 from *Lissodendoryx florida*. Structurally, the natural product contains a 14-membered macrocycle and an azadecalin core that is conserved across the manzamine family of alkaloids. This chapter describes a full account of our synthetic strategy to achieve the first total synthesis of lissodendoric acid A by utilizing a strained cyclic allene Diels–Alder cycloaddition to build the azadecalin core.

#### 2.2 Introduction

Strained aryne intermediates have been used in the synthesis of natural products for the past half century.<sup>1</sup> The first example involved the use of aryne **2.1** in the synthesis of cryptaustoline (**2.4**) by Kametani and coworkers in 1967 (Figure 2.1). More recently, indolyne **2.2** was used in the synthesis of *N*-methylwelwitindolinone C isothiocyanate (**2.5**) by our own lab. In addition to strained arynes, cyclohexyne (**2.3**) has also been explored as a building block in total synthesis, demonstrated by Carreira's 2011 synthesis of guanacastepene N (**2.6**). Although some strained intermediates have seen ample use in the synthesis of natural products,

one subclass that has not been employed in total synthesis is cyclic allenes. The first strained cyclic allene to be generated and trapped in cycloadditions was 1,2-cyclohexadiene (**2.7**), first by Moore and Moser in 1964<sup>2</sup> and subsequently by Wittig and Fritze in 1966.<sup>3</sup> Despite cyclic allenes being known as viable reaction partners in cycloadditions, advancements in their generation and synthetic use were slow to arise. For example, the first strained azacyclic allene (i.e., **2.8a**, Figure 2.1) was generated by Christl and coworkers in 1994.<sup>4</sup> The slow pace of reaction development using strained cyclic allenes was presumably due to the harsh reaction conditions or pyrophoric reagents necessary to generate these fleeting intermediates. It was not until 2009, when Guitián and coworkers developed a silyl triflate precursor to 1,2-cyclohexadiene (**2.7**) activated by mild reaction conditions (i.e., TBAF as a fluoride source at room temperature),<sup>5</sup> that the field of synthetic chemistry began readily considering strained cyclic allenes as a valuable building blocks.<sup>6</sup>

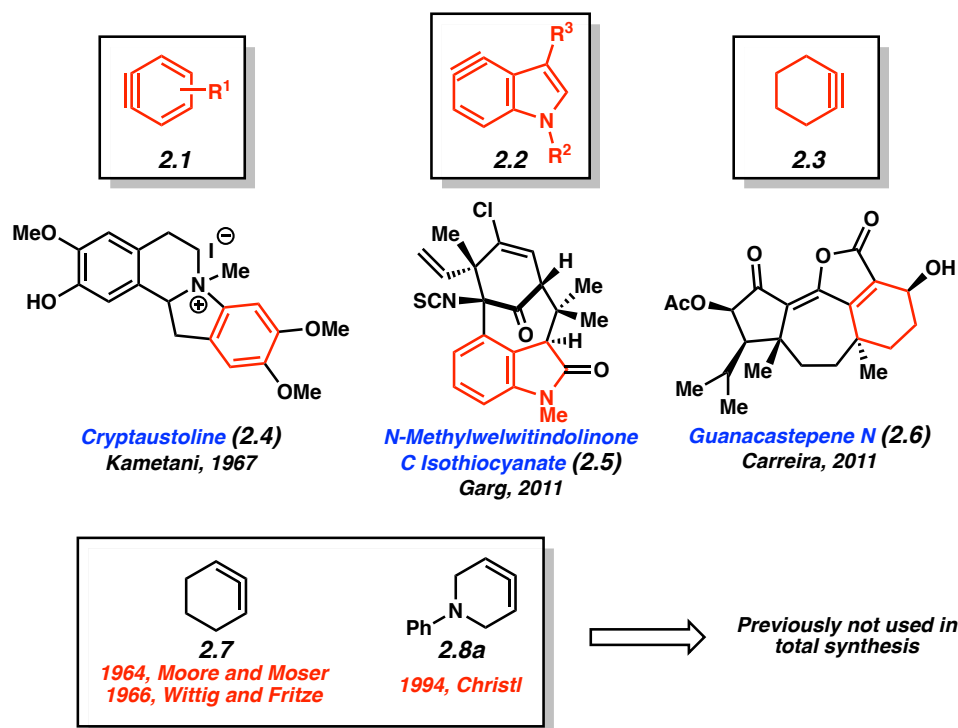


**Figure 2.1.** Select strained intermediates and their use in total synthesis.

Considering the cycloadducts formed via Diels–Alder reactions of strained cyclic allenes, we envisioned using azacyclic allene **2.8** to access the azadecalin cores of manzamine alkaloids such as the family’s namesake, manzamine A (**2.9**), or the more recently isolated manzamine alkaloid, lissodendoric acid A (**2.10**, Figure 2.2). The manzamine family of alkaloids is intriguing due to its broad display of biological activity, such as anti-cancer, insecticidal, anti-bacterial, and anti-inflammatory properties, among others.<sup>7</sup> Specifically, lissodendoric acid A (**2.10**) has been demonstrated to reduce reactive oxygen species in neuroblastoma cells treated with 6-hydroxydopamine, which are employed as an in vitro model for Parkinson’s disease.<sup>8</sup> Lissodendoric acid A (**2.10**) was first isolated in 2017 from the sea sponge *Lissodendoryx florida* which is found in the Sea of Okhotsk, located between Japan and Russia. Structurally, lissodendoric acid A (**2.10**) contains two stereocenters, one of which is quaternary, a 14-membered macrocycle, and the azadecalin core that is conserved across the family of manzamine alkaloids. Prior to the studies shown in Chapter 1,<sup>9</sup> there had been no syntheses of **2.10**. This chapter describes a full account of our efforts to accomplish the first total synthesis of lissodendoric acid A (**2.10**).

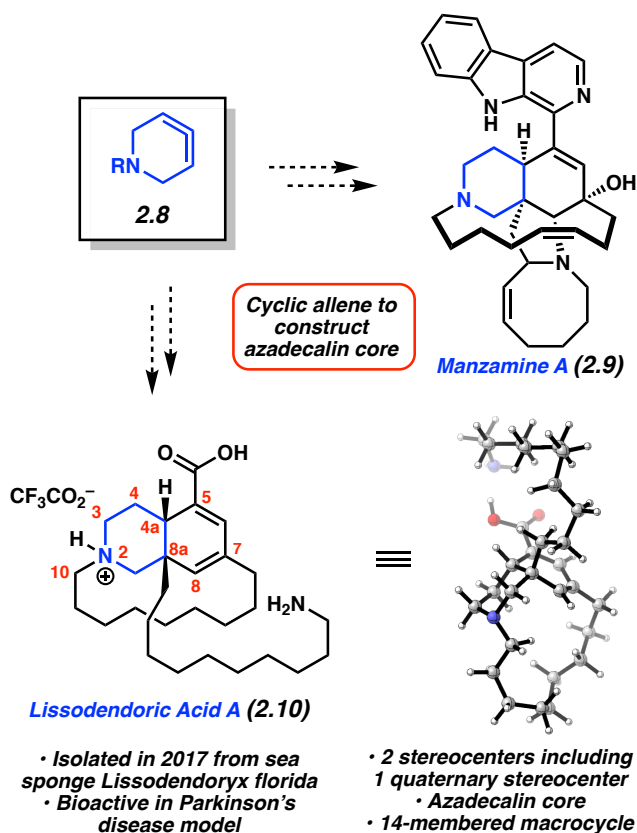


**Figure 2.2.** Envisioned use of an azacyclic allene to construct cores of manzamine alkaloids **2.8** and **2.9** (geometry optimized structure using B3LYP/6-31G\*).

Our laboratory's previous study on azacyclic allene Diels–Alder reactions showed that with an alkyl-substituted allene, such as **2.11**, cycloaddition of furan (**2.12**) preferentially occurs on the double bond distal to the alkyl group, as shown in Figure 2.3a.<sup>6a</sup> In order for an allene, such as **2.14**, to be used in building the azadecalin core of lissodendoric acid A (**2.10**), allene trapping would need to occur on the more electron-rich double bond proximal to the alkyl substituent. We hypothesized that altering the electronics of the trapping partner to an electron-poor diene would influence the regioselectivity of the cycloaddition, such that it would occur on the more electron-rich double bond. Notably, the trapping of allene **2.14** with an electron-poor diene was expected to proceed through and inverse-electron demand Diels–Alder cycloaddition.

We envisioned that a pyrone, such as **2.15**, could serve as a suitable electron-poor diene and afford cycloadduct **2.16** as the desired regioisomer when reacted with in situ generated allene **2.14**. Furthermore, the resulting bridged ring system in **2.16** would prove strategic, as CO<sub>2</sub> could be readily extruded upon heating to unveil a diene, as is present in natural product **2.10**.<sup>10</sup>

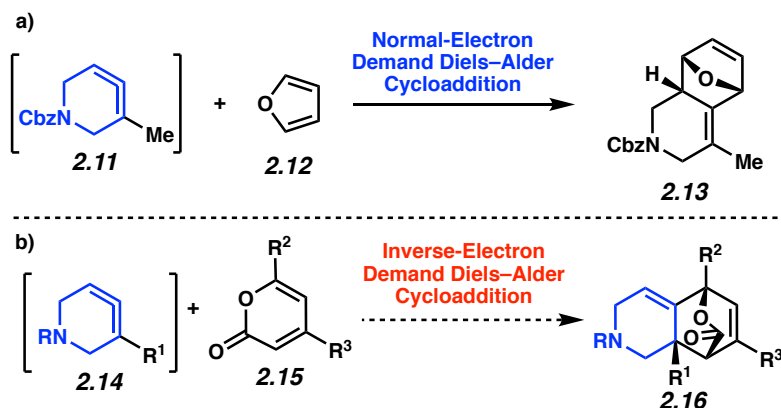


**Figure 2.3.** a) Known cycloaddition of azacyclic allene **2.11**. b) Envisioned inverse-electron demand Diels–Alder cycloaddition.

### 2.3 Model System Studies

With the expectation that an inverse-electron demand Diels–Alder reaction would give the desired regioisomer, we opted to test our hypothesis on a model system. To this end, we designed pyrone **2.20**, which contains a vinyl bromide as a potential cross-coupling handle and a benzyl-protected alcohol that we envisioned could be unveiled and oxidized to the carboxylic acid found in **2.10**. To synthesize pyrone **2.20**, we began with bromination of propiolic acid (**2.17**). Next, a gold-catalyzed cyclization between bromopropiolic acid (**2.18**) and benzyl propargyl ether (**2.19**) afforded desired pyrone **2.20** in 61% yield.<sup>11</sup> Upon treatment of model methyl substituted silyl triflate **2.21** with CsF, allene **2.22** was generated in situ and trapped with

pyrone **2.20** to deliver cycloadduct **2.23** in 48% yield and >20:1 dr. Additionally, this reaction was performed with enantioenriched silyl triflate **2.21** (separated by chiral SFC), which led to cycloadduct **2.23** with 100% stereoretention, demonstrating the excellent stereospecificity of this reaction. With the desired regioisomer formed in the methyl model system, we designed a synthesis of lissodendoric acid A (**2.10**).

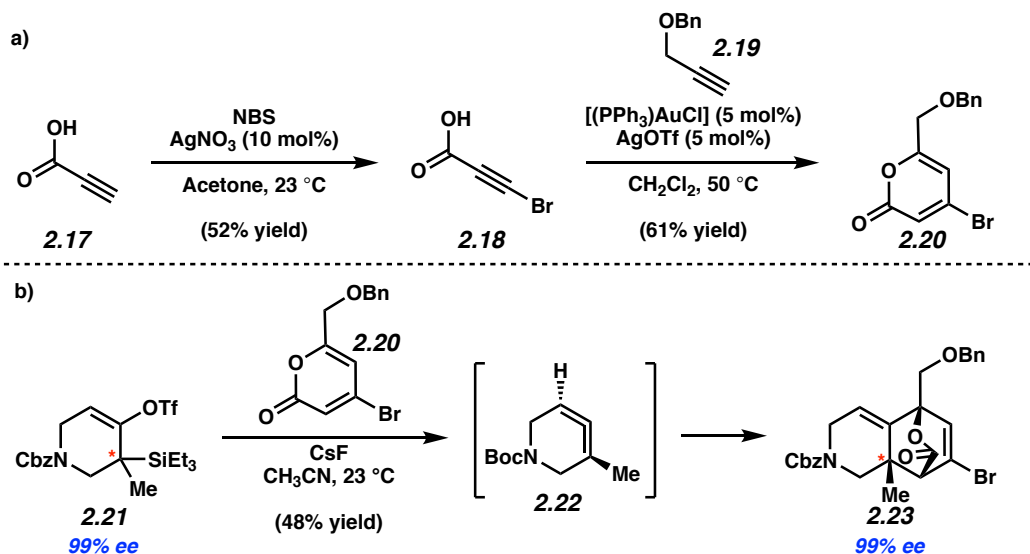


**Figure 2.4.** a) Synthesis of pyrone **2.20**. b) Diels–Alder reaction on model system.

## 2.4 Synthesis of Cycloadduct and Macrocycle en Route to Lissodendoric Acid A

In our first-generation retrosynthetic analysis, we envisioned accessing lissodendoric acid A (**2.10**) from macrocycle **2.24** through redox manipulations of the benzyl-protected alcohol and  $\alpha,\beta$ -unsaturated amide followed by deprotection of the Boc-protected primary amine (Figure 2.5). Macrocycle **2.24** was thought to be available from diene **2.25** through cross-coupling, protecting group manipulations, and ring-closing metathesis. Diene **2.25** could arise from cycloadduct **2.26** via a selective reduction of the tri-substituted olefin over the vinyl bromide

followed by a retro-Diels–Alder reaction to extrude CO<sub>2</sub>. Finally, cycloadduct **2.26** could result from the Diels–Alder reaction between in situ-generated allene **2.27** and readily accessible pyrone **2.20**.

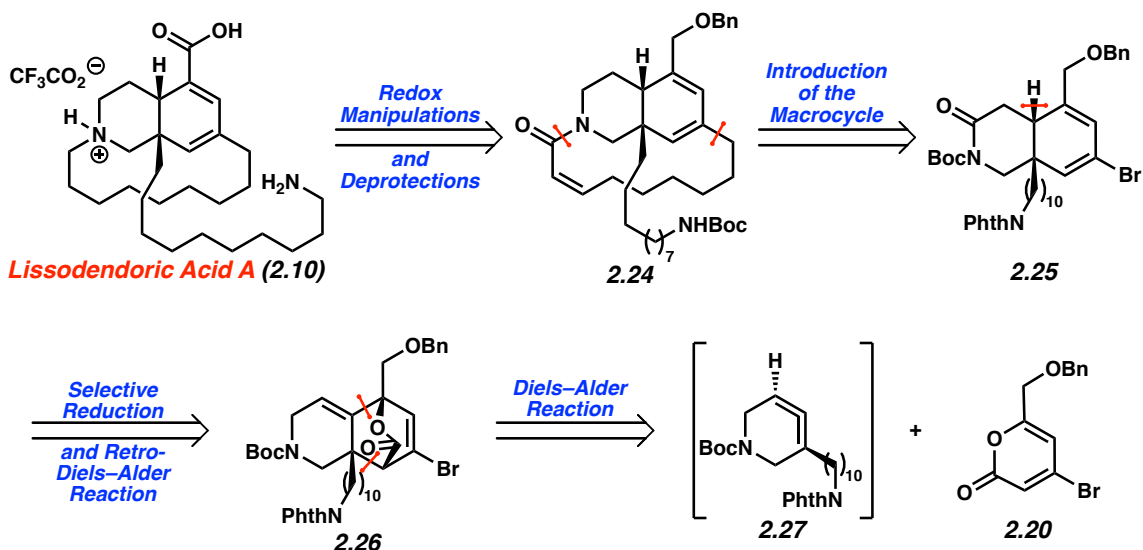


**Figure 2.5.** Retrosynthetic analysis of lissodendoric acid A (**2.10**).

As pyrone **2.20** was already in hand from our model system studies (see Figure 2.4), we aimed to synthesize silyl triflate **2.33**, which we considered a plausible precursor to cyclic allene **2.27** (Figure 2.6). From commercially available  $\alpha$ -bromo ketone **2.28**, formation of the silyl enol ether followed by retro-Brook rearrangement and trapping with ethyl chloroformate delivered carbonate **2.29** in 70% yield over two steps. Upon treatment with Pd(PPh<sub>3</sub>)<sub>4</sub>, carbonate **2.29** underwent allylic alkylation to afford allyl ketone **2.30**.<sup>12</sup> Next, olefin cross-metathesis with alkene **2.31** followed by hydrogenation provided ketone **2.32** in 90% yield over two steps. Finally, triflation of ketone **2.32** occurred readily to deliver silyl triflate **2.33** in 94% yield.



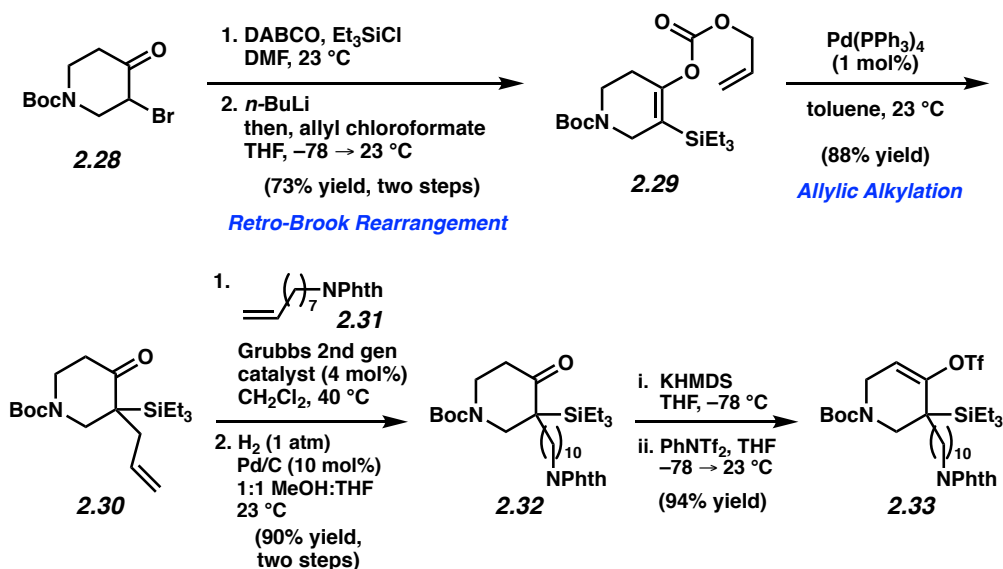


**Figure 2.6.** Synthesis of silyl triflate **2.33**.

With both pyrone **2.20** and silyl triflate **2.33** in hand, the key azacyclic allene Diels–Alder reaction was evaluated (Figure 2.7). Treatment of silyl triflate **2.33** with pyrone **2.20** in the presence of CsF afforded desired cycloadduct **2.26** in 75% yield with excellent diastereoselectivity. This transformation presumably proceeds via allene **2.27** and leads to the formation of two new C–C bonds, three new stereocenters, and the desired azadecalin scaffold. Notably, this reaction can be performed on gram scale. The success of this key Diels–Alder cycloaddition established the strained allene methodology as a viable strategy for constructing the core of lissodendoric acid A (**2.10**). With cycloadduct **2.26** in hand, the remaining challenges in the total synthesis of **2.10** included a selective hydrogenation of the C4–C4a alkene and installation of the macrocycle.

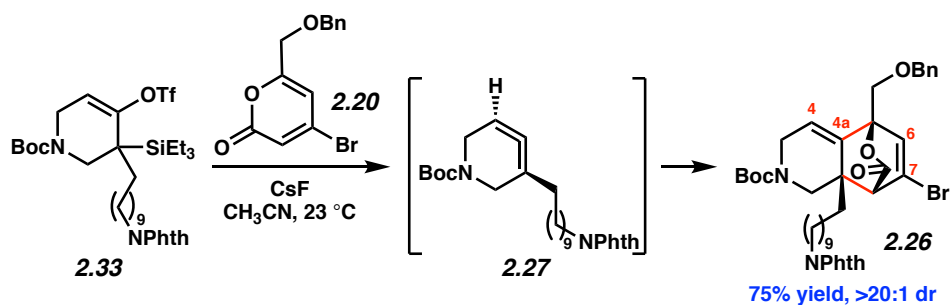


**Figure 2.7.** Diels–Alder cycloaddition using silyl triflate **2.33** en route to **2.10**.

To transform cycloadduct **2.26** to diene **2.25** we first envisioned a selective reduction of the C4–C4a alkene over the reduction of the C6–C7 alkene (Figure 2.8). Unfortunately, efforts to reduce the olefin using traditional metal-catalyzed hydrogenation or diimide reduction conditions were unsuccessful. To distinguish the olefins electronically, cycloadduct **2.26** was subjected to allylic oxidation conditions to access enamide **2.34**. With enamide **2.34** in hand, a Stryker reduction was employed to afford *cis*-decalin **2.35** in 92% yield with excellent diastereoselectivity.<sup>13</sup> Heating bicycle **2.35** in DMSO allowed for the extrusion of CO<sub>2</sub> in a retro-Diels–Alder reaction to provide diene **2.25** in nearly quantitative yield.<sup>10</sup>

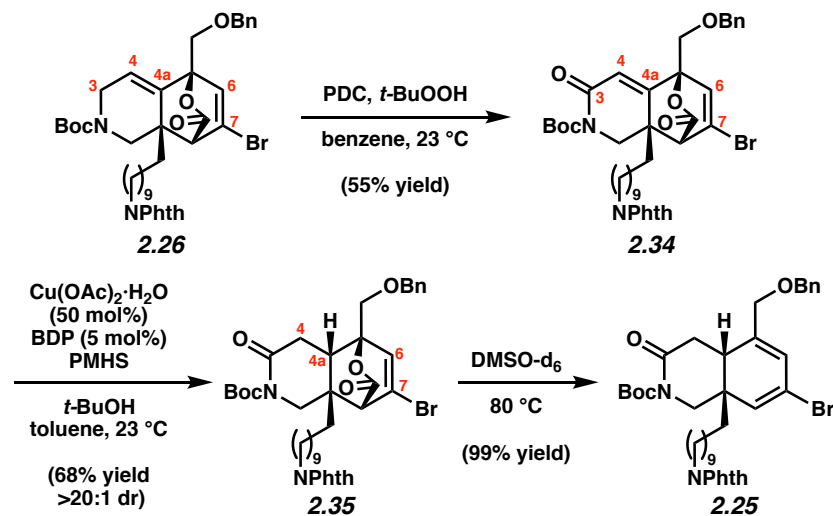


**Figure 2.8.** Manipulations of cycloadduct **2.26** to access diene **2.25**.

Toward the goal of introducing the macrocycle, we prepared intermediate **2.41** using the route shown in Figure 2.9. As we envisioned using olefin metathesis to construct the macrocycle, first, a cross-coupling to install an alkyl chain containing a terminal olefin that could participate in the olefin metathesis was necessary. Negishi coupling between vinyl bromide **2.25** and readily available alkylzinc bromide<sup>14</sup> **2.36** proceeded smoothly, delivering alkene **2.37** in 86% yield. Cross-electrophile coupling reactions<sup>15</sup> between vinyl bromide **2.25** and alkyl bromides were also considered, however, most led to negligible yields of the desired product. Next, it was necessary for amide **2.37** to be reduced to an amine. As traditional LiAlH<sub>4</sub> reductions are not compatible with the phthalimide, protecting group manipulations were therefore required, beginning with removal of the Boc and phthalimide protecting groups from **2.37** to afford primary amine **2.38**. Next, primary amine **2.38** was converted to the corresponding carbamate upon treatment with Boc anhydride. The amide was then reduced to secondary amine **2.39** with LiAlH<sub>4</sub>. Finally, secondary amine **2.39** was acylated using acryloyl chloride (**2.40**) to yield acrylamide **2.41**.

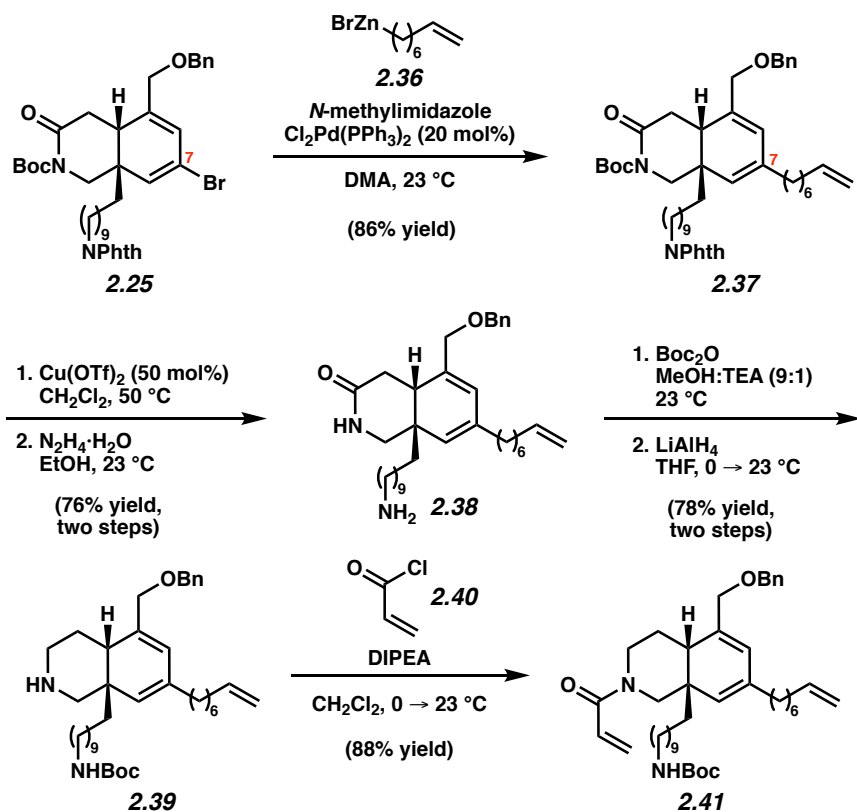


**Figure 2.9.** Elaboration of diene **2.25** to macrocyclization precursor **2.41**.

With alkene **2.41** in hand, the key macrocyclization and functional group manipulations en route to lissodendoric acid A (**2.10**) were performed. First, olefin **2.41** was treated with the Grubbs' 2<sup>nd</sup> generation catalyst to afford macrocycle **2.24** in 73% yield (Figure 2.10).<sup>16</sup> Enamide **2.24** was then reduced to tertiary amine **2.42** through a two-step sequence. Benzyl-protected alcohol **2.42** was next deprotected using  $\text{BCl}_3$  to furnish **2.43** in 77% yield. However, oxidation of alcohol **2.43** to aldehyde **2.44** proved challenging under a variety of different oxidation conditions. To further probe this difficult oxidation, **2.24** was converted to amide **2.45** by 1,4-reduction of the enamide, followed by deprotection of the benzyl-protected alcohol. Treatment of **2.45** with  $\text{MnO}_2$  facilitated smooth oxidation to aldehyde **2.46** in 70% yield. Interestingly, subjecting tertiary amine **2.43** to the same oxidation conditions did not result in formation of an

aldehyde, suggesting that the tertiary amine moiety is responsible for the difficult oxidation of alcohol **2.43**.

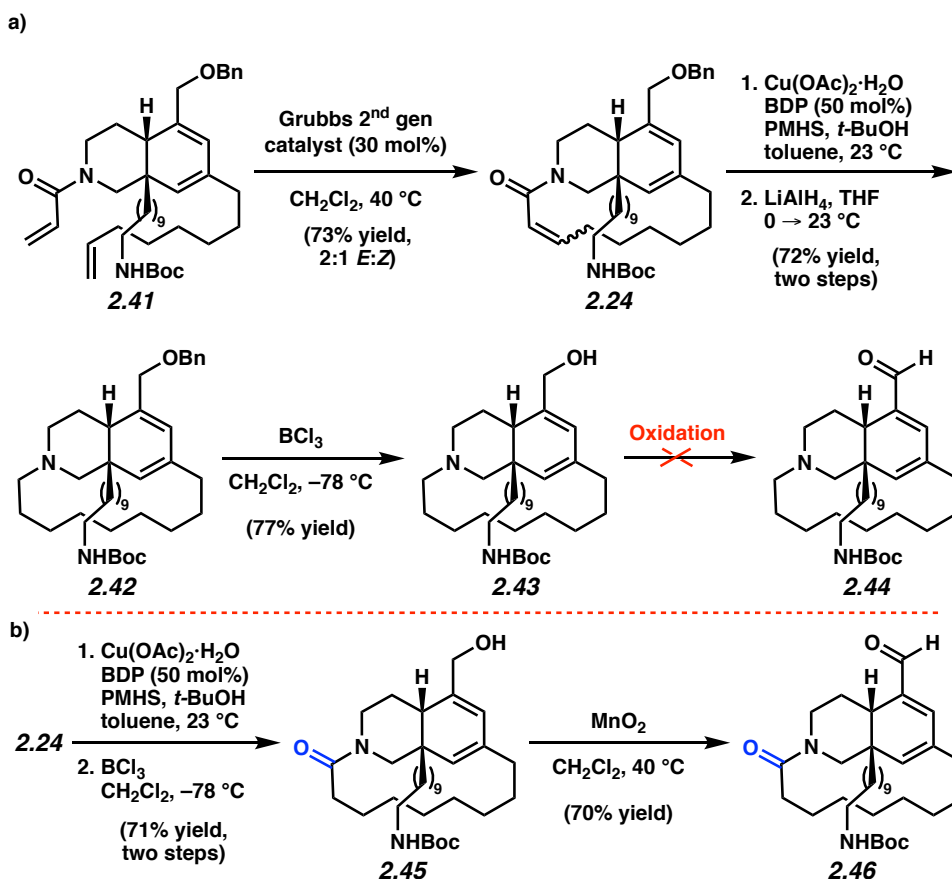


**Figure 2.10.** a) Macrocyclization and attempted oxidation. b) Synthesis of amide **2.45** to allow for oxidation to aldehyde **2.46**.

To circumvent the difficult late-stage oxidation and multiple protecting group manipulations, we opted to alter our cyclic allene Diels–Alder target from cycloadduct **2.26** to cycloadduct **2.47** (Figure 2.11). There are several key changes. First, rather than carrying a benzyl-protected alcohol through the synthesis, an ester would be used. The ester could be readily hydrolyzed to yield a carboxylic acid in the final step of the synthesis, rather than having

to perform late-stage oxidations. Next, we decided to install an alkyl chain with a terminal olefin, which would allow for fewer late-stage manipulations related to introduction of the macrocycle. Finally, rather than swapping out the protecting group on the primary amine from a phthalimide to Boc-protecting group mid-synthesis, we envisioned synthesizing cycloadduct **2.47** bearing a di-Boc-protected primary amine.

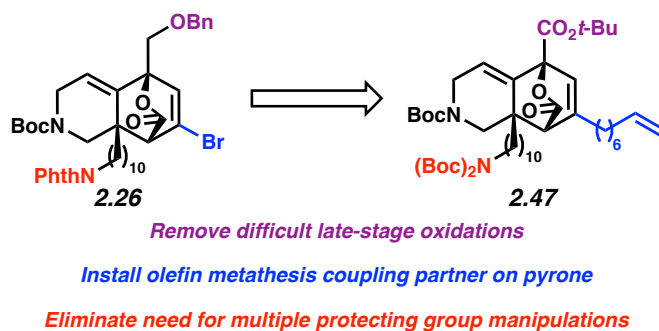


**Figure 2.11.** Revision of strategy to pursue cycloadduct **2.47**.

## 2.5 Revised Route to Lissodendoric Acid A

With a redesigned cycloadduct to target, syntheses of the pyrone and silyl triflate fragments that would lead to formation of cycloadduct **2.47** were pursued. First, starting with commercially available pyrone **2.48**, a one-pot bis-tosylation and esterification reaction to yield *t*-butyl ester pyrone **2.49** was performed (Figure 2.12a). Next, vinyl tosylate **2.49** underwent Negishi coupling with alkyl zinc bromide **2.36** to afford pyrone **2.50** in 80% yield. Our synthesis of silyl triflate **2.53** is shown in Figure 2.12b. In a sequence similar to the one used to prepare silyl triflate **2.33** (see Figure 2.6), allyl ketone **2.30** was elaborated to ketone **2.52** in 79% yield over two steps. Then, deprotonation and triflation of ketone **2.52** using KHMDS and Comins' reagent delivered silyl triflate **2.53**.

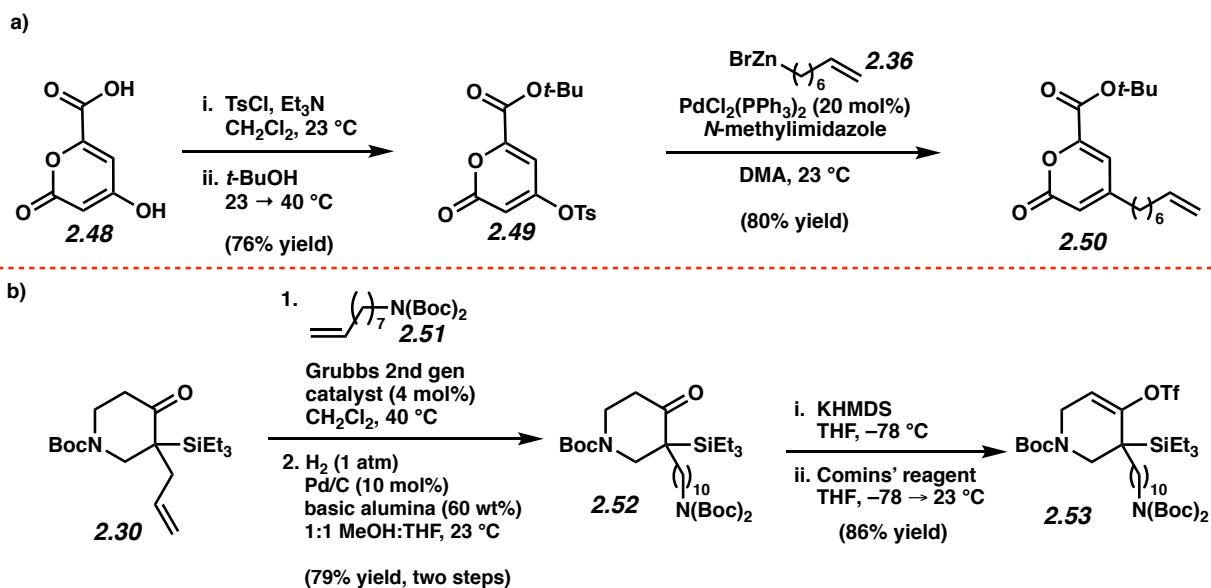


**Figure 2.12.** a) Synthesis of ester-containing pyrone **2.50**. b) Synthesis of silyl triflate **2.53**.

With the highly functionalized substrates in hand (i.e., silyl triflate **2.53** and pyrone **2.50**) the key Diels–Alder cycloaddition was attempted (Figure 2.13). To our delight, the cycloaddition between pyrone **2.50** and in situ-generated allene **2.54** delivered cycloadduct **2.47** in 81% yield and >20:1 dr. This cycloaddition demonstrated that more functionalized substrates are still competent in the strained azacyclic Diels–Alder reaction, which also tolerated substituents on the pyrone that perturbed the electronics. Further details of this key step, including a variant using optically-enriched material, are described in Chapter 1.

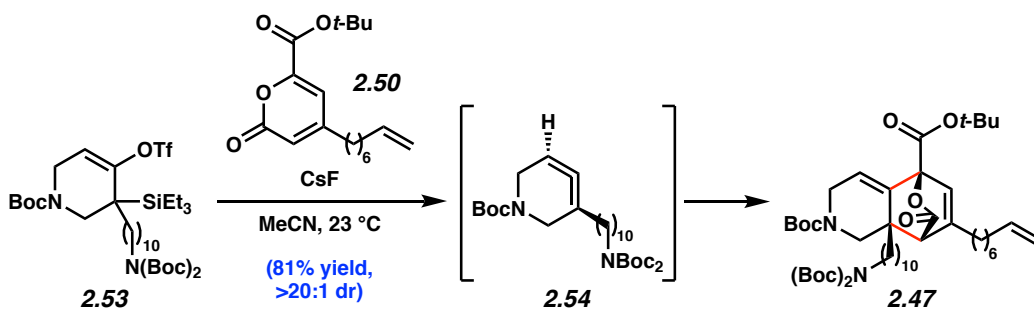


**Figure 2.13.** Diels–Alder cycloaddition using revised strategy.

Next, cycloadduct **2.47** was subjected to a similar synthetic sequence as cycloadduct **2.26** to allow for the selective reduction of the C4–C4a alkene over the C6–C7 alkene through an allylic oxidation and 1,4-reduction sequence to afford *cis*-decalin **2.55** (Figure 2.14). An optimized, one-pot reaction consisting of heating bicycle **2.55** in acetonitrile and subsequent addition of copper triflate allowed for the extrusion of CO<sub>2</sub> in a retro-Diels–Alder reaction and selective removal of two of the three Boc protecting groups to provide diene **2.56** in 68% yield.<sup>17</sup> Reduction of the amide in **2.56** could no longer be performed using LiAlH<sub>4</sub>, as this was expected to reduce the ester as well. Instead, Rh-catalyzed reduction of **2.56** delivered secondary amine **2.57**.<sup>18</sup> To introduce the 14-membered macrocycle, amine **2.57** was acylated with acryloyl chloride (**2.40**) and then treated with the Grubbs' 2<sup>nd</sup> generation catalyst<sup>16</sup> to afford macrocycle **2.58**. Selective reduction of the  $\alpha,\beta$ -unsaturated enamide present in **2.58** to a tertiary amine was necessary. This was successfully carried out in two separate reduction steps; 1,4-reduction under Stryker reaction conditions,<sup>13</sup> followed by Rh-catalyzed reduction<sup>18</sup> afforded desired tertiary amine **2.59** in 34% yield over two steps.



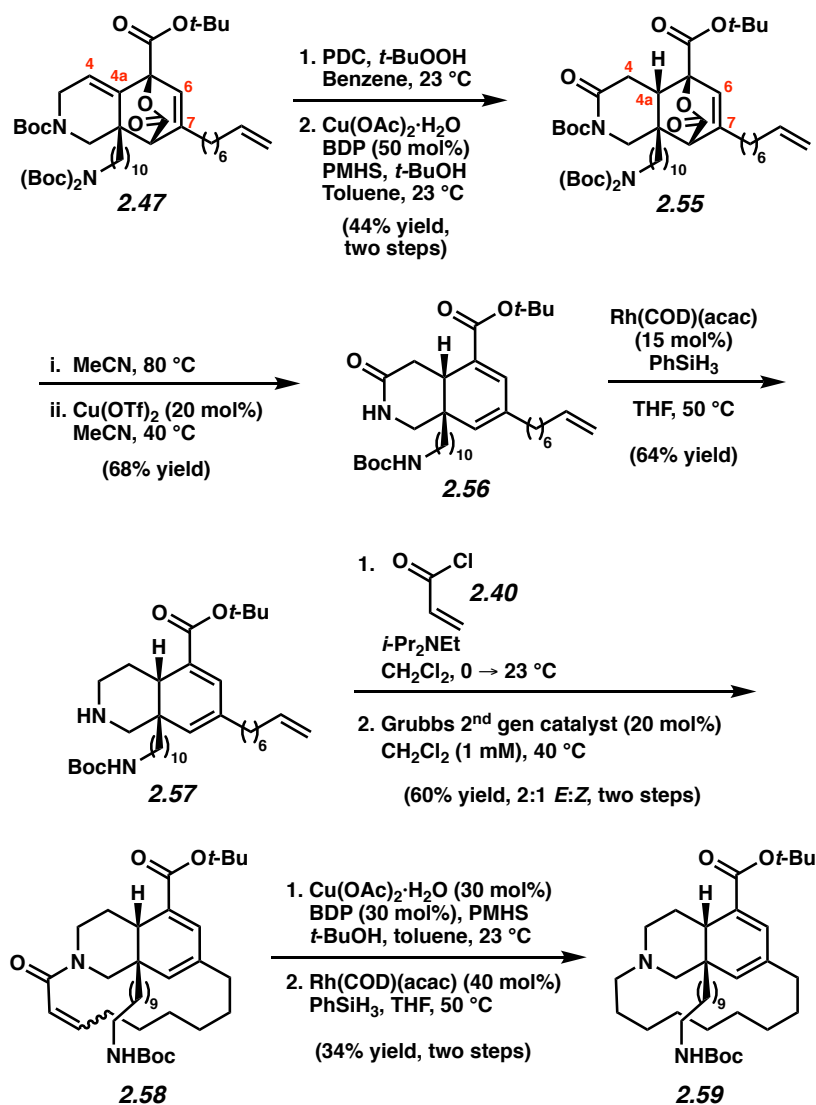


**Figure 2.14.** Elaboration of cycloadduct **2.47** to tertiary amine **2.59**.

Rather than performing three separate reduction steps from secondary amide **2.56** to tertiary amine **2.59**, we envisioned an alternate route where all reductions would be executed in a single step (Figure 2.15). Starting with acylation of secondary amide **2.56**, treatment with acryloyl chloride (**2.40**) afforded macrocyclization precursor **2.60**. Next, ring-closing metathesis supplied macrocycle **2.61** in 83% yield. To complete the synthesis of **2.10**, reduction of the  $\alpha,\beta$ -unsaturated imide present in **31** to a tertiary amine was necessary. Gratifyingly, this sequence

could be achieved in a one-pot procedure using Rh-catalyzed reduction conditions.<sup>18</sup> Finally, protecting group removal using trifluoroacetic acid delivered lissodendoric acid A (**2.10**).

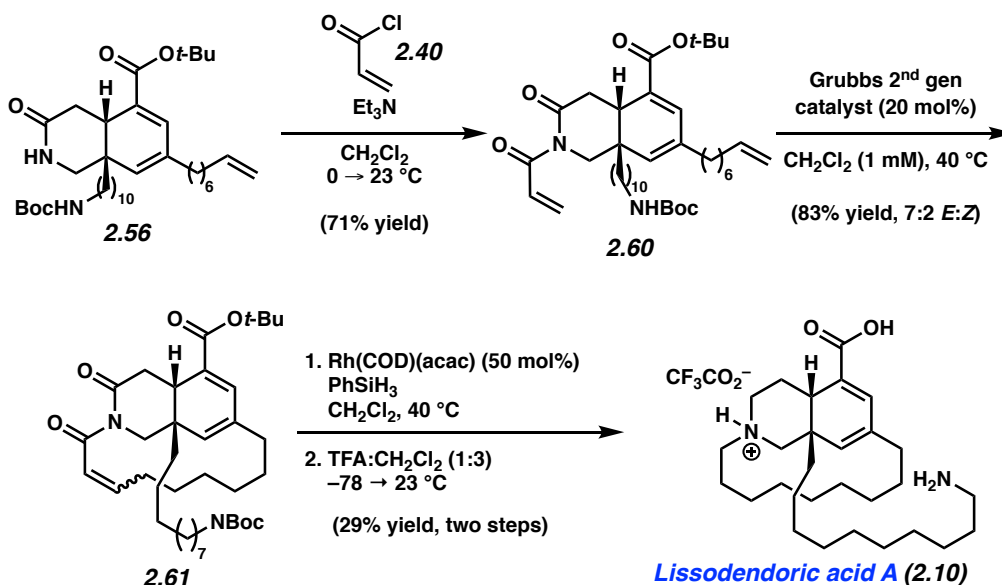


**Figure 2.15.** Optimization of late-stage reductions to access lissodendoric acid A (**2.10**).

## 2.6 Conclusion

This study describes the first total synthesis of the manzamine alkaloid lissodendoric acid A (**2.10**). The strategic use of a cyclic allene Diels–Alder reaction to form the azadecalin core of **2.10** marks the first application of a strained allene in total synthesis. This synthesis showcases the utility of heterocyclic allene chemistry to rapidly build complex scaffolds and could ultimately lead to the increased use of strained cyclic allenes in complex molecule synthesis.

## 2.7 Experimental Section

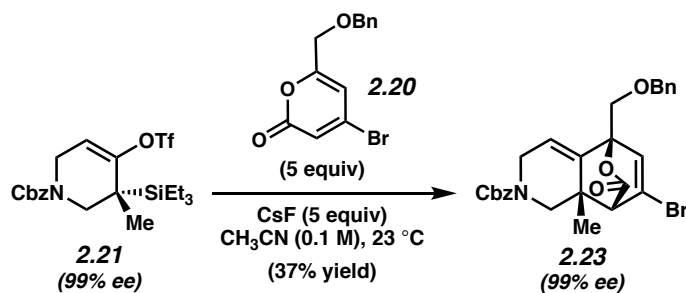
**2.7.1 Materials and Methods.** Unless stated otherwise, reactions were conducted in flame-dried glassware under an atmosphere of nitrogen using anhydrous solvents (either freshly distilled or passed through activated alumina columns). All commercially obtained reagents were used as received unless otherwise specified. 1,4-Diazabicyclo[2.2.2]octane (DABCO) and diisopropylethylamine (DIPEA) were purchased from Acros Organics. AgOTf, NBS, *n*-Butyllithium 2.5 M solution in hexanes (*n*-BuLi), allyl chloroformate, Grubbs' 2<sup>nd</sup> generation catalyst, KHMDS, PDC, *t*-BuOOH 70 wt% in H<sub>2</sub>O, *N*-methylimidazole, Boc<sub>2</sub>O, LiAlH<sub>4</sub> 2.0 M solution in THF, acryloyl chloride (**2.40**), BCl<sub>3</sub> 1.0 M solution in CH<sub>2</sub>Cl<sub>2</sub>, PhSiH<sub>3</sub>, TsCl, and trifluoroacetic acid (TFA) were obtained from Sigma-Aldrich. AgNO<sub>3</sub>, *N*-Phenyl-bis(trifluoromethanesulfonimide) (PhNTf<sub>2</sub>), and triethylsilyl chloride (Et<sub>3</sub>SiCl) were purchased from Oakwood Chemical. CsF, (PPh<sub>3</sub>)AuCl, Pd(PPh<sub>3</sub>)<sub>4</sub>, Cl<sub>2</sub>Pd(PPh<sub>3</sub>)<sub>2</sub>, Cu(OTf)<sub>2</sub>, Rh(COD)(acac), Pd/C, and 1,2-bis(diphenylphosphino)benzene (BDP) were purchased from Strem Chemicals. Copper(II) acetate monohydrate (Cu(OAc)<sub>2</sub>·H<sub>2</sub>O) and hydrazine monohydrate (N<sub>2</sub>H<sub>4</sub>·H<sub>2</sub>O) were purchased from TCI chemicals. Poly(methylhydrosiloxane) (PMHS) was purchased from Alfa-Aesar. *t*-BuOH was purchased from Fisher Scientific.  $\alpha$ -Bromo ketone **2.28** and Comins' reagent were purchased from Combi-Blocks. Et<sub>3</sub>SiCl, allyl chloroformate, and acryloyl chloride (**2.40**) were distilled over CaH<sub>2</sub> prior to use. PMHS and *t*-BuOH were sparged with N<sub>2</sub> prior to use. NBS was recrystallized from H<sub>2</sub>O prior to use. Unless stated otherwise, reactions were performed at 23 °C. Thin-layer chromatography (TLC) was conducted with EMD gel 60 F254 pre-coated plates (0.25 mm) and visualized using anisaldehyde or potassium permanganate staining. Silicycle Siliaflash P60 (particle size 0.040–0.063 mm) was used for flash column chromatography. <sup>1</sup>H-NMR spectra were recorded on Bruker spectrometers (at 400,

500, or 600 MHz) and are reported relative to the residual solvent signal. Data for  $^1\text{H}$ -NMR spectra are reported as follows: chemical shift ( $\delta$  ppm), multiplicity, coupling constant (Hz) and integration.  $^{13}\text{C}$ -NMR spectra were recorded on Bruker spectrometers (at 100, 125, or 150 MHz) and are reported relative to the residual solvent signal. Data for  $^{13}\text{C}$ -NMR spectra are reported in terms of chemical shift ( $\delta$  ppm). IR spectra were obtained on a Perkin-Elmer UATR Two FT-IR spectrometer and are reported in terms of frequency of absorption ( $\text{cm}^{-1}$ ). DART-MS spectra were collected on a Thermo Exactive Plus MSD (Thermo Scientific) equipped with an ID-CUBE ion source, a Vapor Interface (IonSense Inc.), and an Orbitrap mass analyzer. Both the source and MSD were controlled by Excalibur software v. 3.0. The analyte was spotted onto OpenSpot sampling cards (IonSense Inc.) using  $\text{CDCl}_3$  as the solvent. Ionization was accomplished using UHP He (Airgas Inc.) plasma with no additional ionization agents. The mass calibration was carried out using Pierce LTQ Velos ESI (+) and (-) Ion calibration solutions (Thermo Fisher Scientific). Determination of enantiopurity was carried out on a Mettler Toledo SFC (supercritical fluid chromatography) using a Daicel ChiralPak OD-H column. Benzyl propargyl ether (**2.19**) and 3-bromopropionic acid (**2.18**)<sup>19</sup> are known compounds.  $^1\text{H}$  NMR spectral data matched those reported in the literature.

### 2.7.2 Experimental Procedures

Experimental procedures and characterization for compounds **2.18**, **2.20**, **2.49**, **2.50**, **2.47**, **2.55**, **2.60**, **2.61** and **2.10** are reported in Chapter 1.<sup>9</sup>

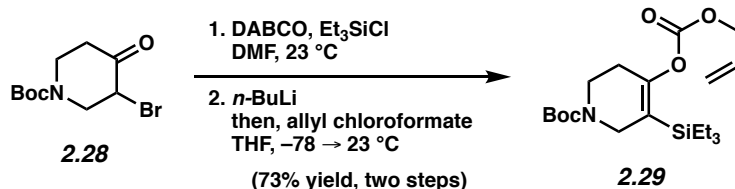
### 2.7.2.1 Model System Diels–Alder Cycloaddition



**Cycloadduct 2.23.** To a solution of silyl triflate **2.21**<sup>6a</sup> (132 mg, 0.0270 mmol, 1.00 equiv) and pyrone **2.20** (40.1 mg, 0.134 mmol, 5.00 equiv) in acetonitrile (0.26 mL, 0.10 M) was added CsF (31.5 mg, 0.134 mmol, 5.00 equiv). The vial was sealed and the reaction was allowed to stir at 23 °C for 16 h. After 16 h, the reaction was filtered over celite (1 cm) using EtOAc (~6 mL) as the eluent and concentrated to a crude oil. The crude oil was purified by preparative thin-layer chromatography (2:1 hexanes:EtOAc) to obtain cycloadduct **2.23** (5.2 mg, 37% yield) as a yellow oil. Cycloadduct **2.23**: *R<sub>f</sub>* 0.24 (9:1 hexanes:EtOAc); <sup>1</sup>H NMR (500 MHz, CDCl<sub>3</sub>): δ 7.40–7.28 (m, 10H), 6.54 (dd, *J* = 11.7, 1.4, 1H), 5.73 (dd, *J* = 26.5, 3.8, 1H), 5.23–5.13 (m, 2H), 4.69–4.65 (m, 2H), 4.32–4.19 (m, 1H), 4.17–3.98 (m, 2H), 3.93 (d, *J* = 10.7, 1H), 3.76 (td, *J* = 19.6, 5.4, 1H), 3.52 (d, *J* = 25.5, 1H), 2.55 (dd, *J* = 16.5, 11.8, 1H), 1.14 (d, *J* = 16.4, 3H); <sup>13</sup>C NMR (125 MHz, CDCl<sub>3</sub>): δ 169.2, 156.2, 155.8, 137.9, 137.5, 137.19, 137.16, 136.6, 136.5, 133.1, 132.8, 128.8, 128.7, 128.6, 128.4, 128.3, 128.23, 128.15, 128.12, 128.07, 119.3, 118.9, 117.5, 117.1, 85.1, 85.0, 74.3, 67.8, 67.7, 67.6, 60.4, 60.3, 49.8, 49.6, 43.0, 42.7, 37.4, 22.1, 22.0; IR (film): 3036, 2929, 2875, 1765, 1702, 1454, 1417, 1264, 1096 cm<sup>-1</sup>; HRMS-APCI (*m/z*) [M – CO<sub>2</sub>]<sup>+</sup> calcd for C<sub>26</sub>H<sub>26</sub>BrNO<sub>3</sub><sup>+</sup>, 479.1091; found 479.1054.

*Note: 2.23 was obtained as a mixture of rotamers. These data represent empirically observed chemical shifts from the <sup>1</sup>H and <sup>13</sup>C NMR spectra.*

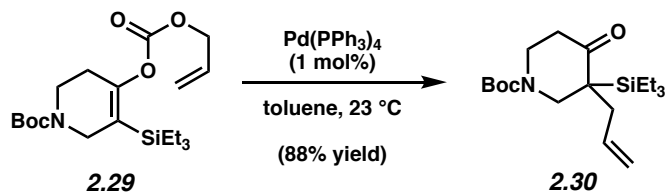
### 2.7.2.2 Synthesis of Silyl Triflate 2.33



**Carbonate 2.29.** To a solution of  $\alpha$ -bromo ketone **2.28** (5.02 g, 18.0 mmol, 1.00 equiv) dissolved in DMF (17.0 mL, 1.10 M) using sonication, was added TESCl (4.85 mL, 28.9 mmol, 1.60 equiv) and DABCO (4.64 g, 41.3 mmol, 2.30 equiv). Then, the reaction was allowed to stir for 21.5 h at 23 °C before being quenched with a saturated aq. solution of NaHCO<sub>3</sub> (60 mL). The reaction mixture was then transferred to a separatory funnel and diluted with water (150 mL). The layers were separated and the aqueous layer was extracted with EtOAc (3 x 50 mL). The combined organic layers were sequentially washed with water (2 x 50 mL) and brine (1 x 50 mL), dried with MgSO<sub>4</sub>, filtered, and concentrated under reduced pressure to provide the crude residue. The crude residue was purified via flash chromatography (100% hexanes → 39:1 hexanes:EtOAc) to obtain the bromo silyl enol ether. A solution of the bromo silyl enol ether (6.00 g, 15.4 mmol, 1.00 equiv) in THF (153 mL, 0.100 M) was cooled to -78 °C and stirred for 1 h. At this point, *n*-BuLi (7.34 mL, 18.3 mmol, 1.20 equiv, 2.60 M in hexanes) was added dropwise over 20 min. The reaction was stirred at -78 °C for 2 h at which point allyl chloroformate (2.44 mL, 22.9 mmol, 1.50 equiv) was added dropwise over 15 min. The reaction was stirred at -78 °C for 10 min, then warmed to 23 °C and stirred for 13 h. At this point the reaction was quenched with a saturated aq. solution of NaHCO<sub>3</sub> (30 mL). The reaction was then transferred to a separatory funnel and diluted with water (30 mL) and the layers were separated. The aqueous layer was extracted with ethyl acetate (3 x 40 mL). The combined organic layers were sequentially washed with water (3 x 40 ml) and brine (40 mL). The organic layer was then

dried with MgSO<sub>4</sub>, filtered, and concentrated under reduced pressure to give a yellow oil. The crude oil was purified via flash chromatography (9:1 hexanes:EtOAc) to obtain carbonate **2.29** (5.8 g, 73% yield over two steps) as a colorless oil. Carbonate **2.29**: R<sub>f</sub> 0.57 (5:1 hexanes:EtOAc); <sup>1</sup>H NMR (500 MHz, CDCl<sub>3</sub>): δ 5.94 (ddt, *J* = 17.2, 10.5, 5.9, 1H), 5.38 (dq, *J* = 17.1, 1.4, 1H), 5.29 (dd, *J* = 10.4, 1.2, 1H), 4.64 (dt, *J* = 5.9, 1.3, 2H), 3.96 (br s, 2H), 3.56 (br s, 2H), 2.38 (br s, 2H), 1.46 (s, 9H), 0.93 (t, *J* = 7.9, 9H), 0.64 (q, *J* = 7.9, 6H); <sup>13</sup>C NMR (125 MHz, CDCl<sub>3</sub>): δ 154.7, 152.9, 150.1, 131.4, 119.5, 118.7, 80.0, 68.9, 45.1, 44.5, 41.0, 40.1, 28.6, 28.2, 28.1, 7.4, 3.1; IR (film): 2954, 2876, 1755, 1698, 1237, 1157 cm<sup>-1</sup>; HRMS-APCI (*m/z*) [M + H]<sup>+</sup> calcd for C<sub>20</sub>H<sub>36</sub>NO<sub>5</sub>Si<sup>+</sup>, 398.2357; found 398.2358.

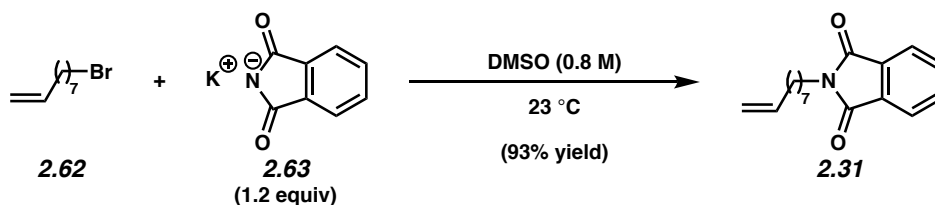
*Note: 2.29 was obtained as a mixture of rotamers. These data represent empirically observed chemical shifts from the <sup>1</sup>H and <sup>13</sup>C NMR spectra.*



**Allyl ketone 2.30.** To a flask in the glovebox was added Pd(PPh<sub>3</sub>)<sub>4</sub> (183 mg, 0.158 mmol, 1.00 mol%). This was taken out of the glove box and dissolved in freshly distilled toluene (50.0 mL). To a solution of allyl carbonate **2.29** (6.30 g, 15.8 mmol, 1.00 equiv) in toluene (108 mL) was added the palladium solution dropwise over 10 min. The reaction was allowed to stir at 23 °C for 1 h before being quenched with hexanes (100 mL). This solution was filtered over a pad of silica (2 cm), washed with EtOAc (100 mL), and was concentrated under reduced pressure to a yellow oil. The crude oil was purified via flash chromatography (9:1 hexanes:EtOAc) to give allyl ketone **2.30** (4.94 g, 88% yield) as a colorless oil. Allyl ketone **2.30**: R<sub>f</sub> 0.52 (5:1

hexanes:EtOAc);  $^1\text{H}$  NMR (500 MHz,  $\text{CDCl}_3$ ):  $\delta$  5.71–5.62 (m, 1H), 5.08–4.92 (m, 2H), 4.09–3.80 (m, 2H), 3.71–3.45 (m, 1H), 3.33–3.13 (m, 1H), 2.89 (br s, 1H), 2.56 (br s, 1H), 2.38 (br s, 1H), 2.06 (br s, 1H), 1.46 (s, 9H), 0.98 (t,  $J = 7.8$ , 9H), 0.78–0.65 (m, 6H);  $^{13}\text{C}$  NMR (125 MHz,  $\text{CDCl}_3$ ):  $\delta$  211.5, 210.8, 154.6, 150.1, 134.8, 117.9, 117.7, 84.0, 80.4, 80.0, 50.5, 49.7, 46.4, 45.6, 42.0, 41.6, 40.1, 37.7, 37.2, 28.5, 28.1, 8.0, 7.5, 3.1, 2.5; IR (film): 2955, 2878, 1688, 1365, 1242, 1165  $\text{cm}^{-1}$ ; HRMS-APCI ( $m/z$ )  $[\text{M} + \text{H}]^+$  calcd for  $\text{C}_{19}\text{H}_{36}\text{NO}_3\text{Si}^+$ , 354.2459; found 354.2456.

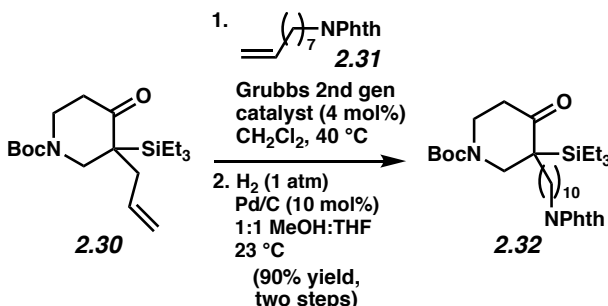
*Note: 2.30 was obtained as a mixture of rotamers. These data represent empirically observed chemical shifts from the  $^1\text{H}$  and  $^{13}\text{C}$  NMR spectra.*



**Phthalimide 2.31.** To a mixture of 9-bromononene (**2.62**, 10.0 g, 48.7 mmol, 1.00 equiv) and potassium phthalimide (**2.63**, 10.8 g, 58.5 mmol, 1.20 equiv) was added DMSO (60.9 mL, 0.800 M) and the reaction mixture was allowed to stir at 23 °C for 16 h. After 16 h, the mixture was transferred to a separatory funnel with water (100 mL) and  $\text{CH}_2\text{Cl}_2$  (100 mL). The layers were separated and the aqueous layer was extracted with  $\text{CH}_2\text{Cl}_2$  (3 x 100 mL). The combined organic layers were dried over  $\text{MgSO}_4$ , filtered, and concentrated under reduced pressure. The crude residue was purified via flash chromatography (9:1 hexanes:EtOAc) to give phthalimide **2.31** (18.5 g, 93% yield) as a white solid. Phthalimide **2.31**:  $R_f$  0.40 (9:1 hexanes:EtOAc);  $^1\text{H}$  NMR (500 MHz,  $\text{CDCl}_3$ ): 7.82 (dd,  $J = 5.5, 3.0$ , 2H), 7.69 (dd,  $J = 5.5, 3.0$ , 2H), 5.78 (ddt,  $J = 17.3, 10.1, 6.7$ , 1H), 4.97 (dq,  $J = 17.1, 1.6$ , 1H), 4.92–4.89 (m, 1H), 3.66 (t,  $J = 7.4$ , 2H), 2.04–1.98



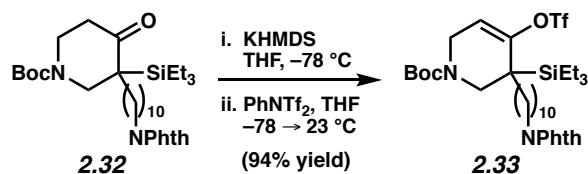
(m, 2H), 1.70–1.61 (m, 2H), 1.38–1.24 (m, 8H);  $^{13}\text{C}$  NMR (125 MHz,  $\text{CDCl}_3$ ):  $\delta$  168.6, 139.2, 133.9, 132.3, 123.3, 114.3, 38.2, 33.8, 29.14, 29.06, 28.9, 28.7, 26.9; IR (film): 3076, 2927, 2855, 1772, 1707, 1394, 1367  $\text{cm}^{-1}$ ; HRMS-APCI ( $m/z$ )  $[\text{M} + \text{H}]^+$  calcd for  $\text{C}_{17}\text{H}_{22}\text{NO}_2^+$ , 272.1645; found 272.1654.



**Ketone 2.32.** A flask in the glove box was charged with Grubbs' 2<sup>nd</sup> Generation catalyst (235 mg, 0.277 mmol, 4.00 mol%), sealed with a septum, and taken out of the glovebox. To this flask was added a solution of allyl ketone **2.30** (2.45 g, 6.93 mmol, 1.00 equiv) and phthalimide **2.31** (9.41 g, 34.7 mmol, 5.00 equiv) in  $\text{CH}_2\text{Cl}_2$  (35 mL, 0.20 M). The flask was equipped with a reflux condenser and the reaction mixture was heated to  $40\text{ }^\circ\text{C}$  and stirred for 16 h at which point it was cooled to  $23\text{ }^\circ\text{C}$ . The solvent was removed under reduced pressure to give a dark brown tacky oil. The crude oil was purified via flash chromatography (100% benzene  $\rightarrow$  9:1 benzene:EtOAc) and repurified via flash chromatography (9:1 hexanes:EtOAc  $\rightarrow$  5:1 hexanes:EtOAc) to give the cross-metathesis product. To a flask was added the cross-metathesis product (1.31 g, 2.19 mmol, 1.00 equiv), Pd/C (233 mg, 0.219 mmol, 10% w/w, 10 mol%), THF (33 mL), and MeOH (33 mL). The flask was evacuated and backfilled with  $\text{H}_2$  from a balloon three times, then left to stir under an atmosphere of  $\text{H}_2$  (1 atm) for 45.5 h. Over this time, the flask was evacuated and backfilled with  $\text{H}_2$  from a balloon 3 times at 20 h, and 30 h. After 45.5 h, the reaction was filtered over celite (4 cm) with  $\text{CH}_2\text{Cl}_2$  as the eluent (150 mL). Evaporation

under reduced pressure afforded the crude residue. The crude residue was purified via flash chromatography (4:1 hexanes:EtOAc) to afford ketone **2.32** (1.25 g, 90% yield over two steps) as a colorless oil. Ketone **2.32**:  $R_f$  0.35 (5:1 hexanes:EtOAc);  $^1\text{H}$  NMR (600 MHz,  $\text{CDCl}_3$ ):  $\delta$  7.84 (dd,  $J = 5.4, 3.0$ , 2H), 7.70 (dd,  $J = 5.4, 3.0$ , 2H), 3.99–3.88 (m, 1H), 3.85–3.72 (m, 1H), 3.72–3.51 (m, 3H), 3.41–3.23 (m, 1H), 2.58 (s, 1H), 2.45–2.32 (m, 1H), 2.03–1.89 (m, 1 H), 1.70–1.63 (m, 2H), 1.46 (s, 9H), 1.35–1.11 (m, 15H), 0.97 (t,  $J = 7.7$ , 9H), 0.75–0.63 (m, 6H);  $^{13}\text{C}$  NMR (125 MHz,  $\text{CDCl}_3$ ):  $\delta$  212.3, 211.5, 168.6, 154.7, 133.9, 132.3, 123.3, 80.5, 80.0, 50.9, 50.5, 50.3, 46.5, 45.8, 42.1, 41.6, 40.0, 38.19, 38.18, 34.0, 33.2, 30.69, 30.66, 30.6, 29.7, 29.57, 29.55, 29.53, 29.47, 29.30, 29.27, 28.7, 28.6, 28.5, 27.1, 26.99, 26.97, 26.9, 25.7, 8.00, 2.67; IR (film): 2928, 2877, 2855, 1714, 1690, 1396  $\text{cm}^{-1}$ ; HRMS-APCI ( $m/z$ )  $[\text{M} + \text{H}]^+$  calcd for  $\text{C}_{34}\text{H}_{55}\text{N}_2\text{O}_5\text{Si}^+$ , 599.3875; found 599.3896.

*Note: 2.32 was obtained as a mixture of rotamers. These data represent empirically observed chemical shifts from the  $^1\text{H}$  and  $^{13}\text{C}$  NMR spectra.*

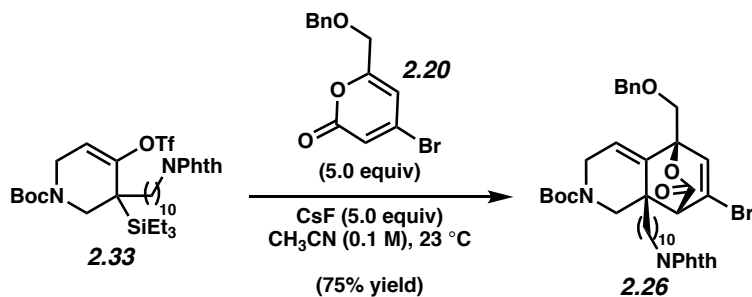


**Silyl triflate 2.33.** A flask in the glovebox was charged with KHMDS (670 mg, 3.36 mmol, 1.20 equiv), sealed with a septum, and taken out of the glovebox. THF (12.0 mL) was then added to the flask and the reaction mixture was cooled to  $-78$  °C. To the solution was added ketone **2.32** (1.73 g, 2.80 mmol, 1.00 equiv) in THF (6.0 mL) dropwise over 10 min at  $-78$  °C. The solution was stirred at  $-78$  °C for 1 h. Then, PhNTf<sub>2</sub> (1.40 g, 3.92 mmol, 1.40 equiv) in THF (6.0 mL) was added dropwise over 5 min at  $-78$  °C. The reaction was then warmed to  $23$  °C and stirred for 2 h. After 2 h, the reaction was quenched with a saturated aq. solution of NaHCO<sub>3</sub> (50 mL)

and diluted with water (50 mL) and Et<sub>2</sub>O (50 mL). The reaction was then transferred to a separatory funnel, the layers were separated, and the aqueous layer was extracted with Et<sub>2</sub>O (3 x 50 mL). The combined organic layers were dried over MgSO<sub>4</sub>, filtered, and concentrated under reduced pressure to provide the crude residue. The crude residue was purified via flash chromatography (19:1 hexanes:EtOAc → 9:1 hexanes:EtOAc) to obtain silyl triflate **2.33** (2.03 g, 94% yield) as a colorless oil. Silyl triflate **2.33**: R<sub>f</sub> 0.64 (5:1 hexanes:EtOAc); <sup>1</sup>H NMR (500 MHz, CDCl<sub>3</sub>): δ 7.83 (dd, *J* = 5.0, 2.9, 2H), 7.70 (dd, *J* = 5.0, 2.9, 2H), 5.65 (s, 1H), 4.17 (dd, *J* = 18.0, 4.1, 1H), 3.89–3.64 (m, 4H), 3.48–3.30 (m, 1H), 1.69–1.63 (m, 2H), 1.61–1.52 (m, 2H), 1.46 (s, 9H), 1.43–1.07 (m, 15H), 0.99 (t, *J* = 7.9, 9H), 0.75–0.65 (m, 6H); <sup>13</sup>C NMR (125 MHz, CDCl<sub>3</sub>): δ 168.60, 168.59, 154.3, 153.5, 133.9, 132.3, 123.3, 122.2, 119.7, 117.1, 114.6, 110.2, 80.5, 47.4, 46.8, 42.3, 41.9, 38.2, 35.6, 35.4, 32.9, 32.6, 30.5, 29.7, 29.60, 29.57, 29.32, 29.29, 28.8, 28.51, 28.48, 27.02, 26.99, 26.96, 25.0, 24.6, 8.1, 2.9, 2.8; IR (film): 2930, 2879, 2856, 1715, 1415, 1396, 1210 cm<sup>-1</sup>; HRMS-APCI (*m/z*) [M + H]<sup>+</sup> calcd for C<sub>35</sub>H<sub>54</sub>F<sub>3</sub>N<sub>2</sub>O<sub>7</sub>SSi<sup>+</sup>, 731.3368; found 731.3384.

*Note: 2.33 was obtained as a mixture of rotamers. These data represent empirically observed chemical shifts from the <sup>1</sup>H and <sup>13</sup>C NMR spectra.*

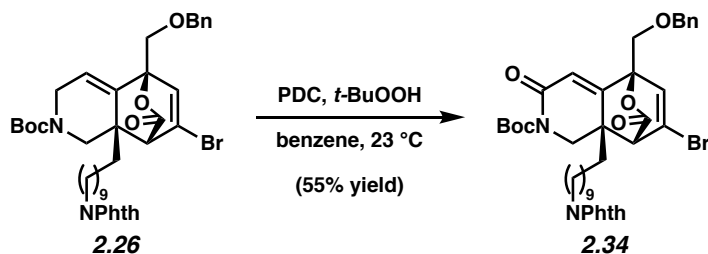
### 2.7.2.3 Diels–Alder Cycloaddition



**Cycloadduct 2.26.** To a solution of silyl triflate **2.33** (555 mg, 0.759 mmol, 1.00 equiv) and pyrone **2.20** (1.12 g, 3.80 mmol, 5.00 equiv) in acetonitrile (7.59 mL) was added CsF (577 mg, 3.80 mmol, 5.00 equiv). The vial was sealed and the reaction was allowed to stir at 23 °C for 16 h. After 16 h, the reaction was filtered over silica (2 cm) using EtOAc (~10 mL) as the eluent and concentrated to a crude oil. The crude oil was purified via flash chromatography (5:1 → 3:1 hexanes:EtOAc) to obtain cycloadduct **2.26** (432 mg, 75% yield) as a yellow foam. Cycloadduct **2.26**:  $R_f$  0.26 (5:1 hexanes:EtOAc); <sup>1</sup>H NMR (600 MHz, CDCl<sub>3</sub>): δ 7.83 (dd,  $J$  = 5.4, 3.0, 2H), 7.69 (dd,  $J$  = 5.4, 3.0, 2H), 7.40–7.31 (m, 5H), 6.53 (dd,  $J$  = 23.8, 2.4, 1H), 5.66 (dd,  $J$  = 26.9, 4.7, 1H), 4.66 (s, 2H), 4.38–4.10 (m, 2H), 4.05–4.01 (m, 1H), 3.92 (d,  $J$  = 10.7, 1H), 3.70–3.63 (m, 3H), 3.61–3.55 (m, 1H), 2.30 (dd,  $J$  = 41.3, 11.6, 1H), 1.69–1.61 (m, 3 H), 1.50–1.45 (m, 9H), 1.36–1.16 (m, 15H); <sup>13</sup>C NMR (150 MHz, CDCl<sub>3</sub>): δ 169.2, 169.1, 168.6, 155.1, 154.9, 138.3, 137.3, 137.2, 134.0, 133.5, 133.0, 132.3, 128.7, 128.3, 128.2, 128.1, 128.1, 123.4, 119.2, 118.8, 117.4, 117.1, 85.2, 85.1, 80.6, 80.4, 74.2, 67.9, 67.8, 57.4, 57.3, 45.6, 44.8, 42.9, 42.5, 40.8, 40.7, 38.2, 34.4, 34.3, 30.0, 29.8, 29.7, 29.6, 29.6, 29.5, 29.3, 29.2; IR (film): 2928, 2855, 1770, 1710, 1395, 1365, 1136 cm<sup>-1</sup>; HRMS-APCI ( $m/z$ ) [ $M - \text{CO}_2$ ]<sup>+</sup> calcd for C<sub>40</sub>H<sub>49</sub>BrN<sub>2</sub>O<sub>5</sub><sup>+</sup>, 716.2819; found 716.2877.

*Note: 2.26 was obtained as a mixture of rotamers. These data represent empirically observed chemical shifts from the <sup>1</sup>H and <sup>13</sup>C NMR spectra.*

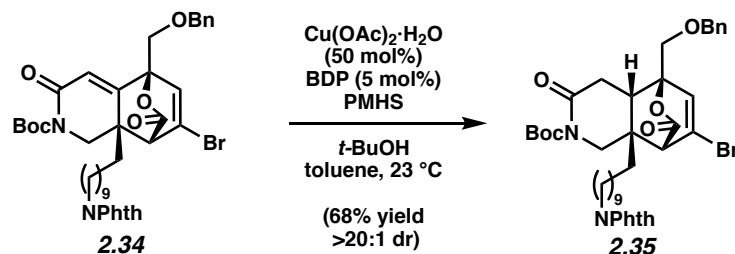
#### 2.7.2.4 Synthesis of Macrocyclization Precursor 2.41



**Enamide 2.34.** To a solution of cycloadduct **2.26** (50.0 mg, 0.0656 mmol, 1.00 equiv) in benzene (6.56 mL, 0.01 M) was added celite (1.00 g), PDC (74.1 mg, 0.197 mmol, 3.00 equiv), and *t*-BuOOH (0.0270 mL, 70 wt% in water, 0.197 mmol, 3.00 equiv). The solution was stirred at 23 °C for 2.5 h. At this point, the solution was filtered over a pad of celite and rinsed with EtOAc (15 mL). The filtrate was diluted with saturated aq. sodium thiosulfate solution (10 mL) and water (15 mL). The solution was transferred to a separatory funnel and the layers were separated. The aqueous layer was extracted with EtOAc (3 x 15 mL). The combined organic layers were washed with water (3 x 15 mL) and brine (15 mL), dried over MgSO<sub>4</sub>, filtered, and concentrated to a crude off-yellow oil. The crude oil was purified via preparative TLC (7:3 hexanes:EtOAc) to obtain enamide **2.34** (28.0 mg, 55% yield) as a yellow foam. Enamide **2.34**: *R<sub>f</sub>* 0.33 (2:1 hexanes:EtOAc); <sup>1</sup>H NMR (500 MHz, CDCl<sub>3</sub>): δ 7.83 (dd, *J* = 5.4, 3.0, 2H), 7.7 (dd, *J* = 5.4, 3.0, 2H), 7.40–7.32 (m, 5H), 6.71 (d, *J* = 2.2, 1H), 5.8 (s, 1H), 4.65 (q, *J* = 17.7, 12.0, 2H), 4.38 (d, *J* = 12.8, 1H), 4.0 (d, *J* = 10.7, 1H), 3.9 (d, *J* = 10.7, 1H), 3.72 (d, *J* = 2.0, 1H), 3.67 (t, *J* = 7.3, 2H), 3.25 (d, *J* = 12.7, 1H), 1.95–1.87 (m, 1H), 1.69–1.63 (m, 3H), 1.53 (s, 9H), 1.34–1.20 (m, 14H); <sup>13</sup>C NMR (125 MHz, CDCl<sub>3</sub>): δ 168.6, 167.8, 162.6, 156.5, 152.1, 136.7, 134.01, 133.95, 132.3, 128.8, 128.4, 128.2, 123.3, 121.6, 116.8, 84.1, 83.9, 74.3, 67.1, 56.9, 49.8, 40.9, 38.2, 34.2, 29.6, 29.5, 29.3, 28.7, 28.1 (3C), 27.0, 23.5; IR (film): 2933, 2854, 1773, 1712, 1395,

1369, 1151  $\text{cm}^{-1}$ ; HRMS-APCI ( $m/z$ )  $[\text{M} - \text{CO}_2]^+$  calcd for  $\text{C}_{40}\text{H}_{47}\text{BrN}_2\text{O}_6^+$ , 731.26903; found 731.26350.

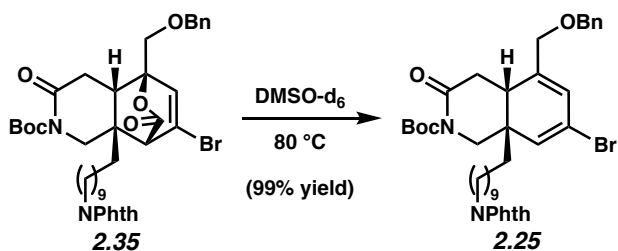
*Note: 2.34 was obtained as a mixture of rotamers. These data represent empirically observed chemical shifts from the  $^1\text{H}$  and  $^{13}\text{C}$  NMR spectra.*



**Amide 2.35.** A flask was charged with copper(II) acetate monohydrate (54.5 mg, 0.273 mmol, 50.0 mol%) and BDP (24.4 mg, 0.0546 mmol, 10.0 mol%). The solids were dissolved in sparged  $t\text{-BuOH}$  (0.520 mL, 5.46 mmol, 10.0 equiv) and toluene (2.10 mL). The contents of the flask were sonicated for 2 minutes and then stirred for 30 minutes, during which the solution turned blue. At this point, PMHS (3.09 mL, 1.64 mmol, 3.00 equiv) was added dropwise over 4 minutes, then the solution was allowed to stir for 40 minutes during which it turned yellow/green. A solution of enamide **2.34** (424 mg, 0.546 mmol, 1.00 equiv) in toluene (2.1 mL, 0.26 M) was then added to the Stryker reagent dropwise over 3 minutes. The reaction then stirred at 23 °C for 21 h, after which it was diluted with EtOAc (30 mL). The solution was transferred to a separatory funnel and washed with 1N NaOH (10 mL), 1N HCl (10 mL), saturated aq.  $\text{NaHCO}_3$  solution (10 mL), and then brine (10 mL). The combined aqueous layers were washed with EtOAc (3 x 10 mL). The organic layers were combined, dried over  $\text{MgSO}_4$ , and concentrated under reduced pressure. The crude material was purified via flash chromatography (9:1  $\rightarrow$  2:1 hexanes:EtOAc) to obtain amide **2.35** (289 mg, 68% yield) as a yellow foam. Amide **2.35**:  $R_f$  0.23 (2:1 hexanes:EtOAc);  $^1\text{H}$  NMR (500 MHz,  $\text{CDCl}_3$ ):  $\delta$  7.84 (dd,  $J = 5.4, 3.0, 2\text{H}$ ),

7.70 (dd,  $J = 5.4, 3.0, 2\text{H}$ ), 7.4–7.3 (m, 5H), 6.46 (d,  $J = 1.9, 1\text{H}$ ), 4.65 (d,  $J = 12.0, 1\text{H}$ ), 4.57 (d,  $J = 12.0, 1\text{H}$ ), 4.24 (d,  $J = 14.0, 1\text{H}$ ), 3.82 (d,  $J = 11.2, 1\text{H}$ ), 3.69–3.64 (m, 3H), 3.59 (d,  $J = 2.0, 1\text{H}$ ), 3.2 (d,  $J = 14.0, 1\text{H}$ ), 2.59 (dd,  $J = 14.6, 5.8, 1\text{H}$ ), 2.28 (dd,  $J = 11.8, 5.8, 1\text{H}$ ), 2.1–2.0 (m, 1H), 1.7–1.6 (m, 3H), 1.52 (s, 9H), 1.34–1.21 (m, 15H);  $^{13}\text{C}$  NMR (125 MHz,  $\text{CDCl}_3$ ):  $\delta$  169.2, 169.0, 168.6, 151.2, 137.0, 134.0, 132.3, 131.0, 128.8, 128.3, 128.1, 123.3, 122.5, 86.6, 84.1, 74.2, 69.1, 56.8, 45.9, 44.7, 43.5, 38.4, 38.2, 37.5, 29.8, 29.6, 29.5, 29.4, 29.3, 28.7, 28.0, 27.0, 23.2; IR (film): 2928, 2855, 1770, 1713, 1396, 1368, 1153  $\text{cm}^{-1}$ ; HRMS-APCI ( $m/z$ )  $[\text{M} - \text{CO}_2]^+$  calcd for  $\text{C}_{40}\text{H}_{49}\text{BrN}_2\text{O}_6^+$ , 733.28468; found 733.27974.

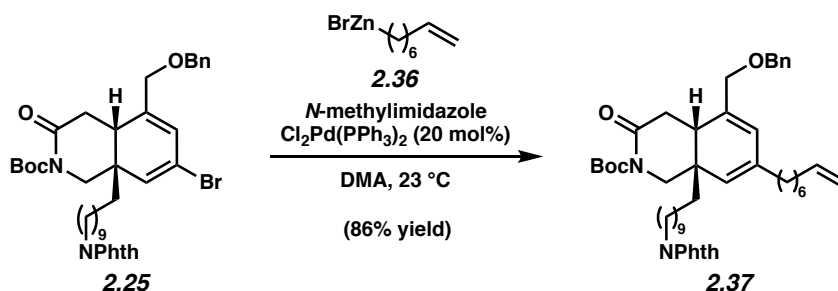
*Note: 2.35 was obtained as a mixture of rotamers. These data represent empirically observed chemical shifts from the  $^1\text{H}$  and  $^{13}\text{C}$  NMR spectra.*



**Diene 2.25.** A vial was charged with enamide **2.35** (129 mg, 0.166 mmol, 1.00 equiv) and  $\text{DMSO-d}_6$  (2.10 mL, 0.0800 M). The vial was heated to 80 °C for 2.5 h, after which it was allowed to cool to 23 °C. The reaction mixture diluted with  $\text{Et}_2\text{O}$  (2 mL) and transferred to a separatory funnel and washed with water (3 x 1 mL). The combined aqueous layers were extracted with  $\text{Et}_2\text{O}$  (2 x 2 mL) and the organic layers were combined, washed with brine (2 mL), and dried over  $\text{MgSO}_4$  to obtain diene **2.25** (120 mg, 99% yield) as a pale-yellow oil. Diene **2.25**:  $R_f$  0.37 (2:1 hexanes:EtOAc);  $^1\text{H}$  NMR (500 MHz,  $\text{CDCl}_3$ ):  $\delta$  7.84 (dd,  $J = 5.4, 3.0, 2\text{H}$ ), 7.71 (dd,  $J = 5.4, 3.0, 2\text{H}$ ), 7.37–7.29 (m, 5H), 5.95 (s, 1H), 5.60 (s, 1H), 4.50 (q,  $J = 27.4, 11.9, 2\text{H}$ ), 4.04 (d,  $J = 13.0, 1\text{H}$ ), 3.90 (d,  $J = 13.8, 1\text{H}$ ), 3.72–3.64 (m, 3H), 3.59 (d,  $J = 13.8, 1\text{H}$ ),

2.58 (dd,  $J = 14.2, 4.6, 1\text{H}$ ), 2.54–2.41 (m, 2H), 1.69–1.62 (m, 3H), 1.53 (s, 9H), 1.33–1.19 (m, 15H);  $^{13}\text{C}$  NMR (125 MHz,  $\text{CDCl}_3$ ):  $\delta$  171.3, 168.6, 151.9, 138.5, 137.8, 134.0, 132.3, 129.3, 128.6, 128.0, 127.8, 124.5, 123.3, 116.8, 83.5, 72.7, 71.0, 51.7, 43.2, 39.6, 38.2, 37.0, 36.8, 30.3, 29.6, 29.5, 29.3, 28.7, 28.1 (2C), 27.0, 23.6; IR (film): 2928, 2854, 1773, 1711, 1396, 1367, 1152  $\text{cm}^{-1}$ ; HRMS-APCI ( $m/z$ )  $[\text{M} + \text{H}]^+$  calcd for  $\text{C}_{40}\text{H}_{50}\text{BrN}_2\text{O}_6^+$ , 733.28468; found 733.27959.

*Note: 2.25 was obtained as a mixture of rotamers. These data represent empirically observed chemical shifts from the  $^1\text{H}$  and  $^{13}\text{C}$  NMR spectra.*

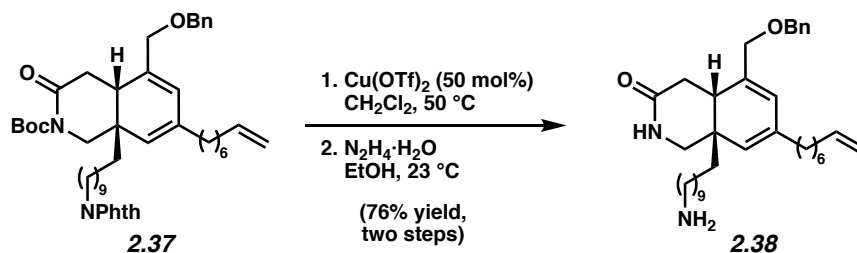


**Diene 2.37.** A flask was charged with vinyl bromide **2.25** (986 mg, 1.34 mmol, 1.00 equiv). To the flask was added bis(triphenylphosphine)palladium(II) chloride (189 mg, 0.269 mmol, 20.0 mol%), 1-methylimidazole (552 mg, 536  $\mu\text{L}$ , 6.72 mmol, 5.00 equiv), and a solution of alkylzinc bromide<sup>14</sup> **2.36** in DMA (1.7 g, 13 mL, 0.52 M, 6.7 mmol, 5.0 equiv). The reaction mixture was stirred at 23  $^\circ\text{C}$  for 19 h. After 19 h, the reaction was quenched with saturated aq.  $\text{NH}_4\text{Cl}$  (10 mL) and diluted with EtOAc (10 mL). The aqueous layer was then diluted with  $\text{H}_2\text{O}$  (10 mL) and extracted with EtOAc (7 x 10 mL). The organic layers were combined, dried over  $\text{MgSO}_4$ , filtered, and concentrated to a crude residue under reduced pressure. The crude residue was purified via flash chromatography (100% benzene  $\rightarrow$  9:1 benzene:EtOAc) to obtain diene **2.37** (886 mg, 86% yield) as a yellow oil. Diene **2.37**:  $R_f$  0.59 (2:1 hexanes:EtOAc);  $^1\text{H}$  NMR (500 MHz,  $\text{CDCl}_3$ ):  $\delta$  7.84 (dd,  $J = 5.3, 2.9, 2\text{H}$ ), 7.70 (dd,  $J = 5.3, 2.9, 2\text{H}$ ), 7.35–7.32 (m, 5H), 5.87–



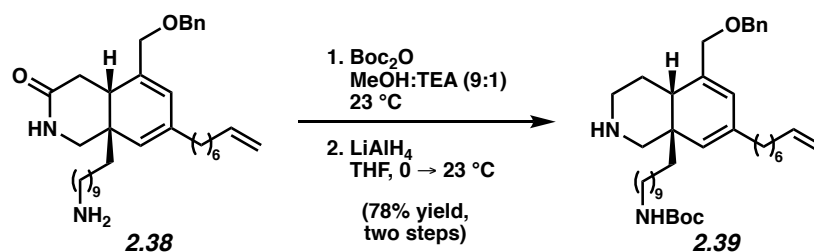
5.72 (m, 2H), 5.02–4.89 (m, 3H), 4.52 (d,  $J = 11.8$ , 1H), 4.45 (d,  $J = 11.8$ , 1H), 4.05 (d,  $J = 12.3$ , 1H), 3.90 (d,  $J = 12.3$ , 1H), 3.69–3.63 (m, 3H), 3.61–3.51 (m, 1H), 2.56 (dd,  $J = 15.0, 5.9$ , 1H), 2.49–2.43 (m, 1H), 2.42–2.32 (m, 1H), 2.08–2.00 (m, 5H), 1.52 (s, 9H), 1.41–1.29 (m, 17H), 1.21–1.17 (m, 8H);  $^{13}\text{C}$  NMR (125 MHz,  $\text{CDCl}_3$ ):  $\delta$  172.2, 168.6, 152.2, 139.2, 138.2, 135.5, 134.4, 134.0, 128.6, 127.80, 127.75, 124.3, 124.0, 123.3, 114.4, 83.1, 72.3, 72.2, 52.6, 40.0, 38.2, 37.6, 37.3, 35.5, 33.9, 30.5, 29.8, 29.71, 29.68, 29.6, 29.3, 29.1, 29.0, 28.8, 28.3, 28.2, 27.0, 23.7, 14.3; IR (film): 2917, 2851, 1773, 1715, 1395  $\text{cm}^{-1}$ ; HRMS-APCI ( $m/z$ )  $[\text{M} + \text{H}]^+$  calcd for  $\text{C}_{48}\text{H}_{65}\text{N}_2\text{O}_6^+$ , 765.48371; found 765.48541.

*Note: 2.37 was obtained as a mixture of rotamers. These data represent empirically observed chemical shifts from the  $^1\text{H}$  and  $^{13}\text{C}$  NMR spectra.*



**Primary amine 2.38.** To a solution of diene **2.37** (886 mg, 1.16 mmol, 1.00 equiv) in  $\text{CH}_2\text{Cl}_2$  (11.6 mL, 0.10 M) was added  $\text{Cu}(\text{OTf})_2$  (209 mg, 579  $\mu\text{mol}$ , 50.0 mol%). The vial was sealed and the reaction mixture was heated to 50  $^\circ\text{C}$  and stirred for 1.5 h. At this point, the reaction mixture was cooled to 23  $^\circ\text{C}$  and quenched with saturated aq.  $\text{NaHCO}_3$  (10 mL). The organic layer was diluted with  $\text{CH}_2\text{Cl}_2$  (10 mL) and the layers were separated. The organic layer was washed with saturated aq.  $\text{NaHCO}_3$  (1 x 10 mL) and water (1 x 10 mL). The combined aqueous layers were washed with  $\text{CH}_2\text{Cl}_2$  (2 x 10 mL). The combined organic layers were dried over magnesium sulfate, filtered, and concentrated under reduced pressure. The crude residue was purified via flash chromatography (3:1 benzene:EtOAc  $\rightarrow$  1:2 Benzene:EtOAc) to obtain the

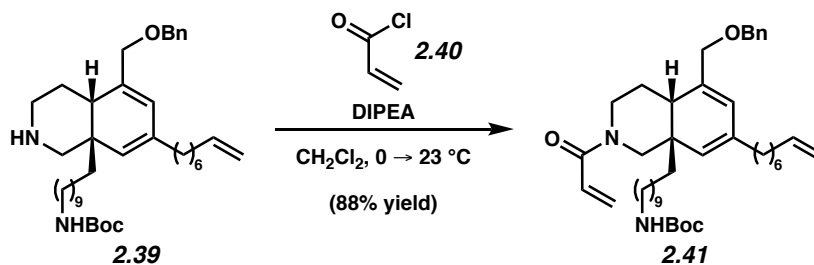
secondary amide as a colorless oil. To a solution of the secondary amine (457 mg, 688  $\mu\text{mol}$ , 1.00 equiv) in ethanol (6.9 mL, 0.10 M) was added hydrazine monohydrate (108 mg, 104  $\mu\text{L}$ , 64% Wt, 1.38 mmol, 2.00 equiv) over 1 min. The reaction was heated to 40  $^{\circ}\text{C}$  and stirred. After 3 h, additional hydrazine monohydrate (104  $\mu\text{L}$ , 64 wt%, 1.38 mmol, 2.00 equiv) was added dropwise to the reaction mixture over 1 min. After 4 h total, the solvent was removed under vacuum. The reaction was diluted with EtOAc (5 mL) and quenched with saturated aq.  $\text{NaHCO}_3$  (5 mL). The layers were separated and the aqueous layer was diluted with  $\text{H}_2\text{O}$  (3 mL) and extracted with EtOAc (3 x 5 mL) and  $\text{CH}_2\text{Cl}_2$  (2 x 5 mL). The organic layers were combined, dried over sodium sulfate and was concentrated under reduced pressure. The crude residue was purified via flash chromatography (9:1  $\text{CH}_2\text{Cl}_2$ :MeOH  $\rightarrow$  1:1  $\text{CH}_2\text{Cl}_2$ :MeOH w/ 5% TEA) to obtain primary amine **2.38** as a colorless oil (330 mg, 76% yield over two steps). Primary amine **2.38**:  $R_f$  0.63 (3:1  $\text{CH}_2\text{Cl}_2$ :MeOH);  $^1\text{H}$  NMR (500 MHz,  $\text{CDCl}_3$ ):  $\delta$  7.40–7.28 (m, 5H), 5.86–5.77 (m, 1H), 5.76 (s, 1H), 5.26 (s, 1H), 5.03–4.96 (m, 1H), 4.96–4.90 (s, 1H), 4.57 (d,  $J = 11.9$ , 1H), 4.52–4.43 (m, 2H), 4.12 (d,  $J = 12.7$ , 1H), 3.92 (d,  $J = 12.9$ , 1H), 3.14–3.04 (m, 2H), 3.01–2.88 (m, 2H), 2.68–2.57 (m, 5H), 2.40 (d,  $J = 12.7$ , 2H), 2.12–1.99 (m, 5H), 1.91 (dd,  $J = 11.8$ , 3.6, 1H), 1.60–1.52 (m, 2H), 1.47–1.41 (m, 15H), 1.34–1.04 (m, 37H); IR (film): 3383, 2923, 2853, 1717, 1043  $\text{cm}^{-1}$ ; HRMS-APCI (m/z)  $[\text{M} + \text{H}]^+$  calcd for  $\text{C}_{35}\text{H}_{55}\text{N}_2\text{O}_2^+$ , 535.42678; found 535.42581.



**Secondary amine 2.39.** To a solution of amide **2.38** (197 mg, 369  $\mu$ mol, 1.00 equiv) dissolved in methanol (3.7 mL, 0.10 M) was added triethylamine (0.41 mL) dropwise over 1 min and Boc<sub>2</sub>O (121 mg, 554  $\mu$ mol, 1.50 equiv). The reaction was stirred at 23 °C for 13 h. After 13 h, the reaction mixture was concentrated to a crude oil. The crude oil was dissolved in EtOAc (5 mL) and quenched with saturated aq. NaHCO<sub>3</sub> (5 mL). The layers were separated and the aqueous layer was washed with EtOAc (3 x 5 mL). The organic layers were combined and washed with brine (1 x 5 mL). The organic layers were combined, dried over sodium sulfate, and concentrated under reduced pressure. The crude residue was purified via flash chromatography (100% DCM → 19:1 DCM:MeOH) to obtain the Boc-protected amine. A solution of the Boc-protected amine (199 mg, 313  $\mu$ mol, 1.00 equiv) in THF (3.1 mL, 0.10 M) was cooled to 0 °C. To this solution was added LiAlH<sub>4</sub> in THF (2.0 M) (784  $\mu$ L, 2.0 M, 1.57 mmol, 5.00 equiv) dropwise over 1 min. The reaction was then warmed to 23 °C and stirred for 4 h. After 4 h, the reaction mixture was cooled to 0 °C and diluted with Et<sub>2</sub>O (2 mL). The reaction mixture was then quenched with water (150  $\mu$ L), 3 M aqueous NaOH (150  $\mu$ L), and water (300  $\mu$ L) and was stirred for 5 min. The mixture was warmed to 23 °C, dried over magnesium sulfate, filtered over a pad of celite, rinsed with EtOAc (10 mL), and concentrated under reduced pressure. The crude residue was purified via flash chromatography (19:1 CH<sub>2</sub>Cl<sub>2</sub>:MeOH → 9:1 CH<sub>2</sub>Cl<sub>2</sub>:MeOH w/ 5% Et<sub>3</sub>N) to obtain secondary amine **2.39** (179 mg, 78% yield over 2 steps). Secondary amine **2.39**: R<sub>f</sub> 0.14 (19:1 CH<sub>2</sub>Cl<sub>2</sub>:MeOH); <sup>1</sup>H NMR (500 MHz, CDCl<sub>3</sub>):  $\delta$  7.39–7.31 (m, 5H), 5.77 (s, 1H), 5.44–5.32 (m, 1H), 5.25 (s, 1H), 5.02–4.88 (m, 1H), 4.60–4.54 (m, 1H), 4.52–4.42 (m, 2H),

4.13–4.09 (m, 1H), 3.92 (d,  $J = 13.0$ , 1H), 3.78–3.69 (m, 1H), 3.68–3.61 (m, 1H), 3.13–3.05 (m, 3H), 3.05–2.94 (m, 2H), 2.46–2.40 (m, 1H), 2.29–2.19 (m, 1H), 2.10–1.85 (m, 17H), 1.67–1.51 (m, 5H), 1.48–1.42 (m, 17H), 1.36–1.06 (m, 67H);  $^{13}\text{C}$  NMR (125 MHz,  $\text{CDCl}_3$ ):  $\delta$  156.1, 139.3, 138.84, 138.79, 138.5, 136.64, 136.57, 131.7, 129.9, 128.5, 127.8, 127.7, 124.8, 122.7, 122.6, 114.3, 79.1, 72.3, 72.0, 68.1, 63.3, 60.5, 58.6, 56.1, 54.4, 44.9, 40.8, 38.5, 37.6, 36.1, 35.5, 33.9, 33.0, 32.7, 32.07, 32.05, 30.8, 30.2, 29.84, 29.81, 29.75, 29.70, 29.64, 29.58, 29.51, 29.49, 29.44, 29.37, 29.2, 29.14, 29.06, 28.9, 28.72, 28.66, 28.58, 27.4, 27.0, 25.9, 25.8, 25.6, 23.8, 22.8, 21.2, 18.6, 18.1, 14.34, 14.27; IR (film): 2925, 2853, 1707, 1455, 1173  $\text{cm}^{-1}$ ; HRMS-APCI ( $m/z$ ) [ $\text{M} + \text{H}$ ] $^+$  calcd for  $\text{C}_{40}\text{H}_{65}\text{N}_2\text{O}_3^+$ , 621.49897; found 621.49822.

*Note: 2.39 was obtained as a mixture of rotamers. These data represent empirically observed chemical shifts from the  $^1\text{H}$  and  $^{13}\text{C}$  NMR spectra.*

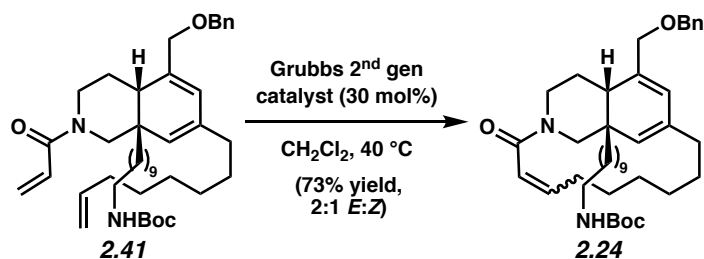


**Acrylamide 2.41.** To a solution of secondary amine **2.39** (163 mg, 262  $\mu\text{mol}$ , 1.00 equiv) in  $\text{CH}_2\text{Cl}_2$  (2.6 mL, 0.10 M) was added N,N-diisopropylethylamine (137  $\mu\text{L}$ , 785  $\mu\text{mol}$ , 3.00 equiv) dropwise over 1 min. The solution was cooled to  $0\text{ }^\circ\text{C}$ . To the stirring solution, acryloyl chloride (**2.40**, 64.0  $\mu\text{L}$ , 785  $\mu\text{mol}$ , 3.00 equiv) was added dropwise over 1 min at  $0\text{ }^\circ\text{C}$ . The reaction was warmed to  $23\text{ }^\circ\text{C}$  and allowed to stir for 1 h. The reaction mixture was quenched with water (3 mL) and diluted with EtOAc (5 mL). The organic layer was washed with saturated aq.  $\text{NaHCO}_3$  (1 x 5 mL). The aqueous layers were extracted with EtOAc (4 x 5 mL) and  $\text{CH}_2\text{Cl}_2$  (1 x 5 mL).

The combined organic layers were dried over sodium sulfate, filtered, and concentrated under reduced pressure. The crude residue was purified via flash chromatography (3:1 hexanes:EtOAc → 1:1 hexanes:EtOAc) to obtain acrylamide **2.41** (155 mg, 88% yield) as a colorless oil. Acrylamide **2.41**:  $R_f$  0.41 (19:1  $\text{NH}_3$  saturated  $\text{CH}_2\text{Cl}_2$ :MeOH);  $^1\text{H}$  NMR (500 MHz,  $\text{CDCl}_3$ ):  $\delta$  7.42–7.31 (m, 5H), 6.63 (ddd,  $J = 90.5, 16.6, 10.7$ , 1H), 6.28 (dd,  $J = 36.6, 16.6$ , 1H), 5.87–5.60 (m, 3H), 5.36–5.07 (m, 1H), 4.98 (d,  $J = 17.0$ , 1H), 4.92 (d,  $J = 10.2$ , 1H), 4.61–4.44 (m, 3H), 4.11 (d,  $J = 12.6$ , 1H), 3.95 (d,  $J = 12.6$ , 1H), 3.91–3.84 (m, 1H), 3.16–3.03 (m, 2H), 2.98–2.84 (m, 1H), 2.55–2.39 (m, 1H), 2.11–1.94 (m, 5H), 1.68–1.61 (m, 2H), 1.44 (s, 13H), 1.40–0.83 (m, 37H);  $^{13}\text{C}$  NMR (125 MHz,  $\text{CDCl}_3$ ):  $\delta$  165.7, 165.4, 156.1, 139.3, 139.2, 138.7, 138.4, 137.9, 136.6, 135.9, 128.7, 128.5, 128.3, 128.03, 127.96, 127.8, 127.3, 125.6, 123.4, 123.0, 114.3, 79.2, 72.5, 72.3, 72.1, 72.0, 53.6, 49.7, 45.9, 42.2, 41.1, 40.8, 40.3, 40.1, 37.1, 37.0, 35.3, 35.2, 33.9, 33.3, 32.1, 30.7, 30.6, 30.2, 29.8, 29.7, 29.6, 29.4, 29.2, 29.1, 29.0, 28.6, 28.4, 27.5, 27.0, 26.3, 24.9, 23.9, 22.8, 14.3; IR (film): 2927, 2854, 1701, 1642, 1453  $\text{cm}^{-1}$ ; HRMS-APCI (m/z)  $[\text{M} + \text{H}]^+$  calcd for  $\text{C}_{43}\text{H}_{67}\text{N}_2\text{O}_4^+$ , 675.50954; found 675.50822.

*Note: 2.41 was obtained as a mixture of rotamers. These data represent empirically observed chemical shifts from the  $^1\text{H}$  and  $^{13}\text{C}$  NMR spectra.*

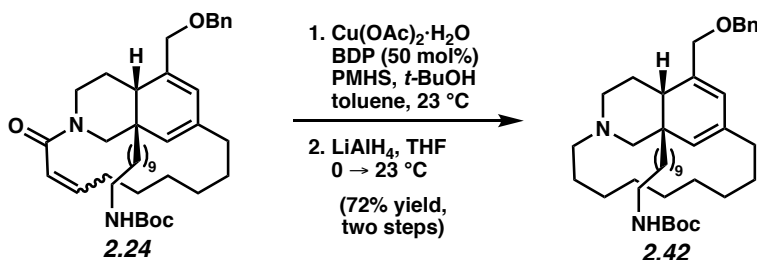
### 2.7.2.5 Macrocyclization and Manipulations of Macrocycle 2.24



**Macrocycle 2.24.** To a flask in the glovebox was added Grubbs' 2<sup>nd</sup> generation catalyst (67.4 mg, 79.3  $\mu$ mol, 30.0 mol%). The flask was then removed from the glovebox and acrylamide **2.41** (179 mg, 264  $\mu$ mol, 1.00 equiv) dissolved in CH<sub>2</sub>Cl<sub>2</sub> (265 mL, 0.001 M) was added. The flask was equipped with a condenser and heated to 40 °C for 20 h. After 20 h, the reaction was removed from heat and the solvent evaporated under reduced pressure. The crude residue was purified via flash chromatography (2:1 hexanes:EtOAc  $\rightarrow$  1:1 hexanes:EtOAc) to obtain macrocycle **2.24** (126 mg, 73% yield) as a brown oil. Macrocycle **2.24**:  $R_f$  0.22 (2:1 Hexanes:EtOAc); <sup>1</sup>H NMR (600 MHz, CDCl<sub>3</sub>):  $\delta$  7.40–7.29 (m, 17H), 6.92 (d,  $J = 14.4$ , 1H), 6.26 (d  $J = 14.4$ , 1H), 6.34–6.22 (m, 2H), 6.06–6.79 (m, 2H), 5.70–5.58 (m, 3H), 5.42–5.21 (m, 1H), 5.07–4.97 (m, 2H), 4.85–4.75 (m, 1H), 4.67–4.41 (m, 12H), 4.16–4.06 (m, 3H), 3.99–3.80 (m, 6H) 3.18–3.03 (m, 8H), 3.02–2.76 (m, 4H), 2.57–2.43 (m, 3H), 2.43–2.30 (m, 3H), 2.21–1.97 (m, 12H), 1.96–1.86 (m, 2H), 1.86–1.75 (m, 3H), 1.49–1.41 (m, 48H), 1.37–1.09 (m, 82H); <sup>13</sup>C NMR (125 MHz, CDCl<sub>3</sub>):  $\delta$  165.6, 156.1, 145.1, 141.1, 138.8, 138.4, 135.4, 134.2, 133.1, 130.3, 129.9, 129.8, 129.2, 128.7, 128.54, 128.49, 128.3, 128.2, 127.8, 127.1, 126.5, 123.8, 123.6, 122.6, 122.1, 79.2, 72.5, 72.2, 72.0, 69.4, 66.5, 64.2, 54.7, 49.0, 42.2, 41.2, 40.8, 40.5, 37.7, 36.8, 33.4, 32.3, 30.7, 30.2, 29.8, 29.74, 29.68, 29.5, 29.4, 29.2, 28.6, 27.9, 27.8, 27.0, 26.6,

26.5, 26.44, 26.36, 24.9, 23.7, 23.5, 22.8, 14.3; IR (film): 2925, 2853, 1717, 1456, 1271  $\text{cm}^{-1}$ ;  
HRMS-APCI (m/z)  $[\text{M} + \text{H}]^+$  calcd for  $\text{C}_{41}\text{H}_{63}\text{N}_2\text{O}_4^+$ , 645.46368; found 645.46298.

*Note: 2.24 was obtained as a mixture of E and Z isomers. These data represent empirically observed chemical shifts from the  $^1\text{H}$  and  $^{13}\text{C}$  NMR spectra.*

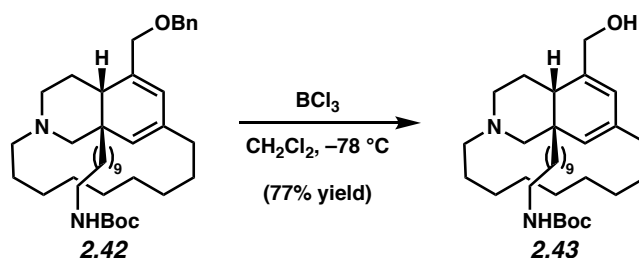


**Tertiary amine 2.42.** To a vial was added copper(II)acetate monohydrate (19.7 mg, 98.8  $\mu\text{mol}$ , 1.00 equiv) and 1,2-bis(diphenylphosphanyl)benzene (BDP) (22.0 mg, 49.4  $\mu\text{mol}$ , 50.0 mol%) . These were dissolved in sparged *t*BuOH (0.190 mL, 1.98 mmol, 20.0 equiv) and toluene (0.38 mL, 0.26 M) and the reaction was stirred for 25 minutes to give a blue solution. At this point PMHS (560  $\mu\text{L}$ , 296  $\mu\text{mol}$ , 3.00 equiv) was added dropwise over 3 min and the solution gradually turned from blue to a yellow/green (~15 min) color. A separate vial was charged with macrocycle **2.24** (63.9 mg, 98.8  $\mu\text{mol}$ , 1.00 equiv), which was dissolved in toluene (0.38 mL). The macrocycle solution was then added to the Strykers reagent solution dropwise over 3 min. The reaction was stirred at 23 °C for 19 h at which point it was diluted with EtOAc (2 mL). The organic layer was washed with 1 N NaOH (2 mL) followed by 1N HCl (2 mL), and saturated aq.  $\text{NaHCO}_3$  (2 mL). The aqueous layers were combined and washed with EtOAc (2 x 2 mL). The organic layers were combined, washed with brine (2 mL), dried over magnesium sulfate, and concentrated under reduced pressure. The crude residue was purified via flash chromatography (9:1 hexanes:EtOAc → 1:1 hexanes:EtOAc) to obtain the amide. A solution of the amide (50.9 mg, 1.00 equiv, 78.4  $\mu\text{mol}$ ) dissolved in THF (0.78 mL, 0.10 M) was cooled to 0 °C. To this

solution was added LiAlH<sub>4</sub> in THF (14.9 mg, 196 μL, 2.0 M, 5.00 equiv, 392 μmol) dropwise over 1 min. The reaction was then warmed to 23 °C and stirred for 40 min. After 40 min, the reaction mixture was cooled to 0 °C and diluted with Et<sub>2</sub>O (1 mL). The reaction mixture was then quenched with water (40 uL), 2 M aqueous NaOH (40 uL), and water (120 uL) and was stirred for 5 min. The mixture was warmed to 23 °C, dried over magnesium sulfate, filtered over a pad of celite, rinsed with EtOAc (10 mL), and concentrated under reduced pressure to obtain tertiary amine **2.42** (38.9 mg, 72% yield over two steps) as a colorless oil that was used without further purification. Tertiary amine **2.42**: R<sub>f</sub> 0.58 (3:1 Hexanes:EtOAc); <sup>1</sup>H NMR (500 MHz, CDCl<sub>3</sub>): δ 7.40–7.31 (m, 5H), 5.64 (s, 1H), 5.28 (s, 1H), 4.59–4.42 (m, 4H), 4.15–4.10 (m, 1H), 3.96–3.91 (m, 1H), 3.14–3.02 (m, 4H), 2.76–2.62 (m, 3H), 2.42–2.33 (m, 2H), 2.31–2.23 (m, 2H), 2.23–2.13 (m, 2H), 2.06–1.96 (m, 2H), 1.82–1.73 (m, 4H), 1.73–1.63 (m, 5H), 1.63–1.53 (m, 6H), 1.44 (m, 28H), 1.37–0.79 (m, 49H); <sup>13</sup>C NMR (125 MHz, CDCl<sub>3</sub>): δ 156.1, 139.6, 138.7, 132.7, 131.1, 128.7, 128.5, 127.8, 127.6, 127.1, 123.3, 79.1, 72.7, 71.7, 65.6, 65.5, 63.1, 63.0, 62.9, 55.9, 52.0, 40.9, 40.8, 39.2, 37.0, 32.7, 30.9, 30.3, 30.2, 29.8, 29.73, 29.70, 29.66, 29.4, 28.6, 28.4, 27.0, 26.8, 25.7, 25.62, 25.57, 25.1, 24.2, 23.9; IR (film): 2925, 2853, 1694, 1365, 1172 cm<sup>-1</sup>; HRMS-APCI (m/z) [M + H]<sup>+</sup> calcd for C<sub>41</sub>H<sub>67</sub>N<sub>2</sub>O<sub>3</sub><sup>+</sup>, 635.51462; found 635.51459.

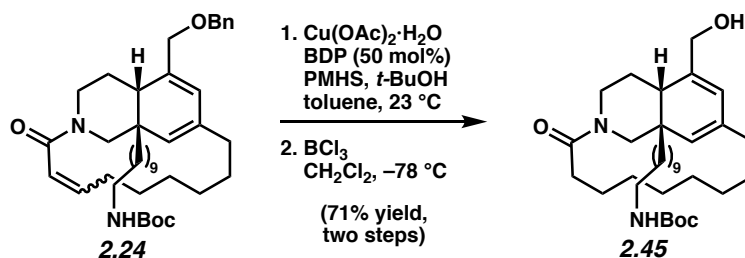
*Note: 2.42 was obtained as a mixture of rotamers. These data represent empirically observed chemical shifts from the <sup>1</sup>H and <sup>13</sup>C NMR spectra.*





**Alcohol 2.43.** A solution of tertiary amine **2.42** (3.8 mg, 6.0  $\mu\text{mol}$ , 1.0 equiv) dissolved in  $\text{CH}_2\text{Cl}_2$  (0.20 mL, 0.030 M) was cooled to  $-78\text{ }^\circ\text{C}$ . To the solution was added boron trichloride in  $\text{CH}_2\text{Cl}_2$  (30  $\mu\text{L}$ , 1.0 M, 30  $\mu\text{mol}$ , 5.0 equiv) dropwise over 1 min. The reaction mixture was stirred at  $-78\text{ }^\circ\text{C}$  for 25 min. The reaction mixture was quenched with saturated aq.  $\text{NaHCO}_3$  (1 mL) and the reaction was allowed to warm to  $23\text{ }^\circ\text{C}$ . The reaction mixture was diluted with  $\text{CH}_2\text{Cl}_2$  (1 mL), the layers were separated, and the aqueous layer was extracted with  $\text{CH}_2\text{Cl}_2$  (3 x 1 mL). The combined organic layers were dried over magnesium sulfate, filtered, and concentrated under reduced pressure. The crude residue was purified via silica plug (2:1 hexanes:EtOAc) to obtain alcohol **2.43** (2.5 mg, 77% yield) as a colorless oil. Alcohol **2.43**:  $R_f$  0.65 (3:1 Hexanes:EtOAc);  $^1\text{H}$  NMR (500 MHz,  $\text{CDCl}_3$ ):  $\delta$  5.70 (s, 1H), 5.32 (s, 1H), 4.48 (s, 1H), 4.21–4.15 (m, 1H), 4.11 (d,  $J = 11.2$ , 1H), 3.14–3.03 (m, 2H), 2.75–2.63 (m, 2H), 2.43–2.34 (m, 1H), 2.29–2.22 (m, 1H), 2.22–2.14 (m, 1H), 2.02–1.94 (m, 1H), 1.86 (dd,  $J = 12.3, 4.9$ , 1H), 1.81–1.76 (m, 1H), 1.72–1.64 (m, 3H), 1.64–1.52 (m, 7H), 1.49–1.39 (m, 18H), 1.38–0.91 (m, 31H);  $^{13}\text{C}$  NMR (125 MHz,  $\text{CDCl}_3$ ):  $\delta$  156.1, 138.2, 134.0, 130.9, 125.5, 79.1, 62.7, 55.8, 51.8, 48.9, 40.9, 40.8, 39.4, 36.7, 32.6, 30.78, 30.75, 30.2, 30.1, 29.8, 29.7, 29.4, 28.6, 28.4, 27.0, 26.8, 25.64, 25.59, 25.5, 25.1, 24.1, 23.7; IR (film): 2927, 2854, 1702, 1249, 1173  $\text{cm}^{-1}$ ; HRMS-APCI (m/z)  $[\text{M} + \text{H}]^+$  calcd for  $\text{C}_{34}\text{H}_{61}\text{N}_2\text{O}_3^+$ , 545.46767; found 545.46665.

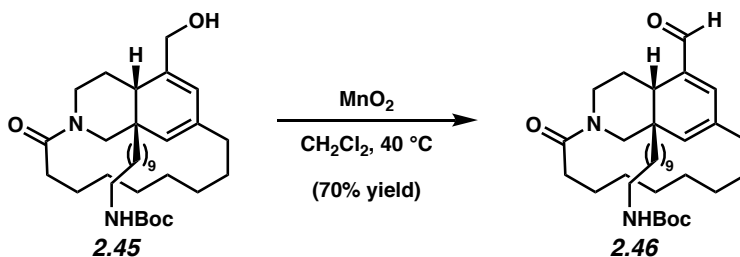
*Note: 2.43 was obtained as a mixture of rotamers. These data represent empirically observed chemical shifts from the  $^1\text{H}$  and  $^{13}\text{C}$  NMR spectra.*



**Alcohol 2.45.** To a vial was added copper(II)acetate monohydrate (19.7 mg, 98.8  $\mu\text{mol}$ , 1.00 equiv) and 1,2-bis(diphenylphosphaneyl)benzene (BDP) (22.0 mg, 49.4  $\mu\text{mol}$ , 50.0 mol%). These were dissolved in sparged *t*BuOH (0.190 mL, 1.98 mmol, 20.0 equiv) and toluene (0.38 mL, 0.26 M) and the reaction was stirred for 25 minutes to give a blue solution. At this point PMHS (560  $\mu\text{L}$ , 296  $\mu\text{mol}$ , 3.00 equiv) was added dropwise over 3 min and the solution gradually turned from blue to a yellow/green color (~15 min). A separate vial was charged with macrocycle **2.24** (63.9 mg, 98.8  $\mu\text{mol}$ , 1.00 equiv) dissolved in toluene (0.38 mL). The macrocycle solution was then added to the Strykers reagent solution dropwise over 3 min. The reaction was stirred at 23 °C for 19 h at which point it was diluted with EtOAc (2 mL). The organic layer was washed with 1 N NaOH (2 mL) followed by 1N HCl (2 mL), and saturated aq.  $\text{NaHCO}_3$  (2 mL). The aqueous layers were combined and washed with EtOAc (2 x 2 mL). The organic layers were combined, washed with brine (2 mL), dried over magnesium sulfate, and concentrated under reduced pressure. The crude residue was purified via flash chromatography (9:1 hexanes:EtOAc  $\rightarrow$  1:1 hexanes:EtOAc) to obtain the amide. A solution of the amide (15.9 mg, 24.5  $\mu\text{mol}$ , 1.00 equiv) dissolved in  $\text{CH}_2\text{Cl}_2$  (0.40 mL, 0.050 M) was cooled to -78 °C. To the solution was added boron trichloride in  $\text{CH}_2\text{Cl}_2$  (123  $\mu\text{L}$ , 1.0 molar, 123  $\mu\text{mol}$ , 5.00 equiv) dropwise over 1 min. The reaction mixture was stirred for 30 min. The reaction mixture was quenched with saturated aq.  $\text{NaHCO}_3$  (1 mL) and the reaction was allowed to warm to 23 °C. The reaction mixture was diluted with  $\text{CH}_2\text{Cl}_2$  (1 mL), the layers were separated, and the

aqueous layer was extracted with CH<sub>2</sub>Cl<sub>2</sub> (3 x 1 mL). The combined organic layers were dried over magnesium sulfate, filtered, and concentrated under reduced pressure. The crude residue was purified via silica plug (1:1 hexanes:EtOAc) to obtain alcohol **2.45** (10.4 mg, 71% yield over two steps) as a colorless oil. Alcohol **2.45**: *R<sub>f</sub>* 0.36 (1:1 Hexanes:EtOAc); <sup>1</sup>H NMR (500 MHz, CDCl<sub>3</sub>): δ 5.77 (s, 1H), 5.36 (s, 1H), 4.83 (d, *J* = 13.6, 1H), 4.50 (s, 1H), 4.14 (dt, *J* = 11.6, 9.1, 2H), 3.83 (d, *J* = 14.2, 1H), 3.15–3.04 (m, 3H), 2.92 (t, *J* = 14.1, 1H), 2.72–2.63 (m, 1H), 2.30 (d, *J* = 13.2, 1H), 2.16–2.05 (m, 3H), 2.05–2.00 (m, 2H), 1.82–1.71 (m, 2H), 1.50–1.35 (m, 28H), 1.35–0.83 (m, 39H); <sup>13</sup>C NMR (125 MHz, CDCl<sub>3</sub>): δ 172.4, 137.1, 135.1, 130.7, 126.3, 49.1, 48.3, 46.2, 40.9, 40.8, 40.1, 36.8, 34.0, 33.4, 30.6, 30.2, 29.64, 29.62, 29.60, 29.4, 28.6, 28.3, 27.0, 26.9, 26.7, 26.5, 26.4, 25.4, 25.1, 23.6; IR (film): 3339, 2927, 2855, 1706, 1628, 1173 cm<sup>-1</sup>; HRMS-APCI (*m/z*) [*M* + *H*]<sup>+</sup> calcd for C<sub>34</sub>H<sub>59</sub>N<sub>2</sub>O<sub>4</sub><sup>+</sup>, 559.44693; found 559.44658.

*Note: 2.45 was obtained as a mixture of rotamers. These data represent empirically observed chemical shifts from the <sup>1</sup>H and <sup>13</sup>C NMR spectra.*

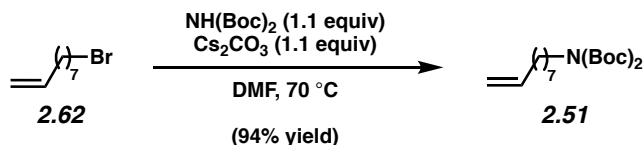


**Aldehyde 2.46.** To a solution of alcohol **2.45** (1.0 mg, 1.8 μmol, 1.0 equiv) in CH<sub>2</sub>Cl<sub>2</sub> (0.3 mL, 0.006 M) was added manganese dioxide (16 mg, 0.18 mmol, 100 equiv) in one portion. The vial was sealed with a Teflon-coated cap and the reaction mixture was heated to 40 °C and stirred for 19 h. After 19 h the reaction mixture was cooled to room temperature, filtered over celite, rinsed with CH<sub>2</sub>Cl<sub>2</sub> (10 mL), and concentrated under reduced pressure to yield aldehyde **2.46** (0.7 mg,

70% yield) as a colorless oil. Aldehyde **2.46**:  $R_f$  0.59 (1:1 Hexanes:EtOAc);  $^1\text{H}$  NMR (500 MHz,  $\text{CDCl}_3$ ):  $\delta$  9.53 (s, 1H), 6.58 (s, 1H), 5.90 (s, 1H), 4.90 (d,  $J = 13.4$ , 1H), 4.50 (s, 1H), 3.80 (d,  $J = 14.1$ , 1H), 3.17–3.05 (m, 2H), 2.99 (td,  $J = 13.3, 2.5$ , 1H), 2.72–2.62 (m, 2H), 2.40–2.31 (m, 2H), 2.22–2.16 (m, 2H), 2.16–2.09 (m, 1H), 1.73–1.65 (m, 2H), 1.50–1.41 (m, 20H), 1.40–0.82 (m, 55H);  $^{13}\text{C}$  NMR (125 MHz,  $\text{CDCl}_3$ ):  $\delta$  192.7, 172.4, 145.3, 140.6, 136.0, 49.0, 46.0, 40.8, 40.4, 37.3, 35.7, 33.9, 33.2, 30.5, 30.2, 29.9, 29.6, 29.5, 29.4, 28.6, 28.4, 27.0, 26.7, 26.3, 26.2, 25.3, 24.8, 23.8, 22.8, 14.3; IR (film): 2926, 2855, 1712, 1672, 1172  $\text{cm}^{-1}$ ; HRMS-APCI ( $m/z$ )  $[\text{M} + \text{H}]^+$  calcd for  $\text{C}_{34}\text{H}_{57}\text{N}_2\text{O}_4^+$ , 557.43128; found 557.43115.

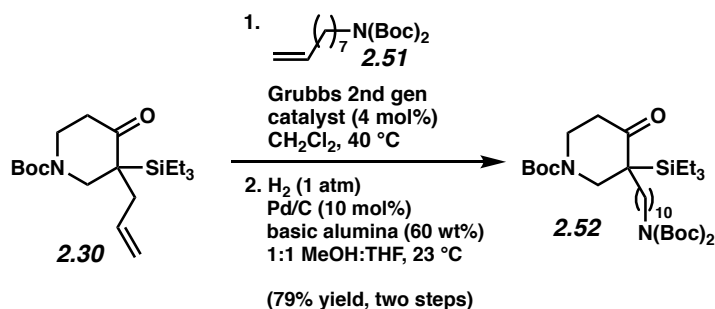
*Note: 2.46 was obtained as a mixture of rotamers. These data represent empirically observed chemical shifts from the  $^1\text{H}$  and  $^{13}\text{C}$  NMR spectra.*

### 2.7.2.6 Synthesis of Silyl Triflate 2.53



**Alkene 2.51.** To a solution of bromide **2.62** (15.0 g, 73.2 mmol, 1.00 equiv) in DMF (360 mL, 0.20 M) was added di-tert-butyl iminodicarbonate (17.5 g, 80.6 mmol, 1.10 equiv) and cesium carbonate (26.2 g, 80.4 mmol, 1.10 equiv). The reaction mixture was heated to 70 °C for 2 h. After this time, the mixture was allowed to cool to room temperature and then was transferred to a separatory funnel with water (500 mL) and  $\text{Et}_2\text{O}$  (200 mL). The layers were separated and the aqueous layer was extracted with  $\text{Et}_2\text{O}$  (3 x 200 mL). The combined organic layers were washed with water (3 x 200 mL) and brine (100 mL), dried over  $\text{MgSO}_4$ , filtered, and concentrated under reduced pressure. The crude residue was purified via flash chromatography (20:1 hexanes:EtOAc) to afford alkene **2.51** (23.4 g, 94 %) as a colorless oil. Alkene **2.51**:  $R_f$  0.47 (9:1

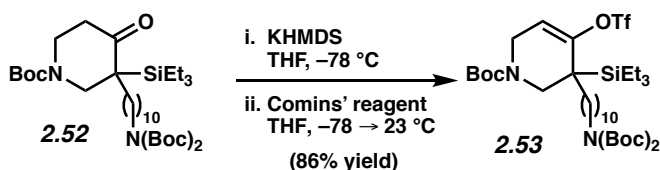
Hexanes:EtOAc);  $^1\text{H}$  NMR (400 MHz,  $\text{CDCl}_3$ ):  $\delta$  5.78 (ddt,  $J = 17.1, 10.2, 6.7$ , 1H), 5.01–4.87 (m, 2H), 3.56–3.48 (m, 2H), 2.05–1.97 (m, 2H), 1.58–1.51 (m, 2H), 1.48 (s, 18H), 1.39–1.31 (m, 2H), 1.31–1.23 (m, 6H);  $^{13}\text{C}$  NMR (100 MHz,  $\text{CDCl}_3$ ):  $\delta$  152.8, 139.2, 114.3, 82.0, 46.6, 33.9, 29.3, 29.14, 29.12, 38.9, 28.2, 26.9; IR (film):  $\text{cm}^{-1}$ ; IR (film): 3078, 2930, 1697, 1367, 1128  $\text{cm}^{-1}$ ; HRMS-APCI (m/z)  $[\text{M} + \text{H}]^+$  calcd for  $\text{C}_{19}\text{H}_{36}\text{NO}_4^+$ , 342.26389; found 342.25999.



**Ketone 2.52.** To a flask in the glovebox was added Grubbs' 2<sup>nd</sup> generation catalyst (50.1 mg, 59.1  $\mu\text{mol}$ , 4.00 mol%). The flask was then removed from the glovebox and silyl ketone **2.30** (522 mg, 1.48 mmol, 1.00 equiv) and alkene **2.51** (2.52 g, 7.38 mmol, 5.00 equiv) dissolved in  $\text{CH}_2\text{Cl}_2$  (7.0 mL, 0.20 M) were added. The flask was fitted with a reflux condenser and heated to 40 °C for 21 h. After this time, the reaction was removed from heat and the solvent evaporated under reduced pressure. The crude residue was purified via flash chromatography (19:1 hexanes:EtOAc  $\rightarrow$  9:1 hexanes:EtOAc) to afford the cross-metathesis product. To a solution of the cross-metathesis product (1.28 g, 1.84 mmol, 1.00 equiv) in THF (28 mL, 0.033 M) and methanol (28 mL) was added basic alumina (1.30 g) and palladium on carbon (203 mg, 10.0 wt%, 191  $\mu\text{mol}$ , 10.0 mol%). The flask was then sparged with  $\text{H}_2$  from a balloon and then left to stir under an atmosphere of  $\text{H}_2$  (1 atm) for 7 h. The reaction was then filtered over celite (3 cm, monster pipette) with  $\text{CH}_2\text{Cl}_2$  as the eluent (50 mL) and the solvent was removed under reduced pressure. The crude residue was purified via flash chromatography (4:1 hexanes:EtOAc) to

afford ketone **2.52** (1.26 g, 79% yield over two steps) as a colorless oil. Ketone **2.52**:  $R_f$  0.56 (4:1 Hexanes:EtOAc);  $^1\text{H}$  NMR (400 MHz,  $\text{CDCl}_3$ ):  $\delta$  4.02–3.60 (m, 3H), 3.56–3.49 (m, 2H), 3.41–3.22 (m, 1H), 2.57 (br s, 1H), 2.45–2.29 (m, 1H), 2.07–1.95 (m, 1H), 1.70–1.61 (m, 1H), 1.53–1.43 (m, 29H), 1.31–1.14 (m, 14H), 0.97 (t,  $J = 7.9$ , 9H), 0.79–0.60 (m, 6H);  $^{13}\text{C}$  NMR (100 MHz,  $\text{CDCl}_3$ ):  $\delta$  152.9, 82.1, 46.7, 40.0, 30.7, 29.7, 29.6, 29.4, 29.2, 28.6, 28.2, 27.0, 25.7, 8.0, 2.5; IR (film): 2928, 2857, 1746, 1694, 1366, 1127  $\text{cm}^{-1}$ ; HRMS-APCI ( $m/z$ )  $[\text{M} + \text{H}]^+$  calcd for  $\text{C}_{36}\text{H}_{69}\text{N}_2\text{O}_7\text{Si}^+$ , 669.48686; found 669.48074.

*Note: 2.52 was obtained as a mixture of rotamers. These data represent empirically observed chemical shifts from the  $^1\text{H}$  and  $^{13}\text{C}$  NMR spectra.*

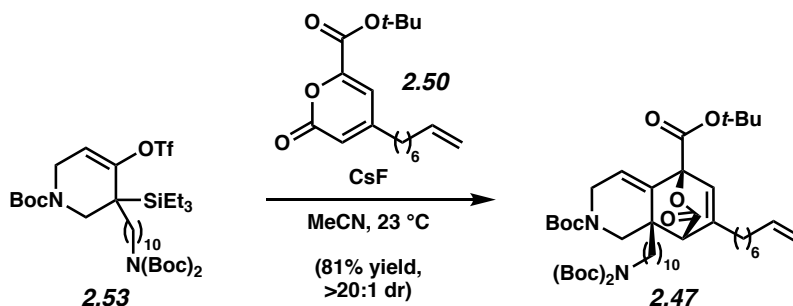


**Silyl Triflate 2.53.** To a flask in the glovebox was added potassium hexamethyldisilazide (697 mg, 3.32 mmol, 1.21 equiv). The flask was then removed from the glovebox and THF (10 mL) was added and it was cooled to  $-78$  °C. To another flask was added silyl ketone **2.52** (1.933 g, 2.75 mmol, 1.00 equiv) and THF (9 mL). The ketone solution was then added dropwise over 10 min to the KHMDS solution at  $-78$  °C. After stirring for 1 h at  $-78$  °C, a third solution of Comins' Reagent (1.29 g, 3.29 mmol, 1.20 equiv) in THF (9 mL) was added dropwise over 5 min at  $-78$  °C. The reaction was then warmed to room temperature and stirred at  $23$  °C for 2 h. After this time, the reaction was quenched with saturated aq.  $\text{NaHCO}_3$  (50 mL) and diluted with water (50 mL) and  $\text{Et}_2\text{O}$  (50 mL). The layers were separated and the aqueous layer was extracted with  $\text{Et}_2\text{O}$  (2 x 50 mL). The combined organic layers were dried over  $\text{MgSO}_4$ , filtered, and concentrated under reduced pressure to provide the crude residue. The crude residue was purified

via flash chromatography (97:3 → 93:7 hexanes:EtOAc) to afford silyl triflate **2.53** (1.92 g, 86% yield) as a colorless oil. Silyl triflate **2.53**:  $R_f$  0.21 (9:1 Hexanes:EtOAc);  $^1\text{H}$  NMR (400 MHz,  $\text{CDCl}_3$ ):  $\delta$  5.66 (br s, 1H), 4.17 (dd,  $J = 17.9, 4.1$ , 1H), 3.92–3.63 (m, 2H), 3.56–3.49 (m, 1H), 3.48–3.31 (m, 1H), 1.65–1.52 (m, 4H), 1.51–1.40 (m, 27H), 1.33–1.15 (m, 15H), 0.99 (t,  $J = 7.9$ , 9H), 0.76–0.65 (m, 6H);  $^{13}\text{C}$  NMR (100 MHz,  $\text{CDCl}_3$ ):  $\delta$  154.3, 152.9, 110.3, 82.1, 80.5, 46.7, 30.6, 30.2, 29.7, 29.6, 29.5, 29.4, 29.2, 28.6, 28.5, 28.2, 27.0, 24.3, 8.1, 2.8; IR (film): 2931, 2856, 1699, 1366, 1127  $\text{cm}^{-1}$ ; HRMS-APCI ( $m/z$ )  $[\text{M} + \text{H}]^+$  calcd for  $\text{C}_{37}\text{H}_{68}\text{F}_3\text{N}_2\text{O}_9\text{SSi}^+$ , 801.43614; found 801.42924.

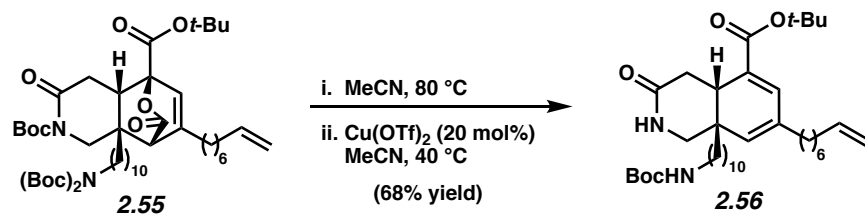
*Note: 2.53 was obtained as a mixture of rotamers. These data represent empirically observed chemical shifts from the  $^1\text{H}$  and  $^{13}\text{C}$  NMR spectra.*

### 2.7.2.7 Diels–Alder Cycloaddition and Elaboration toward Lissodendoric Acid A (2.10)



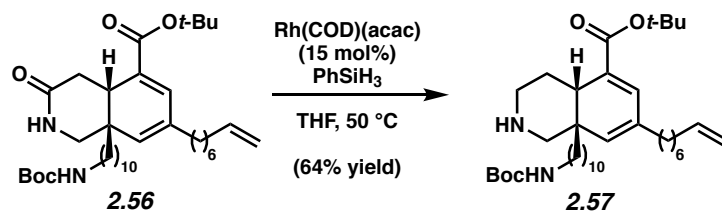
**Cycloadduct 2.47.** To a vial in the glovebox was added CsF (584 mg, 3.84 mmol, 7.38 equiv). This vial was removed from the glovebox and then a separate solution of silyl triflate **2.53** (426 mg, 521  $\mu\text{mol}$ , 1.00 equiv) and pyrone **2.50** (804 mg, 2.62 mmol, 5.00 equiv) in MeCN (5.2 mL) was added to the vial containing cesium fluoride. The reaction mixture was allowed to stir vigorously at 23 °C for 20 h. After this time, the reaction mixture was filtered through a short plug of silica gel (3 cm silica) eluting with 1:1 hexanes:EtOAc (~30 mL) and the concentrated under reduced pressure. The crude residue was purified via flash chromatography (8:1:1

hexanes:CH<sub>2</sub>Cl<sub>2</sub>:Et<sub>2</sub>O → 3:1:1 hexanes:CH<sub>2</sub>Cl<sub>2</sub>:Et<sub>2</sub>O) to afford the cycloadduct **2.47** (369 mg, 81% yield) as yellow oil. Spectral data match those previously reported.<sup>9</sup>



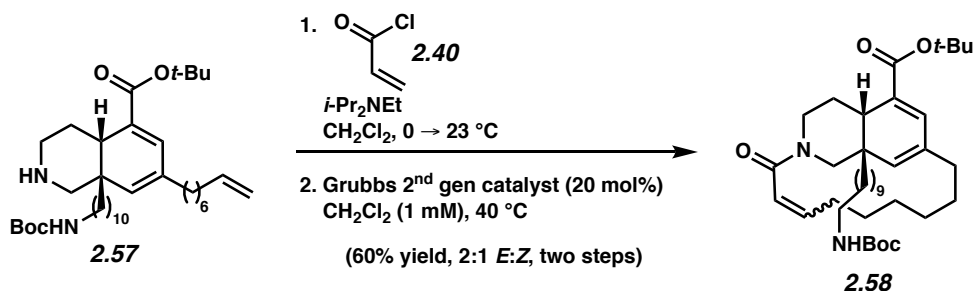
**Diene 2.56.** A vial containing a solution of amide **2.55** (10.0 mg, 11.6 μmol, 1.00 equiv) in acetonitrile (0.39 mL, 0.30 M) was sealed with a Teflon-lined cap and heated to 80 °C for 14.25 h. The solution was then cooled to 23 °C and to the solution was added copper (II) triflate (0.8 mg, 2.3 μmol, 20 mol%) in one portion and the vial was resealed with a Teflon-lined cap. The vial was heated to 40 °C for 1.5 h. The reaction mixture was then allowed to cool to 23 °C and filtered through a short plug of silica gel (0.9 x 2.5 cm silica) eluting with EtOAc (10 mL) and then concentrated under reduced pressure. The crude residue was purified via preparative TLC (1:1 hexanes:EtOAc) to afford diene **2.56** (4.9 mg 68% yield) as a colorless oil. Diene **2.56**: *R<sub>f</sub>* 0.46 (1:1 Hexanes:EtOAc); <sup>1</sup>H NMR (500 MHz, CDCl<sub>3</sub>): δ 6.78 (d, *J* = 1.1, 1H), 5.93 (br s, 1H), 5.80 (ddt, *J* = 17.1, 10.3, 6.7, 1H), 5.53 (s, 1H), 4.99 (ddt, *J* = 17.1, 2.0, 1.6, 1H), 4.96–4.91 (m, 1H), 4.49 (br s, 1H), 3.36–3.24 (m, 2H), 3.16–3.02 (m, 2H), 2.88–2.78 (m, 1H), 2.54 (dd, *J* = 17.3, 7.1, 1H), 2.16–1.99 (m, 5H), 1.64–1.58 (m, 4H), 1.51 (s, 9H), 1.44 (s, 9H), 1.32–1.15 (m, 22H); <sup>13</sup>C NMR (125 MHz, CDCl<sub>3</sub>): δ 173.8, 166.0, 156.1, 139.2, 137.2, 133.8, 133.5, 133.2, 114.4, 81.0, 50.7, 40.8, 38.3, 37.9, 36.0, 35.0, 33.9, 30.5, 30.2, 29.8, 29.63, 29.60, 29.59, 29.54, 29.4, 29.04, 29.01, 28.98, 28.6, 28.5, 28.3, 26.9, 24.4; IR (film): 3315, 2927, 2855, 1698, 1671, 1163 cm<sup>-1</sup>; HRMS-APCI (*m/z*) [*M* + *H*]<sup>+</sup> calcd for C<sub>37</sub>H<sub>63</sub>N<sub>2</sub>O<sub>5</sub><sup>+</sup>, 615.47315; found 615.47783.





**Secondary amine 2.57.** To a vial was added diene **2.56** (65.0 mg, 106  $\mu\text{mol}$ , 1.00 equiv). The vial was then brought into the glovebox and  $[\text{Rh(COD)(acac)}]$  (4.92 mg, 15.9  $\mu\text{mol}$ , 15.0 mol%) was added. The vial was then removed from the glovebox and the mixture was dissolved in THF (1.27 mL, 0.0800 M) and to this solution was added phenylsilane (52.2  $\mu\text{L}$ , 423  $\mu\text{mol}$ , 4.00 equiv). The reaction mixture was then allowed to stir at 50  $^\circ\text{C}$  for 12.5 h. After this time, the reaction mixture allowed to cool to 23  $^\circ\text{C}$  and was then quenched slowly with saturated aq. ammonium fluoride (1.0 mL). The reaction mixture was allowed to stir for 2.5 h at 23  $^\circ\text{C}$  and then was diluted with  $\text{Et}_2\text{O}$  (5 mL), water (5 mL), and 1 M aq NaOH (5 mL). The layers were separated and the aqueous layer was washed with  $\text{Et}_2\text{O}$  (3 x 5 mL). The combined organic layers were dried over  $\text{MgSO}_4$ , filtered, and concentrated under reduced pressure. The crude residue was purified via flash chromatography (100%  $\text{EtOAc}$   $\rightarrow$  100%  $\text{CH}_2\text{Cl}_2$  saturated with  $\text{NH}_3$ ) to afford secondary amine **2.57** (40.8 mg, 64% yield) as a pale yellow oil. Secondary amine **2.57**:  $R_f$  0.26 (9:1  $\text{CH}_2\text{Cl}_2$ : $\text{MeOH}$ );  $^1\text{H}$  NMR (500 MHz,  $\text{CDCl}_3$ ):  $\delta$  6.76 (s, 1H), 5.86–5.74 (m, 1H), 5.58 (s, 1H), 5.04–4.88 (m, 2H), 4.51 (br s, 1H), 3.15–3.04 (m, 2H), 2.99 (d,  $J = 12.3$ , 1H), 2.92–2.82 (m, 1H), 2.46–2.34 (m, 3H), 2.17–2.07 (m, 2H), 2.06–1.99 (m, 3H), 1.65–1.55 (m, 2H), 1.50 (s, 10H), 1.43 (s, 14H), 1.39–1.04 (m, 48H), 0.95–0.78 (m, 6H);  $^{13}\text{C}$  NMR (125 MHz,  $\text{CDCl}_3$ ):  $\delta$  166.8, 156.1, 139.4, 139.2, 136.1, 135.5, 134.2, 133.41, 133.38, 133.03, 133.00, 127.8, 114.3, 114.2, 80.3, 79.1, 55.1, 45.2, 40.8, 39.0, 37.8, 35.2, 34.0, 33.9, 33.6, 33.3, 32.1, 32.0, 30.7, 30.3, 30.2, 29.83, 29.79, 29.75, 29.66, 29.60, 29.56, 29.50, 29.43, 29.41, 29.29, 29.27, 29.21, 29.11, 29.07, 29.01, 28.82, 28.78, 28.68, 28.56, 28.3, 28.21, 28.16, 26.94, 26.86, 26.6, 26.0, 24.0, 23.9,

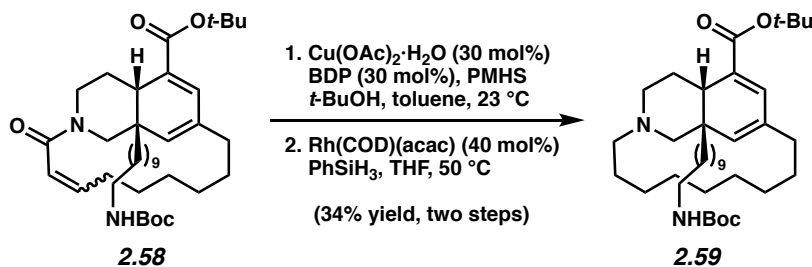
22.8, 14.3, 11.0; IR (film): 2925, 2854, 1699, 1161, 1135  $\text{cm}^{-1}$ ; HRMS-APCI ( $m/z$ )  $[\text{M} + \text{H}]^+$  calcd for  $\text{C}_{37}\text{H}_{65}\text{N}_2\text{O}_4^+$ , 691.49388; found 601.49212.



**Macrocycle 2.58.** A solution of secondary amine **2.57** (5.0 mg, 8.3  $\mu\text{mol}$ , 1.0 equiv) in  $\text{CH}_2\text{Cl}_2$  (0.2 mL) was cooled to  $0^\circ\text{C}$ . To the solution was added *N,N*-diisopropylethylamine (3.2 mg, 4.3  $\mu\text{L}$ , 25  $\mu\text{mol}$ , 3.0 equiv) followed by acryloyl chloride (**2.40**, 2.3 mg, 2.0  $\mu\text{L}$ , 25  $\mu\text{mol}$ , 3.0 equiv). The reaction was allowed to warm to  $23^\circ\text{C}$  and stir for 2 h. The reaction mixture was quenched with water (2 mL) and saturated aq.  $\text{NaHCO}_3$  (2 mL) and diluted with  $\text{Et}_2\text{O}$  (5 mL). The aqueous layer was separated from the organics and washed with  $\text{Et}_2\text{O}$  (2 x 5 mL). The combined organic fractions were dried over  $\text{MgSO}_4$ , filtered, and concentrated under reduced pressure. The crude residue was purified via preparative TLC (7:3 hexanes: $\text{EtOAc}$ ) to afford the acrylamide. To a vial in the glovebox was added Grubbs' 2<sup>nd</sup> generation catalyst (0.8 mg, 20 mol%, 0.9  $\mu\text{mol}$ ). The vial was then removed from the glovebox and then a solution of the acrylamide (3.0 mg, 1.0 equiv, 4.6  $\mu\text{mol}$ ) in sparged  $\text{CH}_2\text{Cl}_2$  (4.6 mL) was added to the vial containing Grubbs' catalyst. The reaction vial was sealed and allowed to stir at  $40^\circ\text{C}$  for 14 h. After this time, the reaction mixture was concentrated under reduced pressure. The crude residue was purified via preparative TLC (7:3 hexanes: $\text{EtOAc}$ ) to afford macrocycle **2.58** (2.7 mg, 60% yield over two steps) as a yellow oil. Macrocycle **2.58**:  $R_f$  0.53 (2:1 Hexanes: $\text{EtOAc}$ );  $^1\text{H}$  NMR (500 MHz,  $\text{CDCl}_3$ ):  $\delta$  6.92 (d,  $J = 14.5$ , 1H), 6.73–6.57 (m, 3H), 6.51–6.22 (m, 1H), 6.08–5.79

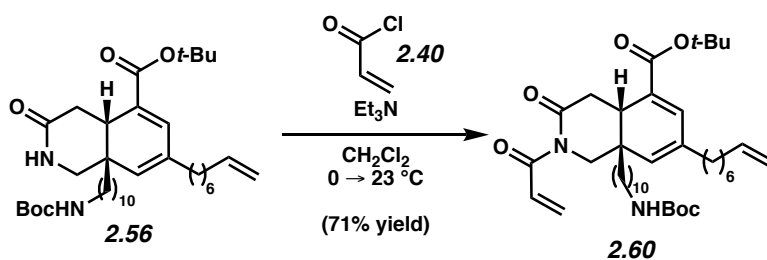
(m, 2H), 5.74–5.30 (m, 2H), 5.19–5.04 (m, 1H), 4.85 (d,  $J = 13.6$ , 1H), 4.63 (d,  $J = 13.6$ , 1H), 4.49 (br s, 2H), 4.05–3.79 (m, 2H), 3.20–2.91 (m, 10H), 2.62–2.49 (m, 5H), 2.46–2.31 (m, 4H), 2.25–2.09 (m, 7H), 2.09–1.97 (m, 8H), 1.74–1.66 (m, 10H), 1.53–1.50 (m, 32H), 1.48–1.41 (m, 51H), 1.38–0.69 (m, 134H);  $^{13}\text{C}$  NMR (125 MHz,  $\text{CDCl}_3$ ):  $\delta$  166.2, 165.2, 156.0, 145.1, 141.4, 135.9, 135.7, 135.0, 134.2, 133.9, 133.1, 132.9, 122.2, 121.9, 80.5, 79.0, 54.5, 48.7, 45.9, 41.9, 40.80, 40.76, 40.6, 38.83, 38.76, 38.4, 37.6, 36.6, 34.1, 33.1, 32.0, 31.9, 30.5, 30.1, 29.7, 29.6, 29.52, 29.46, 29.4, 29.3, 29.1, 28.8, 28.4, 28.2, 28.1, 27.8, 27.7, 27.2, 26.8, 26.44, 26.37, 26.3, 26.1, 24.8, 23.9, 23.6, 23.1, 22.7, 14.1; IR (film): 2926, 2854, 1699, 1275, 1166  $\text{cm}^{-1}$ ; HRMS-APCI (m/z)  $[\text{M} + \text{H}]^+$  calcd for  $\text{C}_{38}\text{H}_{63}\text{N}_2\text{O}_5^+$ , 627.47315; found 627.47344.

*Note: 2.58 was obtained as a mixture of E and Z isomers. These data represent empirically observed chemical shifts from the  $^1\text{H}$  and  $^{13}\text{C}$  NMR spectra.*



**Tertiary amine 2.59.** To a vial was added copper(II) acetate monohydrate (0.78 mg, 3.9  $\mu\text{mol}$ , 30 mol%) and 1,2-bis(diphenylphosphino)benzene (BDP) (1.8 mg, 3.9  $\mu\text{mol}$ , 30 mol%). These were dissolved in sparged toluene (1.5 mL) and  $t\text{-BuOH}$  (25  $\mu\text{L}$ , 0.26 mmol, 20 equiv) the reaction mixture was allowed to stir for 30 min to give a blue solution. At this point PMHS (75 mg, 74  $\mu\text{L}$ , 39  $\mu\text{mol}$ , 3.0 equiv) was added dropwise over 1 min and the solution gradually turned from blue to a yellow/green color (30 min). A separate vial was charged with macrocycle **2.58** (8.2 mg, 13  $\mu\text{mol}$ , 1.00 equiv) and was dissolved in toluene (1.5 mL). The macrocycle

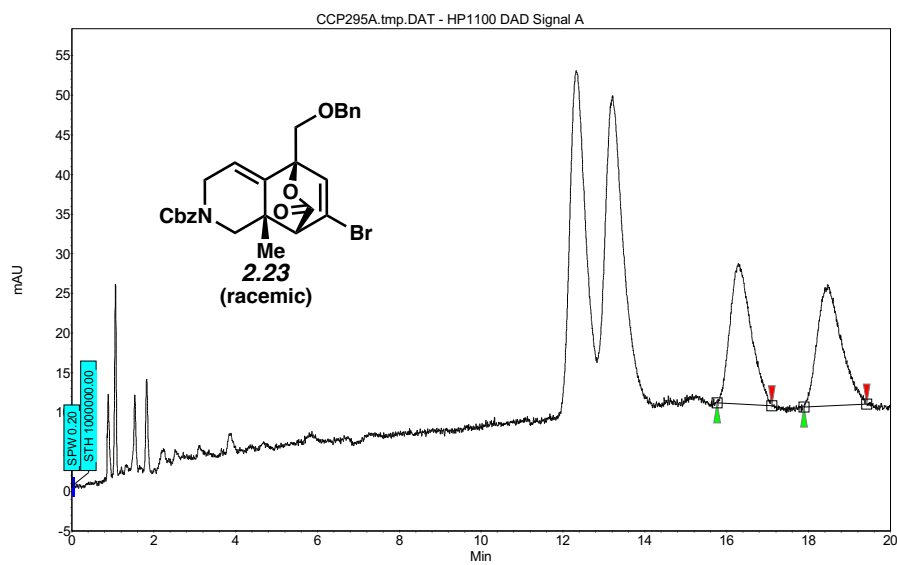
solution was then added to the Strykers reagent dropwise over 3 min. The reaction mixture was allowed to stir at 23 °C for 19.5 h. After this time, the reaction mixture was passed through a plug of silica gel (1 x 3 cm) eluting with EtOAc (50 mL). The crude residue was purified via preparative TLC (65:35 hexanes:EtOAc) to afford the amide. To a vial was added the amide (3.0 mg, 1.0 equiv, 4.8 μmol). The vial was then brought into the glovebox and Rh(COD)(acac) (0.6 mg, 40 mol%, 2 μmol) was added. The vial was then removed from the glovebox and the mixture was dissolved in THF (0.3 mL) and to this solution was added phenylsilane (2.6 mg, 3.0 μL, 5.0 equiv, 24 μmol). The vial was sealed with a Teflon-lined cap and the reaction mixture was then heated to 50 °C and stirred for 14.5 h. After this time, the reaction mixture was allowed to cool to 23 °C and was then quenched slowly with saturated aq. ammonium fluoride (0.5 mL). The reaction mixture was allowed to stir for 30 min at 23 °C and then diluted with Et<sub>2</sub>O (5 mL), water (5 mL), and 1 M aq NaOH (5 mL). The layers were separated and the aqueous layer was washed with Et<sub>2</sub>O (2 x 5 mL). The combined organic layers were dried over MgSO<sub>4</sub>, filtered, and concentrated under reduced pressure. The crude residue was purified via preparative TLC (9:1 hexanes:EtOAc) to afford tertiary amine **2.59** (1.2 mg, 34% yield over two steps) as a colorless oil. Tertiary amine **2.59**: *R<sub>f</sub>* 0.80 (4:1 Hexanes:EtOAc); <sup>1</sup>H NMR (500 MHz, CDCl<sub>3</sub>): δ 6.69 (s, 1H), 5.59 (s, 1H), 4.48 (br s, 1H), 3.16–3.01 (m, 2H), 2.73 (dd, *J* = 10.9, 1.2, 1H), 2.69–2.61 (m, 1H), 2.41–2.05 (m, 6H), 1.80 (d, *J* = 11.0, 1H), 1.75–1.66 (m, 3H), 1.50 (s, 9H), 1.44 (s, 9 H), 1.34–1.02 (m, 31H); <sup>13</sup>C NMR (125 MHz, CDCl<sub>3</sub>): δ 167.0, 139.4, 134.5, 134.0, 131.6, 80.0, 62.9, 55.8, 51.7, 40.8, 39.7, 38.6, 36.8, 32.6, 30.8, 30.5, 30.2, 29.9, 29.71, 29.69, 29.4, 28.6, 28.4, 28.3, 27.03, 26.96, 25.6, 25.54, 29.50, 25.1, 24.03, 24.00; IR (film): 2926, 2853, 1697, 1249, 1164 cm<sup>-1</sup>; HRMS-APCI (*m/z*) [*M* + *H*]<sup>+</sup> calcd for C<sub>38</sub>H<sub>67</sub>N<sub>2</sub>O<sub>4</sub><sup>+</sup>, 615.50954; found 615.50877.



**Imide 2.60:** A solution of amide **2.56** (55.0 mg, 1.00 equiv, 89.4  $\mu\text{mol}$ ) in  $\text{CH}_2\text{Cl}_2$  (0.90 mL, 0.10 M) was cooled to  $0^\circ\text{C}$ . To this solution was added triethylamine (27.2 mg, 37.4  $\mu\text{L}$ , 3.00 equiv, 268  $\mu\text{mol}$ ) followed by acryloyl chloride (**2.40**, 24.3 mg, 21.9  $\mu\text{L}$ , 3.00 equiv, 268  $\mu\text{mol}$ ) dropwise over 1 min. The reaction was allowed to warm to  $23^\circ\text{C}$  and stir for 15 h. The reaction mixture was quenched with water (1 mL) and saturated aq.  $\text{NaHCO}_3$  (1 mL) and diluted with  $\text{Et}_2\text{O}$  (2 mL). The layers were separated and the aqueous layer was washed with  $\text{Et}_2\text{O}$  (3 x 1 mL). The combined organic layers were dried over  $\text{MgSO}_4$ , filtered, and concentrated under reduced pressure. The crude residue was purified by flash chromatography (5:1 hexanes: $\text{EtOAc}$ ) to afford imide **2.60** (42.5 mg, 71% yield) as a colorless oil. Spectral match those previously reported.<sup>9</sup>

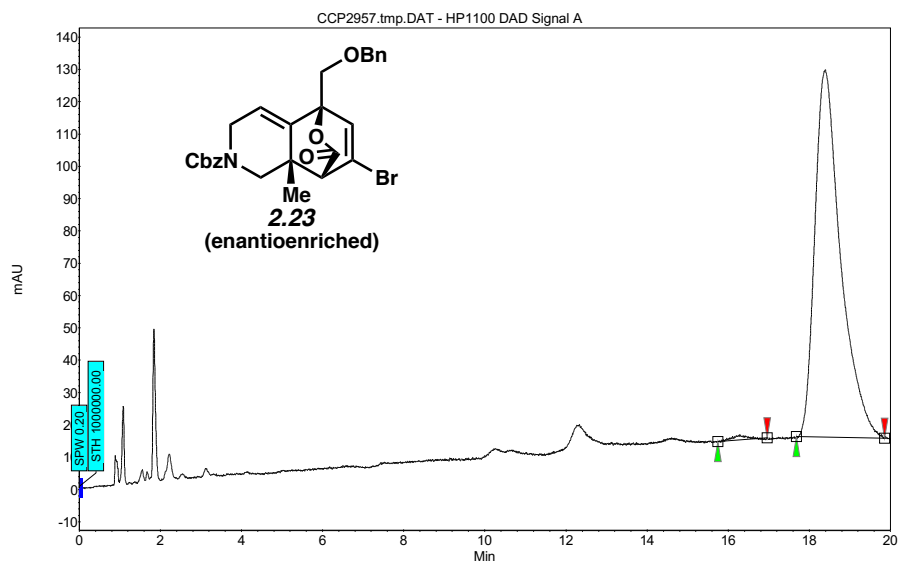
### 2.7.2.8 Verification of Enantioenrichment of Cycloadduct **2.23**:

Compound	Method Column/Temp.	Solvent	Method Flow Rate	Retention Times (min)	Enantiomeric Ratio (er)
<p><b>2.23</b> (racemic)</p>	Diacel ChiralPak OD-H / $35^\circ\text{C}$	15% isopropanol in $\text{CO}_2$	2 mL/min	16.29/18.47	~50.5:49.5
<p><b>2.23</b> (enantioenriched)</p>	Diacel ChiralPak OD-H / $35^\circ\text{C}$	15% isopropanol in $\text{CO}_2$	2 mL/min	16.29/18.40	~99.4:0.6



Index	Name	Time			RT Offset	Quantity	Height	Area	
		[Min]	[Min]	[Min]				[μV]	[μV.Min]
1	UNKNOWN	15.76	16.29	17.11	0.00	50.46	17.8	10.5	50.462
2	UNKNOWN	17.89	18.47	19.42	0.00	49.54	15.3	10.3	49.538
Total						100.00	33.1	20.8	100.000

**Figure 2.16.** SFC trace of racemic **2.23**.



Index	Name	Time			RT Offset	Quantity	Height	Area	
		[Min]	[Min]	[Min]				[μV]	[μV.Min]
1	UNKNOWN	15.74	16.29	16.96	0.00	0.58	1.6	0.5	0.585
2	UNKNOWN	17.69	18.40	19.86	0.00	99.42	113.7	83.6	99.415
Total						100.00	115.3	84.1	100.000

**Figure 2.17.** SFC trace of enantioenriched **2.23**.

## **2.8 Spectra Relevant to Chapter Two:**

### **Total Synthesis of Lissodendoric Acid A**

Francesca M. Ippoliti, Nathan J. Adamson, Laura G. Wonilowicz,

Evan R. Darzi, Joyann S. Donaldson, and Neil K. Garg.

*Manuscript in preparation.*

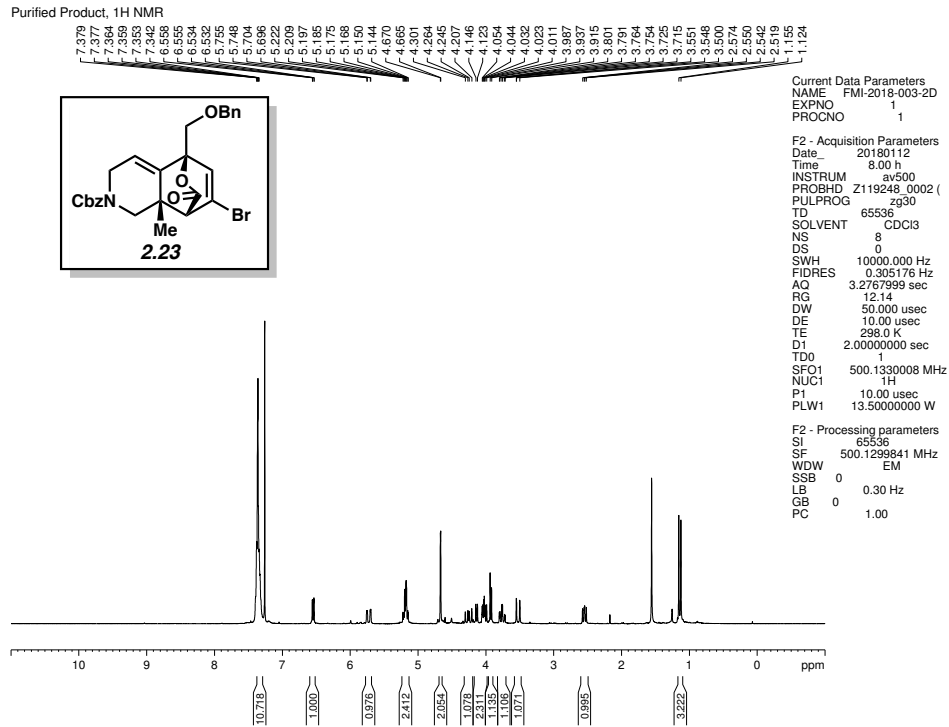


Figure 2.18. <sup>1</sup>H NMR (500 MHz, CDCl<sub>3</sub>) of compound 2.23.

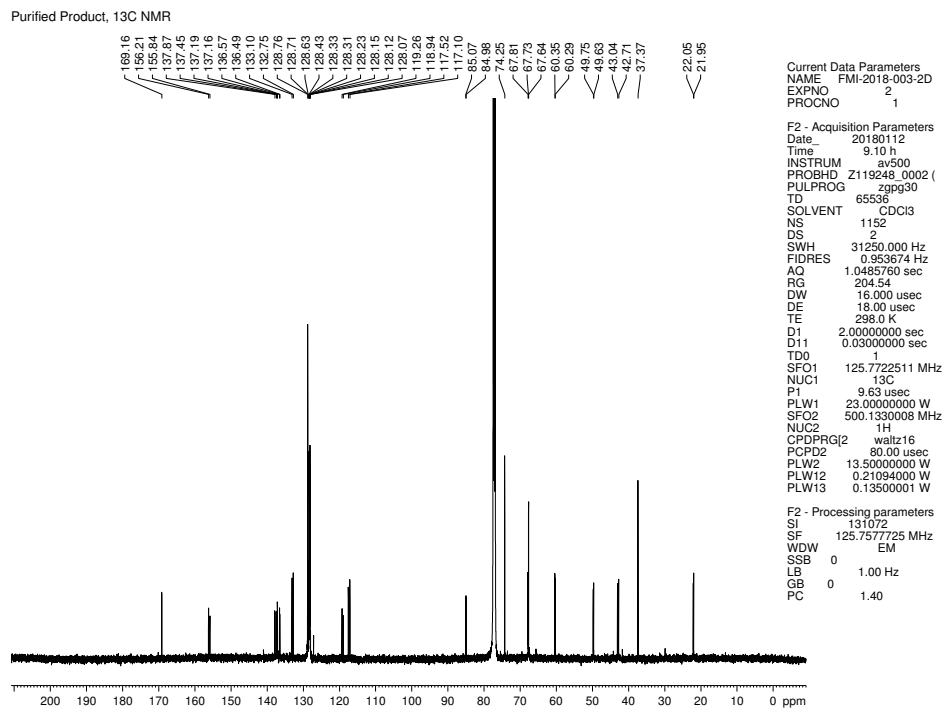


Figure 2.19. <sup>13</sup>C NMR (125 MHz, CDCl<sub>3</sub>) of compound 2.23.



Purified Product, <sup>1</sup>H NMR

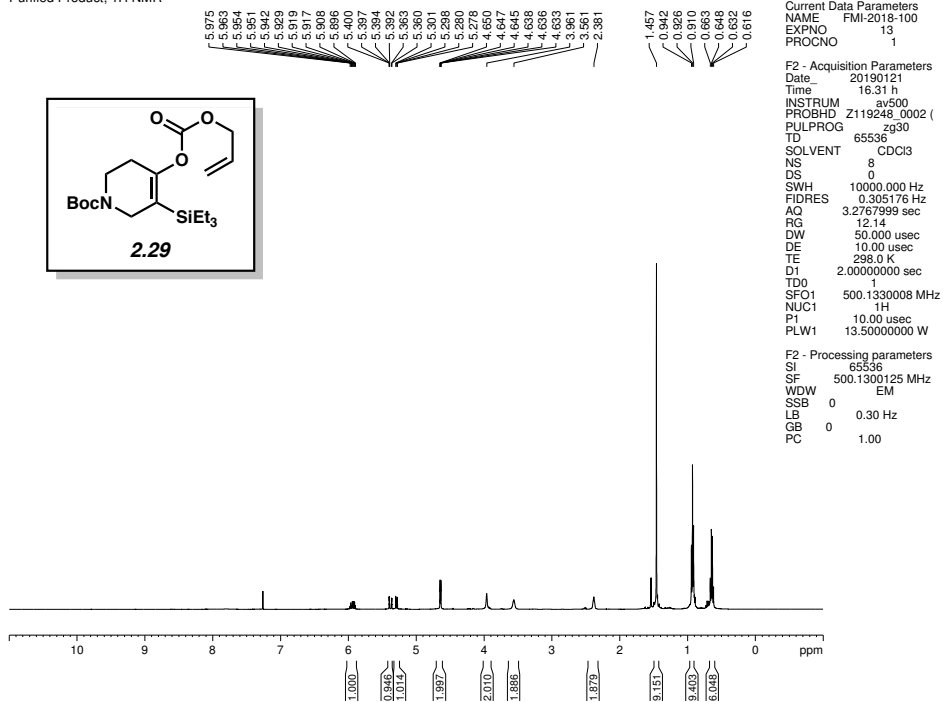
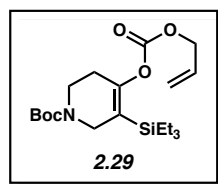


Figure 2.20. <sup>1</sup>H NMR (500 MHz, CDCl<sub>3</sub>) of compound 2.29.

Purified Product, <sup>13</sup>C NMR

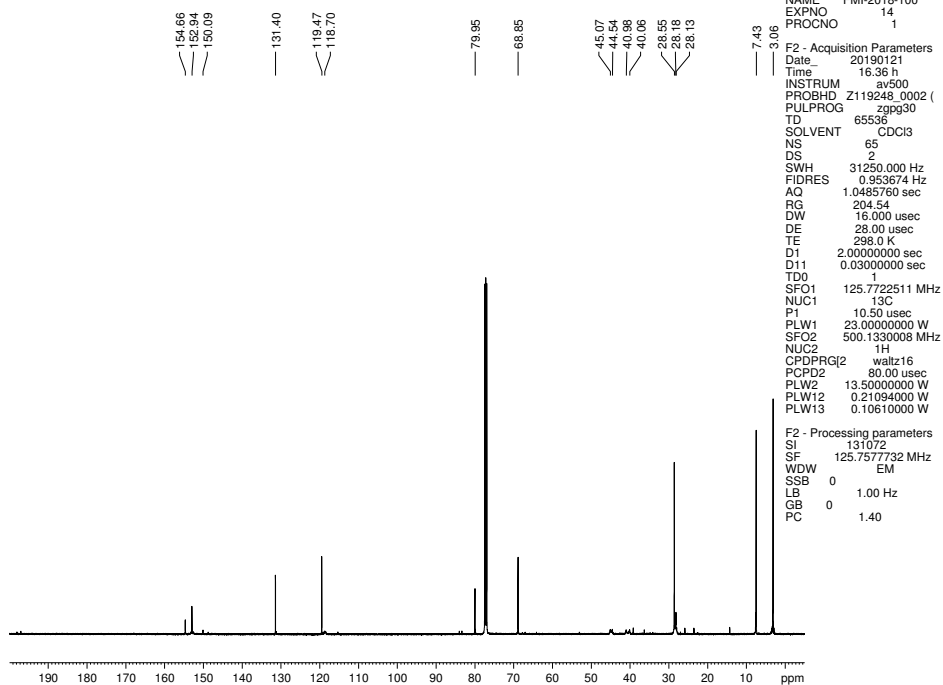


Figure 2.21. <sup>13</sup>C NMR (125 MHz, CDCl<sub>3</sub>) of compound 2.29.



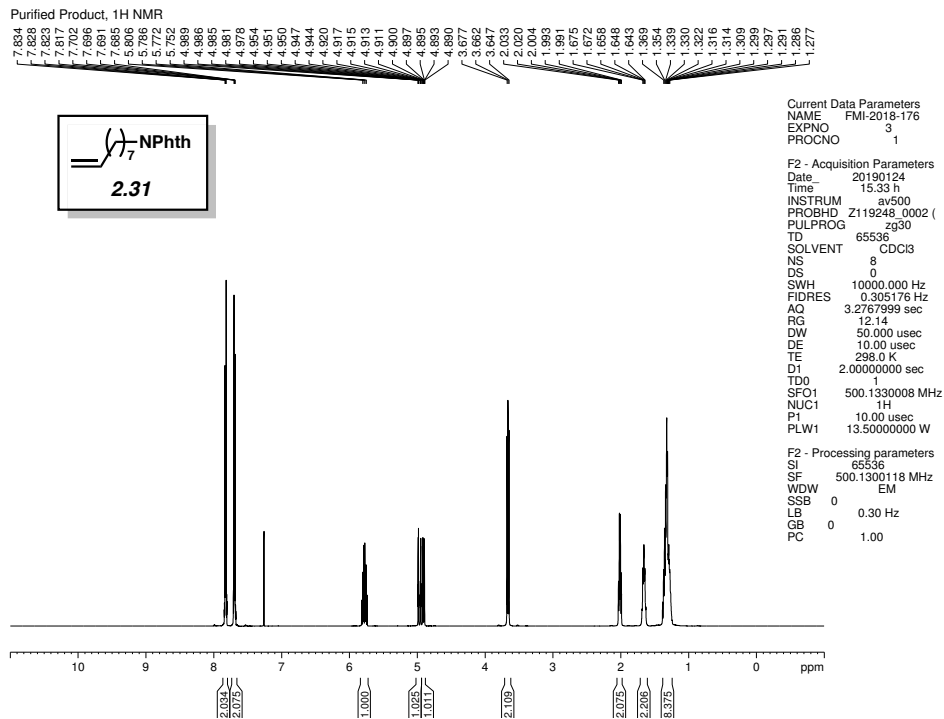


Figure 2.24. <sup>1</sup>H NMR (500 MHz, CDCl<sub>3</sub>) of compound 2.31.

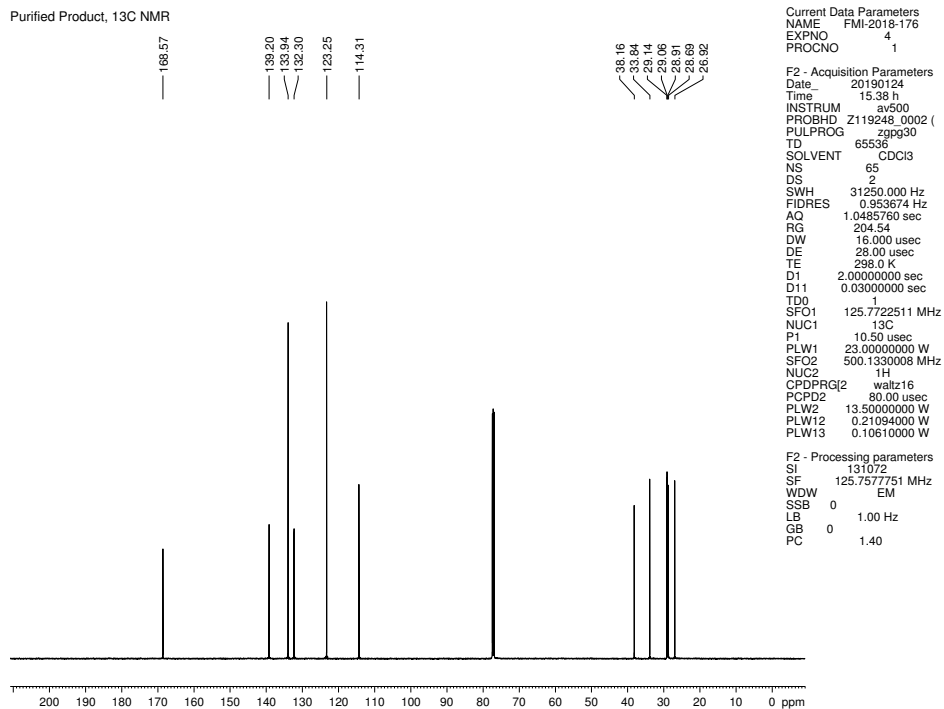


Figure 2.25. <sup>13</sup>C NMR (125 MHz, CDCl<sub>3</sub>) of compound 2.31.

Purified Product, <sup>1</sup>H NMR

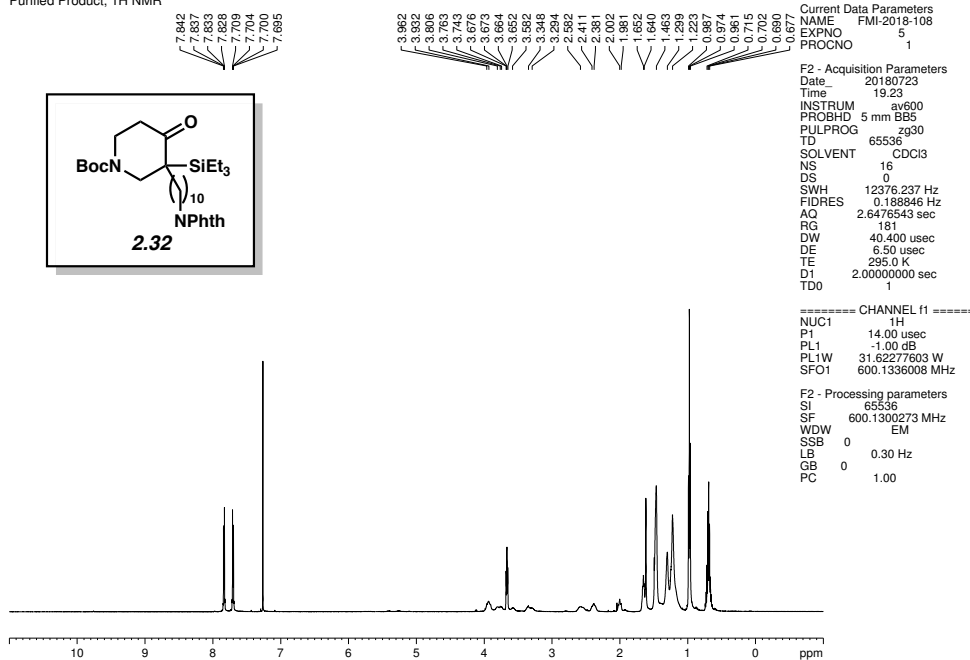
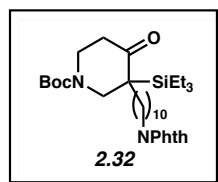


Figure 2.26. <sup>1</sup>H NMR (600 MHz, CDCl<sub>3</sub>) of compound 2.32.

Purified Product, <sup>13</sup>C NMR

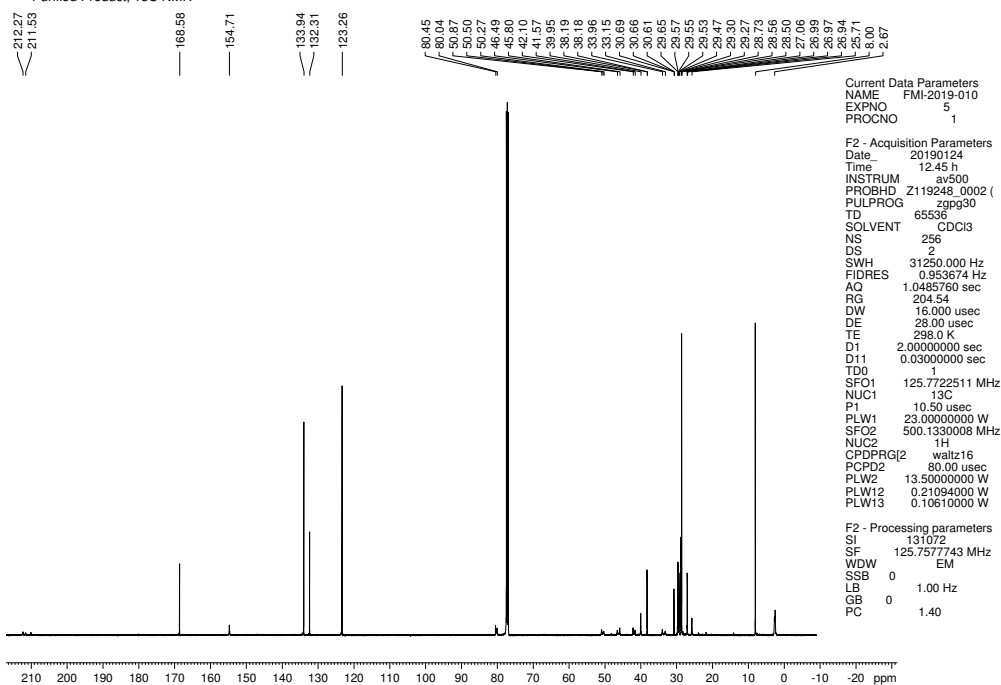


Figure 2.27. <sup>13</sup>C NMR (125 MHz, CDCl<sub>3</sub>) of compound 2.32.

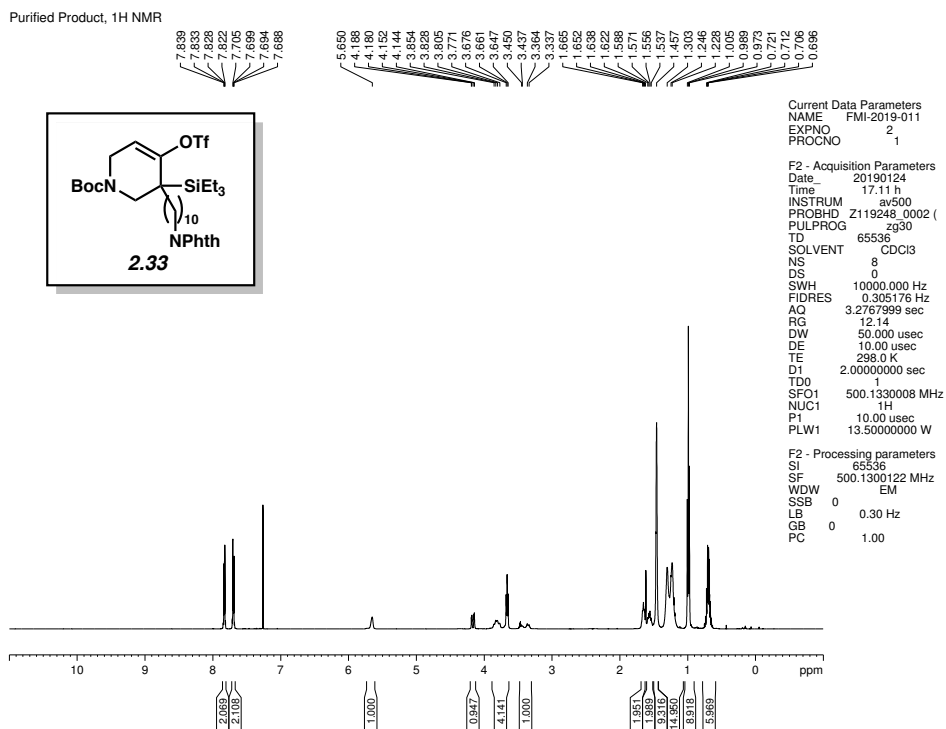


Figure 2.28. <sup>1</sup>H NMR (500 MHz, CDCl<sub>3</sub>) of compound 2.33.

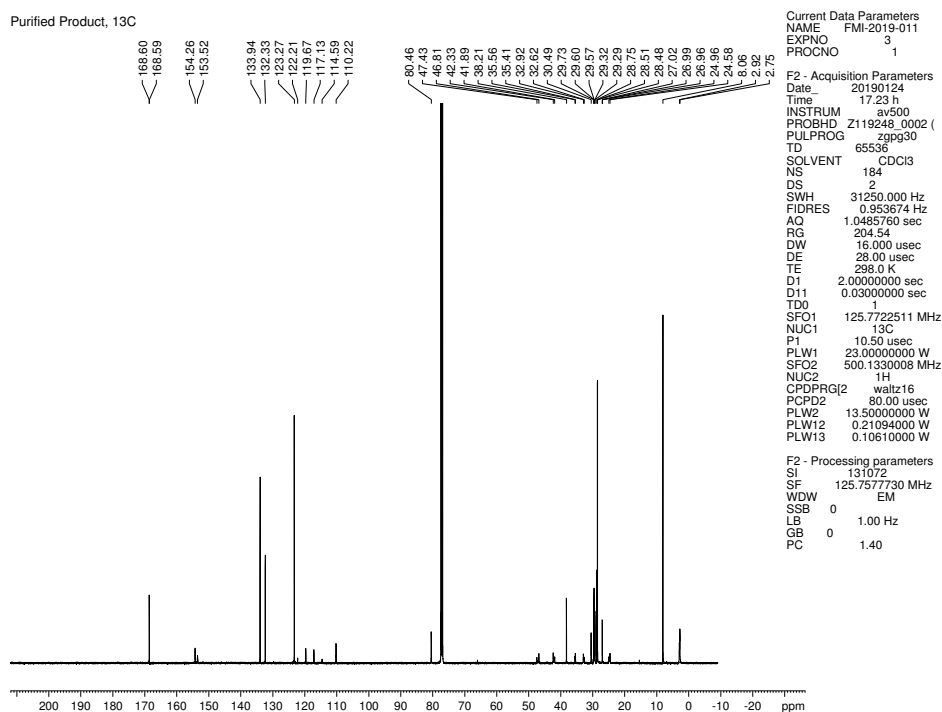


Figure 2.29. <sup>13</sup>C NMR (125 MHz, CDCl<sub>3</sub>) of compound 2.33.



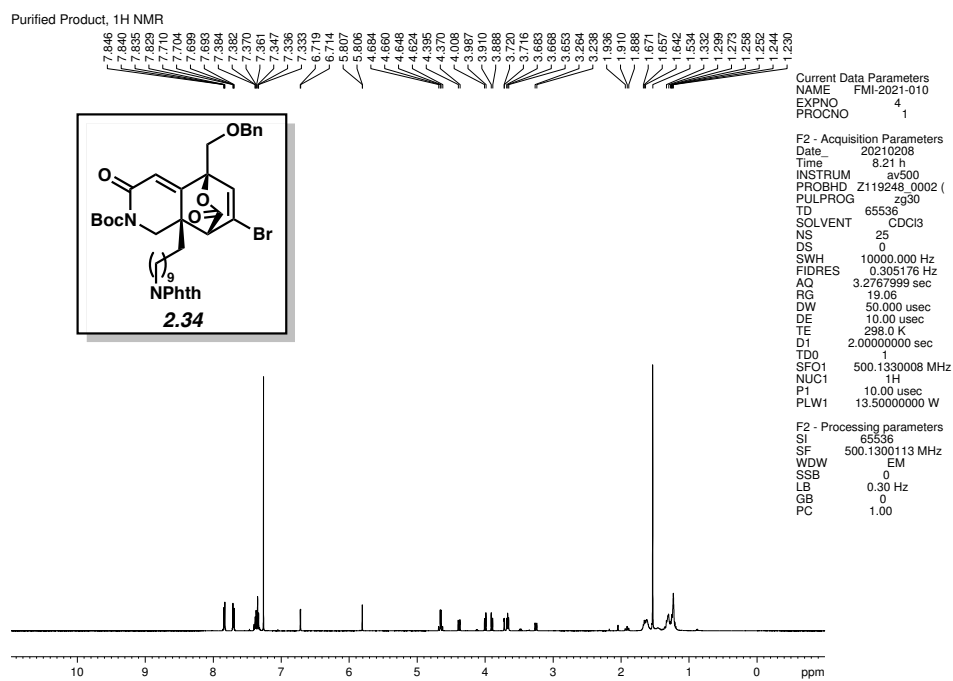


Figure 2.32. <sup>1</sup>H NMR (500 MHz, CDCl<sub>3</sub>) of compound 2.34.

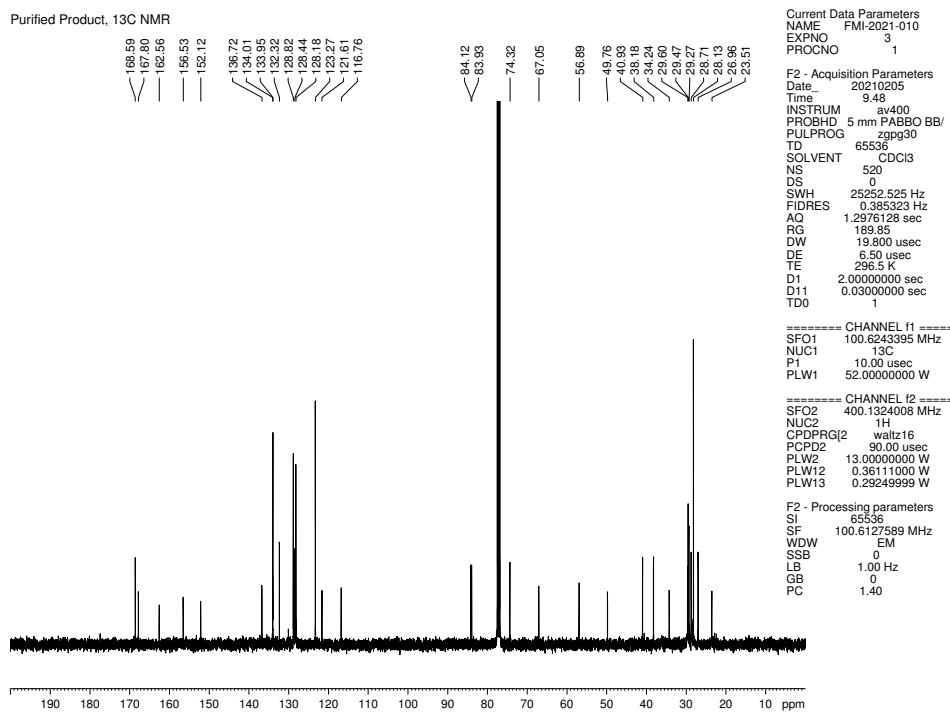


Figure 2.33. <sup>13</sup>C NMR (100 MHz, CDCl<sub>3</sub>) of compound 2.34.

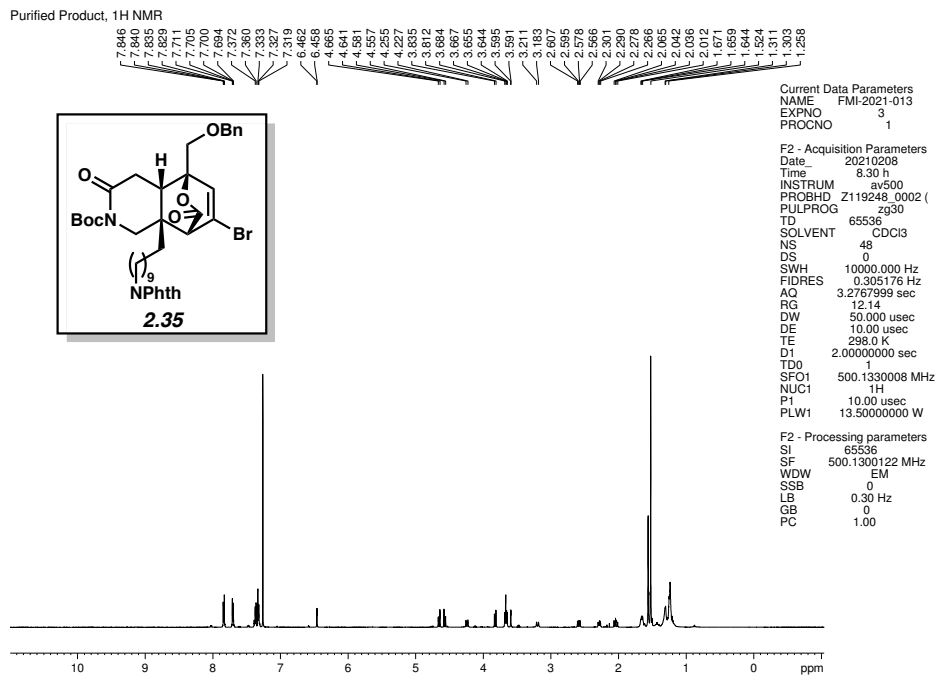


Figure 2.34. <sup>1</sup>H NMR (500 MHz, CDCl<sub>3</sub>) of compound 2.35.

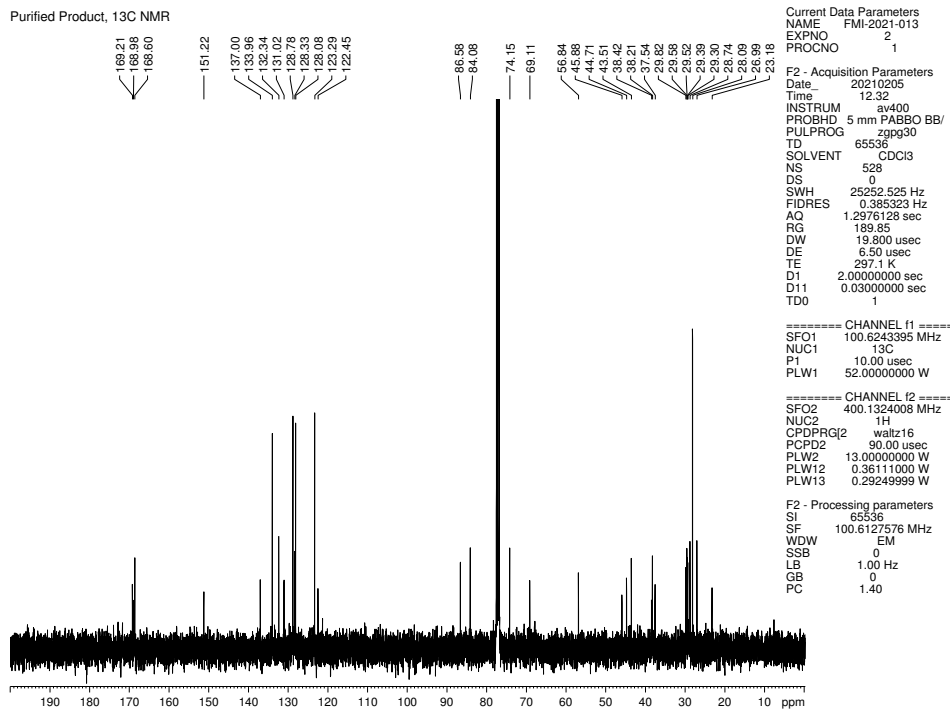


Figure 2.35. <sup>13</sup>C NMR (100 MHz, CDCl<sub>3</sub>) of compound 2.35.



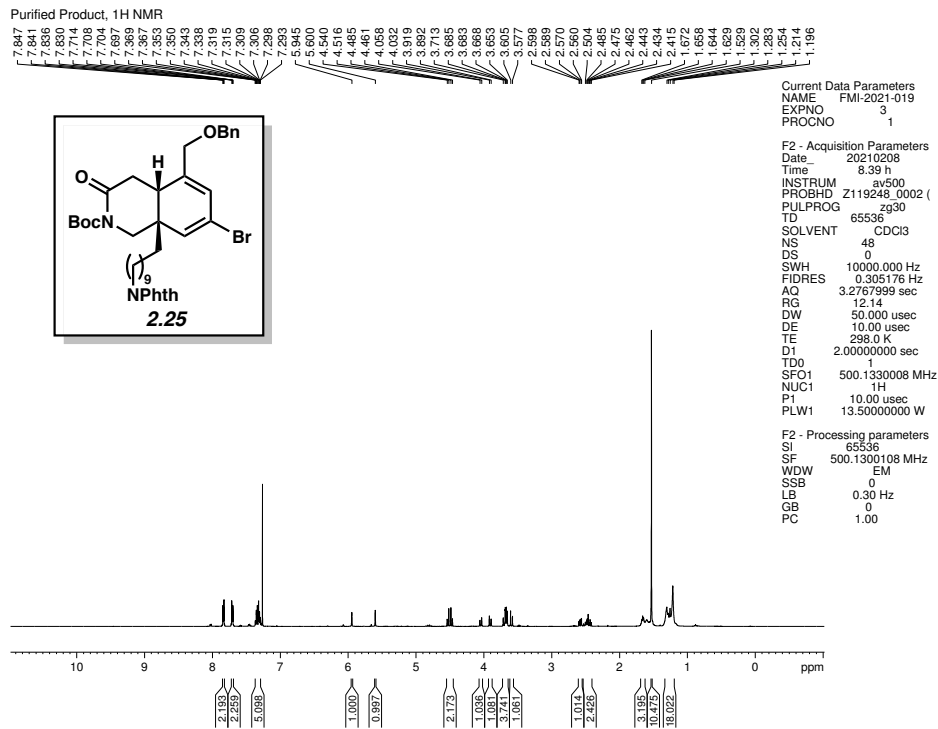


Figure 2.36. <sup>1</sup>H NMR (500 MHz, CDCl<sub>3</sub>) of compound 2.25.

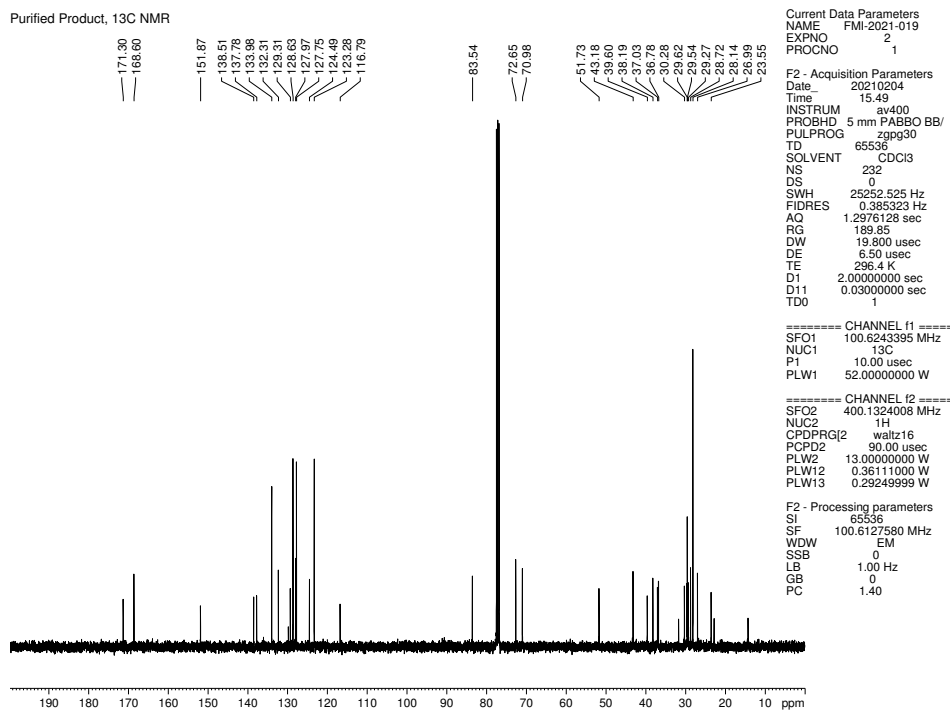


Figure 2.37. <sup>13</sup>C NMR (100 MHz, CDCl<sub>3</sub>) of compound 2.25.

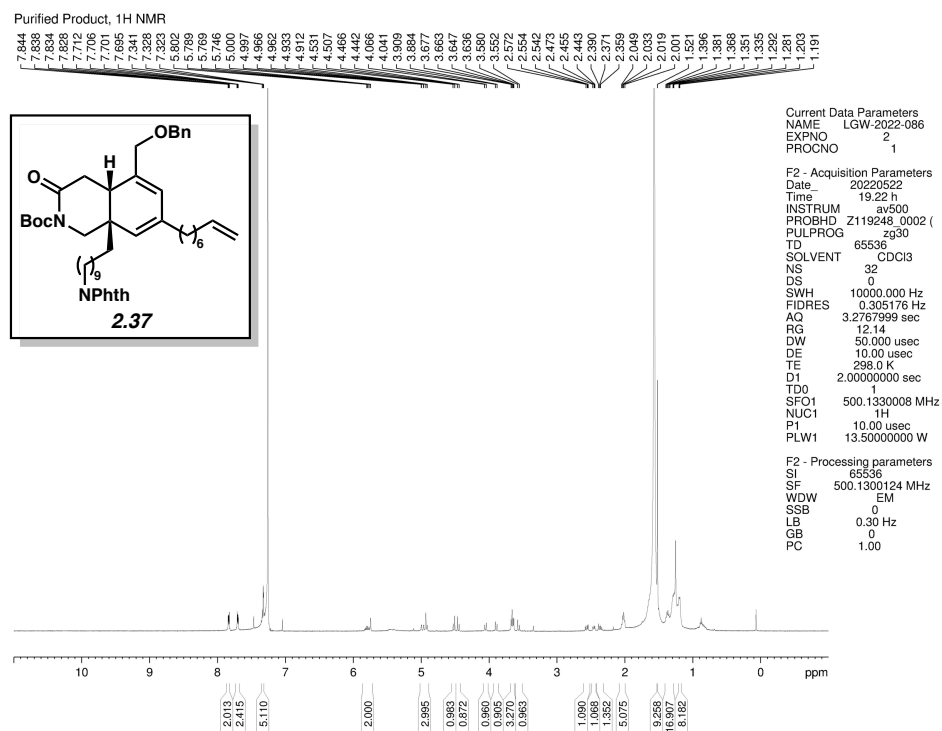


Figure 2.38. <sup>1</sup>H NMR (500 MHz, CDCl<sub>3</sub>) of compound 2.37.

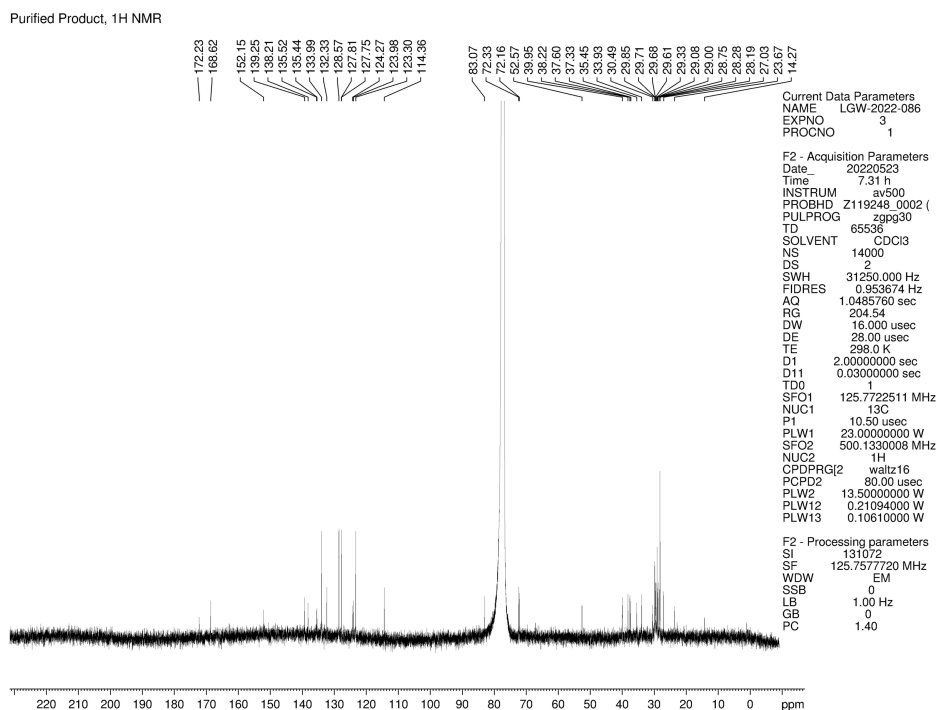


Figure 2.39. <sup>13</sup>C NMR (125 MHz, CDCl<sub>3</sub>) of compound 2.37.

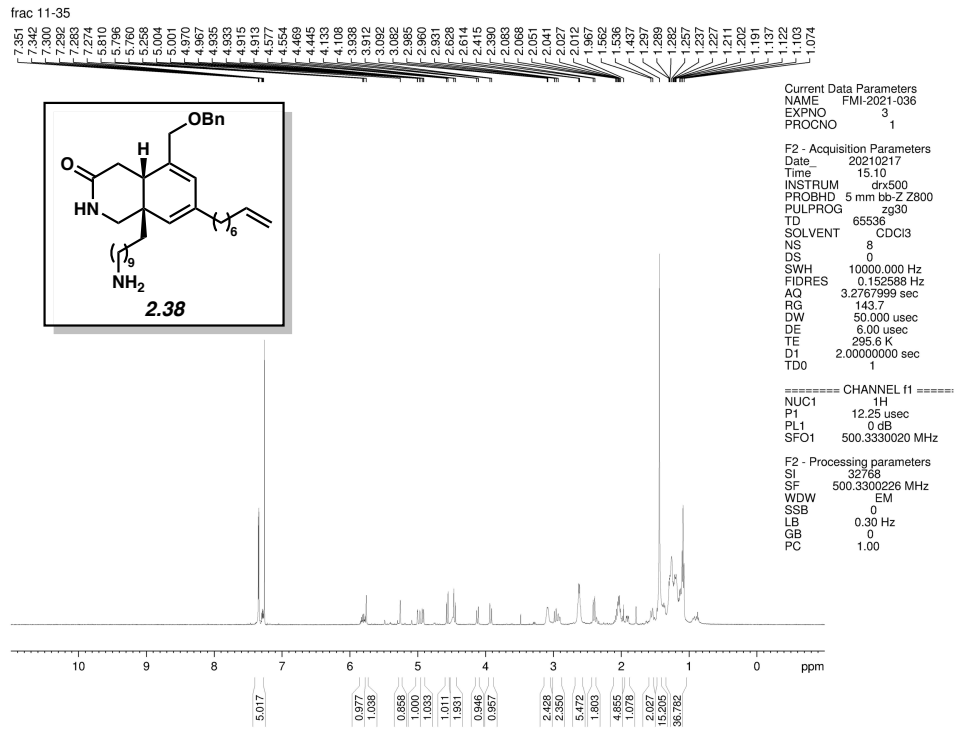


Figure 2.40.  $^1\text{H}$  NMR (500 MHz,  $\text{CDCl}_3$ ) of compound 2.38.



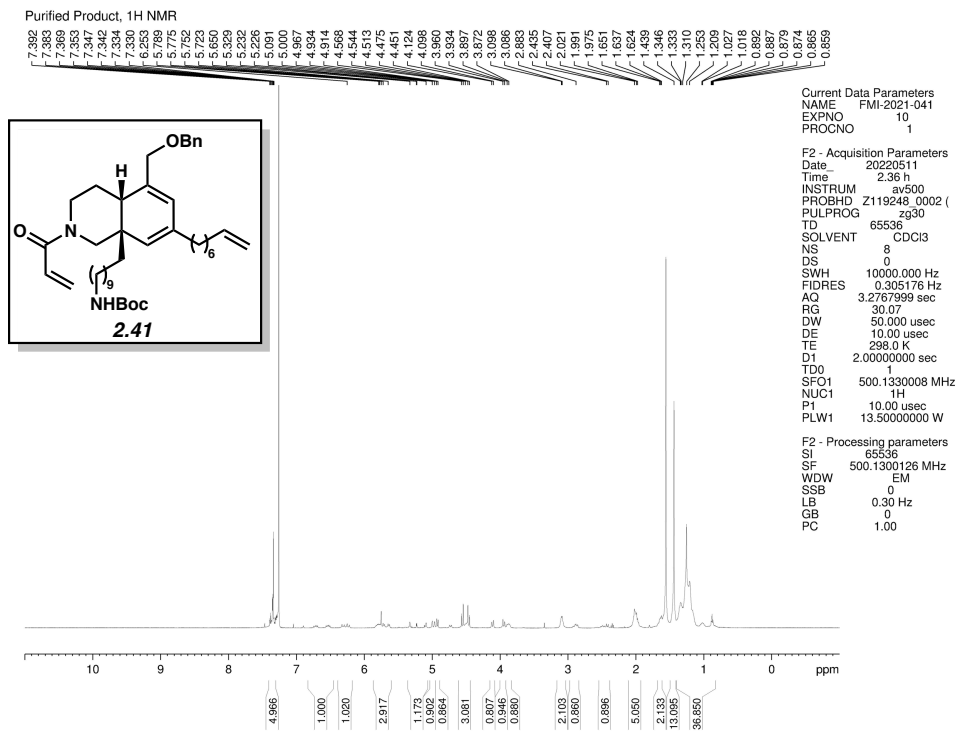


Figure 2.43. <sup>1</sup>H NMR (500 MHz, CDCl<sub>3</sub>) of compound 2.41.

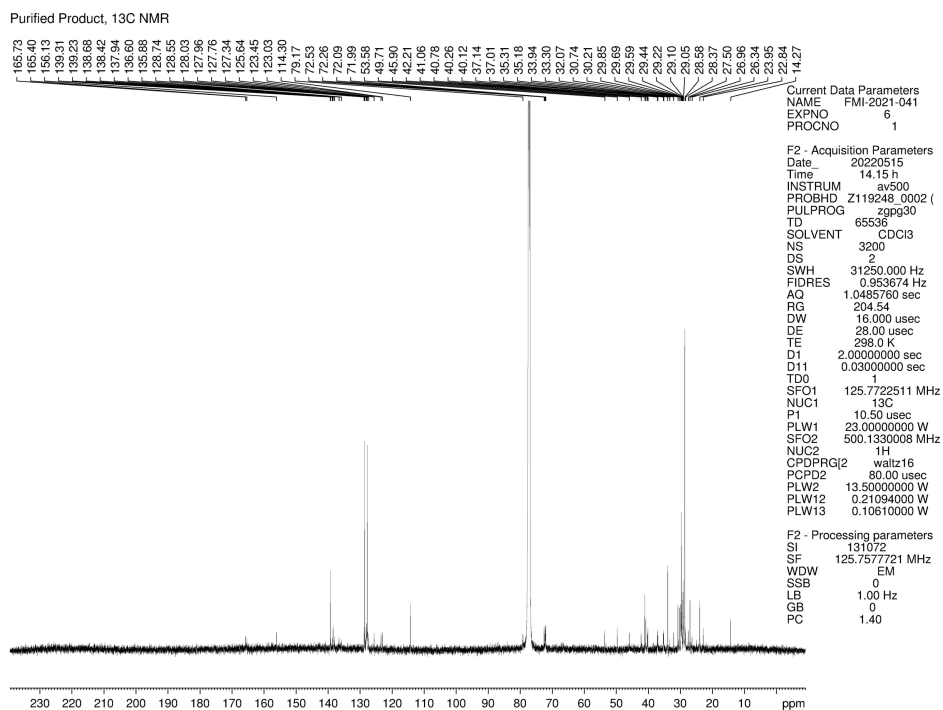


Figure 2.44. <sup>13</sup>C NMR (125 MHz, CDCl<sub>3</sub>) of compound 2.41.

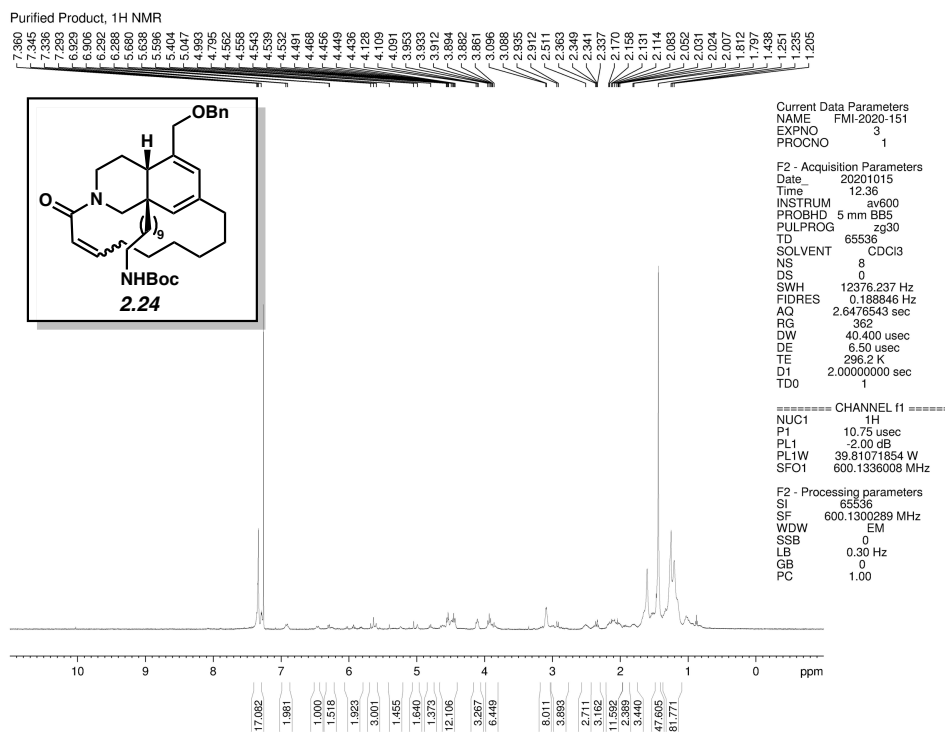


Figure 2.45. <sup>1</sup>H NMR (600 MHz, CDCl<sub>3</sub>) of compound 2.24.

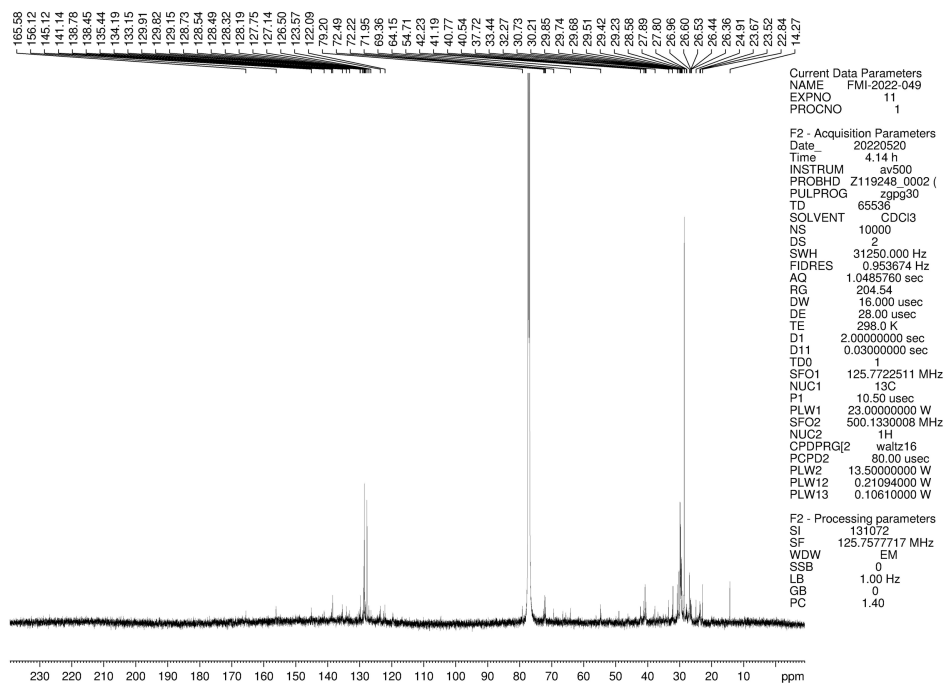


Figure 2.46. <sup>13</sup>C NMR (125 MHz, CDCl<sub>3</sub>) of compound 2.24.

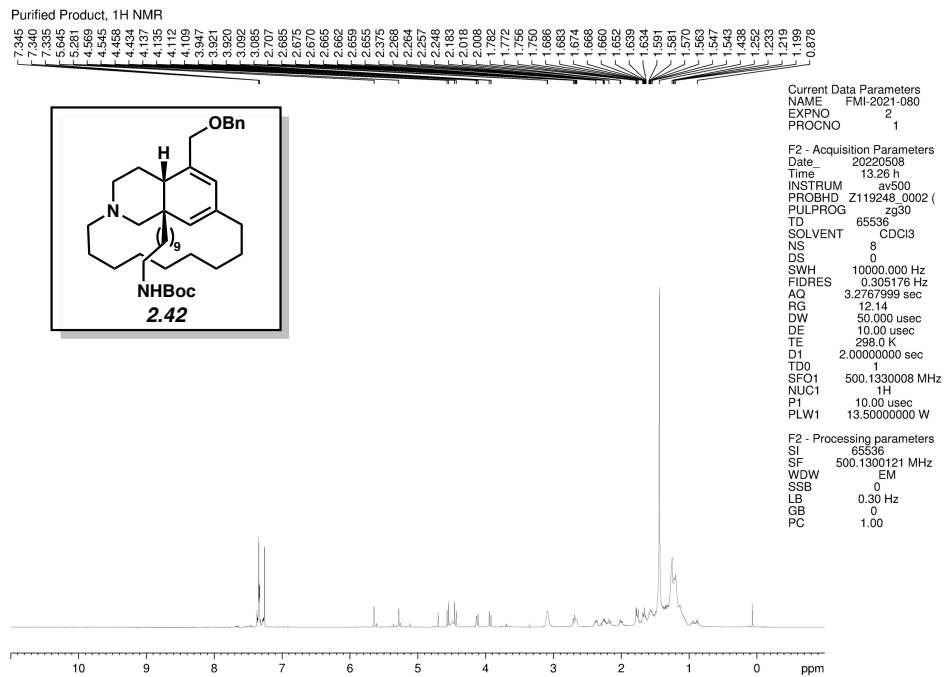


Figure 2.47. <sup>1</sup>H NMR (500 MHz, CDCl<sub>3</sub>) of compound 2.42.

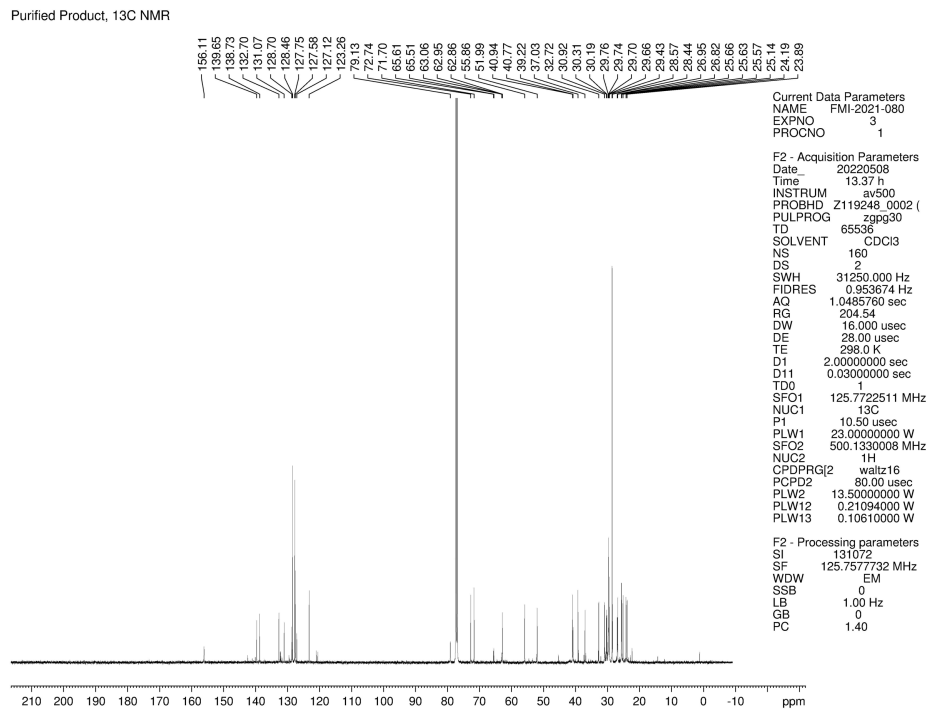


Figure 2.48. <sup>13</sup>C NMR (125 MHz, CDCl<sub>3</sub>) of compound 2.42.

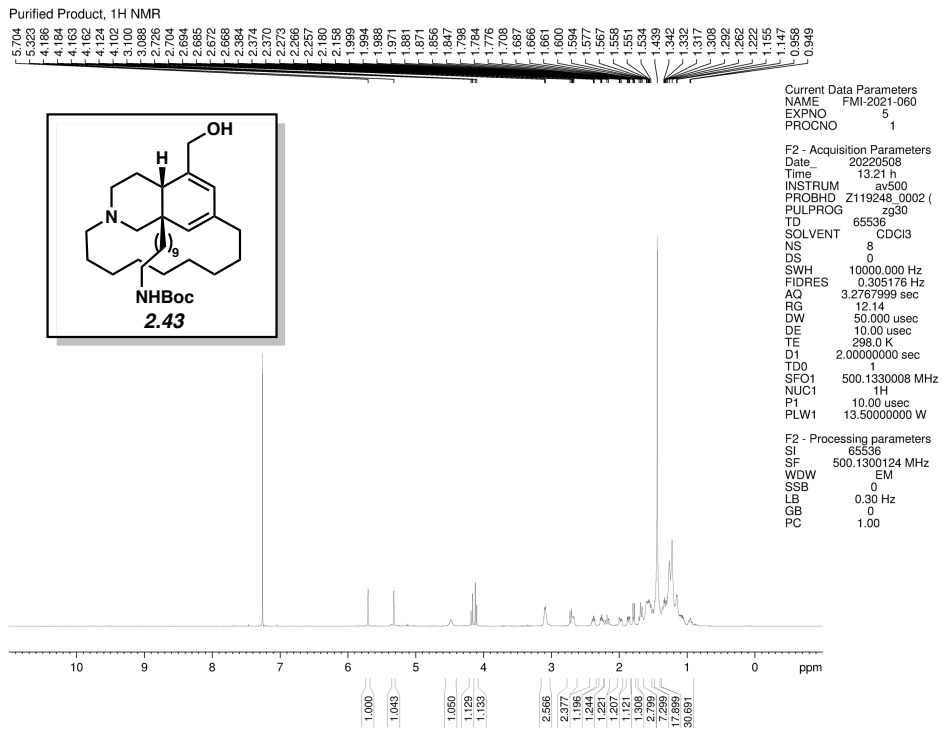


Figure 2.49. <sup>1</sup>H NMR (500 MHz, CDCl<sub>3</sub>) of compound **2.43**.

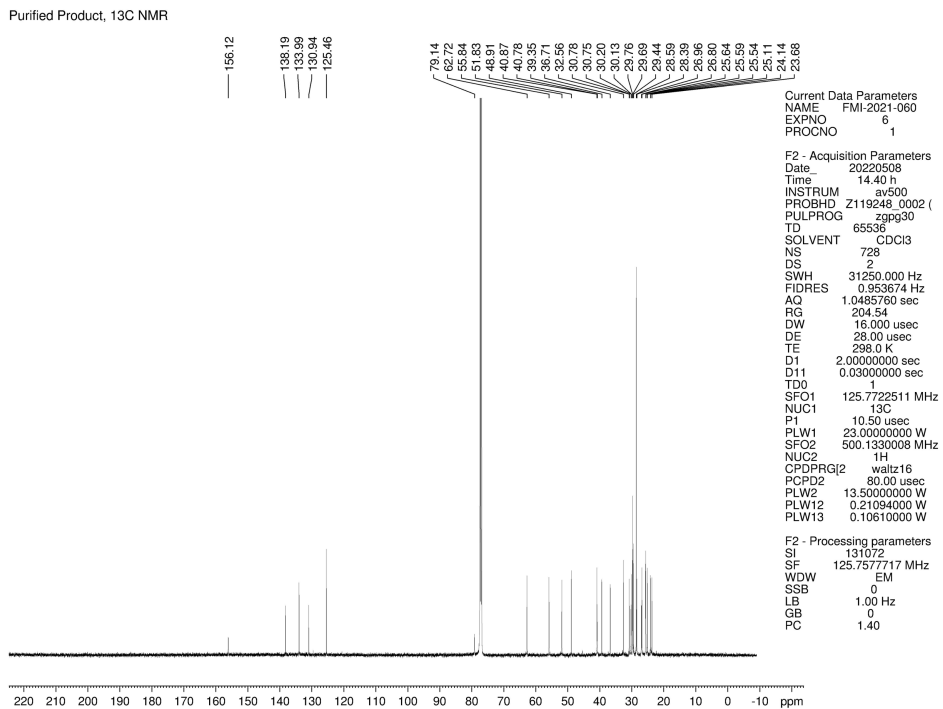


Figure 2.50. <sup>13</sup>C NMR (125 MHz, CDCl<sub>3</sub>) of compound **2.43**.



Purified Product, <sup>1</sup>H NMR

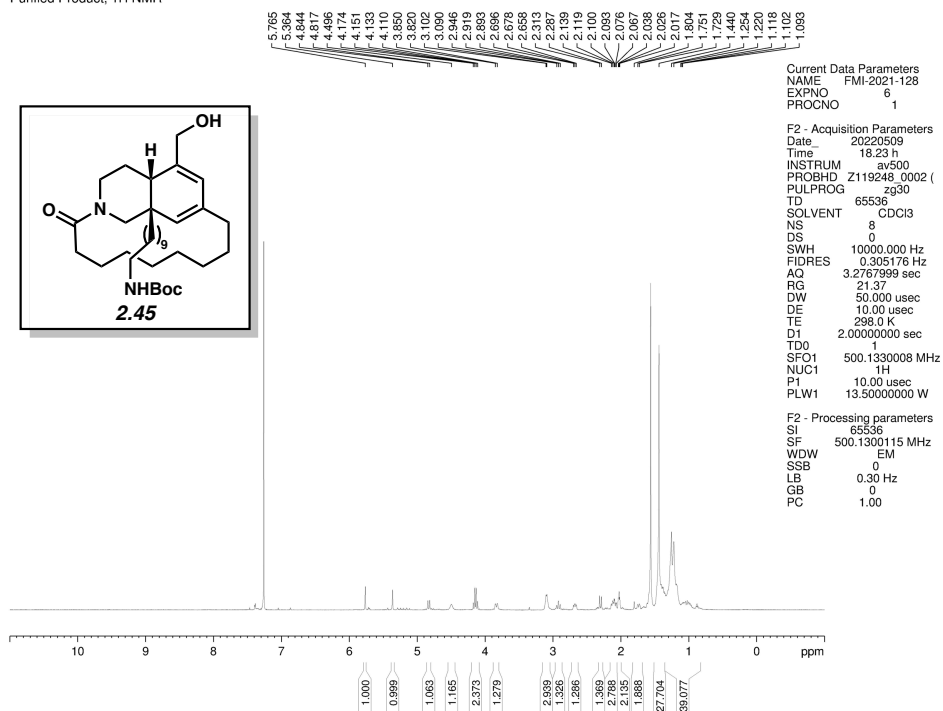


Figure 2.51. <sup>1</sup>H NMR (500 MHz, CDCl<sub>3</sub>) of compound 2.45.

Purified Product, <sup>13</sup>C NMR

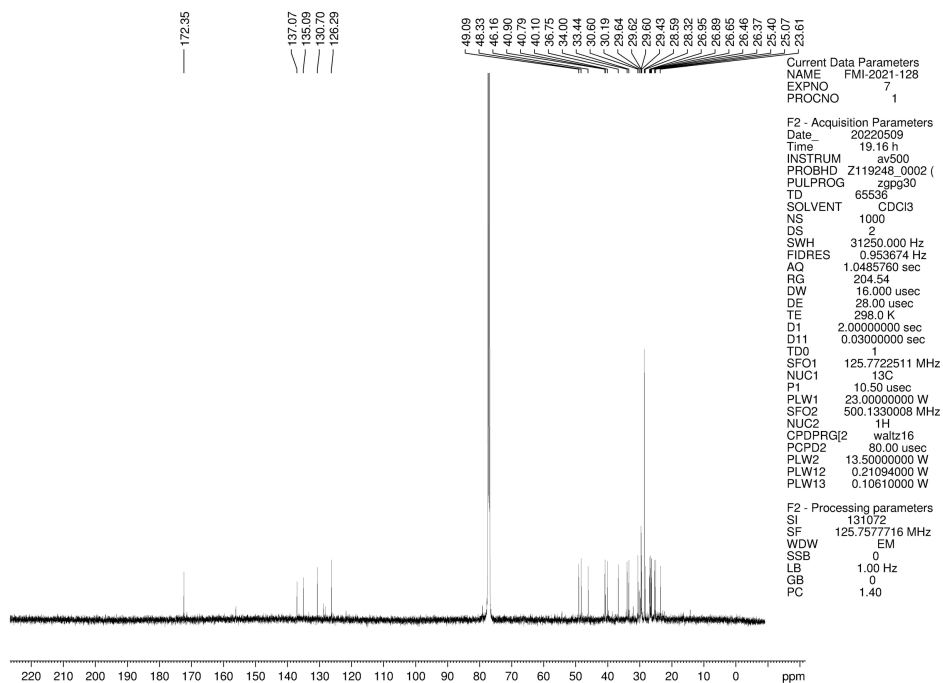


Figure 2.52. <sup>13</sup>C NMR (125 MHz, CDCl<sub>3</sub>) of compound 2.45.

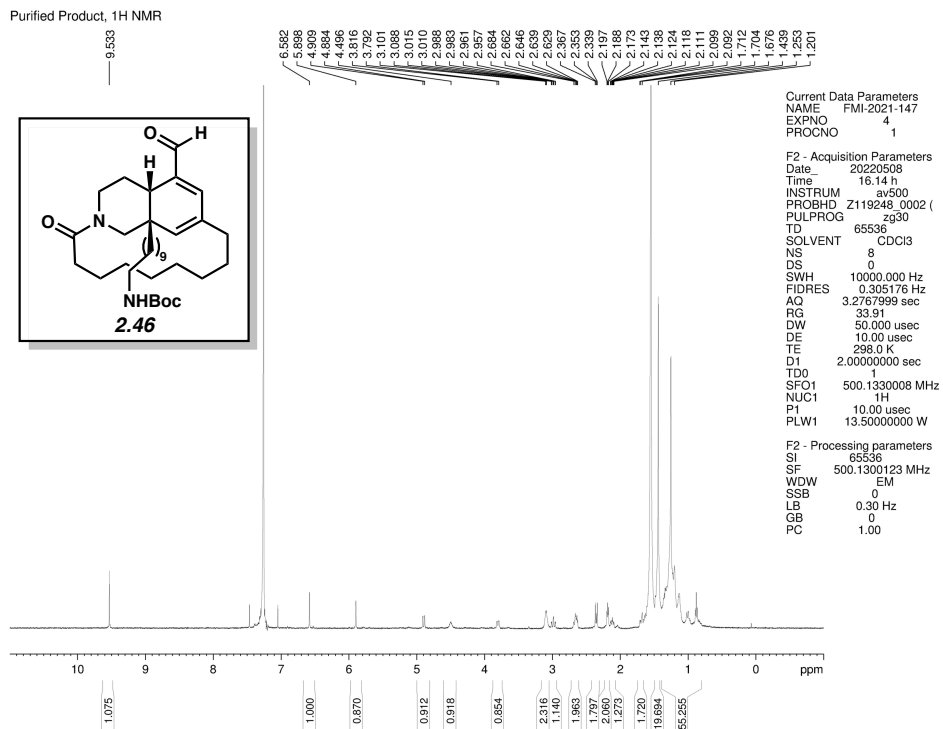


Figure 2.53. <sup>1</sup>H NMR (500 MHz, CDCl<sub>3</sub>) of compound 2.46.

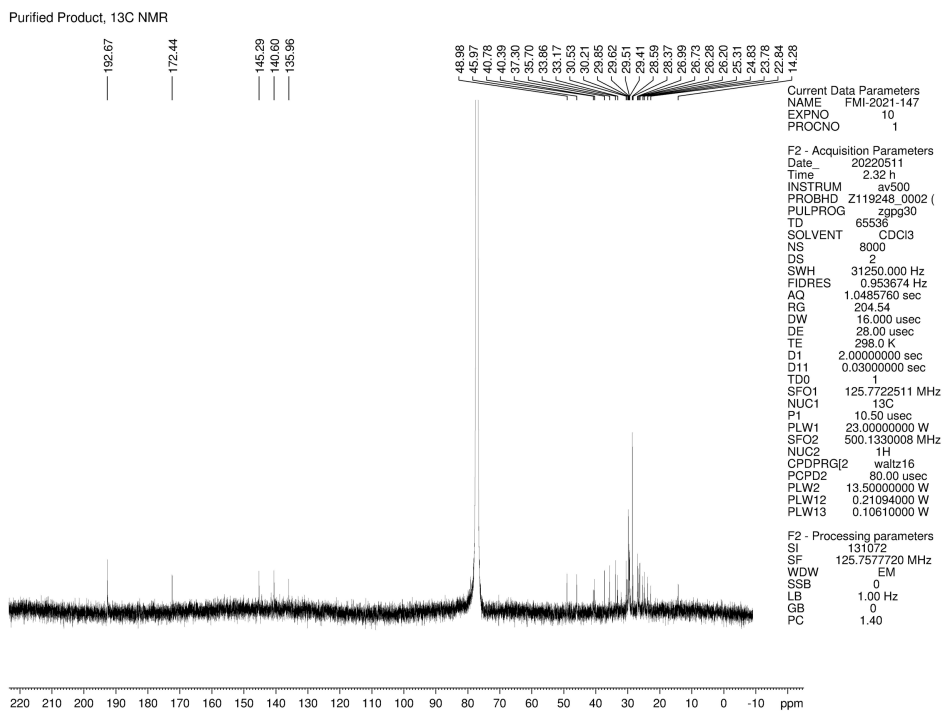


Figure 2.54. <sup>13</sup>C NMR (125 MHz, CDCl<sub>3</sub>) of compound 2.46.

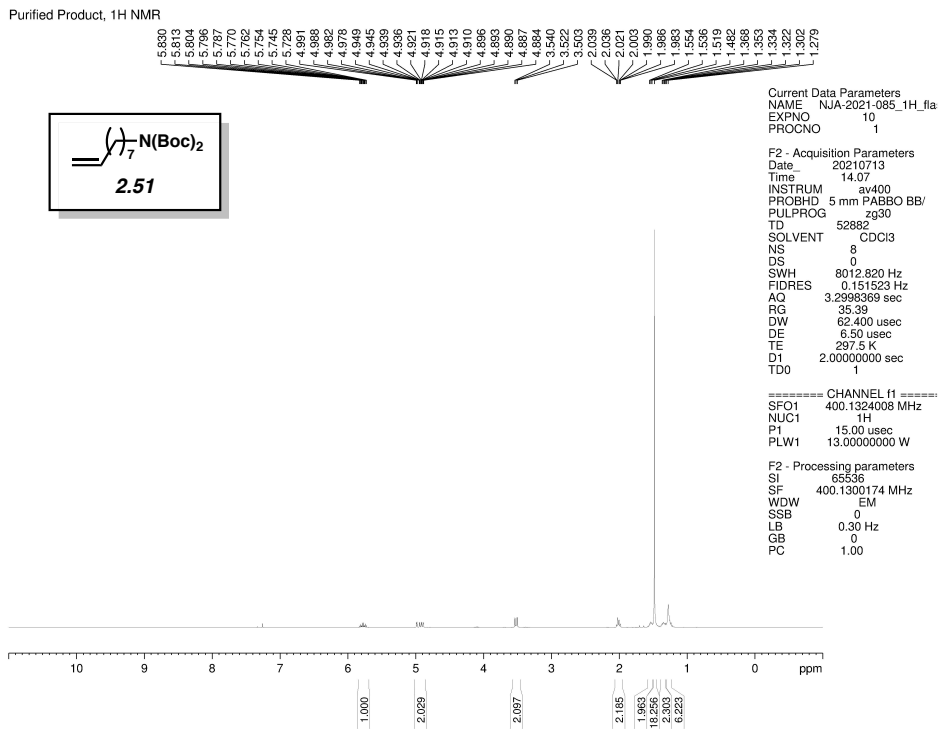


Figure 2.55. <sup>1</sup>H NMR (400 MHz, CDCl<sub>3</sub>) of compound 2.51.

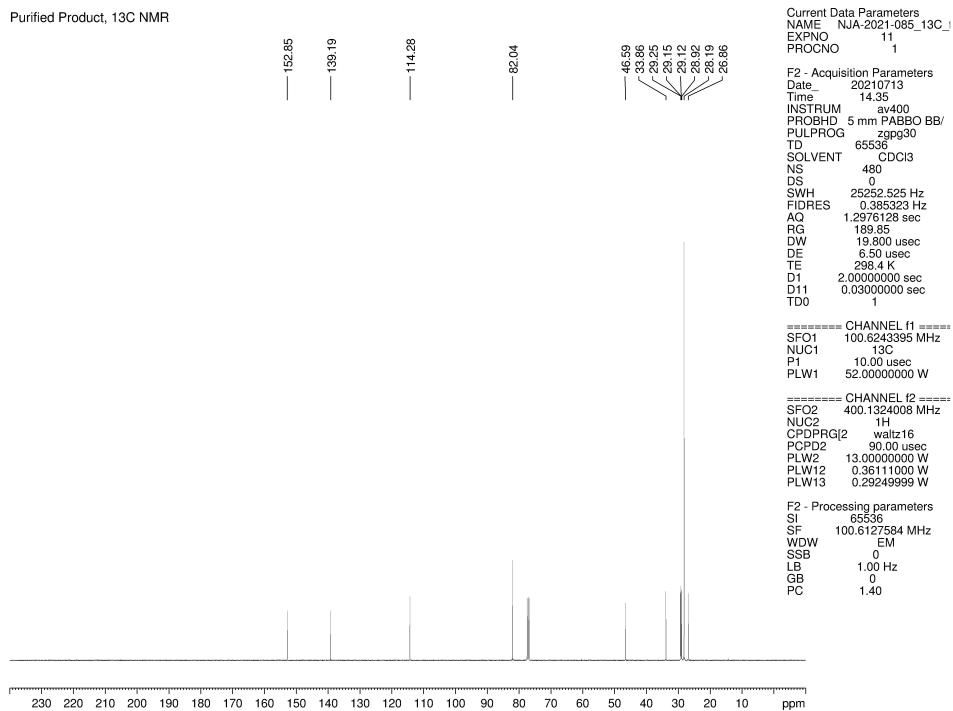


Figure 2.56. <sup>13</sup>C NMR (100 MHz, CDCl<sub>3</sub>) of compound 2.51.

Purified Product, <sup>1</sup>H NMR

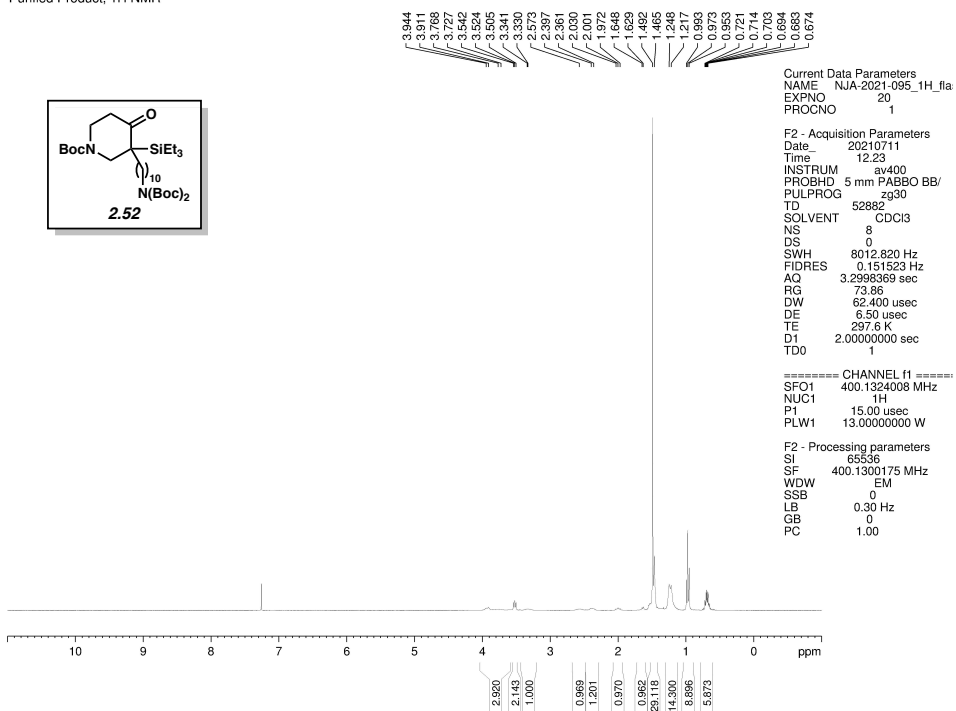


Figure 2.57. <sup>1</sup>H NMR (400 MHz, CDCl<sub>3</sub>) of compound 2.52.

Purified Product, <sup>13</sup>C NMR

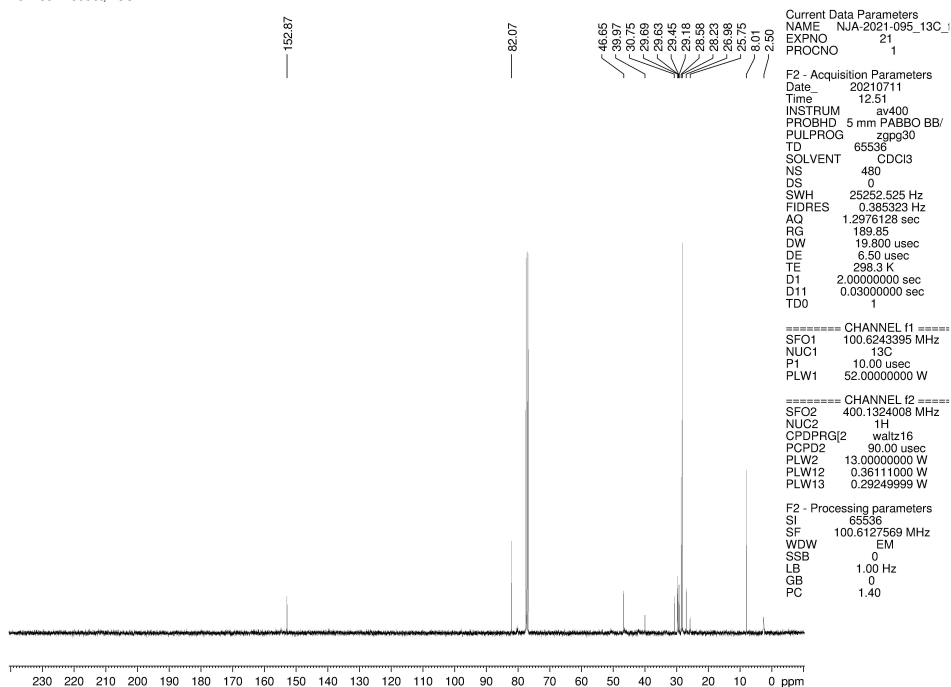


Figure 2.58. <sup>13</sup>C NMR (100 MHz, CDCl<sub>3</sub>) of compound 2.52.



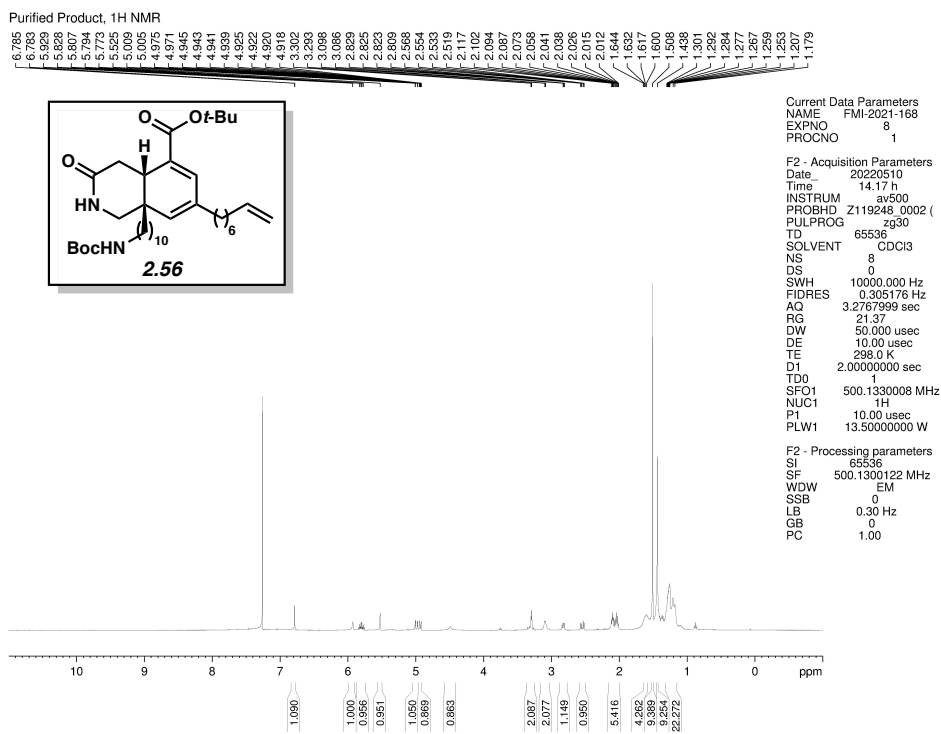


Figure 2.61. <sup>1</sup>H NMR (500 MHz, CDCl<sub>3</sub>) of compound 2.56.

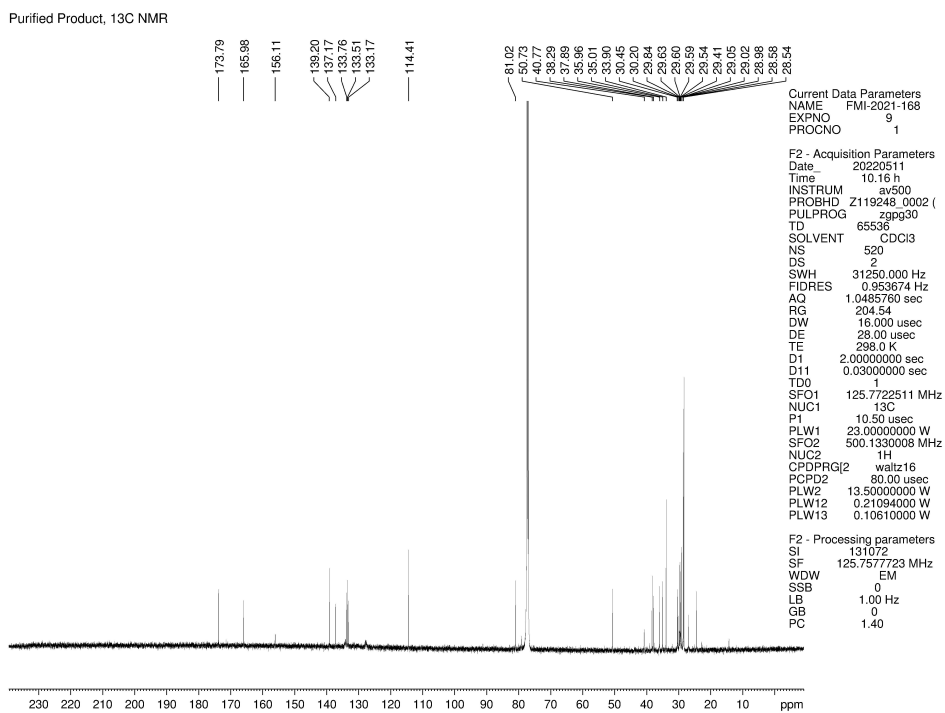


Figure 2.62. <sup>13</sup>C NMR (125 MHz, CDCl<sub>3</sub>) of compound 2.56.

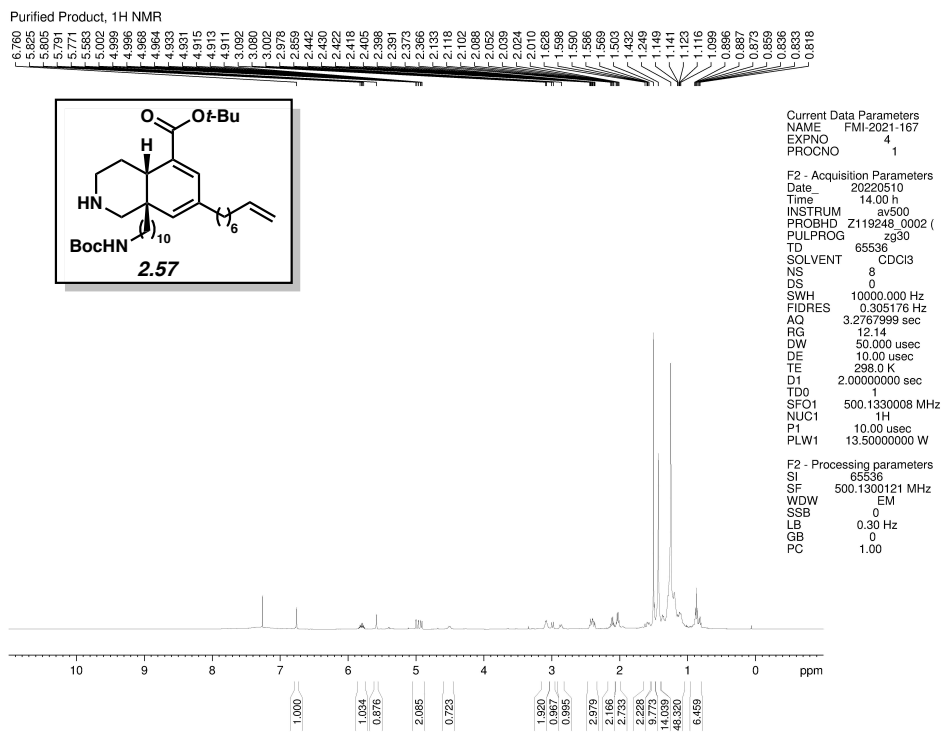


Figure 2.63. <sup>1</sup>H NMR (500 MHz, CDCl<sub>3</sub>) of compound 2.57.

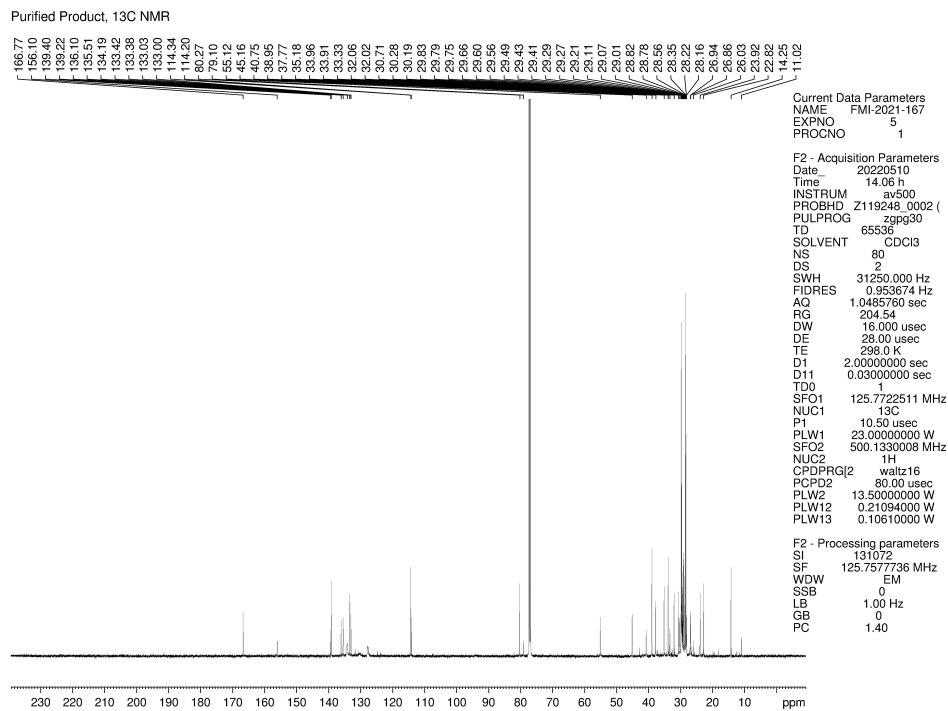


Figure 2.64. <sup>13</sup>C NMR (125 MHz, CDCl<sub>3</sub>) of compound 2.57.

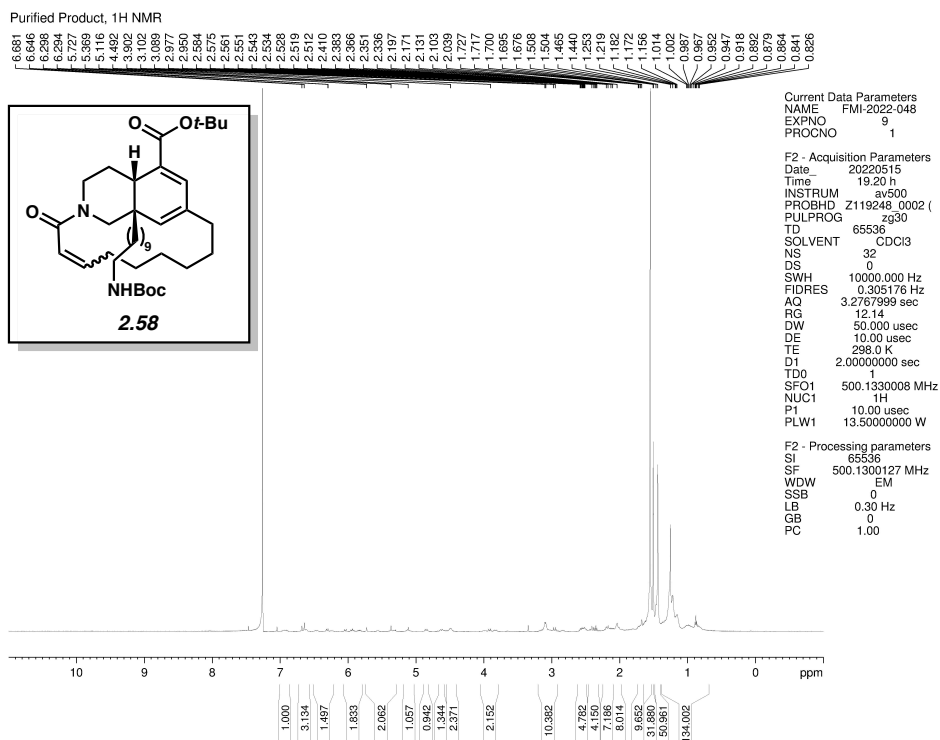


Figure 2.65. <sup>1</sup>H NMR (500 MHz, CDCl<sub>3</sub>) of compound 2.58.

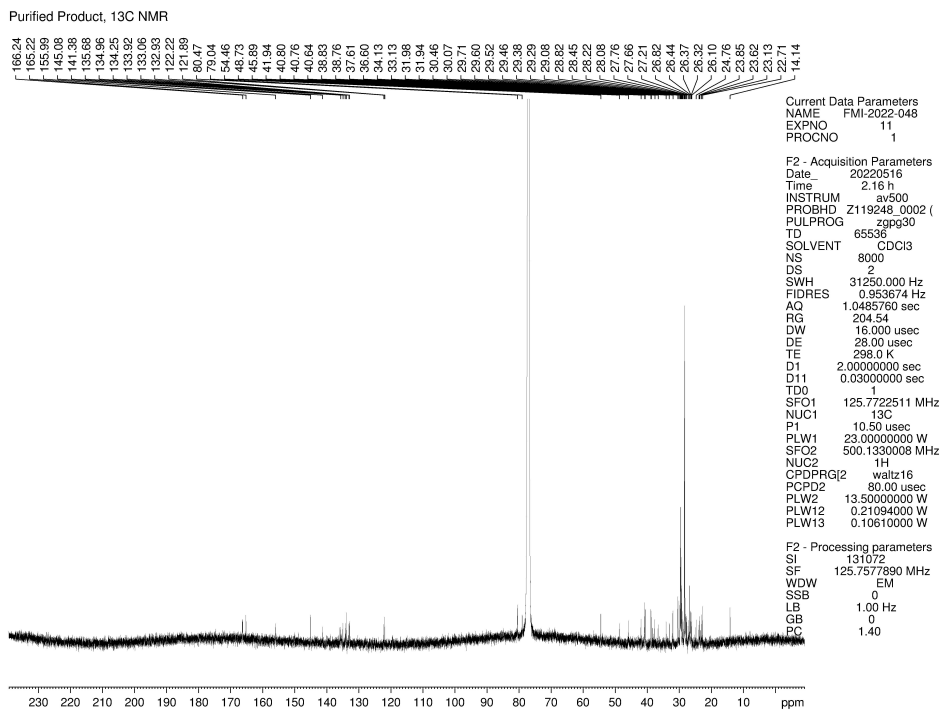


Figure 2.66. <sup>13</sup>C NMR (125 MHz, CDCl<sub>3</sub>) of compound 2.58.



Purified Product, <sup>1</sup>H NMR

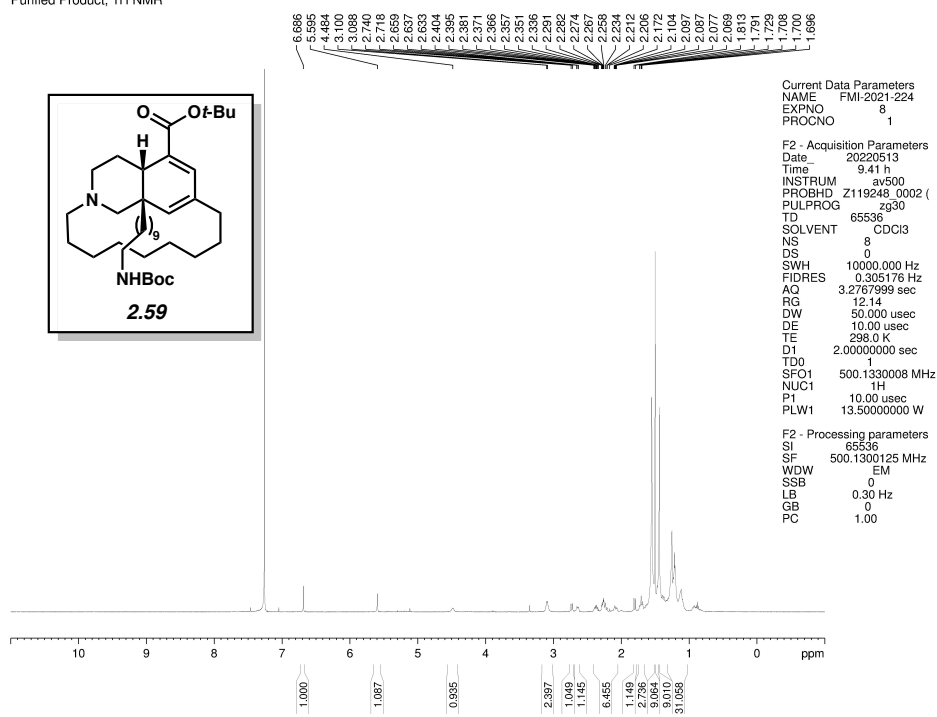


Figure 2.67. <sup>1</sup>H NMR (500 MHz, CDCl<sub>3</sub>) of compound 2.59.

Purified Product, <sup>13</sup>C NMR

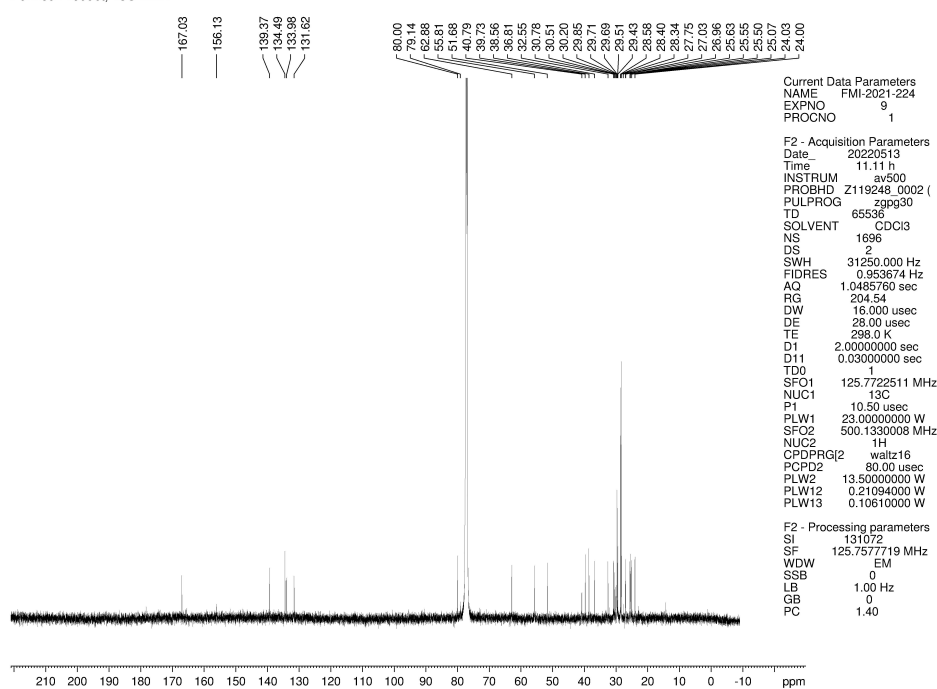


Figure 2.68. <sup>13</sup>C NMR (125 MHz, CDCl<sub>3</sub>) of compound 2.59.

## 2.9 Notes and References

- (1) a) Tadross, P. M.; Stoltz, B. M. A Comprehensive History of Arynes in Natural Product Total Synthesis. *Chem. Rev.* **2012**, *112*, 3550–3577. b) Gampe, C. M.; Carreira, E. M. Arynes and Cyclohexyne in Natural Product Synthesis. *Angew. Chem., Int. Ed.* **2012**, *51*, 3766–3778. c) Takikawa, H.; Nishii, A.; Sakai, T.; Suzuki, K. Aryne-Based Strategy in the Total Synthesis of Naturally Occurring Polycyclic Compounds. *Chem. Soc. Rev.* **2018**, *47*, 8030–8056. d) Anthony, S. M.; Wonilowicz, L. G.; McVeigh, M. S.; Garg, N. K. Leveraging Fleeting Strained Intermediates to Access Complex Scaffolds. *JACS Au* **2021**, *1*, 897–912.
- (2) a) Moser, W. M. The Reactions of gem-Dihalocyclopropanes with Organometallic Reagents. Ph. D. Thesis. Massachusetts Institute of Technology, Cambridge, MA, 1964; b) Moore, W. R.; Moser, W. R. The Reaction of 6,6-Dibromobicyclo[3.1.0]hexane with Methylithium. Efficient Trapping of 1,2-Cyclohexadiene by Styrene. *J. Org. Chem.* **1970**, *35*, 908–912.
- (3) Wittig, G.; Fritze, P. On the Intermediate Occurrence of 1,2-Cyclohexadiene. *Angew. Chem., Int. Ed.* **1966**, *5*, 846.
- (4) Christl, M.; Braun, M.; Wolz, E.; Wagner, W. 1-Phenyl-1-aza-3,4-cyclohexadien, das erste Isodihydropyridin: Erzeugung und Abfangreaktionen. *Chem. Ber.* **1994**, *127*, 1137–1142.
- (5) Quintana, I.; Peña, D.; Pérez, D.; Guitián, E. Generation and Reactivity of 1,2-Cyclohexadiene under Mild Reaction Conditions. *Eur. J. Org. Chem.* **2009**, 5519–5524
- (6) a) Barber, J. S.; Yamano, M. M.; Ramirez, M.; Darzi, E. R.; Knapp, R. R.; Liu, F.; Houk, K. N.; Garg, N. K. Diels–Alder Cycloadditions of Strained Azacyclic Allenes. *Nat.*

- Chem.* **2018**, *10*, 953–960; b) Lofstrand, V. A.; McIntosh, K. C.; Almealmadi, Y. A.; West, F. G. Strain-Activated Diels–Alder Trapping of 1,2-Cyclohexadienes: Intramolecular Capture by Pendent Furans. *Org. Lett.* **2019**, *21*, 6231–6234; c) Westphal, M. V.; Hudson, L.; Mason, J. W.; Pradeilles, J. A.; Zécric, F.; J.; Briner, K.; Schreiber, S. L. Water-Compatible Cycloadditions of Oligonucleotide-Conjugated Strained Allenes for DNA-Encoded Library Synthesis. *J. Am. Chem. Soc.* **2020**, *142*, 7776–7782.
- (7) Radwan, M.; Hanora, A.; Khalifa, S.; Abou-El-Ela, S. H. Manzamines. *Cell Cycle* **2012**, *11*, 1765–1772.
- (8) Lyakhova, E. G.; Kolesnikova, S. A.; Kalinovsky, A. I.; Berdyshev, D. V.; Pisllyagin, E. A.; Kuzmich, A. S.; Popov, R. S.; Dmitrenok, P. S.; Makarieva, T. N.; Stonik, V. A. Lissodendoric Acids A and B, Manzamine-Related Alkaloids from the Far Eastern Sponge *Lissodendoryx florida*. *Org. Lett.* **2017**, *19*, 5320–5323.
- (9) Ippoliti, F. M.; Adamson, N. J.; Wonilowicz, L. G.; Darzi, E. R.; Donaldson, J. S.; Garg, N. K. Total Synthesis of Lissodendoric Acid A via Stereospecific Trapping of a Strained Cyclic Allene. *Manuscript in preparation*.
- (10) Abdullahi, M. H.; Thompson, L. M.; Bearpark, M. J.; Vinader, V.; Afarinkia, K. The Role of Substituents in Retro Diels–Alder Extrusion of CO<sub>2</sub> from 2(*H*)-Pyrone Cycloadducts. *Tetrahedron* **2016**, *72*, 6021–6024.
- (11) Luo, T.; Dai, M.; Zheng, S.-L.; Schreiber, S. L. Syntheses of  $\alpha$ -Pyrone Using Gold-Catalyzed Coupling Reactions. *Org. Lett.* **2011**, *13*, 2834–2836.
- (12) a) Trost, B. M.; Xu, J.; Schmidt, T. Palladium-Catalyzed Decarboxylative Asymmetric Allylic Alkylation of Enol Carbonates. *J. Am. Chem. Soc.* **2009**, *131*, 18343–18357; b)

- Weaver, J. D.; Recio, A.; Grenning, A. J.; Tunge, J. A. Transition Metal-Catalyzed Decarboxylative Allylation and Benzylolation Reactions. *Chem. Rev.* **2011**, *111*, 1846–1913.
- (13) Baker, B. A.; Bošković, Z. V.; Lipshutz, B. H. (BDP)CuH: A “Hot” Stryker’s Reagent for Use in Achiral Conjugate Reductions. *Org. Lett.* **2008**, *10*, 289–292.
- (14) Huo, S. Highly Efficient, General Procedure for the Preparation of Alkylzinc Reagents from Unactivated Alkyl Bromides and Chlorides. *Org. Lett.* **2003**, *5*, 423–425.
- (15) Everson, D. A.; Weix, D. J. Cross-Electrophile Coupling: Principles of Reactivity and Selectivity. *J. Org. Chem.* **2014**, *79*, 4793–4798.
- (16) a) Chatterjee, A. K.; Morgan, J. P.; Scholl, M.; Grubbs, R. H. Synthesis of Functionalized Olefins by Cross and Ring-Closing Metathesis. *J. Am. Chem. Soc.* **2000**, *122*, 3783–3784;  
b) Chatterjee, A. K.; Choi, T.-L.; Sanders, D. P.; Grubbs, R. H. A General Model for Selectivity in Olefin Cross Metathesis. *J. Am. Chem. Soc.* **2003**, *125*, 11360–11370.
- (17) Evans, V.; Mahon, M. F.; Webster, R. L. A mild, copper-catalysed amide deprotection strategy: use of *tert*-butyl as a protecting group. *Tetrahedron* **2014**, *70*, 7593–7597.
- (18) Das, S.; Li, Y.; Lu, L.-Q.; Junge, K.; Beller, M. A General and Selective Rhodium-Catalyzed Reduction of Amides, *N*-Acyl Amino Esters, and Dipeptides Using Phenylsilane. *Chem. Eur. J.* **2016**, *22*, 7050–7053.
- (19) Luo, T.; Dai, M.; Zheng, S.-L.; Schreiber, S. L. Syntheses of  $\alpha$ -Pyrone Using Gold-Catalyzed Coupling Reactions. *Org. Lett.* **2011**, *13*, 2834–2836.

## CHAPTER THREE

### Concise Approach to Cyclohexyne and 1,2-Cyclohexadiene Precursors

Jason V. Chari,<sup>†</sup> Francesca M. Ippoliti,<sup>†</sup> and Neil K. Garg.

*J. Org. Chem.* **2019**, *84*, 3652–3655.

#### 3.1 Abstract

Silyl triflate precursors to cyclic alkynes and allenes serve as valuable synthetic building blocks. We report a concise and scalable synthetic approach to prepare the silyl triflate precursors to cyclohexyne and 1,2-cyclohexadiene. The strategy involves a retro-Brook rearrangement of an easily accessible cyclohexanone derivative, followed by triflation protocols. This simple, yet controlled, method should enable the further study of strained alkynes and allenes in chemical synthesis.

#### 3.2 Introduction

The existence of arynes, cyclic alkynes, and cyclic allenes was once considered scientific conjecture.<sup>1</sup> However, following a series of seminal studies in the 1950s and 1960s by Roberts and Wittig, strained intermediates such as benzyne (**3.1**), cyclohexyne (**3.2**), and 1,2-cyclohexadiene (**3.3**) were experimentally validated (Figure 3.1).<sup>2</sup> In the modern era, these intermediates and their derivatives, such as heterocycles **3.4** and **3.5**, have become valuable synthetic building blocks. Indeed, these strained intermediates have been used to synthesize important ligands,<sup>3</sup> agrochemicals,<sup>4</sup> medicinal agents,<sup>5</sup> natural products,<sup>6</sup> and materials.<sup>7</sup> Studies

of **3.1–3.5** have also led to new insights regarding reactivities and selectivities,<sup>8,9,10</sup> particularly as a result of the distortion/interaction model investigated by Houk.<sup>11</sup>

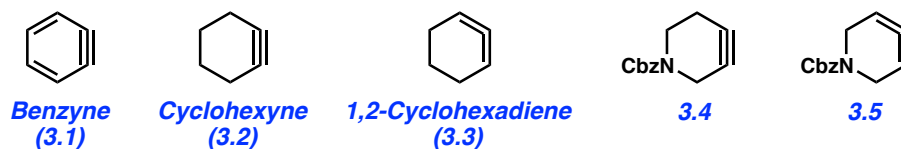


**Figure 3.1.** Strained cyclic alkynes and allenes.

In comparison to arynes, strained cyclic alkynes and allenes are less well-studied. However, as exemplified in Figure 3.2 in the context of **3.2** and **3.3**, cyclic alkynes and allenes can be trapped in an array of cycloadditions to give a diverse range of products.<sup>6,9,10</sup> For example, cycloadducts **3.7**, **3.9**, and **3.11** have been obtained by (3+2) and (4+2) cycloadditions of cyclohexyne (**3.2**).<sup>9c,15</sup> Analogously, **3.13**, **3.15**, and **3.16** have been prepared using (3+2), (2+2), and (4+2) cycloaddition reactions of 1,2-cyclohexadiene (**3.3**).<sup>9b,d,12,15</sup> In all cases, the reactions proceed by the controlled formation of two new bonds, which may be either carbon–carbon bonds or carbon–heteroatom bonds. By virtue of using heteroatom-containing trapping agents, the carbocyclic strained intermediates can be used to access heterocyclic products (e.g., **3.7**, **3.9**, **3.11**, **3.13**, **3.16**) that are of value to the pharmaceutical community. Lastly, it should be noted that the cycloadducts can bear one or more stereocenters, as seen in **3.11**, **3.13**, **3.15**, and **3.16**. In the case of substituted variants of **3.3**, it has been shown that regioselectivities, relative stereochemistry, and even absolute stereochemistry can be controlled in reactions of cyclic allenes, thus boding well for future synthetic applications.<sup>9,10,13</sup>

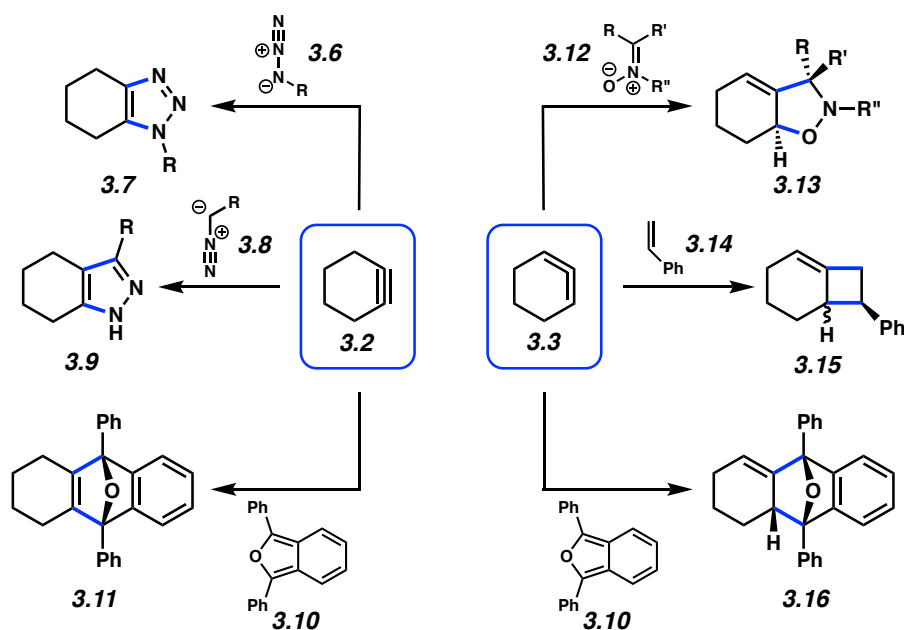


**Figure 3.2.** Cycloadditions of cyclohexyne (**3.2**) and 1,2-cyclohexadiene (**3.3**).

Given the synthetic utility of **3.2** and **3.3** (and derivatives thereof), chemists have sought to design practical synthetic precursors to these strained intermediates. Kobayashi's breakthrough in the context of benzyne<sup>14</sup> has unveiled silyl triflates as ideal precursors to strained intermediates by enabling mild reaction conditions, as will be highlighted later. In seminal studies, Guitián and co-workers demonstrated that silyl triflate precursors to **3.2** and **3.3** could be synthesized from cyclohexenone (**3.17**) (Figure 3.3).<sup>9a,b</sup> As depicted, Guitián's approach initially utilized trimethylsilyl groups. The sequence involves  $\alpha$ -bromination of **3.17**, ketone protection and silylation, followed by deprotection to give **3.18**. 1,4-Reduction of **3.18** furnishes intermediate **3.19a**, which can undergo direct triflation to give cyclohexyne precursor **3.20a**. Alternatively, protonation of **3.19a**, followed by kinetic enolate formation and triflation, delivers 1,2-cyclohexadiene precursor **3.21a**. Our laboratory questioned if intermediates reminiscent of **3.19a** could be more rapidly accessed by another means. However, it should be emphasized that

during our efforts, Mori disclosed an elegant method to prepare triethylsilyl derivatives **3.20b** and **3.21b**.<sup>15</sup> Silyl enol ether **3.22** was treated with LDA and *t*-BuOK. This led to allylic deprotonation, followed by in situ silyl migration, to afford **3.23**. Triflation of **3.23** provided 1,2-cyclohexadiene precursor **3.21b**. On the other hand, the authors found that **3.23** could isomerize to **3.19b** under modified reaction conditions, which, in turn, underwent triflation to give cyclohexyne precursor **3.20b**. It should be noted that silyl triflates **3.20b** and **3.21b** required purification by conventional chromatography, followed by size-exclusion chromatography-HPLC. Nonetheless, Mori's use of **3.22** as the key building block offers a clever strategy.

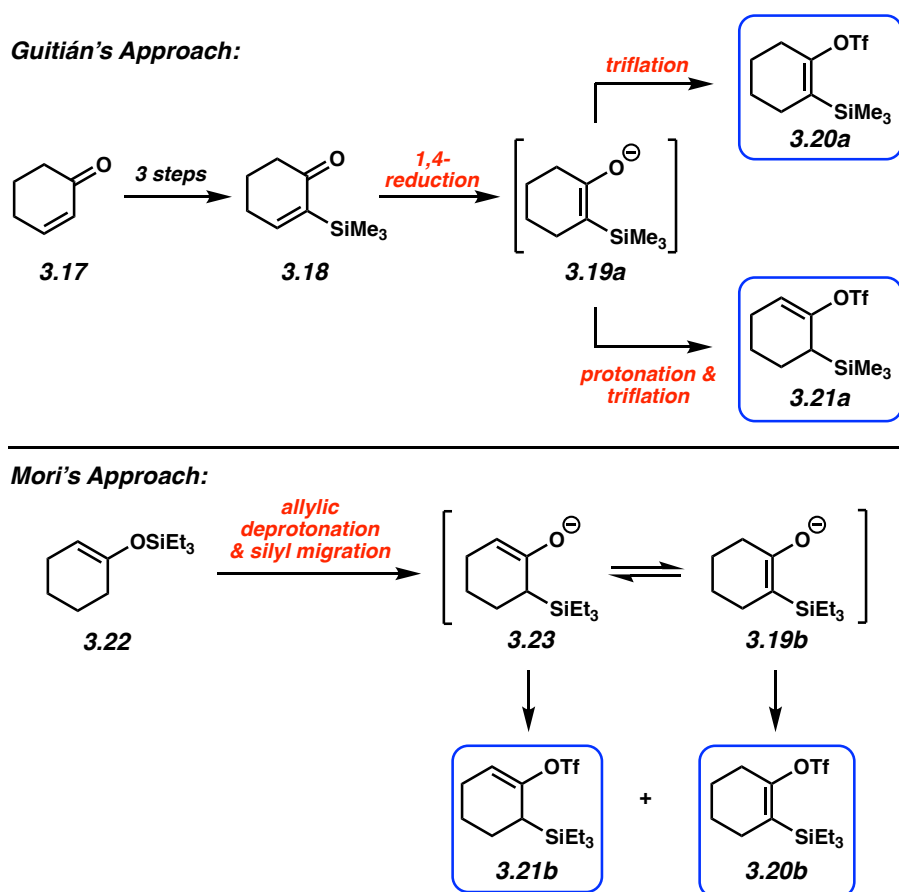


**Figure 3.3.** Synthetic approaches to cyclohexyne precursors **3.20a** and **3.20b** and 1,2-cyclohexadiene precursors **3.21a** and **3.21b**.



### 3.3 Results and Discussion

We have developed an alternative means to access **3.20b** and **3.21b**, which is depicted in Figure 3.4. Our route begins with  $\alpha$ -bromo-cyclohexanone (**3.24**), which is commercially available or can be easily prepared from cyclohexanone.<sup>16</sup> Treatment of **3.24** with DABCO and triethylsilyl chloride in DMF at 0 °C gives silyl enol ether **3.25** as a single constitutional isomer. Next, we perform halogen-metal exchange using *sec*-BuLi. This proceeds with retro-Brook rearrangement to intercept anionic intermediate **3.19b** in a highly controlled and concise manner. This strategy was conceived based on the well-established retro-Brook approach to aryne precursors.<sup>17</sup> Following rearrangement, simply quenching **3.19b** with PhNTf<sub>2</sub> provides cyclohexyne precursor **3.20b** in 97% yield. Alternatively, **3.19b** can be quenched by the addition of aqueous sodium bicarbonate to furnish  $\alpha$ -silyl ketone **3.26** in 95% yield. Our laboratory has previously reported the final step, wherein **3.26** can be converted to **3.21b** by kinetic enolate formation, followed by triflation. This earlier result is depicted based on the literature yield.<sup>9d</sup> The routes to silyl triflates **3.20b** and **3.21b** are only two and three steps from **3.24**, respectively, and notably do not require challenging chromatographic separations. Furthermore, all steps can be performed on gram scale.

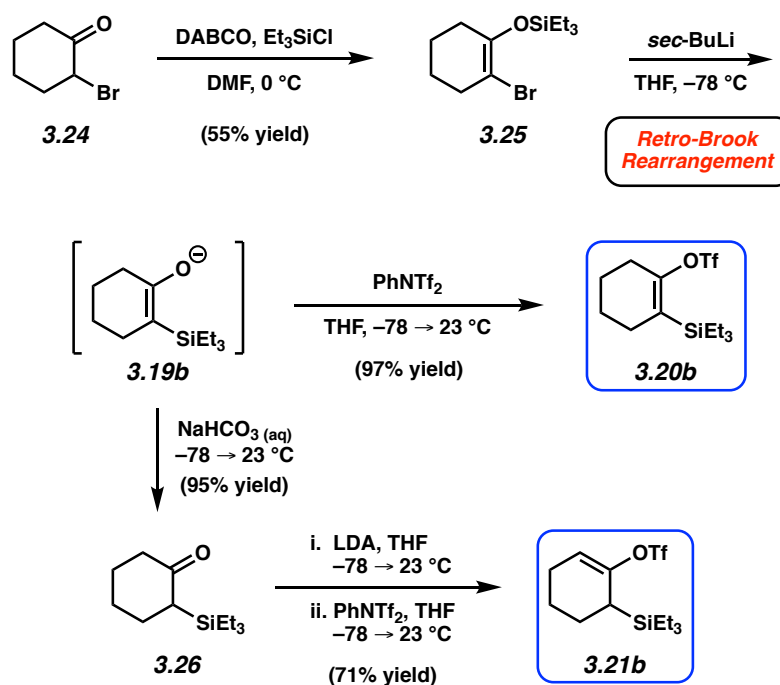


**Figure 3.4.** Retro-Brook approach to silyl triflates **3.20b** and **3.21b**.

To illustrate the mildness and simplicity of strained cyclic alkyne and allene chemistry using silyl triflate precursors, two known examples from the literature are depicted (Figure 3.5). In the first, silyl triflate **3.20b** is treated with **3.10** in the presence of TBAF in THF.<sup>15</sup> This presumably leads to the formation of **3.2** in situ, which undergoes cycloaddition to give Diels–Alder adduct **3.11**. In the second example, silyl triflate **3.21b** is treated with CsF using nitron **3.27** as the trapping agent.<sup>9d</sup> Interception of 1,2-cyclohexadiene (**3.3**) gives **3.28**. The reactions proceed without the rigorous exclusion of water or oxygen, with 1.5–2.0 equivalents of the trapping agents, and with minimal byproduct formation. As such, silyl triflates **3.20b** and **3.21b** can be transformed to value-added products using simple reaction conditions.

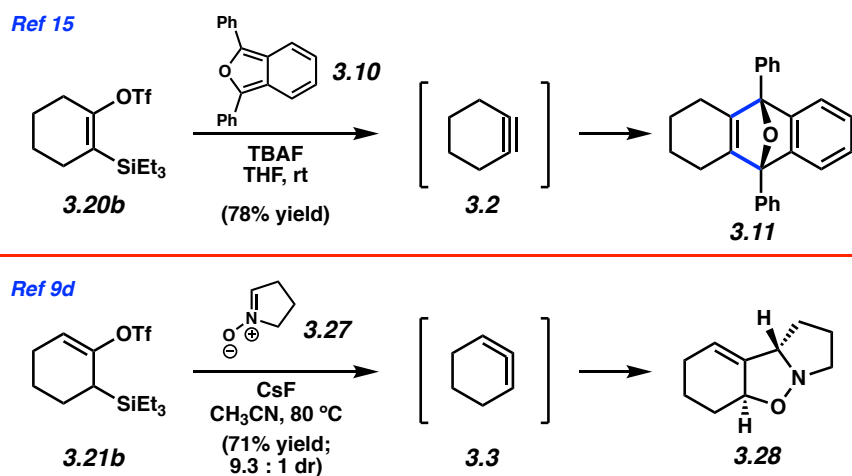


**Figure 3.5.** Examples of Cycloadditions Using Silyl Triflates **3.20b** and **3.21b**.

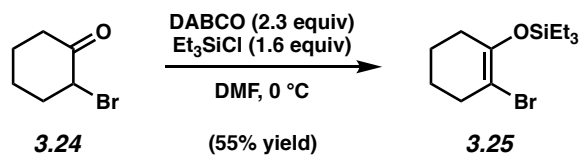
### 3.4 Conclusion

In summary, we have developed a concise approach to silyl triflate precursors to cyclohexyne (**3.2**) and 1,2-cyclohexadiene (**3.3**). Our strategy relies on a retro-Brook rearrangement of a readily available silyl enol ether. The resulting enolate intermediate can be diverted through two different sequences. Direct triflation gives cyclohexyne precursor **3.20b**, whereas protonation, followed kinetic enolization and triflation affords 1,2-cyclohexadiene precursor **3.21b**. We expect this concise and controlled strategy to access silyl triflate precursors will ultimately enable further studies involving strained alkynes and allenes in chemical synthesis.

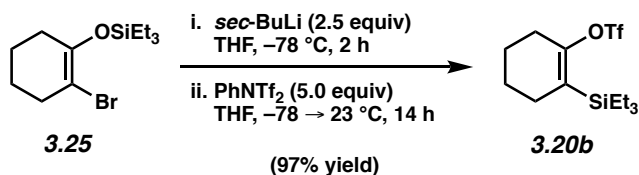
### 3.5 Experimental Section

**3.5.1 Materials and Methods.** Unless stated otherwise, reactions were conducted in flame-dried glassware under an atmosphere of nitrogen using anhydrous solvents (either freshly distilled or passed through activated alumina columns). All commercially obtained reagents were used as received unless otherwise specified. 1,4-Diazabicyclo[2.2.2]octane (DABCO) was purchased from Acros Organics. *Sec*-Butyllithium 1.4 M solution in cyclohexane (*sec*-BuLi) and cyclohexanone were obtained from Sigma-Aldrich. *N*-Phenyl-bis(trifluoromethanesulfonimide) and triethylsilyl chloride (TESCl) were purchased from Oakwood Chemical. Cyclohexanone and TESCl were distilled over CaH<sub>2</sub> prior to use. Unless stated otherwise, reactions were performed at 23 °C. Thin-layer chromatography (TLC) was conducted with EMD gel 60 F254 pre-coated plates (0.25 mm) and visualized using anisaldehyde or potassium permanganate staining. Silicycle Siliaflash P60 (particle size 0.040–0.063 mm) was used for flash column chromatography. <sup>1</sup>H-NMR spectra were recorded on Bruker spectrometers (at 500 MHz) and are reported relative to the residual solvent signal. Data for <sup>1</sup>H-NMR spectra are reported as follows: chemical shift ( $\delta$  ppm), multiplicity, coupling constant (Hz) and integration. <sup>13</sup>C-NMR spectra were recorded on Bruker spectrometers (at 100 MHz) and are reported relative to the residual solvent signal. Data for <sup>13</sup>C-NMR spectra are reported in terms of chemical shift ( $\delta$  ppm). IR spectra were obtained on a Perkin-Elmer UATR Two FT-IR spectrometer and are reported in terms of frequency of absorption (cm<sup>-1</sup>). DART-MS spectra were collected on a Thermo Exactive Plus MSD (Thermo Scientific) equipped with an ID-CUBE ion source, a Vapor Interface (IonSense Inc.), and an Orbitrap mass analyzer. Both the source and MSD were controlled by Excalibur software v. 3.0. The analyte was spotted onto OpenSpot sampling cards (IonSense Inc.) using CDCl<sub>3</sub> as the solvent. Ionization was accomplished using UHP He (Airgas Inc.) plasma with no additional ionization agents. The mass calibration was carried out using Pierce LTQ Velos ESI (+) and (-) Ion calibration solutions (Thermo Fisher Scientific).

### 3.5.2 Experimental Procedures

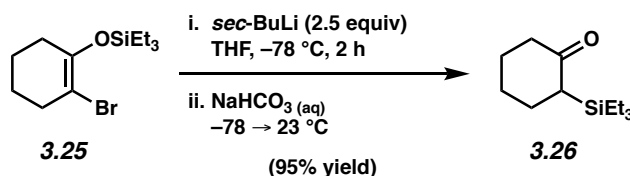


**Silyl enol ether 3.25.** To a stirred solution of known bromo ketone **3.24**<sup>16</sup> (2.01 g, 11.3 mmol, 1.00 equiv) in DMF (10.3 mL, 1.10 M) at 0 °C was added DABCO (2.93 g, 26.1 mmol, 2.30 equiv) and TESCl (3.1 mL, 18 mmol, 1.6 equiv) sequentially. The reaction mixture was stirred for 45 min before being quenched with deionized H<sub>2</sub>O (5 mL). The reaction was then allowed to warm to 23 °C before being diluted with hexanes (20 mL) and H<sub>2</sub>O (20 mL). The layers were separated and the aqueous layer was extracted with hexanes (3 x 25 mL). The combined organic layers were dried over MgSO<sub>4</sub>, filtered, and concentrated under reduced pressure. The resultant crude oil was purified via flash chromatography (100% hexanes) to afford silyl enol ether **3.25** (1.81 g, 55% yield) as a colorless oil. Silyl enol ether **3.25**: *R<sub>f</sub>* 0.40 (100% hexanes); <sup>1</sup>H-NMR (500 MHz, CDCl<sub>3</sub>): δ 2.48–2.44 (m, 2H), 2.18–2.14 (m, 2H), 1.74–1.67 (m, 2H), 1.67–1.61 (m, 2H), 1.01 (t, *J* = 7.9, 9H), 0.71 (q, *J* = 7.9, 6H); <sup>13</sup>C{<sup>1</sup>H}-NMR (100 MHz, CDCl<sub>3</sub>): δ 146.7, 102.2, 34.4, 31.6, 24.6, 23.2, 6.9, 5.8; IR (film): 2937, 2876, 1666, 1215 cm<sup>-1</sup>; HRMS–APCI (*m/z*) [M + H]<sup>+</sup> calcd for C<sub>12</sub>H<sub>24</sub>BrOSi<sup>+</sup>, 291.0780; found, 291.0780.



**Cyclohexyne precursor 3.20b.** A solution of silyl enol ether **3.25** (1.01 g, 3.47 mmol, 1.00 equiv) in THF (25 mL, 0.14 M) was cooled to -78 °C and *sec*-BuLi (0.84 M in cyclohexane, 10 mL, 8.7 mmol, 2.5 equiv) was added dropwise over 13 min. After stirring at -78 °C for 2 h, *N*-

Phenyl-bis(trifluoromethanesulfonimide) (6.19 g, 17.3 mmol, 5.00 equiv) as a solution in THF (15 mL, 1.2 M) was added dropwise over 15 min. After stirring at  $-78\text{ }^{\circ}\text{C}$  for 10 minutes, the reaction mixture was allowed to warm to  $23\text{ }^{\circ}\text{C}$ . After stirring at  $23\text{ }^{\circ}\text{C}$  for 14 h, the reaction was quenched with sat. aq.  $\text{NaHCO}_3$  (40 mL). The layers were separated and the aqueous layer was extracted with EtOAc (3 x 40 mL). The combined organic layers were dried over  $\text{MgSO}_4$ , filtered, and concentrated under reduced pressure. The resulting crude oil was purified via flash chromatography (100% hexanes) using silica gel neutralized with triethylamine to afford cyclohexyne precursor **3.20b** (1.15 g, 97% yield) as a light yellow oil. Cyclohexyne precursor **3.20b**:  $R_f$  0.52 (100% hexanes); Spectral data match those previously reported.<sup>15</sup>



**$\alpha$ -Silyl ketone 3.26.** To a solution of silyl enol ether **3.25** (1.00 g, 3.43 mmol, 1.00 equiv) in THF (40 mL, 0.085 M) at  $-78\text{ }^{\circ}\text{C}$  was added *sec*-BuLi (0.84 M in cyclohexane, 10 mL, 8.6 mmol, 2.5 equiv) dropwise over 13 min. The solution was stirred for 2 h at  $-78\text{ }^{\circ}\text{C}$ , then the reaction was quenched with sat. aq.  $\text{NaHCO}_3$  (15 mL) and allowed to warm to  $23\text{ }^{\circ}\text{C}$ . The reaction mixture was then diluted with EtOAc (15 mL) and  $\text{H}_2\text{O}$  (15 mL). The layers were then separated and the aqueous layer was extracted with EtOAc (3 x 25 mL). The combined organic layers were then dried over  $\text{MgSO}_4$ , filtered, and concentrated under reduced pressure. The resulting crude oil was purified by flash chromatography (100% hexanes  $\rightarrow$  9:1 hexanes:EtOAc) to afford silyl ketone **3.26** (691 mg, 95% yield) as a light yellow oil. Silyl ketone **3.26**:  $R_f$  0.39 (9:1 hexanes:EtOAc); spectral data match those previously reported.<sup>15</sup>

### 3.6 Spectra Relevant to Chapter Three:

#### Concise Approach to Cyclohexyne and 1,2-Cyclohexadiene Precursors

Jason V. Chari,<sup>†</sup> Francesca M. Ippoliti,<sup>†</sup> and Neil K. Garg.

*J. Org. Chem.* **2019**, *84*, 3652–3655.

Purified Product, 1H NMR

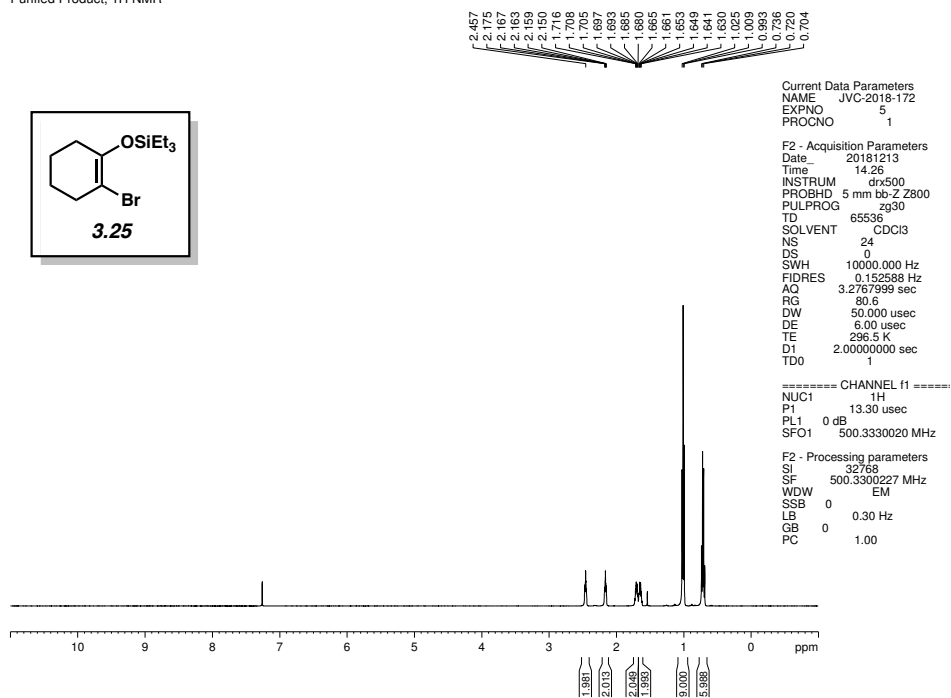
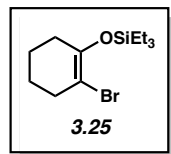


Figure 3.6. <sup>1</sup>H NMR (500 MHz, CDCl<sub>3</sub>) of compound 3.25.

Purified Product, 13C NMR

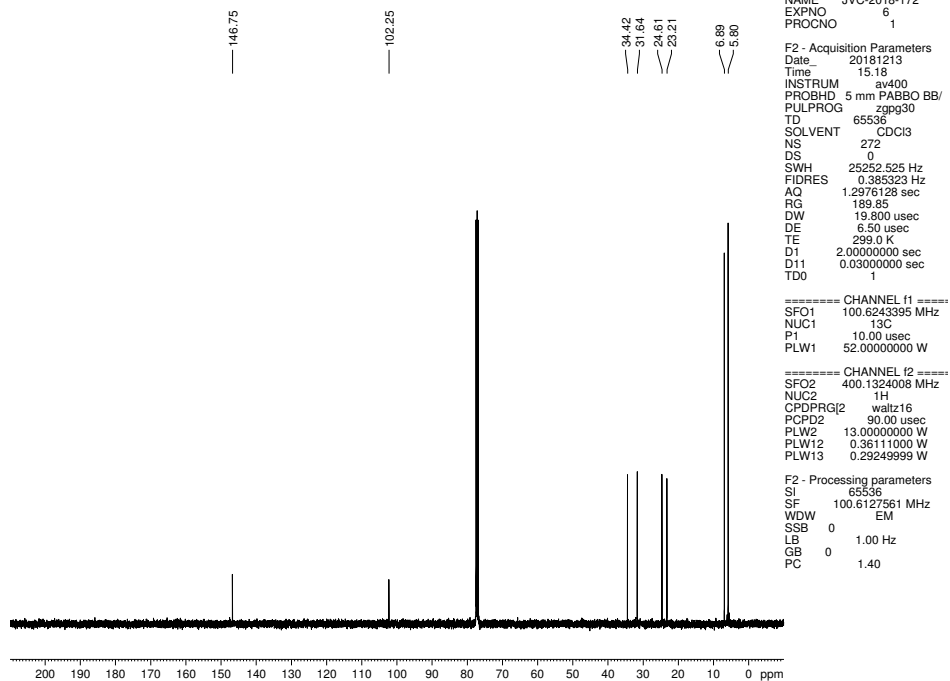


Figure 3.7. <sup>13</sup>C NMR (100 MHz, CDCl<sub>3</sub>) of compound 3.25.



Purified Product, 1H NMR

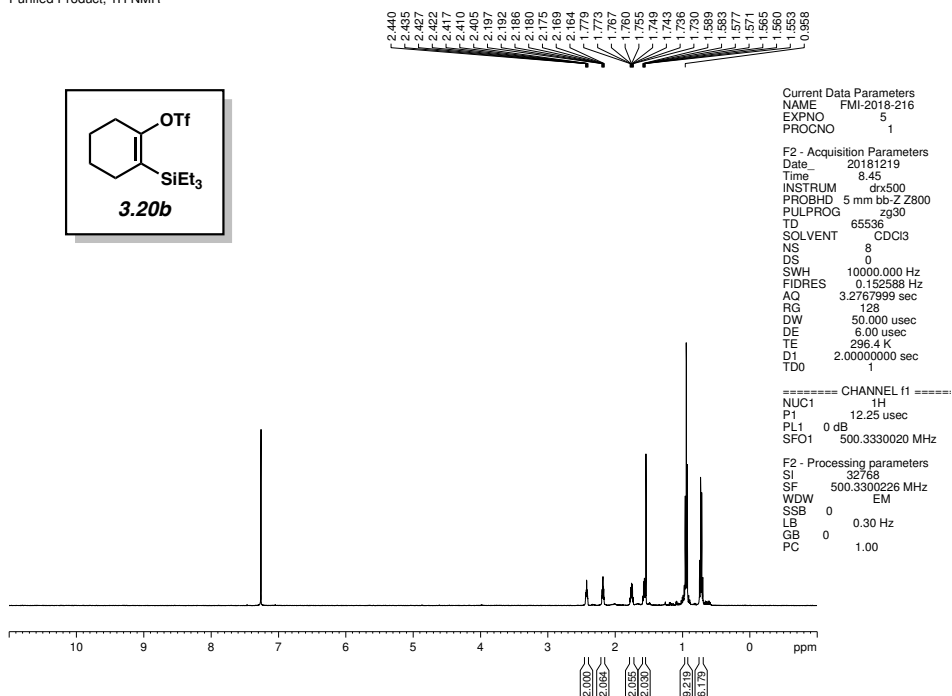


Figure 3.8. <sup>1</sup>H NMR (500 MHz, CDCl<sub>3</sub>) of compound **3.20b**.

Purified Product, 1H NMR

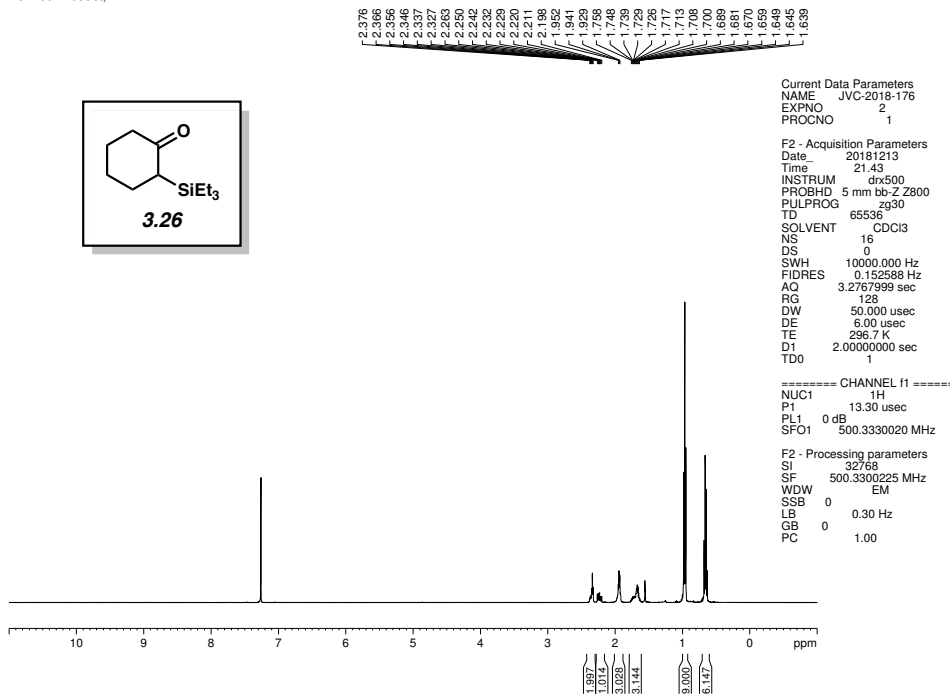


Figure 3.9. <sup>1</sup>H NMR (500 MHz, CDCl<sub>3</sub>) of compound **3.26**.

### 3.7 Notes and References

- (1) For reviews of arynes and related strained intermediates, see: (a) Bronner, S. M.; Goetz, A. E.; Garg, N. K. Understanding and Modulating Indolyne Regioselectivities. *Synlett* **2011**, *18*, 2599–2604. (b) Tadross, P. M.; Stoltz, B. M. A Comprehensive History of Arynes in Natural Product Total Synthesis. *Chem. Rev.* **2012**, *112*, 3550–3577. (c) Gampe, C. M.; Carreira, E. M. Arynes and Cyclohexyne in Natural Product Synthesis. *Angew. Chem., Int. Ed.* **2012**, *51*, 3766–3778. (d) Dubrovskiy, A. V.; Markina, N. A.; Larock, R. C. Use of Benzyne for the Synthesis of Heterocycles. *Org. Biomol. Chem.* **2013**, *11*, 191–218. (e) Hoffman, R. W.; Suzuki, K. A “Hot, Energized” Benzyne. *Angew. Chem., Int. Ed.* **2013**, *52*, 2655–2656. (f) Goetz, A. E.; Garg, N. K. Enabling the Use of Heterocyclic Arynes in Chemical Synthesis. *J. Org. Chem.* **2014**, *79*, 846–851. (g) Yoshida, S.; Hosoya, T. The Renaissance and Bright Future of Synthetic Aryne Chemistry. *Chem. Lett.* **2015**, *44*, 1450–1460. (h) Takikawa, H.; Nishii, A.; Sakai, T.; Suzuki, K. Aryne-Based Strategy in the Total Synthesis of Naturally Occurring Polycyclic Compounds. *Chem. Soc. Rev.* **2018**, *47*, 8030–8056. (i) Dhokale, R. A.; Mhaske, S. B. Transition-Metal-Catalyzed Reactions Involving Arynes. *Synthesis* **2018**, *50*, 1–16.
- (2) (a) Roberts, J. D.; Simmons, H. E.; Carlsmith, L. A.; Vaughn, C. W. Rearrangement in the Reaction of Chlorobenzene-1-C<sup>14</sup> with Potassium Amide. *J. Am. Chem. Soc.* **1953**, *75*, 3290–3291. (b) Scardiglia, F.; Roberts, J. D. Evidence for Cyclohexyne as an Intermediate in the Coupling of Phenyllithium with 1-Chlorocyclohexene. *Tetrahedron* **1957**, *1*, 343–344. (c) Wittig, G.; Fritze, P. On the Intermediate Occurrence of 1,2-

- Cyclohexadiene. *Angew. Chem., Int. Ed.* **1966**, *5*, 846. (d) Wenk, H. H.; Winkler, M.; Sander, W. One Century of Aryne Chemistry. *Angew. Chem., Int. Ed.* **2003**, *42*, 502–528.
- (3) (a) Surry, D. S.; Buchwald, S. L. Biaryl Phosphane Ligands in Palladium-Catalyzed Amination. *Angew. Chem., Int. Ed.* **2008**, *47*, 6338–6361. (b) Mauger, C. C.; Mignani, G. A. An Efficient and Safe Procedure for the Large-Scale Pd-Catalyzed Hydrazone of Aromatic Chlorides Using Buchwald Technology. *Org. Proc. Res. Dev.* **2004**, *8*, 1065–1071.
- (4) Schleth, F.; Vettiger, T.; Rommel, M.; Tobler, H. "Process for the Preparation of Pyrazole Carboxylic Acid Amides" WO2011131544 A1, Oct 27, 2011.
- (5) (a) Carroll, F. I.; Robinson, T. P.; Brieady, L. E.; Atkinson, R. N.; Mascarella, S. W.; Damaj, M. I.; Martin, B. R.; Navarrio, H. A. Synthesis and Nicotinic Acetylcholine Receptor Binding Properties of Bridged and Fused Ring Analogues of Epibatidine. *J. Med. Chem.* **2007**, *50*, 6383–6391. (b) Kamitani, T.; Kigasawa, K.; Hiragi, M.; Wagatsuma, N.; Uryu, T.; Araki, K. Syntheses of Heterocyclic Compounds. 509. Syntheses of Analgesics. 34. Synthesis of 3-Hydroxy-*N*-Cyclopropylmethyl-9-Azamorphan. *J. Med. Chem.* **1973**, *16*, 301–303. (c) Heindel, N. D.; Fives, W. P.; Lemke, T. F.; Rowe, J. E.; Snady, H. W. Synthesis, Transformation, and General Pharmacologic Activity in 1,4-Benzodiazepine-3,5-diones. *J. Med. Chem.* **1971**, *14*, 1233–1235. (d) Bell, M. R.; Zalay, A. W.; Oesterlin, R.; Schane, P.; Potts, G. Basic Ethers of 1-(*p*-Hydroxyphenyl)-2-Phenyl-1,2,3,4-Tetrahydroquinoline and 1-(*p*-Hydroxyphenyl)-2-Phenyl Indole. Antifertility Agents. *J. Med. Chem.* **1970**, *13*, 664–668. (e) Willis, P. G.; Pavlova, O. A.; Chefer, S. I.; Vaupel, D. B.; Mukhin, A. G.; Horti,

- A. G. Synthesis and Structure-Activity Relationship of a Novel Series of Aminoalkylindoles with Potential of Imaging the Neuronal Cannabinoid Receptor by Positron Emission Tomography. *J. Med. Chem.* **2005**, *48*, 5813–5822. (f) Jacob, III, P. Sulfur Analogues of Psychotomimetic Agents. Monothio Analogues of Mescaline and Isomescaline. *J. Med. Chem.* **1981**, *24*, 1348–1353. (g) Coe, J. W.; Brooks, P. R.; Wirtz, M. C.; Bashore, C. G.; Bianco, K. E.; Vetelino, M. G.; Arnold E. P.; Lebel, L. A.; Fox, C. B.; Tingley, III, F. D.; Schulz, D. W.; Davis, T. I.; Sands, S. B.; Mansbach, R. S; Rollema, H.; O'Neill, B. T. 3,5-Bicyclic Aryl Piperidines: A Novel Class of  $\alpha 4\beta 2$  Neuronal Nicotinic Receptor Partial Agonists for Smoking Cessation. *Bioorg. Med. Chem. Lett.* **2005**, *15*, 4889–4897.
- (6) For examples of arynes and other strained cyclic alkynes in total synthesis, see: (a) Kou, K. G. M.; Pflueger, J. J.; Kiho, T.; Morrill, L. C.; Fisher, E. L.; Clagg, K.; Lebold, T. P.; Kisunzu, J. K.; Sarpong, R. A Benzyne Insertion Approach to Hetsisine-Type Diterpenoid Alkaloids: Synthesis of Cossonidine (Davisine). *J. Am. Chem. Soc.* **2018**, *140*, 8105–8109. (b) Goetz, A. E.; Silberstein, A. L.; Corsello, M. A.; Garg, N. K. Concise Enantiospecific Total Synthesis of Tubingensin A. *J. Am. Chem. Soc.* **2014**, *136*, 3036–3039. (c) Neog, K.; Borah, A.; Gogoi, P. Palladium(II)-Catalyzed C–H Bond Activation/C–C and C–O Bond Formation Reaction Cascade: Direct Synthesis of Coumestans. *J. Org. Chem.* **2016**, *81*, 11971–11977. (d) Neumeyer, M.; Kopp, J.; Brückner, R. Controlling the Substitution Pattern of Hexasubstituted Naphthalenes by Aryne/Siloxyfuran Diels–Alder Additions: Regio and Stereocontrolled Synthesis of Arizonin C1 Analogs. *Eur. J. Org. Chem.* **2017**, 2883–2915. (e) Corsello, M. A.; Kim, J.;

- Garg, N. K. Total Synthesis of (–)-Tubingensin B Enabled by the Strategic Use of an Aryne Cyclization. *Nat. Chem.* **2017**, *9*, 944–949. (f) Gampe, C. M.; Carreira, E. M. Total Syntheses of Guanacastepenes N and O. *Angew. Chem., Int. Ed.* **2011**, *50*, 2962–2965.
- (7) Lin, J. B.; Shah, T. J.; Goetz, A. E.; Garg, N. K.; Houk, K. N. Conjugated Trimeric Scaffolds Accessible from Indolyne Cyclotrimerizations: Synthesis, Structure, and Electronic Properties. *J. Am. Chem. Soc.* **2017**, *139*, 10447–10455.
- (8) Fine Nathel, N. F.; Morrill, L. A.; Mayr, H.; Garg, N. K. Quantification of the Electrophilicity of Benzyne and Related Intermediates. *J. Am. Chem. Soc.* **2016**, *138*, 10402–10405.
- (9) (a) Atanes, N.; Escudero, S.; Pérez, D.; Guitián, E.; Castedo, L. Generation of Cyclohexyne and its Diels–Alder Reaction with  $\alpha$ -Pyrones. *Tetrahedron Lett.* **1998**, *39*, 3039–3040. (b) Quintana, I.; Peña, D.; Pérez, D.; Guitián, E. Generation and Reactivity of 1,2-Cyclohexadiene under Mild Reaction Conditions. *Eur. J. Org. Chem.* **2009**, 5519–5524. (c) Medina, J. M.; McMahon, T. C.; Jiménez-Osés, G.; Houk, K. N.; Garg, N. K. Cycloadditions of Cyclohexynes and Cyclopentyne. *J. Am. Chem. Soc.* **2014**, *136*, 14706–14709. (d) Barber, J. S.; Styduhar, E. D.; Pham, H. V.; McMahon, T. C.; Houk, K. N.; Garg, N. K. Nitrene Cycloadditions of 1,2-Cyclohexadiene. *J. Am. Chem. Soc.* **2016**, *138*, 2512–2515. (e) Lofstrand, V. A.; West, F. G. Efficient Trapping of 1,2-Cyclohexadienes with 1,3-Dipoles. *Chem. Eur. J.* **2016**, *22*, 10763–10767.
- (10) (a) McMahon, T. C.; Medina, J. M.; Yang, Y.-F.; Simmons, B. J.; Houk, K. N.; Garg, N. K. Generation and Regioselective Trapping of a 3,4-Piperidyne for the Synthesis of Functionalized Heterocycles. *J. Am. Chem. Soc.* **2015**, *137*, 4082–4085. (b) Tlais, S. F.;

- Danheiser, R. L. *N*-Tosyl-3-Azacyclohexyne. Synthesis and Chemistry of a Strained Cyclic Ynamide. *J. Am. Chem. Soc.* **2014**, *136*, 15489–15492. (c) Christl, M.; Braun, M.; Wolz, E.; Wagner, W. 1-Phenyl-1-aza-3,4-cyclohexadien, das erste Isodihydropyridin: Erzeugung und Abfangreaktionen. *Chem. Ber.* **1994**, *127*, 1137–1142. (d) Shah, T. K.; Medina, J. M.; Garg, N. K. Expanding the Strained Alkyne Toolbox: Generation and Utility of Oxygen-Containing Strained Alkynes. *J. Am. Chem. Soc.* **2016**, *138*, 4948–4954. (e) Barber, J. S.; Yamano, M. M.; Ramirez, M.; Darzi, E. R.; Knapp, R. R.; Liu, F.; Houk, K. N.; Garg, N. K. Diels–Alder Cycloadditions of Strained Azacyclic Allenes. *Nat. Chem.* **2018**, *10*, 953–960. (f) Johnson, R. P. Strained Cyclic Cumulenes. *Chem. Rev.* **1989**, *89*, 1111–1124. (g) Nendel, M.; Tolbert, L. M.; Herring, L. E.; Islam, M. N.; Houk, K. N. Strained Allenes as Dienophiles in the Diels–Alder Reaction: An Experimental and Computational Study. *J. Org. Chem.* **1999**, *64*, 976–983.
- (11) (a) Bronner, S. M.; Goetz, A. E.; Garg, N. K. Understanding and Modulating Indolyne Regioselectivities. *Synlett* **2011**, 2599–2604. (b) Medina, J. M.; Mackey, J. L.; Garg, N. K.; Houk, K. N. The Role of Aryne Distortions, Steric Effects, and Charges in Regioselectivities of Aryne Reactions. *J. Am. Chem. Soc.* **2014**, *136*, 15798–15805. (c) Cheong, P. H.-Y.; Paton, R. S.; Bronner, S. M.; Im, G.-Y. J.; Garg, N. K.; Houk, K. N. Indolyne and Aryne Distortions and Nucleophilic Regioselectivities. *J. Am. Chem. Soc.* **2010**, *132*, 1267–1269.
- (12) Moore, W. R.; Moser, W. R. The Reaction of 6,6-Dibromobicyclo[3.1.0]hexane with Methyllithium. Efficient Trapping of 1,2-Cyclohexadiene by Styrene. *J. Org. Chem.* **1970**, *35*, 908–912.

- (13) Christl, M.; Fischer, H.; Arnone, M.; Engels, B. 1-Phenyl-1,2-cyclohexadiene: Astoundingly High Enantioselectivities on Generation in a Doering–Moore–Skattebøl Reaction and Interception by Activated Olefins. *Chem. Eur. J.* **2009**, *15*, 11266–11272.
- (14) Himeshima, Y.; Sonoda, T.; Kobayashi, H. Fluoride-induced 1,2-Elimination of *o*-Trimethylsilylphenyl Triflate to Benzyne Under Mild Conditions. *Chem. Lett.* **1983**, *12*, 1211–1214.
- (15) Inoue, K.; Nakura, R.; Okano, K.; Mori, A. One-Pot Synthesis of Silylated Enol Triflates from Silyl Enol Ethers for Cyclohexynes and 1,2-Cyclohexadienes. *Eur. J. Org. Chem.* **2018**, 3343–3347.
- (16) Zhang, G.-B.; Wang, F.-X.; Du, J.-Y.; Qu, H.; Ma, X.-Y.; Wei, M.-X.; Wang, C.-T.; Li, Q.; Fan, C.-A. Toward the Total Synthesis of Palhinine A: Expedient Assembly of Multifunctionalized Isotwistane Ring System with Contiguous Quaternary Stereocenters. *Org. Lett.* **2012**, *14*, 3696–3699.
- (17) Peña, D.; Cobas, A.; Pérez, D.; Guitián, E. An Efficient Procedure for the Synthesis of *ortho*-Trialkylsilylaryl Triflates: Easy Access to Precursors of Functionalized Arynes. *Synthesis* **2002**, *2002*, 1454–1458.

## CHAPTER FOUR

### Synthesis of 8-Hydroxygeraniol

Francesca M. Ippoliti,<sup>†</sup> Joyann S. Barber,<sup>†</sup> Yi Tang, and Neil K. Garg.

*J. Org. Chem.* **2018**, *83*, 11323–11326.

#### 4.1 Abstract

An operationally simple protocol for the conversion of geranyl acetate to 8-hydroxygeraniol is reported. The convenient two-step procedure relies on an efficient, chemo- and regioselective SeO<sub>2</sub>-promoted oxidation, followed by straightforward deacetylation. This facile means to prepare 8-hydroxygeraniol is expected to enable biosynthetic studies pertaining to thousands of monoterpene indole alkaloids.

#### 4.2 Introduction

Monoterpene indole alkaloids (MIAs) have provided chemists and biologists with the inspiration to pursue countless scientific endeavors.<sup>1,2,3,4</sup> To-date, over 3,000 MIAs have been discovered, many of which possess striking biological activity. Select examples of MIAs are the notorious poison strychnine (**4.1**) and the life-changing anticancer drug vinblastine (**4.2**), both of which are shown in Figure 4.1. All MIAs are prepared by Nature through a remarkable biosynthetic pathway, which has been under investigation for decades.<sup>1,5,6,7,8,9,10,11</sup>

This Chapter focuses on 8-hydroxygeraniol (**4.3**, Figure 4.1), an early biosynthetic precursor to MIA's. 8-Hydroxygeraniol (**4.3**) is made biosynthetically through a controlled enzymatic oxidation of geraniol<sup>6</sup> before being elaborated to nepetalactol (**4.4**).<sup>12</sup> Many further biosynthetic manipulations ultimately give rise to strictosidine (**4.5**), the last common biosynthetic



precursor to all MIAs. Given the relative simplicity of **4.3**, compared to its successors in the biosynthetic pathway (e.g., **4.5**), it has been used to enable several biosynthetic studies, including the biosynthesis of nepetalactol (**4.4**)<sup>13,14</sup> and the biosynthesis of strictosidine (**4.5**).<sup>15</sup>

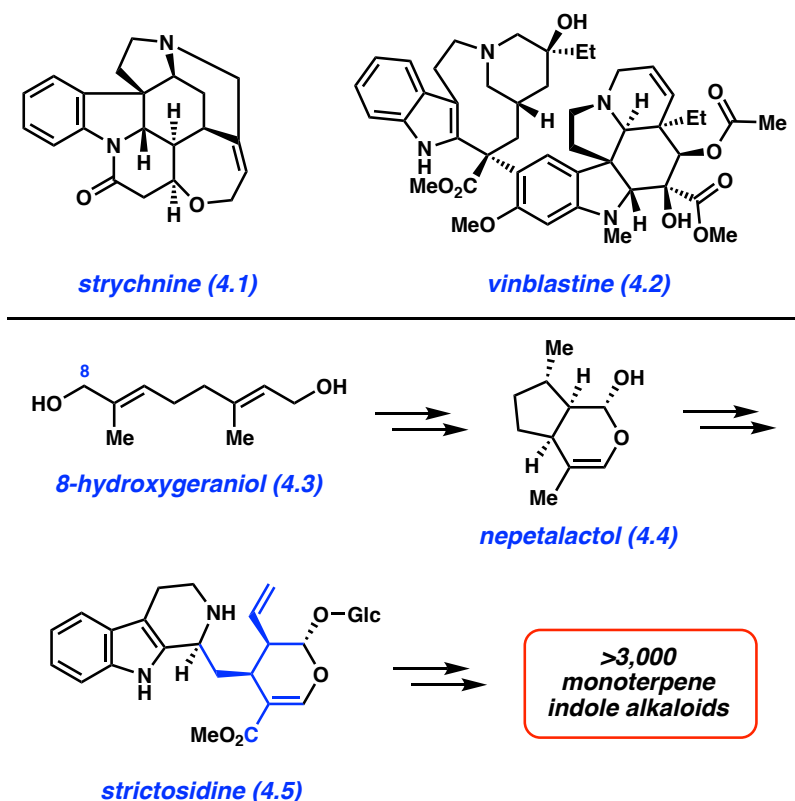


**Figure 4.1.** Role of 8-hydroxygeraniol (**4.3**) in the biosynthesis of all monoterpene indole alkaloids, including strychnine (**4.1**) and vinblastine (**4.2**).

### 4.3 Previous Approaches and Nomenclature Discussion

Several synthetic approaches to 8-hydroxygeraniol (**4.3**) have been reported in the literature (Figure 4.2). The earliest reports appeared back-to-back in 1970, where multistep synthetic routes were developed beginning from either levulinaldehyde (**4.6**)<sup>16</sup> or dehydrolinalool (**4.7**).<sup>17</sup> An alternative strategy was reported by Williams and Lin, which involved

photocycloaddition of **4.8** and **4.9**, with subsequent elaboration using a thermolysis / Cope rearrangement strategy.<sup>18</sup> Perhaps the most direct approach relies on the use of geranyl acetate (**4.10**) as the starting material. In this regard, Kobayashi has reported a procedure for the C8-oxidation of **4.10** using stoichiometric SeO<sub>2</sub>, which proceeds in low yields and with extensive over-oxidation to the corresponding enal.<sup>19</sup> Around the same time, Sharpless reported a similar protocol that relies on catalytic SeO<sub>2</sub> and stoichiometric *t*-butyl hydroperoxide.<sup>20</sup> This procedure, which has subsequently been repeated with similar results,<sup>21</sup> leads to significant recovery of starting material<sup>20</sup> with some minimization of the over-oxidation byproduct (i.e., 45% yield of the desired alcohol and 19% enal<sup>21</sup>). A promising biocatalytic approach to 8-hydroxygeraniol (**4.3**) using a cytochrome P450 has also been described,<sup>21</sup> although it has yet to be rendered practical for material throughput.

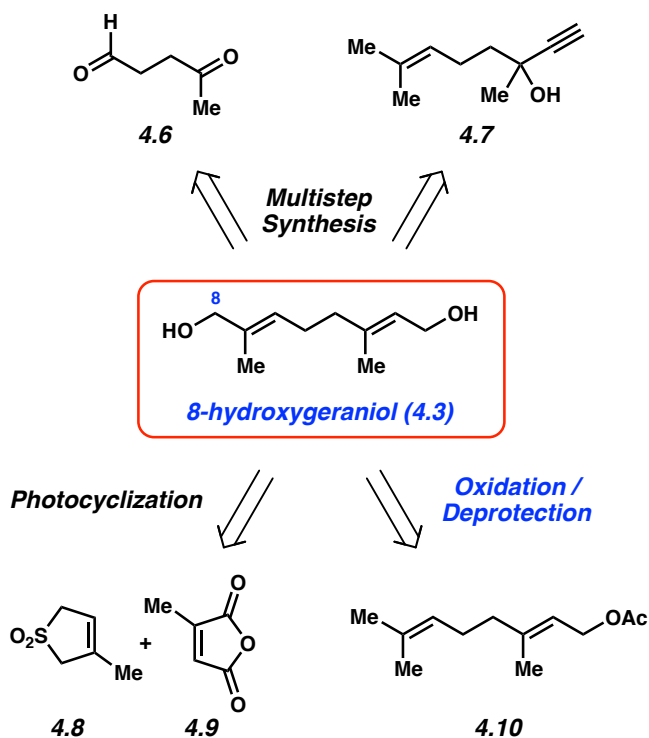


**Figure 4.2.** Various approaches to 8-hydroxygeraniol (**4.3**).

One further point regarding 8-hydroxygeraniol (**4.3**) and its naming should be noted. Throughout the aforementioned literature and other sources, the compound is often referred to as “10-hydroxygeraniol” instead (Figure 4.3).<sup>6,7,12,13,16,17,18,19</sup> We believe this is a simple nomenclature error that has propagated for many decades. Similarly, 8-oxogeraniol (**4.11**), the biosynthetic successor to 8-hydroxygeraniol (**4.3**), has been referred to as “10-oxogeraniol.”<sup>7,12,22</sup> From a nomenclature standpoint, this is also incorrect. We suggest the chemical and biosynthetic community use the “8-” prefix going forward for 8-hydroxygeraniol (**4.3**) to minimize confusion, as this is consistent with IUPAC standards where “8” should reflect the longest carbon chain in the molecule, with C8 being the *trans* substituent on the alkene.<sup>23,24</sup> Additionally, the “8-” prefix is accepted according to various enzymology resources.<sup>25,26</sup>

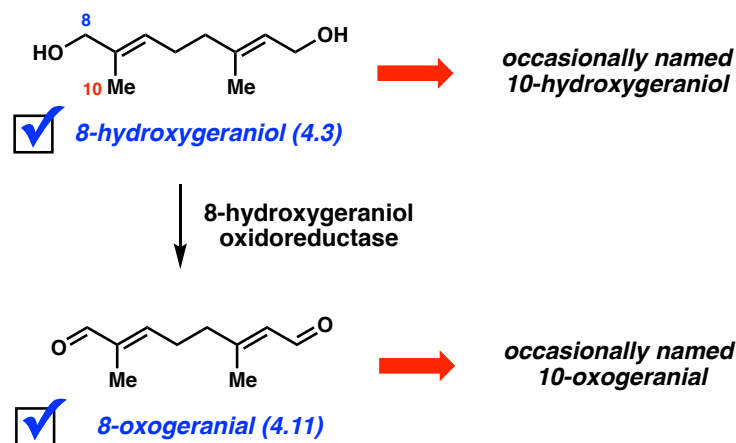


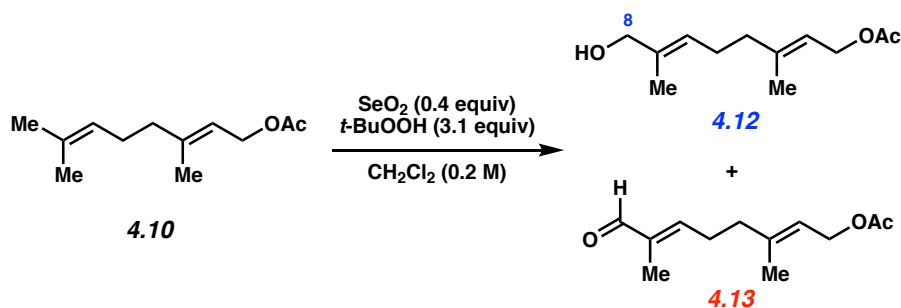
**Figure 4.3.** Confusion surrounding the naming of 8-hydroxygeraniol (**4.3**) and its biosynthetic successor 8-oxogeraniol (**4.11**).

#### 4.4 Synthesis Development

With the aim of developing a practical procedure for the preparation of 8-hydroxygeraniol (**4.3**) to enable our biosynthetic studies,<sup>14</sup> we opted to pursue the chemo- and regioselective allylic

oxidation of geranyl acetate (**4.10**), shown in Figure 4.2, as a starting point. Select results from our efforts to reproduce and optimize the catalytic SeO<sub>2</sub> oxidation procedure are provided in Table 4.1. As shown in entries 1 and 2, the oxidation could be performed at 0 °C. After 5 h, significant amounts of unreacted geranyl acetate (**4.10**) remained (entry 1). However, longer reaction times at 0 °C showed promise for increasing the conversion (entry 2). For the sake of developing a more convenient protocol that would not require cooling for extended periods of time, we attempted the oxidation at 23 °C. After 30 minutes or 1 h, significant recovery of unreacted substrate **4.10** was observed (entries 3 and 4, respectively). When the reaction was performed for 1.5 h, a more desirable ratio was obtained (entry 5), with the desired product **4.12** being formed in 61% yield. At longer reaction times of 5 h, substrate **4.10** could be fully consumed; however, competitive over-oxidation to enal **4.13** was observed (entry 6). Overall, entry 5 conditions were deemed ideal because of the convenience of the experimental protocol (23 °C, 1.5 h) and the optimal yield of **4.12** obtained.

**Table 4.1.** Optimization of SeO<sub>2</sub>-promoted oxidation of **4.10**.<sup>a</sup>



Entry	Temperature	Time	Ratio of <b>4.10</b> : <b>4.12</b> : <b>4.13</b> <sup>a</sup>	Yield of <b>4.12</b> <sup>a</sup>
1	0 °C	5 h	27 : 68 : 4	43%
2	0 °C	7 h	11 : 82 : 7	57%
3	23 °C	30 min	42 : 55 : 2	43%
4	23 °C	1 h	28 : 67 : 5	57%
5	23 °C	1.5 h	19 : 73 : 8	61%
6	23 °C	5 h	0 : 52 : 48	24%

<sup>a</sup> Ratios and yields were determined by <sup>1</sup>H NMR analysis of the crude reaction mixtures (1,3,5-trimethoxybenzene was used as an external standard).

With practical reaction conditions in hand for the efficient oxidation of geranyl acetate (**4.10**), we performed the preparation of 8-hydroxygeraniol (**4.3**) on 3 mmol scale, as shown in Figure 4.4. SeO<sub>2</sub>-promoted oxidation of **4.10** proceeded smoothly under our optimized conditions in just 1.5 h at 23 °C. This gave the desired C8-hydroxylated product **4.12** in 64% isolated yield. Subsequent treatment of **4.12** with K<sub>2</sub>CO<sub>3</sub> in methanol at 23 °C smoothly delivered 8-hydroxygeraniol (**4.3**) in 83% yield after flash column chromatography. This exceedingly simple protocol can be used to synthesize multi-mmol quantities of **4.3**.

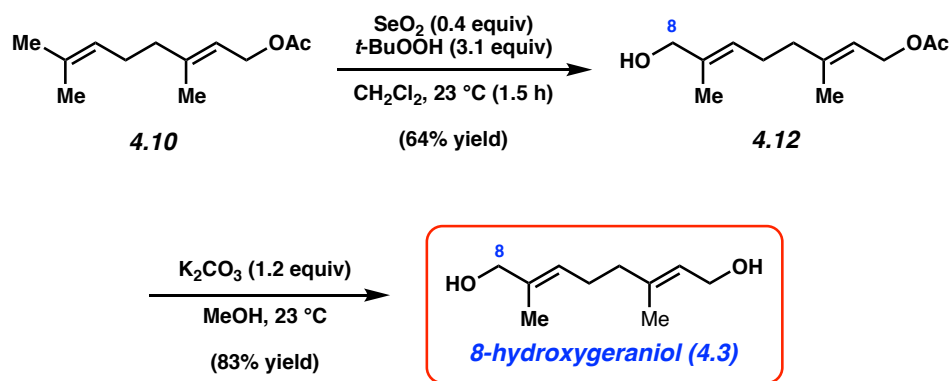


**Figure 4.4.** Preparation of 8-hydroxygeraniol (4.3) on 3 mmol scale.

#### 4.5 Conclusion

In summary, we have developed a simple and convenient procedure to synthesize 8-hydroxygeraniol (4.3). The procedure involves a regio- and chemoselective oxidation, followed by methanolysis. Both transformations are performed at ambient temperature and can be used to easily access multi-mmol quantities of 4.3. We expect this protocol will enable biosynthetic investigations pertaining to thousands of monoterpene indole alkaloids.

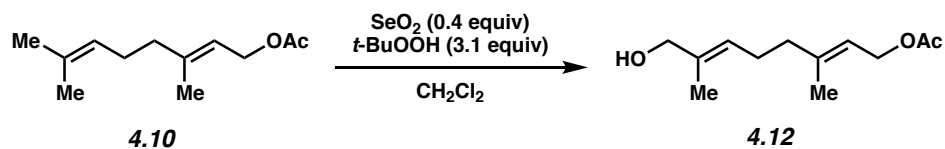
## 4.6 Experimental Section

### 4.6.1 Materials and Methods

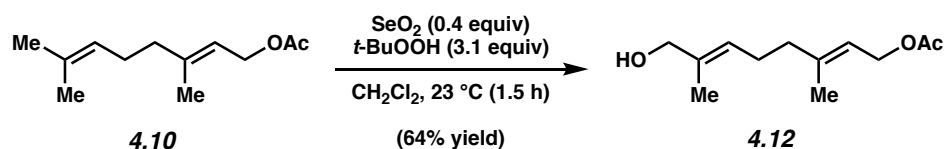
Unless stated otherwise, reactions were conducted in flame-dried glassware under an atmosphere of nitrogen using anhydrous solvents (either freshly distilled or passed through activated alumina columns). All commercially obtained reagents were used as received unless otherwise specified. Geranyl acetate (**4.10**) and potassium carbonate were purchased from Alfa Aesar. Selenium dioxide and *tert*-butyl hydroperoxide solution (~5.5 M in decane, over 4Å molecular sieves) were obtained from Sigma Aldrich. Reaction temperatures were controlled using an IKAmag temperature modulator, and unless stated otherwise, reactions were performed at 23 °C. Thin-layer chromatography (TLC) was conducted with EMD gel 60 F254 pre-coated plates (0.25 mm) and visualized using anisaldehyde staining. Silicycle Siliaflash P60 (particle size 0.040–0.063 mm) was used for flash column chromatography. <sup>1</sup>H-NMR spectra were recorded on Bruker spectrometers (at 500 MHz) and are reported relative to the residual solvent signal. Data for <sup>1</sup>H-NMR spectra are reported as follows: chemical shift ( $\delta$  ppm), multiplicity, coupling constant (Hz) and integration. <sup>13</sup>C-NMR spectra were recorded on Bruker spectrometers (at 125 MHz) and are reported relative to the residual solvent signal. Data for <sup>13</sup>C-NMR spectra are reported in terms of chemical shift. IR spectra were obtained on a Perkin-Elmer UATR Two FT-IR spectrometer and are reported in terms of frequency of absorption ( $\text{cm}^{-1}$ ). DART-MS spectra were collected on a Thermo Exactive Plus MSD (Thermo Scientific) equipped with an ID-CUBE ion source and a Vapor Interface (IonSense Inc.). Both the source and MSD were controlled by Excalibur software v. 3.0. The analyte was spotted onto OpenSpot sampling cards (IonSense Inc.) using CH<sub>2</sub>Cl<sub>2</sub> as the solvent. Ionization was accomplished using UHP He (Airgas Inc.) plasma with no additional

ionization agents. The mass calibration was carried out using Pierce LTQ Velos ESI (+) and (-) Ion calibration solutions (Thermo Fisher Scientific).

#### 4.6.2 Experimental Procedures



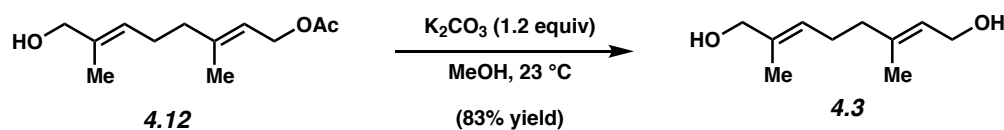
**Representative Procedure for Optimization of Oxidation (Table 4.1, entry 3 is used as an example).** To a flame-dried 10-mL round bottom flask equipped with a magnetic stir bar and selenium dioxide (23.4 mg, 0.20 mmol, 0.4 equiv) under N<sub>2</sub> was added CH<sub>2</sub>Cl<sub>2</sub> (2.5 mL, 0.20 M), *tert*-butyl hydroperoxide (5.5 M in decane, 0.29 mL, 1.58 mmol, 3.1 equiv), and geranyl acetate (4.10, 109 μL, 0.509 mmol, 1.0 equiv). After stirring for 30 min at 23 °C, water (2 mL) and EtOAc (10 mL) were added, and the reaction was transferred to a separatory funnel. The layers were separated and the organic layer was washed successively with deionized water (2 x 5 mL), saturated aqueous NaHCO<sub>3</sub> (1 x 5 mL), deionized water (1 x 5 mL), and brine (1 x 5 mL). The organic layer was dried over MgSO<sub>4</sub>, filtered, and concentrated under reduced pressure. To the resulting crude product, 1,3,5-trimethoxybenzene (28.3 mg, 0.33 equiv) was added as an external standard. The ratio and yields were determined by <sup>1</sup>H NMR analysis.



**8-Hydroxygeranyl acetate (4.12):** To a flame-dried 100-mL round bottom flask equipped with a magnetic stir bar and selenium dioxide (226 mg, 2.04 mmol, 0.4 equiv) under N<sub>2</sub> was added CH<sub>2</sub>Cl<sub>2</sub> (25 mL, 0.20 M), *tert*-butyl hydroperoxide (5.5 M in decane, 2.9 mL, 15.8 mmol, 3.1



equiv), and geranyl acetate (**4.10**, 1.09 mL, 5.09 mmol, 1.0 equiv). After stirring for 1.5 h at 23 °C, the reaction mixture was concentrated under reduced pressure. The crude oil was transferred to a separatory funnel with EtOAc (50 mL). The organic layer was washed successively with deionized water (2 x 20 mL), saturated aqueous NaHCO<sub>3</sub> (1 x 20 mL), deionized water (1 x 10 mL), and brine (1 x 10 mL). The combined aqueous layers were back-extracted with EtOAc (1 x 80 mL). The combined organic layers were dried over Na<sub>2</sub>SO<sub>4</sub>, filtered, and concentrated under reduced pressure. The resulting crude oil was purified via flash chromatography (6:1 → 2:1 hexanes:EtOAc) to afford 8-hydroxygeranyl acetate (**4.12**, 688 mg, 64% yield) as a colorless oil. 8-Hydroxygeranyl acetate (**4.12**): R<sub>f</sub> 0.43 (2:1 hexanes:EtOAc); <sup>1</sup>H NMR (500 MHz, CDCl<sub>3</sub>): δ 5.39–5.31 (m, 2H), 4.58 (d, *J* = 7.1, 2H), 3.99 (s, 2H), 2.17 (dt, *J* = 7.4, 7.4, 2H), 2.11–2.07 (m, 2H), 2.05 (s, 3H), 1.71 (s, 3H), 1.66 (s, 3H); <sup>13</sup>C NMR (125 MHz, CDCl<sub>3</sub>): δ 171.4, 141.9, 135.4, 125.4, 118.8, 69.0, 61.6, 39.2, 25.8, 21.2, 16.5, 13.8; IR (film): 3424, 2919, 2860, 1736, 1671, 1229 cm<sup>-1</sup>; HRMS-APCI (*m/z*) [M + H]<sup>+</sup> calcd for C<sub>12</sub>H<sub>21</sub>O<sub>3</sub><sup>+</sup>, 213.1485; found, 213.1478. Spectral data match those previously reported.<sup>14</sup>



**8-Hydroxygeraniol (4.3).** A flame-dried 50-mL round bottom flask equipped with a magnetic stir bar was charged with 8-hydroxygeranyl acetate (**4.12**, 633 mg, 2.98 mmol, 1 equiv) and methanol (19 mL, 0.16 M). Potassium carbonate (495 mg, 3.58 mmol, 1.2 equiv) was added in one portion. After stirring at 23 °C for 2.5 h, the solvent was removed under reduced pressure, and the reaction mixture was transferred to a separatory funnel with deionized water (10 mL). The aqueous layer was extracted with diethyl ether (3 x 20 mL). The combined organic layers were washed

successively with 0.5 M aqueous HCl (1 x 10 mL), saturated aqueous NaHCO<sub>3</sub> (1 x 10 mL), brine (1 x 10 mL) and deionized water (1 x 10 mL). Next, the organic layers were dried over MgSO<sub>4</sub>, filtered, and concentrated under reduced pressure. The resulting crude oil was purified via flash chromatography (1:1 hexanes:EtOAc) to afford 8-hydroxygeraniol (**4.3**, 490 mg, 83% yield) as a light yellow oil. 8-Hydroxygeraniol (**4.3**): R<sub>f</sub> 0.18 (1:1 hexanes:EtOAc); <sup>1</sup>H NMR (500 MHz, CDCl<sub>3</sub>): δ 5.41–5.34 (m, 2H), 4.14 (d, *J* = 6.9, 2H), 3.98 (s, 2H), 2.17 (dt, *J* = 7.5, 7.1, 2H), 2.09–2.04 (m, 2H), 1.67 (s, 3H), 1.65 (s, 3H), 1.44 (br s, 2H); <sup>13</sup>C NMR (125 MHz, CDCl<sub>3</sub>): δ 139.1, 135.3, 125.6, 123.9, 68.9, 59.4, 39.1, 25.8, 16.3, 13.8; IR (film): 3307, 2916, 2859, 1669, 999 cm<sup>-1</sup>; HRMS-APCI (*m/z*) [M + H]<sup>+</sup> calcd for C<sub>10</sub>H<sub>19</sub>O<sub>2</sub><sup>+</sup>, 171.1380; found, 171.1375. Spectral data match those previously reported.<sup>14</sup>

## 4.7 Spectra Relevant to Chapter Four:

### Synthesis of 8-Hydroxygeraniol

Francesca M. Ippoliti,<sup>†</sup> Joyann S. Barber,<sup>†</sup> Yi Tang, and Neil K. Garg.

*J. Org. Chem.* **2018**, *83*, 11323–11326.

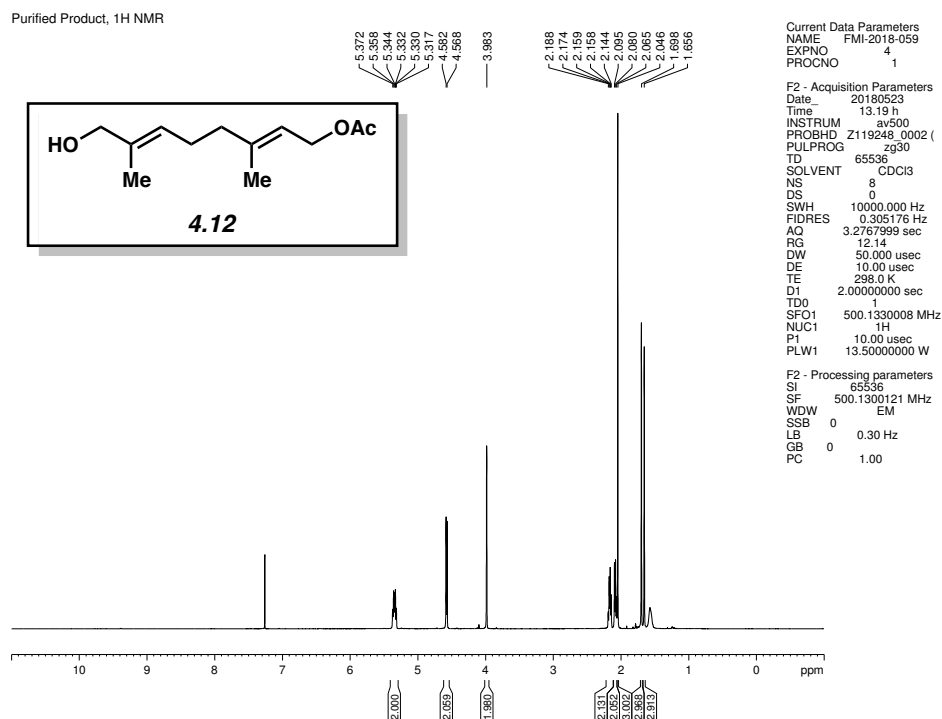


Figure 4.5. <sup>1</sup>H NMR (500 MHz, CDCl<sub>3</sub>) of compound 4.12.

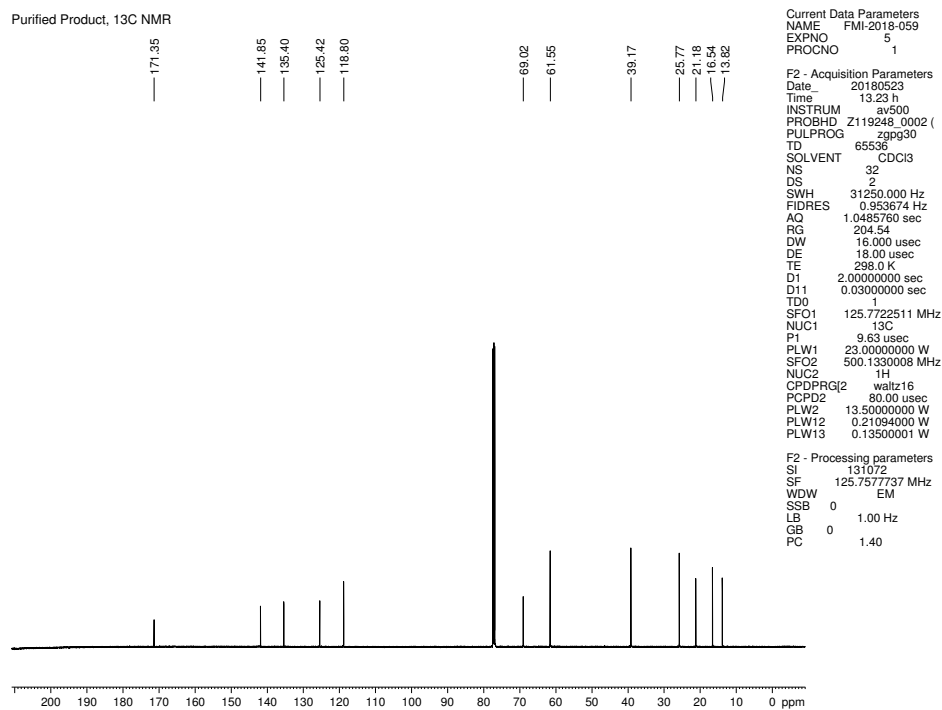


Figure 4.6. <sup>13</sup>C NMR (125 MHz, CDCl<sub>3</sub>) of compound 4.12.

Purified Product, <sup>1</sup>H NMR

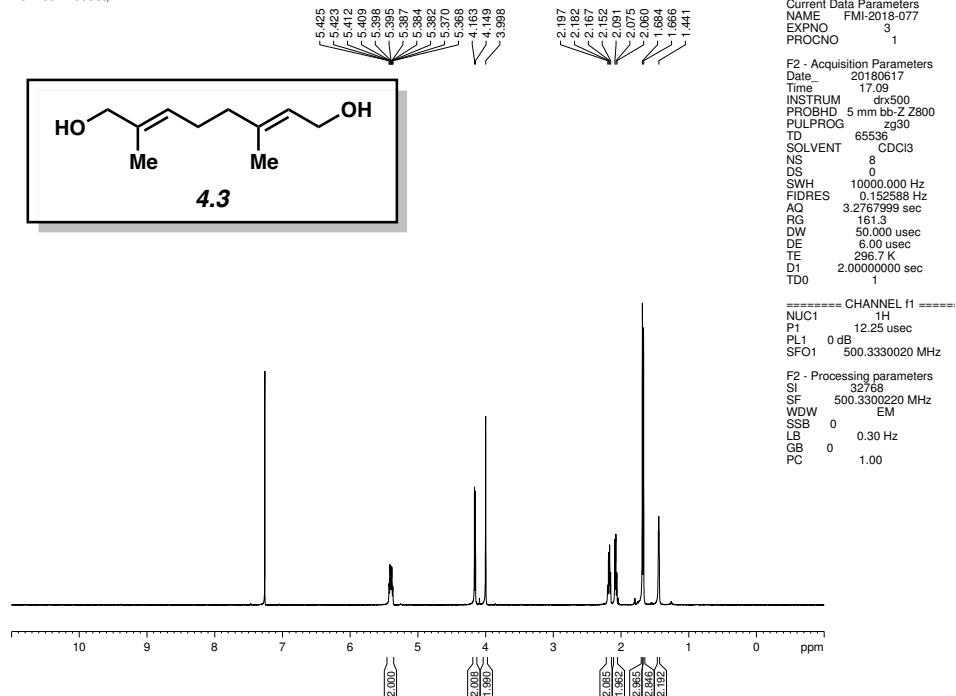


Figure 4.7. <sup>1</sup>H NMR (500 MHz, CDCl<sub>3</sub>) of compound 4.3.

Purified Product, <sup>13</sup>C NMR

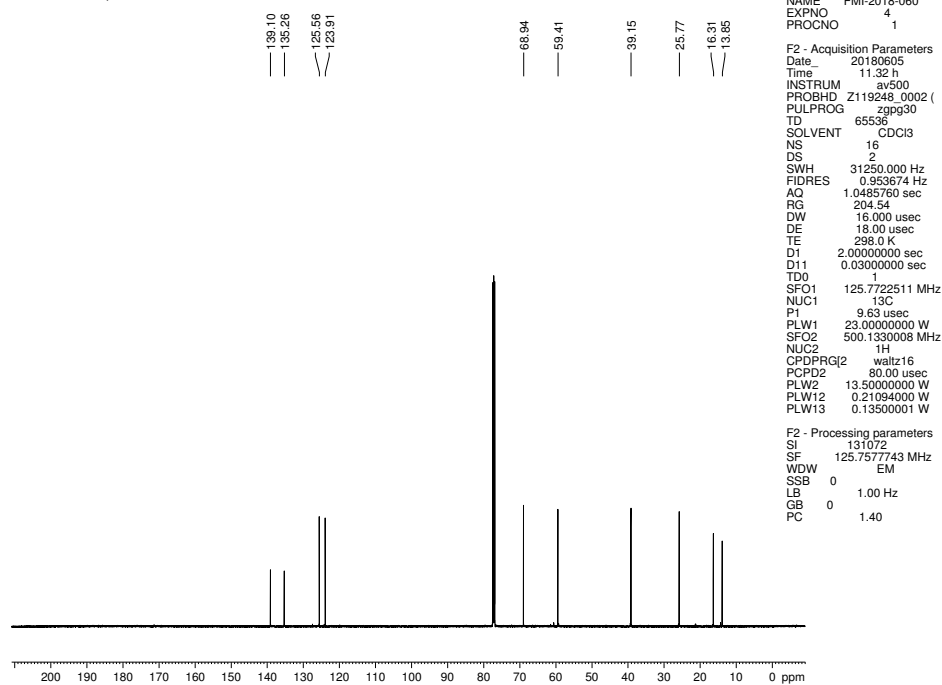


Figure 4.8. <sup>13</sup>C NMR (125 MHz, CDCl<sub>3</sub>) of compound 4.3.

#### 4.8 Notes and References

- (1) O'Connor, S. E.; Maresh, J. J. Chemistry and Biology of Monoterpene Indole Alkaloid Biosynthesis. *Nat. Prod. Rep.* **2006**, *23*, 532–547.
- (2) Pickens, L. B.; Tang, Y.; Chooi, Y.-H. Metabolic Engineering for the Production of Natural Products. *Annu. Rev. Chem. Biomol. Eng.* **2011**, *2*, 211–236.
- (3) O'Connor, S. E. Strategies for Engineering Plant Natural Products: The Iridoid-Derived Monoterpene Indole Alkaloids of *Catharanthus roseus*. In *Methods in Enzymology*; Hopwood, D. A., Ed.; Academic Press: 2012; 515, pp 189–206.
- (4) Pritchett, B. P.; Stoltz, B. M. Enantioselective Palladium-Catalyzed Allylic Alkylation Reactions in the Synthesis of *Aspidosperma* and Structurally Related Monoterpene Indole Alkaloids. *Nat. Prod. Rep.* **2018**, *35*, 559–574.
- (5) Pan, Q.; Mustafa, N. R.; Tang, K.; Choi, Y. H.; Verpoorte, R. Monoterpenoid Indole Alkaloids Biosynthesis and its Regulation in *Catharanthus roseus*: A Literature Review. *Phytochem. Rev.* **2016**, *15*, 221–250.
- (6) Madyastha, K. M.; Meehan, T. D.; Coscia, C. J. Characterization of a Cytochrome P-450 Dependent Monoterpene Hydroxylase from the Higher Plant *Vinca rosea*. *Biochemistry* **1976**, *15*, 1097–1102.
- (7) Ikeda, H.; Esaki, N.; Nakai, S.; Hashimoto, K.; Uesato, S.; Soda, K.; Fujita, T. Acyclic Monoterpene Primary Alcohol: NADP<sup>+</sup> Oxidoreductase of *Rauwolfia serpentina* Cells: The Key Enzyme in Biosynthesis of Monoterpene Alcohols. *J. Biochem.* **1991**, *109*, 341–347.

- (8) Madyastha, K. M.; Guarnaccia, R.; Baxter, C.; Coscia, C. J. *S*-Adenosyl-L-methionine: Loganic Acid Methyltransferase: A Carboxyl-Alkylating Enzyme from *Vinca rosea*. *J. Biol. Chem.* **1973**, *248*, 2497–2501.
- (9) Irmeler, S.; Schröder, G.; St-Pierre, B.; Crouch, N. P.; Hotze, M.; Schmidt, J.; Strack, D.; Matern, U.; Schröder, J. Indole Alkaloid Biosynthesis in *Catharanthus roseus*: New Enzyme Activities and Identification of Cytochrome P450 CYP72A1 as Secologanin Synthase. *Plant J.* **2000**, *24*, 797–804.
- (10) Stöckigt, J.; Zenk, M. H. Isovincoside (Strictosidine), the Key Intermediate in the Enzymatic Formation of Indole Alkaloids. *FEBS Lett.* **1977**, *79*, 233–237.
- (11) Caputi, L.; Franke, J.; Farrow, S. C.; Chung, K.; Payne, R. M. E.; Nguyen, T.-D.; Dang, T.-T. T.; Carqueijeiro, I. S. T.; Koudounas, K.; de Bernonville, T. D.; Ameyaw, B.; Jones, D. M.; Vieira, I. J. C.; Courdavault, V.; O'Connor, S. E. Missing Enzymes in the Biosynthesis of the Anticancer Drug Vinblastine in Madagascar Periwinkle. *Science* **2018**, *360*, 1235–1239.
- (12) Krithika, R.; Srivastava, P. L.; Rani, B.; Kolet, S. P.; Chopade, M.; Soniya, M.; Thulasiram, H. V. Characterization of 10-Hydroxygeraniol Dehydrogenase from *Catharanthus roseus* Reveals Cascaded Enzymatic Activity in Iridoid Biosynthesis. *Sci. Rep.* **2015**, *5*, 8258.
- (13) Campbell, A.; Bauchart, P.; Gold, N. D.; Zhu, Y.; De Luca, V.; Martin, V. J. J. Engineering of a Nepetalactol-Producing Platform Strain of *Saccharomyces cerevisiae* for the Production of Plant Seco-Iridoids. *ACS Synth. Biol.* **2016**, *5*, 405–414.
- (14) Billingsley, J. M.; DeNicola, A. B.; Barber, J. S.; Tang, M.-C.; Horecka, J.; Chu, A.; Garg, N. K.; Tang, Y. Engineering the Biocatalytic Selectivity of Iridoid Production in *Saccharomyces cerevisiae*. *Metab. Eng.* **2017**, *44*, 117–125.

- (15) Brown, S.; Clastre, M.; Courdavault, V.; O'Connor, S. E. De novo Production of the Plant-derived Alkaloid Strictosidine in Yeast. *Proc. Natl. Acad. Sci.* **2015**, *112*, 3205–3210.
- (16) Escher, S.; Loew, P.; Arigoni, D. The Role of Hydroxygeraniol and Hydroxynerol in the Biosynthesis of Loganin and Indole Alkaloids. *Chem. Commun.* **1970**, 823–825.
- (17) Battersby, A. R.; Brown, S. H.; Payne, T. G. Preparation and Isolation of Deoxyloganin: Its Role as Precursor of Loganin and the Indole Alkaloids. *Chem. Commun.* **1970**, 827–828.
- (18) Williams, J. R.; Lin, C. Photocycloaddition of 2,5-Dihydrothiophen *SS*-Dioxides to  $\alpha,\beta$ -Unsaturated Cyclic Anhydrides. Synthesis of 10-Hydroxygeraniol. *J. Chem. Soc. Chem. Commun.* **1981**, 752–753.
- (19) Inouye, H.; Ueda, S.-I.; Uesato, S.-I.; Kobayashi, K. Studies on Monoterpene Glucosides and Related Natural Products. XXXVII. Biosynthesis of the Iridoid Glucosides in *Lamium amplexicaule*, *Deutzia crenata* and *Galium spurium* var. *echinospermon*. *Chem. Pharm. Bull.* **1978**, *26*, 3384–3394.
- (20) Umbreit, M. A.; Sharpless, K. B. Allylic Oxidation of Olefins by Catalytic and Stoichiometric Selenium Dioxide with *tert*-Butyl Hydroperoxide. *J. Am. Chem. Soc.* **1977**, *99*, 5526–5528.
- (21) Bogazkaya, A. M.; von Bühler, C. J.; Kriening, S.; Busch, A.; Seifert, A.; Pleiss, J.; Laschat, S.; Urlacher, V. B. Selective Allylic Hydroxylation of Acyclic Terpenoids by CYP154E1 from *Thermobifida fusca* YX. *Beilstein J. Org. Chem.* **2014**, *10*, 1347–1353.
- (22) Geu-Flores, F.; Sherden, N. H.; Courdavault, V.; Burlat, V.; Glenn, W. S.; Wu, C.; Nims, E.; Cui, Y.; O'Connor, S. E. An Alternative Route to Cyclic Terpenes by Reductive Cyclization in Iridoid Biosynthesis. *Nature* **2012**, *492*, 138–142.



- (23) IUPAC. Nomenclature of Organic Chemistry, Sections A, B, C, D, E, F, and H. Pergamon Press: Oxford, 1979.
- (24) Acyclic Terpenes. In *System of Nomenclature for Terpene Hydrocarbons*; Advances in Chemistry Series; American Chemical Society, 1955; 14, pp. 12–14.
- (25) Swiss Institute of Bioinformatics. ExPASy. ENZYME entry: EC 1.14.14.83. <https://enzyme.expasy.org/EC/1.14.14.83> (accessed June 18, 2018).
- (26) Kyoto University Bioinformatics Center. KEGG. Enzyme 1.14.14.83. [https://www.genome.jp/dbget-bin/www\\_bget?ec:1.14.13.152](https://www.genome.jp/dbget-bin/www_bget?ec:1.14.13.152) (accessed June 18, 2018).

## CHAPTER FIVE

### Cell-Free Total Biosynthesis of Plant Terpene Natural Products using an Orthogonal Cofactor Regeneration System

Undramaa Bat-Erdene,<sup>†</sup> John M. Billingsley,<sup>†</sup> William C. Turner, Benjamin R. Lichman, Francesca M. Ippoliti, Neil K. Garg, Sarah E. O'Connor, and Yi Tang.

*ACS Catal.* **2021**, *11*, 9898–9903.

#### 5.1 Abstract

Here we report the one-pot, cell-free enzymatic synthesis of the plant monoterpene nepetalactol starting from the readily available geraniol. A pair of orthogonal cofactor regeneration systems permitted NAD<sup>+</sup>-dependent geraniol oxidation followed by NADPH-dependent reductive cyclization without isolation of intermediates. The orthogonal cofactor regeneration system maintained a high ratio of NAD<sup>+</sup> to NADH and a low ratio of NADP<sup>+</sup> to NADPH. The overall reaction contains four biosynthetic enzymes, including a soluble P450; and five accessory and cofactor regeneration enzymes. Furthermore, addition of a NAD<sup>+</sup>-dependent dehydrogenase to the one-pot mixture led to ~1 g/L of nepetalactone, the active cat attractant in catnip.

#### 5.2 Introduction

One-pot, cell-free synthesis of complex molecules using purified enzymes is a powerful technology to access natural products that are otherwise difficult to produce.<sup>1</sup> This approach has been named total biosynthesis<sup>2</sup> or synthetic biochemistry.<sup>3</sup> Compared to synthetic chemistry approaches, “cell-free” biosynthesis exploits the precise regio- and stereoselectivities of enzymes to perform chemical transformations of unprotected substrates under mild reaction conditions.

Cell-free biosynthesis platforms can also outperform microbial *in vivo* biosynthesis by eliminating competing metabolic pathways to overcome potential toxicity.<sup>4,5</sup> Moreover, cell-free bioproduction benefits from modular and flexible pathway implementation, rapid design-build-test-learn cycles, and can approach theoretical conversion.<sup>6,7</sup> Notwithstanding the increasing number of examples of cell-free biosynthesis, a number of challenges exist which limit the utility. In particular, efficient and orthogonal cofactor supply and regeneration is an ever-present obstacle, especially for more complex pathways in which multiple (redox) cofactors are involved. Numerous approaches have been developed to address this obstacle, including reengineering of enzyme cofactor specificity,<sup>8</sup> use of chemically orthogonal unnatural cofactors<sup>9,10</sup> and in an impressive demonstration, the use of a molecular rheostat and synthetic purge valve to manage excess cofactor buildup.<sup>11,12</sup>

Indeed, balancing cofactor usage is especially important in systems where both reductive and oxidative reactions are involved. When the biosynthetic pathway uses a single type of cofactor, such as NAD(H) or NADP(H), concomitant oxidation of reducing equivalents upon substrate reduction serves to regenerate oxidizing equivalents, and vice versa. During active metabolism, however, estimated ratios of NAD<sup>+</sup>:NADH range from 200:1 to 600:1,<sup>13</sup> whereas estimated ratios of NADP<sup>+</sup>:NADPH range from 1:30 to 1:200.<sup>13</sup> Thus, many biosynthetic pathway enzymes have evolved to use different types of cofactors. Indeed, natural product biosynthetic logic frequently employ both NAD<sup>+</sup>-dependent oxidation and NADPH-dependent reduction steps.<sup>14,15,16,17</sup> Without an orthogonal cofactor regeneration system, combining all the enzymes in one pot will lead to futile redox cycles. Therefore, to achieve one-pot reconstitution of such pathways, it is essential to eliminate crosstalk when regenerating both cofactors. The situation is more complex when the thermodynamic equilibrium requires high concentrations of the correct cofactor which is true for

many of the NAD(P)H-dependent oxidoreductases.<sup>18</sup> Since the enzymes rely on a high ratio of the correct cofactor i.e.,  $\text{NAD}^+:\text{NADH}$  or  $\text{NADPH}:\text{NADP}^+$ , maintaining an optimal ratio is key to drive the reaction to completion. In this study, we addressed the requirement of an orthogonal cofactor regeneration system to accomplish the one-pot cell-free synthesis of *cis-trans* nepetalactol (5.1, Figure 5.1).

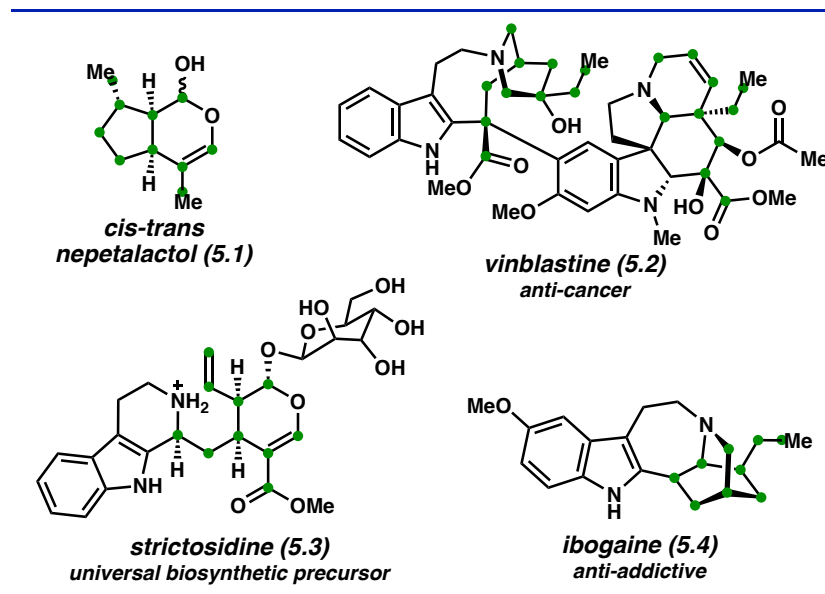


**Figure 5.1.** *Cis-trans* nepetalactol (5.1) serves as the ten-carbon terpene core of strictosidine (5.3), the biosynthetic precursor to vinblastine (5.2), ibogaine (5.4), and ~3,000 additional monoterpene indole alkaloids.

### 5.3 Results and Discussion

Biosynthesis of *cis-trans* nepetalactol (5.1, also referred to hereafter as “nepetalactol”) from geraniol (5.5) requires  $\text{NAD}^+$ -dependent oxidation and NADPH-dependent reductive cyclization (Figure 5.2). Geranyl pyrophosphate (GPP) is hydrolyzed by geraniol synthase to give geraniol (5.5).<sup>19</sup> Regiospecific hydroxylation of one of the terminal methyl groups by the P450 geraniol-8-hydroxylase (G8H) provides 8-hydroxygeraniol (5.6).<sup>20</sup> Next, tandem and reversible

NAD<sup>+</sup>-dependent oxidation of **5.6** by geraniol oxidoreductase (GOR) generates the dialdehyde 8-oxogeranial (**5.9**) (via either 8-hydroxygeranial (**5.7**) or 8-oxogeraniol (**5.8**).<sup>21</sup> Stereoselective reduction of **5.9** using NADPH to an enol intermediate by iridoid synthase (ISY), followed by enzyme-assisted cyclization by a major latex protein-like enzyme (MLPL) result in **5.1**.<sup>22,23</sup> **5.9** can spontaneously form ring-opened iridodials **5.12**, which can also be derived through the ring opening of **5.1**, albeit at a slow rate.<sup>24</sup> Dehydrogenation of **5.1** by nepetalactol-related short-chain reductase/dehydrogenase 1 (NEPS1) forms nepetalactone (**5.11**), which is a potent insect repellent and the active cat-attractant in catnip.<sup>25</sup> Nepetalactol (**5.1**) can be further modified into strictosidine (**5.3**), precursor to >3,000 members of the monoterpene indole alkaloid family (Figure 5.1). Establishing cost-effective routes to nepetalactol (**5.1**) and its derivatives is therefore an objective for both synthetic chemists and synthetic biologists.

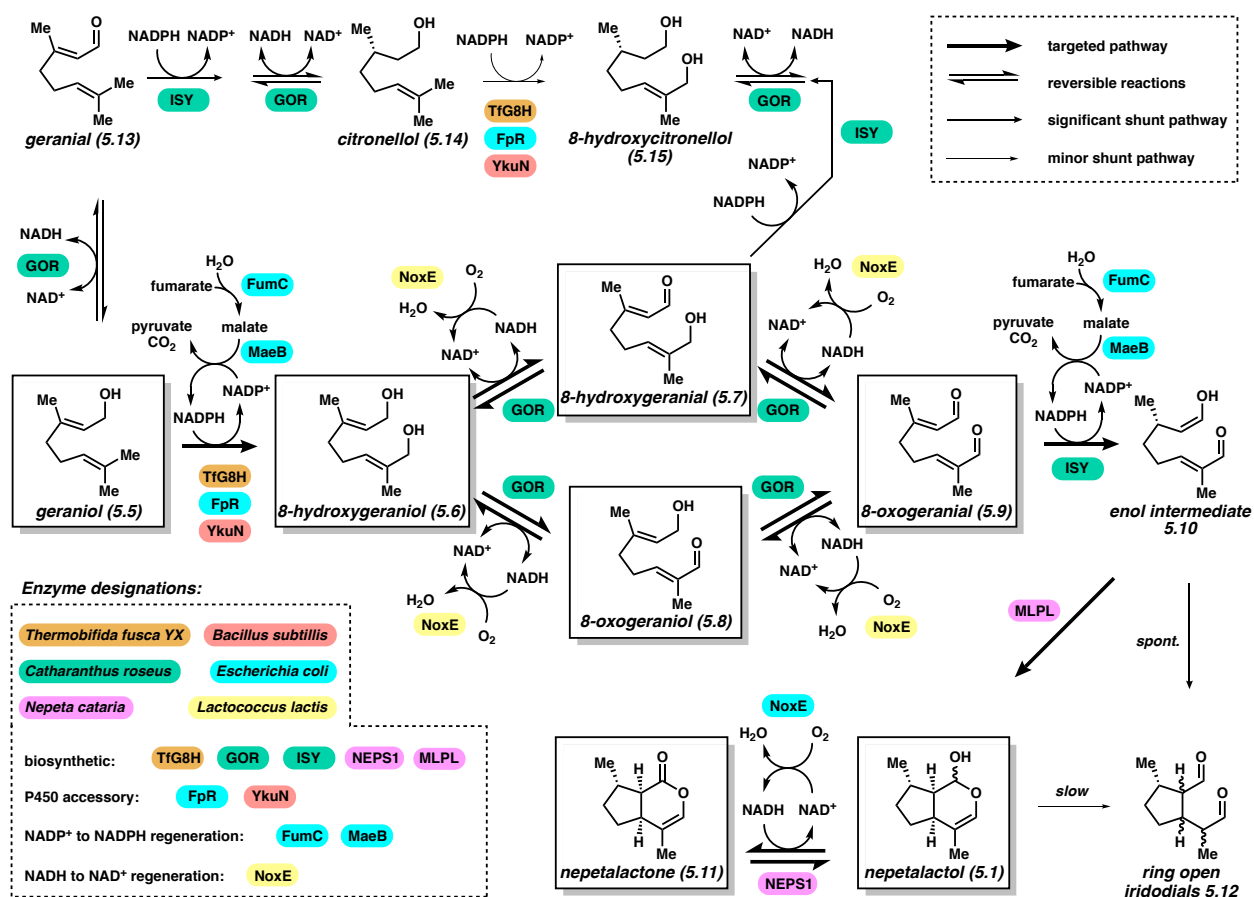


**Figure 5.2.** Biosynthesis of nepetalactol (5.1) and nepetalactone (5.11) along with possible shunt products. On pathway intermediates are boxed. Cofactor regeneration enzymes are only shown for main pathway reactions.

Initial efforts to recapitulate nepetalactol (5.1) production using cell-free biosynthesis were prompted by the expensive cost from commercial vendors, the low titers observed in microbial hosts,<sup>26,27,28,29</sup> and difficulties in implementing synthetic routes.<sup>30,31,32,33,34,35</sup> Reported syntheses suffer from low yields and enantioselectivities; or rely on the costly synthon (-)-citronellol as an enantiopure starting material.<sup>30–35</sup> To perform cell-free biosynthesis, geraniol (5.5) was selected as the starting material because of its high abundance as an essential oil and low cost. Since the plant homologues of G8H are membrane-bound and not suitable for *in vitro* biocatalysis, a functionally

equivalent, soluble bacterial P450 was used. CYP154E1 (TfG8H) from *Thermobifida fusca* YX was reported to perform the same hydroxylation as G8H and can be reductively regenerated by the NADPH-dependent cytochrome P450 flavodoxin/ferredoxin reductase (FpR from *Escherichia coli*) and flavodoxin (YkuN) from *Bacillus subtilis*.<sup>36,37</sup> Using TfG8H, FpR and YkuN, we were able to observe hydroxylation of **5.5** to 8-hydroxygeraniol (**5.6**).<sup>38</sup> We next confirmed the oxidation of **5.6** to 8-hydroxygeranial (**5.7**), 8-oxogeraniol (**5.8**) and 8-oxogeranial (**5.9**) when combined with GOR and excess NAD<sup>+</sup>.<sup>38</sup> The reaction was observed to reach an equilibrium between these four compounds due to depletion of cofactor and reaction reversibility. Upon incubation of **5.9** (330 mg/L) together with ISY and MLPL, nepetalactol (**5.1**) was almost exclusively formed using excess NADPH, with a small amount of ring-opened iridodials **5.12** being detected. ISY could utilize both NADPH and NADH as reducing cofactors, albeit showing strong preference for NADPH.

Despite demonstration of competent *in vitro* activities of the individual enzymes, one-pot synthesis of **5.1** from **5.5** as shown in Figure 5.2 using sub-stoichiometric amounts of cofactors is challenging. First, an orthogonal cofactor regeneration system is required to regenerate NAD<sup>+</sup> from NADH (for the GOR oxidation step), while not oxidizing NADPH, which is required for TfG8H and ISY turnover. Similarly, the cofactor regeneration system must also regenerate NADPH from NADP<sup>+</sup>, while not reducing NAD<sup>+</sup> to NADH. Second, the enzyme activities of the regeneration systems must be carefully tuned to match the differential reactivities TfG8H, GOR and ISY. The oxidation of **5.6** to **5.9** is stepwise and readily reversible, and thus can accumulate mono-aldehyde intermediates **5.7** and **5.8** (Figure 5.2). With **5.7**, ene-reduction catalyzed by ISY followed by aldehyde reduction catalyzed by GOR can give irrecoverable shunt products such as 8-

hydroxycitronellol **5.15**. Hence, the ratio of  $\text{NAD}^+$  to NADH available for GOR oxidation must be well-controlled.

For the oxidizing enzyme that can selectively oxidize NADH instead of NADPH, we use the NADH-oxidase (NoxE) from *Lactococcus lactis*.<sup>38,39</sup> When coupled, 10  $\mu\text{M}$  GOR and 5  $\mu\text{M}$  NoxE were able to fully convert 340 mg/L **5.6** to **5.9** in the presence of limiting 100  $\mu\text{M}$   $\text{NAD}^+$  within 1 hour.<sup>38</sup> In contrast, a cost-effective NADPH regeneration system that does not reduce  $\text{NAD}^+$  was not readily available. The conventional glucose-6-phosphate (G6P) dehydrogenase or glyceraldehyde-3-phosphate (GAP) dehydrogenase, which convert G6P to 6-phospho-D-glucono-1,5-lactone and GAP to 1,3-bisphosphoglycerate, respectively,<sup>40,41</sup> use the expensive substrates G6P and GAP. Other NADPH-regeneration enzymes such as glucose-1-dehydrogenase and isocitrate dehydrogenase were also not suitable due to their non-specific cofactor usage or high substrate cost. Combining the requirements of cofactor orthogonality, ease of enzyme expression and cost effectiveness, we chose a two-enzyme system which consists of fumarate hydratase (FumC) and  $\text{NADP}^+$ -dependent malic enzyme (MaeB) from *Escherichia coli*. MaeB catalyzes the decarboxylation of (*S*)-malate to generate pyruvate in a strictly  $\text{NADP}^+$ -dependent manner.<sup>42</sup> While (*S*)-malate acid is relatively expensive, it can be readily generated from the hydration of the inexpensive fumarate by FumC. In addition to its cofactor selectivity, the decarboxylation reaction catalyzed by MaeB is irreversible and thus drives the coupled reaction forward. Cloning and characterization of MaeB and FumC confirmed that the two-enzyme system displayed excellent selectivity towards  $\text{NADP}^+$  over  $\text{NAD}^+$  in the presence of fumarate.<sup>38</sup> To test this system in catalysis, we performed the coupled reaction of TfG8H/FpR/YkuN and FumC/MaeB with limiting concentrations of NADPH. Full conversion of 310 mg/L (2 mM) geraniol (**5.5**) to 8-hydroxygeraniol (**5.6**) with 5  $\mu\text{M}$  TfG8H, 10  $\mu\text{M}$  FpR, 10  $\mu\text{M}$  YkuN, 1  $\mu\text{M}$  FumC, 10  $\mu\text{M}$  MaeB



and 100  $\mu\text{M}$  NADPH was observed within 1.5 hours.<sup>38</sup> This full conversion establishes a robust *in vitro* P450 biocatalytic reaction, which typically requires excess NADPH due to suboptimal electron transfer between the P450 and its partner enzymes.<sup>43</sup> The FumC/MaeB regeneration system was also fully compatible with ISY and MLPL and supported the full conversion of 330 mg/L (2 mM) **5.9** to nepetalactol (**5.1**) in the presence of 0.5  $\mu\text{M}$  ISY, 5  $\mu\text{M}$  MLPL, 1  $\mu\text{M}$  FumC, 10  $\mu\text{M}$  MaeB and 100  $\mu\text{M}$  NADPH.<sup>38</sup> Neither TfG8H- nor ISY-catalyzed reaction was inhibited by the accumulated pyruvate.<sup>38</sup>

With an orthogonal cofactor regeneration system in hand, a one-pot enzymatic synthesis of nepetalactol (**5.1**) was attempted using all purified enzymes. As expected from the substrate promiscuity of ISY and GOR (Figure 5.2), incubation of all nine enzymes along with 310 mg/L **5.5** led to a number of shunt products. Although **5.9** was produced (15% yield), a considerable amount of citronellol (**5.14**) and 8-hydroxycitronellol (**5.15**) were formed (Figure 5.2).<sup>38</sup> Alcohol **5.14** is formed when **5.5** is oxidized to geranial (**5.13**) by GOR, which then undergoes eneduction by ISY, followed by a GOR-catalyzed reduction (Figure 5.2). To reduce the formation of **5.14** which is an irrecoverable shunt product, we used a multi-step, one-pot approach in which ISY was added after G8H and GOR reactions were completed. A 200  $\mu\text{L}$ -scale, two-step approach was successful in producing a higher amount of nepetalactol (**5.1**, 65% yield).<sup>38</sup> However, the formation of shunt products remained and was particularly problematic in a larger scale reaction (10 mL).<sup>38</sup> We hypothesized formation of **5.14** is due to low G8H hydroxylation activity caused by oxygen transport deficiency in the reaction vessel, which led to the  $\text{O}_2$ -independent GOR oxidation and subsequent conversion to **5.14**.<sup>22, 23, 44</sup> When the agitation rate was raised from 250 rpm to 300 rpm, aggregation and precipitation of enzymes were observed.

To eliminate the formation of **5.14** and **5.15** as major shunt products, a one-pot drop-in strategy was pursued, where the biosynthetic enzymes were added sequentially after the upstream reaction was completed. As an initial test, 310 mg/L **1** was incubated with TfG8H, FpR, YkuN, FumC, MaeB along with 100  $\mu$ M NADPH and 6 mM fumarate for 2 hours. Upon full conversion of **5.5** to **5.6**, GOR, NoxE and 100  $\mu$ M NAD<sup>+</sup> were added directly to the mixture, which was incubated for 2 additional hours. Finally, ISY, MLPL and 6 mM fumarate were added and reacted for 2 hours. This scheme fully converted 3.1 mg geraniol (**5.5**) to nepetalactol (**5.1**) in a 10 mL reaction mixture,<sup>38</sup> forming >3 mg nepetalactol (**5.1**) in the reaction (>95% conversion). We then increased the amount of substrate added to the reaction through the addition of multiple aliquots of **5.5** (Figure 5.3A). The G8H reaction was supplemented with an additional 310 mg/L geraniol (**5.5**) and 6 mM fumarate every 1.5 hours, and substrate hydroxylation was monitored (Figure 5.3A, trace i-iv). Our NADPH-regeneration system supported hydroxylation of a combined 930 mg/L of **5.5** to **5.6** within 4.5 hours. Subsequent addition of GOR and reaction for two hours led to complete conversion of **5.6** to **5.7**, **5.8**, and **5.9**, and only very minor amounts of **5.13** (Figure 5.3A, trace v). Finally, addition of ISY and MLPL resulted in the formation of 940 mg/L of nepetalactol (**5.1**) (93% yield) in two additional hours (Figure 5.3A, trace vi). Overall, this one-pot mixture operating at the 10 mL scale produced ~1 g/L of **5.1** after 8.5 hours (Figure 5.3A, trace vi).

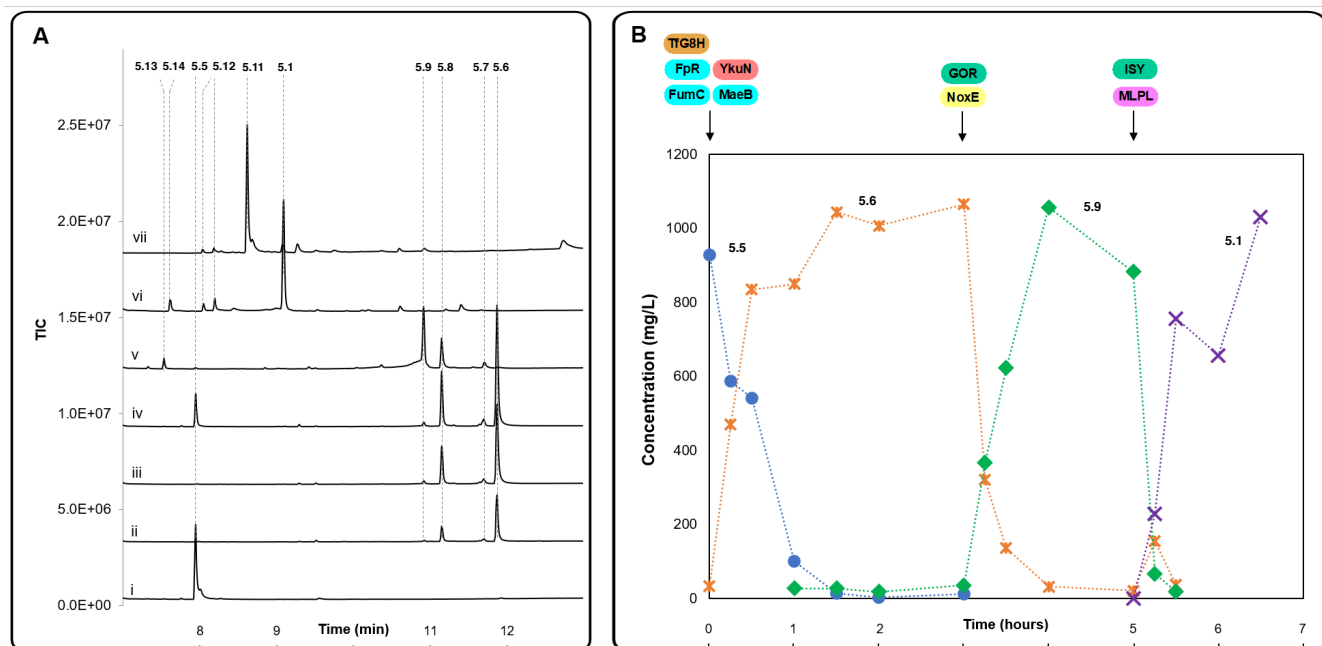


**Figure 5.3.** One pot enzymatic synthesis of nepetalactol (**5.1**) and nepetalactone (**5.11**) using an orthogonal cofactor regeneration system. **(A)** GC-MS chromatograms for 10 mL-scale one-pot conversion of 6 mM geraniol (**5.5**) to nepetalactol (**5.1**) and nepetalactone (**5.11**). Final reaction contained 925.5 mg/L geraniol (**5.5**), 5  $\mu$ M TfG8H, 10  $\mu$ M FpR, 10  $\mu$ M YkuN, 10  $\mu$ M GOR, 0.5  $\mu$ M ISY, 5  $\mu$ M MLPL, 1  $\mu$ M FumC, 10  $\mu$ M MaeB, 100  $\mu$ M NADPH, 100  $\mu$ M NAD<sup>+</sup> and 18 mM fumarate in BTP buffer (pH 9.0) unless otherwise specified. (i) starting material, 2 mM **5.5**, (ii) 1.5-hour reaction with TfG8H, (iii) additional 1.5-hour reaction with TfG8H and an additional aliquot of 2 mM **5.5** added, (iv) additional 1.5-hour reaction with TfG8H and an additional aliquot of 2 mM **5.5** added, (v) 2-hour reaction after GOR was added to (iv), (vi) 2-hour reaction after ISY and MLPL were added to (v), (vii) 2-hour reaction after ISY/MLPL and NEPS1 were added to (v). Peak identities were deduced from GC-MS and by comparison to authentic standards (see Supporting Information). **(B)** Substrate (**5.5**, blue circle) and products' (**5.6**, orange star; **5.9**, green diamond; **5.1**, purple cross) concentrations measured over time, with

timing of added enzymes indicated with arrows atop. The reaction condition is as specified above with starting **5.5** concentration of 957 mg/L (6.2 mM).

Encouraged by this result in Figure 5.3A, we performed the 10 mL reaction with starting batch concentration of **5.5** at 957 mg/L (6.2 mM) (Figure 5.3B),<sup>38</sup> with no additional aliquots. The concentrations of **5.5**, **5.6**, **5.9** and **5.1** were measured and plotted as a function of time in Figure 5.3B. GOR and NoxE was added after three hours when all of **5.5** were converted to **5.6**; while ISY and MLPL were added after five hours when all of **5.6** were converted to **5.9**. After two additional hours, all of the **5.9** were converted to **5.1** with a final concentration of ~ 1 g/L.

To probe the compatibility of the one-pot reaction with downstream biosynthetic enzymes that act on **5.1**, the nepetalactol-related short-chain reductase/dehydrogenase (NEPS1) was introduced to form **5.11**. Since NEPS1 utilizes NAD<sup>+</sup> to convert nepetalactol (**5.1**) to nepetalactone (**5.11**), it was added to the reaction mixture at the same time as ISY and MLPL without any additional cofactors or coenzymes. The near complete conversion of **5.5** to **5.11** (930 mg/L) was observed after 8.5 hours (Figure 5.3A, trace vii).<sup>38</sup> Production of nepetalactone (**5.1**) by recycling sub-stoichiometric concentrations of each nicotinamide cofactor corresponds to 180- and 120-fold decreases in the required molar loading of NAD<sup>+</sup> and NADPH, respectively.

## 5.4 Conclusion

In summary, we report the production of nearly 1 g/L nepetalactol (**5.1**) or nepetalactone (**5.11**) from geraniol (**5.5**) through the use of a pair of orthogonal cofactor regeneration enzymes. The reaction requires up to five biosynthetic and five auxiliary enzymes and can be operated in a one-pot fashion. Our results highlight a major advantage permitted by cell-free systems – the precise temporal control of enzymatic action which is difficult to program via metabolic engineering.<sup>45,46,47,48</sup> Future protein engineering efforts aimed at lowering ISY promiscuity, or implementing shunt metabolite rescue,<sup>49</sup> could further simplify the reaction sequence. Our system produces nepetalactol (**5.1**) at a titer ~130-fold greater than the highest reported in a microbial platform.<sup>28</sup> Depending on the estimated cost of protein,<sup>38</sup> our total material cost ranges from 60 USD to 120 USD to generate 1 g of **5.1**, which is significantly lower than current commercial sources. Our platform establishes a cost-effective method to produce **5.1**, which is useful in the biosynthetic investigation and synthesis of the monoterpene indole alkaloid natural products.

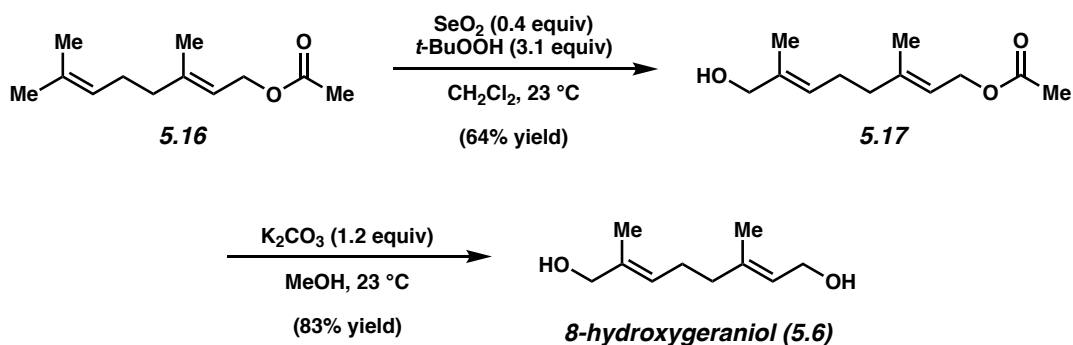
## 5.5 Experimental Section

### 5.5.1 Materials and Methods

Unless stated otherwise, reactions were conducted in flame-dried glassware under an atmosphere of nitrogen using anhydrous solvents (passed through activated alumina columns). All commercially obtained reagents were used as received. Geranyl acetate (**5.16**) and potassium carbonate were purchased from Alfa Aesar. Selenium dioxide and *tert*-Butyl hydroperoxide solution (~5.5 M in decane, over 4Å molecular sieves) were obtained from Sigma Aldrich. Dess-Martin periodinane (DMP) was purchased from Combi-Blocks. Reaction temperatures were controlled using an IKAmag temperature modulator, and unless stated otherwise, reactions were performed at 23 °C. Thin-layer chromatography (TLC) was conducted with EMD gel 60 F254 pre-coated plates (0.25 mm) and visualized using anisaldehyde staining. Silicycle Siliaflash P60 (particle size 0.040–0.063 mm) was used for flash column chromatography.

### 5.5.2 Experimental Procedures

#### 5.5.2.1 Synthesis of 8-Hydroxygeraniol (**5.6**)

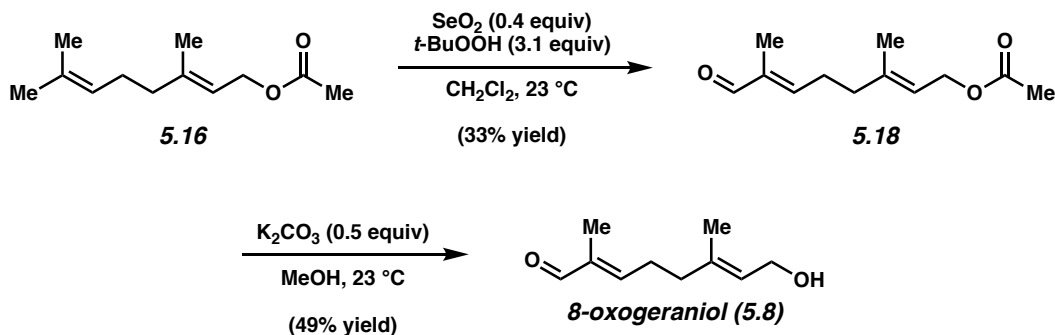


**8-Hydroxygeranyl acetate (5.17):** To a flame-dried 100-mL round bottom flask equipped with a magnetic stir bar and selenium dioxide (226 mg, 2.04 mmol, 0.400 equiv) under  $\text{N}_2$  was added  $\text{CH}_2\text{Cl}_2$  (25 mL, 0.20 M), *tert*-butyl hydroperoxide (5.5 M in decane, 2.9 mL, 16 mmol, 3.1 equiv), and geranyl acetate (**5.16**, 1.09 mL, 5.09 mmol, 1.00 equiv). After stirring for 1.5 h at 23 °C, the

reaction mixture was concentrated under reduced pressure. The crude oil was transferred to a separatory funnel with EtOAc (50 mL). The organic layer was washed successively with deionized water (2 x 20 mL), saturated aqueous NaHCO<sub>3</sub> (1 x 20 mL), deionized water (1 x 10 mL), and brine (1 x 10 mL). The combined aqueous layers were extracted with EtOAc (1 x 80 mL). The combined organic layers were dried over Na<sub>2</sub>SO<sub>4</sub>, filtered, and concentrated under reduced pressure. The resulting crude oil was purified via flash chromatography (6:1 → 2:1 hexanes:EtOAc) to afford 8-hydroxygeranyl acetate (**5.17**, 688 mg, 64% yield) as a colorless oil. <sup>1</sup>H-NMR spectral data match those previously reported.<sup>50</sup>

**8-Hydroxygeraniol (5.6):** A flame-dried 50-mL round bottom flask equipped with a magnetic stir bar was charged with 8-hydroxygeranyl acetate (**5.17**, 633 mg, 2.98 mmol, 1.00 equiv) and methanol (19 mL, 0.16 M). Potassium carbonate (495 mg, 3.58 mmol, 1.20 equiv) was added in one portion. After stirring at 23 °C for 2.5 h, the solvent was removed under reduced pressure, and the reaction mixture was transferred to a separatory funnel with deionized water (10 mL). The aqueous layer was extracted with diethyl ether (3 x 20 mL). The combined organic layers were washed successively with 0.5 M aqueous HCl (1 x 10 mL), saturated aqueous NaHCO<sub>3</sub> (1 x 10 mL), brine (1 x 10 mL) and deionized water (1 x 10 mL). Next, the organic layers were dried over MgSO<sub>4</sub>, filtered, and concentrated under reduced pressure. The resulting crude oil was purified via flash chromatography (1:1 hexanes:EtOAc) to afford 8-hydroxygeraniol (**5.6**, 490 mg, 83% yield) as a light yellow oil. <sup>1</sup>H-NMR spectral data match those previously reported.<sup>50</sup>

### 5.5.2.2 Synthesis of 8-Oxogeraniol (5.8)



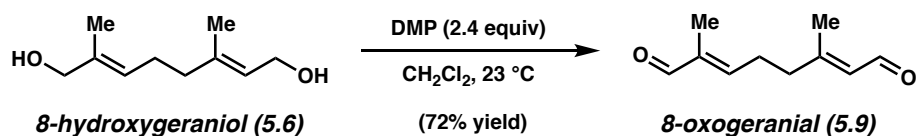
**8-Oxogeranyl acetate (5.18):** A 500 mL round bottom flask was equipped with a magnetic stir bar and flame-dried then cooled under N<sub>2</sub>. Selenium dioxide (1.36 g, 12.2 mmol, 0.400 equiv), CH<sub>2</sub>Cl<sub>2</sub> (150 mL, 0.20 M), *tert*-butyl hydroperoxide (5.5 M in decane, 17 mL, 95 mmol, 3.1 equiv), and geranyl acetate (**5.16**, 6.55 mL, 30.6 mmol, 1.00 equiv) were added to the flask. After stirring for 21 h at 23 °C, the reaction mixture was concentrated to an oil under reduced pressure. To the crude oil, EtOAc (100 mL) was added and the reaction was transferred to a separatory funnel. The organic layer was washed successively with deionized water (2 x 20 mL), saturated aqueous NaHCO<sub>3</sub> (1 x 20 mL), deionized water (1 x 20 mL), and brine (1 x 20 mL). The combined aqueous layers were extracted with EtOAc (100 mL). The combined organic layers were dried over MgSO<sub>4</sub>, filtered, and concentrated under reduced pressure. The crude oil was purified via flash chromatography (6:1 hexanes:EtOAc) to afford 8-oxogeranyl acetate (**5.18**, 2.14 g, 33% yield) as a colorless oil. <sup>1</sup>H-NMR spectral data match those previously reported.<sup>51</sup>

**8-Oxogeraniol (5.8):** To a flame-dried 25 mL round bottom flask charged with a stir bar and cooled under N<sub>2</sub>, 8-oxogeranyl acetate (**5.18**, 309 mg, 1.47 mmol, 1.00 equiv) was dissolved in methanol (9.2 mL, 0.16 M). To the stirring solution was added potassium carbonate (102 mg, 0.736 mmol, 0.500 equiv) and the solution was stirred at 23 °C for 2.5 h. After 2.5 h, the solvent was



removed under reduced pressure, deionized water (10 mL) and diethyl ether (10 mL) were added to the crude oil, and the reaction was transferred to a separatory funnel. The layers were separated and the aqueous layer was extracted with diethyl ether (3 x 10 mL). The combined organic layers were washed with brine (1 x 10 mL). The organic layers were then dried over Na<sub>2</sub>SO<sub>4</sub>, filtered, and concentrated under reduced pressure. The crude oil was purified by flash chromatography (2:1 hexanes:EtOAc) to afford 8-oxogeraniol (**5.8**, 122 mg, 49% yield) as a light yellow oil. <sup>1</sup>H-NMR spectral data match those previously reported.<sup>51</sup>

### 5.5.2.3 Synthesis of 8-Oxogeraniol (**5.9**)



**8-Oxogeraniol (5.9):** To a flame-dried 250 mL round bottom flask equipped with a stir bar and cooled under N<sub>2</sub>, 8-hydroxygeraniol (**5.6**, 1.00 g, 5.87 mmol, 1.00 equiv), DMP (5.98 g, 14.1 mmol, 2.40 equiv), and CH<sub>2</sub>Cl<sub>2</sub> (59 mL, 0.10 M) were added. The flask was purged with N<sub>2</sub> and stirred at 23 °C for 1 h. After 1 h, the reaction was quenched with 1:1:1 sat. aq. NaHCO<sub>3</sub>:sat. aq. Na<sub>2</sub>S<sub>2</sub>O<sub>3</sub>: H<sub>2</sub>O (60 mL) and was transferred to a separatory funnel. The aqueous layer was extracted with CH<sub>2</sub>Cl<sub>2</sub> (3 x 60 mL). The combined organic layers were dried over Mg<sub>2</sub>SO<sub>4</sub>, filtered, and concentrated in vacuo. The crude residue was purified via flash chromatography (4:1 Hex:EtOAc) to afford 8-oxogeraniol (**5.9**, 705 mg, 72% yield) as a light yellow oil. <sup>1</sup>H-NMR spectral data match those previously reported.<sup>51</sup>

### 5.5.3 Synthetic Biology Details

The details for strains and general culture conditions, DNA manipulation and cloning, protein expression and purification, *in vitro* enzymatic reactions, and supplemental tables and figures are reported in the literature.<sup>38</sup>

## 5.6 Notes and References

- (1) Hayashi, Y. Pot Economy and One-Pot Synthesis. *Chem. Sci.* **2016**, *7*, 866–880.
- (2) Roberts, A. A.; Ryan, K. S.; Moore, B. S.; Gulder, T. A. M. Total (Bio)Synthesis: Strategies of Nature and of Chemists. *Top. Curr. Chem.* **2010**, *297*, 149–203.
- (3) Bowie, J. U.; Sherkhanov, S.; Korman, T. P.; Valliere, M. A.; Opgenorth, P. H.; Liu, H. Synthetic Biochemistry: The Bio-Inspired Cell-Free Approach to Commodity Chemical Production. *Trends Biotechnol.* **2020**, *38*, 766–778.
- (4) Korman, T. P.; Opgenorth, P. H.; Bowie, J. U. A Synthetic Biochemistry Platform for Cell Free Production of Monoterpenes from Glucose. *Nat. Commun.* **2017**, *8*, 15526.
- (5) Sherkhanov, S.; Korman, T. P.; Chan, S.; Faham, S.; Liu, H.; Sawaya, M. R.; Hsu, W.-T.; Vikram, E.; Cheng, T.; Bowie, J. U. Isobutanol Production Freed from Biological Limits Using Synthetic Biochemistry. *Nat. Commun.* **2020**, *11*, 4292.
- (6) Claassens, N. J.; Burgener, S.; Vögeli, B.; Erb, T. J.; Bar-Even, A. A Critical Comparison of Cellular and Cell-Free Bioproduction Systems. *Curr. Opin. Biotechnol.* **2019**, *60*, 221–229.
- (7) Dudley, Q. M.; Karim, A. S.; Jewett, M. C. Cell-Free Metabolic Engineering: Biomanufacturing beyond the Cell. *Biotechnol. J.* **2015**, *10*, 69–82.
- (8) Black, W. B.; Zhang, L.; Mak, W. S.; Maxel, S.; Cui, Y.; King, E.; Fong, B.; Sanchez Martinez, A.; Siegel, J. B.; Li, H. Engineering a Nicotinamide Mononucleotide Redox Cofactor System for Biocatalysis. *Nat. Chem. Biol.* **2020**, *16*, 87–94.
- (9) King, E.; Maxel, S.; Li, H. Engineering Natural and Noncanonical Nicotinamide Cofactor-Dependent Enzymes: Design Principles and Technology Development. *Curr. Opin. Biotechnol.* **2020**, *66*, 217–226.

- (10) Richardson, K. N.; Black, W. B.; Li, H. Aldehyde Production in Crude Lysate- and Whole Cell-Based Biotransformation Using a Noncanonical Redox Cofactor System. *ACS Catal.* **2020**, *10*, 8898–8903.
- (11) Opgenorth, P. H.; Korman, T. P.; Iancu, L.; Bowie, J. U. A Molecular Rheostat Maintains ATP Levels to Drive a Synthetic Biochemistry System. *Nat. Chem. Biol.* **2017**, *13*, 938–942.
- (12) Opgenorth, P. H.; Korman, T. P.; Bowie, J. U. A Synthetic Biochemistry Molecular Purge Valve Module That Maintains Redox Balance. *Nat. Commun.* **2014**, *5*, 4113.
- (13) Walsh, C. T.; Tang, Y. *The Chemical Biology of Human Vitamins*; RSC Publishing, 2018.
- (14) Walsh, C. T.; Tang, Y. *Natural Product Biosynthesis: Chemical Logic and Enzymatic Machinery*; RSC Publishing, 2017.
- (15) Tang, M.-C.; Zou, Y.; Watanabe, K.; Walsh, C. T.; Tang, Y. Oxidative Cyclization in Natural Product Biosynthesis. *Chem. Rev.* **2017**, *117*, 5226–5333.
- (16) Morris, J. S.; Caldo, K. M. P.; Liang, S.; Facchini, P. J. PR10/Bet v1-like Proteins as Novel Contributors to Plant Biochemical Diversity. *ChemBioChem* **2021**, *22*, 264–287.
- (17) Lichman, B. R. The Scaffold-Forming Steps of Plant Alkaloid Biosynthesis. *Nat. Prod. Rep.* **2021**, *38*, 103–129.
- (18) Sellés Vidal, L.; Kelly, C. L.; Mordaka, P. M.; Heap, J. T. Review of NAD(P)H-Dependent Oxidoreductases: Properties, Engineering and Application. *Biochim. Biophys. Acta BBA - Proteins Proteomics* **2018**, *1866*, 327–347.
- (19) Brown, S.; Clastre, M.; Courdavault, V.; O'Connor, S. E. De Novo Production of the Plant-Derived Alkaloid Strictosidine in Yeast. *Proc. Natl. Acad. Sci.* **2015**, *112*, 3205–3210.

- (20) Collu, G.; Unver, N.; Peltenburg-Looman, A. M. G.; van der Heijden, R.; Verpoorte, R.; Memelink, J. Geraniol 10-Hydroxylase, a Cytochrome P450 Enzyme Involved in Terpenoid Indole Alkaloid Biosynthesis. *FEBS Lett.* **2001**, *508*, 215–220.
- (21) Miettinen, K.; Dong, L.; Navrot, N.; Schneider, T.; Burlat, V.; Pollier, J.; Woittiez, L.; van der Krol, S.; Lugan, R.; Ilc, T.; Verpoorte, R.; Oksman-Caldentey, K.-M.; Martinoia, E.; Bouwmeester, H.; Goossens, A.; Memelink, J.; Werck-Reichhart, D. The Seco-Iridoid Pathway from *Catharanthus Roseus*. *Nat. Commun.* **2014**, *5*, 3606.
- (22) Geu-Flores, F.; Sherden, N. H.; Courdavault, V.; Burlat, V.; Glenn, W. S.; Wu, C.; Nims, E.; Cui, Y.; O'Connor, S. E. An Alternative Route to Cyclic Terpenes by Reductive Cyclization in Iridoid Biosynthesis. *Nature* **2012**, *492*, 138–142.
- (23) Lichman, B. R.; Godden, G. T.; Hamilton, J. P.; Palmer, L.; Kamileen, M. O.; Zhao, D.; Vaillancourt, B.; Wood, J. C.; Sun, M.; Kinser, T. J.; Henry, L. K.; Rodriguez-Lopez, C.; Dudareva, N.; Soltis, D. E.; Soltis, P. S.; Buell, C. R.; O'Connor, S. E. The Evolutionary Origins of the Cat Attractant Nepetalactone in Catnip. *Sci. Adv.* **2020**, *6*, eaba0721.
- (24) Lindner, S.; Geu-Flores, F.; Bräse, S.; Sherden, N. H.; O'Connor, S. E. Conversion of Substrate Analogs Suggests a Michael Cyclization in Iridoid Biosynthesis. *Chem. Biol.* **2014**, *21*, 1452–1456.
- (25) Lichman, B. R.; Kamileen, M. O.; Titchiner, G. R.; Saalbach, G.; Stevenson, C. E. M.; Lawson, D. M.; O'Connor, S. E. Uncoupled Activation and Cyclization in Catmint Reductive Terpenoid Biosynthesis. *Nat. Chem. Biol.* **2019**, *15*, 71–79.
- (26) Campbell, A.; Bauchart, P.; Gold, N. D.; Zhu, Y.; De Luca, V.; Martin, V. J. J. Engineering of a Nepetalactol-Producing Platform Strain of *Saccharomyces Cerevisiae* for the Production of Plant Seco-Iridoids. *ACS Synth. Biol.* **2016**, *5*, 405–414.

- (27) Billingsley, J. M.; DeNicola, A. B.; Barber, J. S.; Tang, M.-C.; Horecka, J.; Chu, A.; Garg, N. K.; Tang, Y. Engineering the Biocatalytic Selectivity of Iridoid Production in *Saccharomyces Cerevisiae*. *Metab. Eng.* **2017**, *44*, 117–125.
- (28) Yee, D. A.; DeNicola, A. B.; Billingsley, J. M.; Creso, J. G.; Subrahmanyam, V.; Tang, Y. Engineered Mitochondrial Production of Monoterpenes in *Saccharomyces Cerevisiae*. *Metab. Eng.* **2019**, *55*, 76–84.
- (29) Duan, Y.; Liu, J.; Du, Y.; Pei, X.; Li, M. *Aspergillus oryzae* Biosynthetic Platform for *de Novo* Iridoid Production. *J. Agric. Food Chem.* **2021**, *69*, 2501–2511.
- (30) Kouda, R.; Yakushiji, F. Recent Advances in Iridoid Chemistry: Biosynthesis and Chemical Synthesis. *Chem. – Asian J.* **2020**, *15*, 3771–3783.
- (31) Lee, S.; Paek, S.-M.; Yun, H.; Kim, N.-J.; Suh, Y.-G. Enantioselective Total Synthesis of a Natural Iridoid. *Org. Lett.* **2011**, *13*, 3344–3347.
- (32) Sim, J.; Yoon, I.; Yun, H.; An, H.; Suh, Y.-G. Divergent Synthetic Route to New Cyclopenta[*c*]Pyran Iridoids: Syntheses of Jatamanin A, F, G and J, Gastrolactone and Nepetalactone. *Org. Biomol. Chem.* **2016**, *14*, 1244–1251.
- (33) Harnying, W.; Neudörfl, J.-M.; Berkessel, A. Enantiospecific Synthesis of Nepetalactones by One-Step Oxidative NHC Catalysis. *Org. Lett.* **2020**, *22*, 386–390.
- (34) Sakai, K.; Ishiguro, Y.; Funakoshi, K.; Ueno, K.; Suemune, H. A Novel Synthesis of Cis-3,4-Disubstituted Cyclopentanones. *Tetrahedron Lett.* **1984**, *25*, 961–964.
- (35) Suemune, H.; Oda, K.; Saeki, S.; Sakai, K. A New Conversion Method from (–)-Limonene to Nepetalactones. *Chem. Pharm. Bull.* **1988**, *36*, 172–177.

- (36) Bühler, C. von; Le-Huu, P.; Urlacher, V. B. Cluster Screening: An Effective Approach for Probing the Substrate Space of Uncharacterized Cytochrome P450s. *ChemBioChem* **2013**, *14*, 2189–2198.
- (37) Bakkes, P. J.; Riehm, J. L.; Sagadin, T.; Rühlmann, A.; Schubert, P.; Biemann, S.; Girhard, M.; Hutter, M. C.; Bernhardt, R.; Urlacher, V. B. Engineering of Versatile Redox Partner Fusions That Support Monooxygenase Activity of Functionally Diverse Cytochrome P450s. *Sci. Rep.* **2017**, *7*, 9570.
- (38) Supplemental tables and figures are reported in the literature: Bat-Erdene, U.; Billingsley, J. M.; Turner, W. C.; Lichman, B. R.; Ippoliti, F. M.; Garg, N. K.; O'Connor, S. E.; Tang, Y. Cell-Free Total Biosynthesis of Plant Terpene Natural Products Using an Orthogonal Cofactor Regeneration System. *ACS Catal.* **2021**, *11*, 9898–9903.
- (39) Lopez de Felipe, F.; Hugenholtz, J. Purification and Characterisation of the Water Forming NADH-Oxidase from *Lactococcus lactis*. *Int. Dairy J.* **2001**, *11*, 37–44.
- (40) Spaans, S. K.; Weusthuis, R. A.; Van Der Oost, J.; Kengen, S. W. M. NADPH-Generating Systems in Bacteria and Archaea. *Front. Microbiol.* **2015**, *6*, 742.
- (41) Mordhorst, S.; Andexer, J. N. Round, Round We Go – Strategies for Enzymatic Cofactor Regeneration. *Nat. Prod. Rep.* **2020**, *37*, 1316–1333.
- (42) Bologna, F. P.; Andreo, C. S.; Drincovich, M. F. *Escherichia coli* Malic Enzymes: Two Isoforms with Substantial Differences in Kinetic Properties, Metabolic Regulation, and Structure. *J. Bacteriol.* **2007**, *189*, 5937–5946.
- (43) Morlock, L. K.; Böttcher, D.; Bornscheuer, U. T. Simultaneous Detection of NADPH Consumption and H<sub>2</sub>O<sub>2</sub> Production Using the Ampliflu™ Red Assay for Screening of P450 Activities and Uncoupling. *Appl. Microbiol. Biotechnol.* **2018**, *102*, 985–994.

- (44) Lichman, B. R.; Kamileen, M. O.; Titchiner, G. R.; Saalbach, G.; Stevenson, C. E. M.; Lawson, D. M.; O'Connor, S. E. Uncoupled Activation and Cyclization in Catmint Reductive Terpenoid Biosynthesis. *Nat. Chem. Biol.* **2018**, *15*, 71–79.
- (45) Olson, E. J.; Hartsough, L. A.; Landry, B. P.; Shroff, R.; Tabor, J. J. Characterizing Bacterial Gene Circuit Dynamics with Optically Programmed Gene Expression Signals. *Nat. Methods* **2014**, *11*, 449–455.
- (46) Chavez, A.; Scheiman, J.; Vora, S.; Pruitt, B. W.; Tuttle, M.; Iyer, E. P. R.; Lin, S.; Kiani, S.; Guzman, C. D.; Wiegand, D. J.; Ter-Ovanesyan, D.; Braff, J. L.; Davidsohn, N.; Housden, B. E.; Perrimon, N.; Weiss, R.; Aach, J.; Collins, J. J.; Church, G. M. Highly Efficient Cas9-Mediated Transcriptional Programming. *Nat. Methods* **2015**, *12*, 326–328.
- (47) Zalatan, J. G.; Lee, M. E.; Almeida, R.; Gilbert, L. A.; Whitehead, E. H.; La Russa, M.; Tsai, J. C.; Weissman, J. S.; Dueber, J. E.; Qi, L. S.; Lim, W. A. Engineering Complex Synthetic Transcriptional Programs with CRISPR RNA Scaffolds. *Cell* **2015**, *160*, 339–350.
- (48) Lee, Y. J.; Hoynes-O'Connor, A.; Leong, M. C.; Moon, T. S. Programmable Control of Bacterial Gene Expression with the Combined CRISPR and Antisense RNA System. *Nucleic Acids Res.* **2016**, *44*, 2462–2473.
- (49) Schwander, T.; Schada von Borzyskowski, L.; Burgener, S.; Cortina, N. S.; Erb, T. J. A Synthetic Pathway for the Fixation of Carbon Dioxide in Vitro. *Science* **2016**, *354*, 900–904.
- (50) Ippoliti, F. M.; Barber, J. S.; Tang, Y.; Garg, N. K. Synthesis of 8-Hydroxygeraniol. *J. Org. Chem.* **2018**, *83*, 11323–11326.



- (51) Dawson, G. W.; Pickett, J. A.; Smiley, D. W. M. The Aphid Sex Pheromone Cyclopentanoids: Synthesis in the Elucidation of Structure and Biosynthetic Pathways. *Bioorg. Med. Chem.* **1996**, *4*, 351–361.

## CHAPTER SIX

### Gaming Stereochemistry

Francesca M. Ippoliti, Melinda M. Nguyen, Amber J. Reilly, and Neil K. Garg.

*Nat. Rev. Chem.* Accepted Article. DOI: 10.1038/s41570-022-00395-5

#### 6.1 Abstract

R/S Chemistry is a free, game-based learning tool for students to practice stereochemical assignments in an interactive setting, leading to increased student engagement in the topic.

#### 6.2 Introduction

Stereochemistry is an essential concept in introductory organic chemistry courses. Learning the concepts of stereochemistry, however, requires students to visualize the structures of molecules in three dimensions when in textbooks they are typically presented in just two. There is thus a barrier for students new to organic chemistry to understand how molecules are oriented in 3D space.<sup>1,2</sup> The lack of familiarity many students have with this type of visualization makes differentiating between stereoisomers and learning to assign absolute configurations challenging.<sup>3</sup>

Traditionally, students practice stereochemical assignments by working on textbook problems that use molecules with little connection to their everyday lives. Consequently, assigning R and S stereocenters can sometimes be uninteresting. Seeking to increase excitement about stereochemical assignments, we turned to game-based learning. Game-based learning techniques enable students to be more actively engaged than when working through problems

from a textbook.<sup>4</sup> Digital games, in particular, enable instant feedback on problem-solving in a way not possible with traditional homework problems. Games for learning a variety of chemistry concepts have been developed and used in the classroom with success.<sup>5,6,7,8</sup>

To develop an effective game-based tool for practicing stereochemical assignments, we set out the following criteria: 1) the assignment process must be laid out in a clear and stepwise manner, 2) both 2D and 3D modes of molecular structure visualization should be provided, 3) the molecules used as examples must be relevant to the lives of students, and 4) the interface must be both game-like and easy to use. On this basis, we assembled a team comprising ourselves, undergraduate and graduate students,<sup>9</sup> and computing expert Dr Daniel Caspi (Element TwentySix) to create R/S Chemistry: a game-based learning resource where students can practice stereochemical assignment on organic molecules in an interactive environment. R/S Chemistry is available for free and the website works on both computers and smartphones.

### **6.3 User Interface and Features of R/S Chemistry**

R/S Chemistry features a simple and intuitive user interface that is comprised of two modes, 'Learn' and 'Expert'. Within each mode, the user can select between three levels of difficulty. Next, the 2D structure of a molecule commonly found in everyday life (for example, ibuprofen, sucrose) spins onto the screen, with a fact about the molecule's purpose to prime the user for the really fun part: assigning the stereochemistry! In 'Learn' mode, the user assigns priorities to each atom bonded to the stereocenter by dragging the corresponding numbered, colored circles to each atom (Figure 6.1a). The user is not able to continue to the next step until the priorities have been properly assigned. This stepwise approach helps students identify any issues they are having with priority assignments, and still provides the opportunity for 3D

visualization once the priorities are established. To aid the user in visualizing the chemical structure, an interactive 3D molecule is also displayed on the page. After the atoms are numbered by priority, the user must then translate the three highest priority atoms onto a Newman projection using the colored circles (Figure 6.1b). Finally, with the Newman projection complete, the user must identify the stereocenter as either R or S. After an answer is chosen, the user's response is identified as correct or incorrect, and a detailed explanation is displayed (Figure 6.1c). This explanation describes both the reasoning behind the priority ranking of each substituent and why the stereocenter is then assigned as either R or S. 'Expert' mode provides a more streamlined experience for the user, for example, by omitting the Newman projection step and imposing time limitations.

a) **MODE: LEARN** Step 1  
 Drag the numbers to assign priorities

While the opposite enantiomer of thalidomide was prescribed to treat morning sickness, this enantiomer of thalidomide resulted in birth defects.

b) **MODE: LEARN** Step 2  
 Complete the Newman Projection and assign R or S configuration

Hint: drag and drop the 1, 2 and 3, assuming substituent 4 is in the back!

c) **Awesome Job!**  
 Score: 20

- 1 N → Highest atomic number of 7
- 2 C → atomic number of 6 (TIE)  
 This carbon is attached to 1 O and 1 N. Atomic number of O = 8.  
 → Highest priority in the tie-breaker
- 3 C → atomic number of 6 (TIE)  
 This carbon is attached to 1 C and 2 H's. Atomic number of C = 6.  
 → Lowest priority in the tie-breaker
- 4 H → Lowest atomic number of 1

**NEXT MOLECULE**

**Figure 6.1.** The R/S Chemistry user interface. a) Step 1 prompts users to assign substituent priorities around a stereocenter. b) In ‘Learn’ mode, Step 2 displays a Newman projection for the user to help determine stereochemical assignment. c) A detailed explanation of the correct stereochemical assignment is given after the user submits an answer.

Many features of R/S Chemistry render it an effective game-like learning tool. In Step 1 of ‘Learn’ mode, if the user incorrectly ranks the substituents, the colored circles ‘shake’. The ability to move to Step 2 is suspended until the substituents are correctly ranked. This immediate feedback during the process of assigning stereocenters allows the students to learn by trial-and-

error, unlike practicing textbook problems. We used colors in R/S Chemistry both to serve as a visual aid for ranking substituents around the stereocenter and to make the interface more vibrant. The timed feature of the ‘Expert’ mode makes playing R/S Chemistry more test-like, while contributing to its game-like feeling. After exiting the game, the user will also get a score that correlates to encouraging phrases on a pop-up banner with confetti. Additionally, there are three different music options to use while playing R/S Chemistry. All of these features contribute to making R/S Chemistry an engaging, game-like learning resource.

#### **6.4 Feedback from Students**

R/S Chemistry was piloted in an undergraduate organic chemistry lecture course at the University of California, Los Angeles (UCLA), while students were learning about stereochemistry in their course. Of note, this resource is best used as a supplement to traditional stereochemical assignment problems, rather than as a replacement. Surveys completed by over 450 students were overwhelmingly positive. A large majority of the students surveyed found R/S Chemistry fun and engaging (95% either agreed or strongly agreed). In comparison to stereochemistry assignment problems traditionally found in textbooks, 95% of students agreed or strongly agreed that R/S Chemistry was more engaging, and most preferred to learn stereochemistry via R/S Chemistry (86% of students agreed or strongly agreed). 98% agreed or strongly agreed that they would recommend R/S Chemistry to a friend who is learning about stereochemistry.

Students appreciated having a molecular visualization tool built into the R/S Chemistry interface, which is based on the technology we had previously developed for QRChem.net.<sup>10</sup> One student noted, “Viewing molecules in 3D is imperative to understanding stereochemistry. I had a

model set myself, but getting walked through problems step by step while being able to rotate and look at a 3D model on screen was almost more helpful. Also, because the program is free, R/S Chemistry is a great resource for financially struggling students who may not be able to fit a model kit into their budget.” Some students explained that they were motivated to learn stereochemistry because the game was fun and interactive, and they also appreciated the instant feedback given to them, which increased their pace of learning compared to textbook problems.

R/S Chemistry delivers a convenient platform to show students that organic molecules are ubiquitous in the world around us. By contrast to most conventional textbook problems, all of the molecules in R/S Chemistry have descriptions that showcase their relevance to everyday life. Pharmaceuticals (for example, Lipitor), fragrances (for example, limonene), biomolecules (for example, adrenaline), and many others are featured. For example, one entry states: “Thalidomide was a medicine taken by pregnant women to treat morning sickness. Tragically, its racemization in the body resulted in birth defects.” Not only does this description inform the user of the purpose of the molecule, but it also highlights the importance of differentiating enantiomers. Clearly establishing this link between organic molecules and their broader societal impact can promote greater student interest. 81% of students agreed or strongly agreed that the inclusion of molecules of practical relevance helped to increase their engagement.

## **6.5 Global Impact and Conclusion**

R/S Chemistry has been used by students across the globe. According to data collected by Google Analytics, R/S Chemistry has already surpassed 24,000 users in 110 countries to date. Currently, R/S chemistry is most used in the United States, Australia, Germany, and Canada, but it is also used in parts of the world with limited access to the internet, including in Guyana,

Mongolia, and Myanmar. The widespread use of this resource and the results from our survey suggest that students would eagerly welcome and benefit from the development of game-based learning resources. In fact, 98% of students we surveyed either agreed or strongly agreed that they would like to see more educators develop free learning resources that use modern technology. Thus, we hope R/S Chemistry will not only help students learn and practice stereochemical assignments, but will also inspire other chemistry educators to design and develop interactive, globally-accessible, free resources for STEM education.



## 6.6 References

- (1) Wu, H.-K.; Shah, P. Exploring Visuospatial Thinking in Chemistry Learning. *Sci. Educ.* **2004**, *88*, 465–492.
- (2) Tuckey, H.; Selvaratnam, M.; Bradely, J. Identification and Rectification of Student Difficulties Concerning Three-Dimensional Structures, Rotation, and Reflection. *J. Chem. Educ.* **1991**, *68*, 460–464.
- (3) Kuo, M.-T.; Jones, L. L.; Pulos, S. M.; Hyslop, R. M. The Relationship of Molecular Representations, Complexity, and Orientation to the Difficulty of Stereochemistry Problems. *Chem. Educator* **2004**, *9*, 321–327.
- (4) Jan, M.; Gaydos, M. What is Game-Based Learning? Past, Present, and Future. *Educational Technology* **2016**, *56*, 6–11.
- (5) Winter, J. Playing with Chemistry. *Nat. Rev. Chem.* **2018**, *2*, 4–5.
- (6) Smaldone, R. A.; Thompson, C. M.; Evans, M.; Voit, W. Teaching Science through Video Games. *Nat. Chem.* **2017**, *9*, 97–102.
- (7) da Silva Júnior, J. N.; Sousa Lima, M. A.; Xerez Moreira, J. V.; Oliveira Alexandre, F. S.; de Almeida, D. M.; de Oliveira, M. d. C. F.; Melo Leite Junior, A. J. Stereogame: An Interactive Computer Game that Engages Students in Reviewing Stereochemistry Concepts. *J. Chem. Educ.* **2017**, *94*, 248–250.
- (8) Winter, J.; Wentzel, M.; Ahluwalia, S. Chairs!: A Mobile Game for Organic Chemistry Students to Learn the Ring Flip of Cyclohexane. *J. Chem. Educ.* **2016**, *93*, 1657–1659.
- (9) Garg, N. K. Empowering Students to Innovate: Engagement in Organic Chemistry Teaching. *Angew. Chem., Int. Ed.* **2018**, *57*, 15612–15613.

- (10) Dang, J.; Lin, B.; Yuan, J.; Schwartz, S. T.; Shah, R. M.; Garg, N. K. Smart Access to 3D Structures. *Nat. Rev. Chem.* **2018**, *2*, 95–96.

## CHAPTER SEVEN

### Advancing Global Chemical Education Through Interactive Teaching Tools

Francesca M. Ippoliti,<sup>†</sup> Jason V. Chari,<sup>†</sup> and Neil K. Garg.

*Chem. Sci.* **2022**, *13*, 5790–5796.

#### 7.1 Abstract

This chapter highlights our recent efforts to develop interactive resources in chemical education for worldwide usage. First, we highlight online tutorials that connect organic chemistry to medicine and popular culture, along with game-like resources for active learning. Next, we describe efforts to aid students in learning to visualize chemical structures in three dimensions. Finally, we present recent approaches toward engaging children and the general population through organic chemistry coloring and activity books. Collectively, these tools have benefited hundreds of thousands of users worldwide. We hope to promote a spirit of innovation in chemical education and spur the development of additional free, interactive, and widely accessible chemical education resources.

#### 7.2 Introduction

As researchers, we devote the majority of our professional efforts, and often even free time, to thinking about and addressing challenges we face in the laboratory. Simultaneously, we have come to realize the impact we researchers are poised to make—and have an obligation to make—when it comes to science education and scientific literacy. Scientific literacy, as described by the *National Academy of Sciences*, “means that a person can ask, find, or determine answers to

questions derived from curiosity about everyday experiences. It means that a person has the ability to describe, explain, and predict natural phenomena.”<sup>1</sup> In other words, scientific literacy pertains to more than simply the ability to recite scientific facts; it extends to an individual’s own judgment and decisions when it comes to science and therefore represents a complex, but critical issue. Heightening the value and importance of scientific literacy, scientific misinformation represents a growing problem in the age of social media.<sup>2</sup>

The key to addressing *global* scientific literacy lies in how we educate and, importantly, ensuring the accessibility of educational resources. As we consider chemical education, an all-too-common historical approach involves memorization and recitation of facts. This approach can be counterproductive in many ways and lead to negative perceptions by students. With regard to accessibility, resources for chemical education vary widely throughout the world, with many students not having access to costly textbooks, molecular model kits, or sometimes instructors.

Toward addressing these challenges,<sup>2</sup> we have taken a keen interest in developing non-traditional educational platforms<sup>3</sup> that focus on growing students’ critical thinking and problem-solving skills. In particular, these tools serve to put students “in the driver’s seat” by compelling them to actively engage and connect with the material. Furthermore, many of our resources seek to make chemistry relatable and engaging to the students by incorporating real-world applications and examples. Engagement is known to correlate well with learning outcomes.<sup>4</sup> In addition, we have sought to create educational tools that are available online for worldwide use given that 4.95+ billion people have internet access already (and this figure is expected to grow).<sup>5</sup> Moreover, the COVID-19 era of virtual education has created an even greater need for readily accessible online teaching materials. Indeed, studies have demonstrated a marked decline in student engagement in

virtual settings during the pandemic.<sup>6</sup> The creation of effective online teaching materials not only benefits students studying chemistry, but also engages the broader population in our field.

Herein, we highlight our efforts to develop interactive and widely accessible resources that are available to all students. These resources were each created by teams comprised of individuals with diverse sets of experiences and backgrounds. This included undergraduate and graduate students, postdoctoral researchers, high school students, and even children. This allowed us to target a variety of audiences by better understanding challenges that exist in different stages of learning scientific topics. Critical to all of these projects was our collaboration with Dr. Daniel Caspi of Element26, Inc. who is a computing expert and master of creating user interfaces across various platforms.

### **7.3 Development and Application of Interactive Online Learning Tools**

An important means of engaging students in chemistry is in relating course content to students' everyday lives. As an example, connecting organic chemistry to biology and popular culture helps to demonstrate that the course material is highly relevant to the students' lives, even if they do not intend to pursue further studies in that field. In particular, we hoped to engage students whose studies are not primarily focused in the area of chemistry.

With this in mind, we sought to create an online platform that connects chemistry concepts to medicine and popular culture. This ultimately led us to create BACON (Biology And Chemistry Online Notes, [learnbacon.com](http://learnbacon.com)), an online set of tutorials that serve as a vehicle for students to make extensive connections between organic chemistry, human health, and popular culture (Figure 7.1).<sup>7</sup> BACON consists of sixteen learning modules that cover organic chemistry topics such as 'Stereochemistry and Chirality,' 'Diels–Alder and Pericyclic Reactions,' and 'Polymers.' Each

module highlights several examples of the topic in both medicine and popular culture to deepen students' understanding of both the concepts and their importance. We also strive to keep these modules relevant to current topics, such as highlighting CRISPR gene editing technologies—which were the subject of the 2020 Nobel Prize in Chemistry<sup>8</sup>—as well as updated popular culture references that mention these scientific breakthroughs. Importantly, the tutorials also highlight members of the scientific community from underrepresented backgrounds in chemistry.

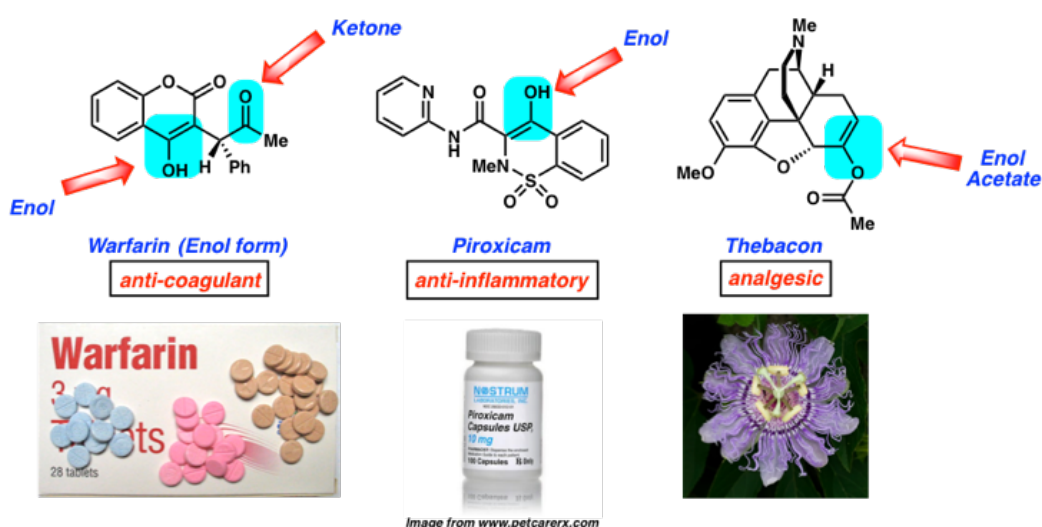


**Figure 7.1.** A selected example from BACON (Biology and Chemistry Online Notes), an online set of tutorials that connect organic chemistry to human health and popular culture.

As mentioned earlier, we have prioritized the creation of online teaching tools for chemical education in order to not only impact our local community, but also countries around the world. With respect to its global impact, BACON has been used by over 228,000 people in 169 different countries,<sup>9</sup> and over 165 universities have integrated BACON into some of their chemistry curricula.<sup>10</sup>

In addition to online learning modules, we have also sought to develop game-based learning tools that create fun and interactive learning environments for students. For example, the smartphone app Backside Attack (Figure 7.2) was launched to help students interact directly with a fundamental chemical reaction, the  $S_N2$  reaction. This topic was specifically chosen as it involves several critical concepts that appear throughout undergraduate organic chemistry curricula. These concepts include nucleophilicity, electrophilicity, and the effect of sterics and solvents on reaction outcomes. This free smartphone app was conceived of and developed by undergraduate students who had used BACON in their organic chemistry coursework. These students appreciated the connections between biology, popular culture, and chemistry, but also envisioned a game-like resource that could help students learn the nuances of a new concept through an entertaining and interactive format. Backside Attack involves an enticing user interface, where participants launch a nucleophile from a syringe into a “solution” containing an electrophile with which it can react. The user is then prompted to draw an arrow-pushing mechanism for the reaction. Next, the user must physically tap repeatedly on the screen to simulate the energy required to overcome the activation barrier for the  $S_N2$  reaction. Finally, the user is tasked with answering a textbook-style problem about the material covered in the level. This free application allows students to explore each aspect of the  $S_N2$  reaction, which is anticipated to provide greater engagement with and absorption of the material. The “Chem Yourself” feature provides an opportunity for users to share their progress with their friends by creating a fun and personalized, chemistry-themed image. Other innovative games have also been created to help students connect with chemistry concepts, such as those developed by Alchemie.<sup>11</sup> Overall, these tools provide exciting opportunities for students to learn challenging concepts in an interactive and fun environment.

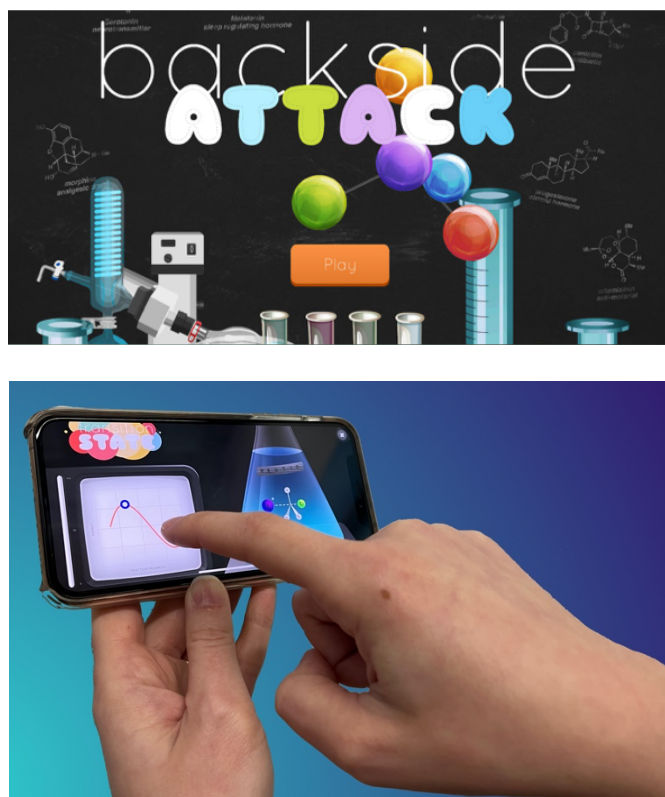


**Figure 7.2.** Backside Attack, a smartphone game that challenges students to master the  $S_N2$  reaction, an important reaction in undergraduate organic chemistry coursework.

#### 7.4 Teaching in Three Dimensions

A crucial skill for any chemistry student is the ability to visualize chemical structures. In particular, understanding chemical structures in two dimensions and carrying this knowledge into three dimensions is central to introductory coursework in chemistry. This involves concepts such as Valence Shell Electron Pair Repulsion (VSEPR) theory, chirality, and stereochemistry. Although these concepts make up a critical foundation of chemistry education, they consistently represent major obstacles for students, with reports of these challenges dating back to the 1940s.<sup>12</sup> Common teaching tools such as physical model kits, while powerful in many cases, can sometimes be inconvenient or costly. Alternatively, one might consider leveraging modern technology to



address this challenge. This offers an immense opportunity for chemistry educators to innovate by developing new interactive tools that facilitate the visualization of chemical structures. Such tools offer the potential to not only aid in students' understanding of three-dimensional structures, but also in generating excitement about these fundamental concepts.

Given the need for alternative approaches to teach students how to visualize chemical structures, we sought to develop a resource that takes advantage of smartphone technology. Our vision was to create a resource that would allow students to visualize any chemical structure instantly and without the need for a physical model kit. Toward achieving this, we opted to leverage the wide utility of quick-response (QR) code technology and in 2018, launched QR Chem (QRChem.net).<sup>13</sup> This project was initially led by a team of undergraduate students, who were later joined by graduate students for further development of the content. This site allows educators and researchers to create QR codes, as well as bit.ly URLs, that link directly to a three-dimensional structure of interest (Figure 7.3). As an example, an instructor may create and present a QR code to a class of students, each of whom can then scan the QR code using their smartphone's built-in camera to open the interactive structure directly on their device. The student is then able to rotate, as well as zoom-in and zoom-out on, the chemical structure in order to compare it to a two-dimensional representation that is also displayed on the screen (an example of this is shown in Figure 7.3).

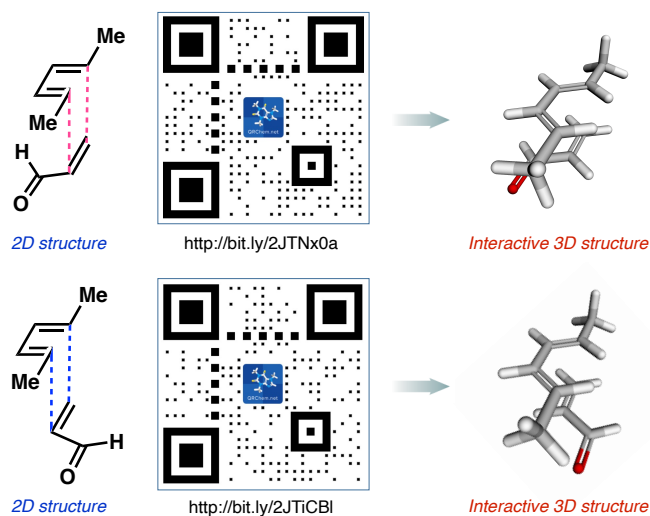


**Figure 7.3.** QR Chem, a site that allows students, instructors, and researchers to create QR codes that link to interactive 3D structures. In this example, two potential scenarios for the classic Diels–Alder reaction are depicted, each leading to different isomeric outcomes.

Since the initial launch of QR Chem, we have created a Molecule of the Day page for the site that showcases over fifty different molecules with important societal impact. This module takes the form of slide-based presentations with embedded QR codes that link to three-dimensional structures, as well as provide interesting information about each molecule. Additionally, the Lesson Plans page on the site contains useful slide-based presentations with embedded QR codes that cover a variety of topics that rely on the visualization of chemical structures (e.g., the Diels–Alder reaction, as depicted in Figure 7.3). It should also be noted that any user can generate a sharable QR code by simply uploading a 2D and 3D structure file, or submitting a valid PubChem CID number for virtually any molecule of interest. In our own experience, QR Chem helped to facilitate interactive learning in courses taught remotely.<sup>14</sup> QR codes generated from QR Chem can also be found in Wikipedia entries, as well as in some textbooks.<sup>15</sup> Excitingly, QR Chem has been used by over 62,000 people in over 150 countries.

In addition to being able to visualize chemical structures, assigning a stereocenter on a molecule is a critical skill for organic chemistry students. We sought to create a learning tool to help teach this skill while also being more interactive and engaging than textbook-based approaches. We envisioned that a game-like interface could serve to achieve this, as such a platform would provide the ability for students to receive direct feedback as they learn how to assign stereocenters and put their knowledge to the test. R/S Chemistry (RSCchemistry.com), launched in 2019, represents our interactive solution to this challenge of learning how to assign stereocenters (Figure 7.4). As with QR Chem, the idea for this resource was originally devised by undergraduate students, with graduate students joining the team later to develop the content. It features multiple levels of gameplay with both a guided ‘Learn’ mode and a timed ‘Expert’ mode for all levels of student mastery. R/S Chemistry leverages the visualization technology used in QR Chem to include interactive three-dimensional structures that assist in the stereochemical assignments. In selecting example molecules for the game, we sought to highlight compounds with broad societal impact, such as medicines and fragrances, to help students connect with the content. Of note, such connections are often missing in traditional teaching tools, further underscoring the need for alternative educational approaches that showcase them. Since its launch, R/S Chemistry has been used by more than 21,000 people in over 100 countries.<sup>16</sup>

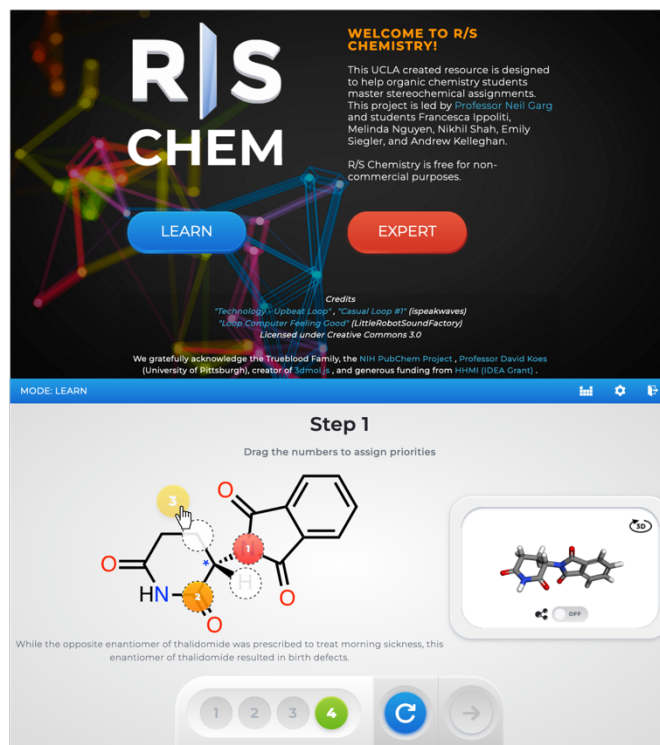


**Figure 7.4.** R/S Chemistry, a resource for students to practice assigning stereocenters in a game-like environment.

Advances in modern technology continue to provide new opportunities for chemical visualization, and, in turn, new areas for innovation. Virtual Reality (VR) and Augmented Reality (AR) technology enable the creation of immersive environments for teaching in three dimensions. Excitingly, these technologies offer the ability to teach abstract concepts that may be very challenging to describe in detail using traditional teaching tools. Several examples of immersive VR<sup>17,18</sup> and AR<sup>19</sup> technology in chemical education have been reported, many of which provide compelling evidence that implementation of virtual reality tools improve student performance. For example, Kurushkin and co-workers have demonstrated that the implementation of a virtual reality program called MEL Chemistry VR in coursework at ITMO University in Russia has improved undergraduate students' ability to grasp challenging concepts pertaining to atomic structure.<sup>17a</sup>

Additionally, Diaconescu and co-workers developed a VR laboratory session to teach advanced inorganic chemistry students about metal coordination and molecular orbitals, which resulted in higher exam scores by the students who participated in the VR session compared to those who did not.<sup>17b</sup> Compelling smartphone-based applications that employ AR technology have also been developed, including Isomers AR by Alchemie,<sup>20</sup> a game that allows users to build and discover new molecules in 3D without the need for a specialized headset. We have also begun to adapt content from QR Chem into a virtual reality interface (VRChem.net) to create an immersive environment where students can view and interact with three-dimensional structures, as well as learn about important molecules that connect to their everyday lives.

## 7.5 Reaching New Audiences

A crucial aspect of addressing scientific literacy lies in connecting with audiences outside of higher education. As a personal anecdote, one of us (N.K.G.) noticed that his daughter was particularly afraid of chemicals from an early age. Before trying a new food, she would often ask, “does it have chemicals in it?” and express wariness about the food. However, once it was explained to her that chemicals make up everything around her, including her favorite things, she became more curious about which chemicals were part of her daily life. We saw this as an opportunity to expand our impact as scientists and educators to a younger generation. In particular, we envisioned that introducing chemistry to children through fun and engaging activities could serve to reduce the negative association they have with the word “chemical.” In considering interactive activities that children are familiar with, we opted to develop a coloring book about organic molecules. The final product, *The Organic Coloring Book*, features molecules such as sucrose, cellulose, and chlorophyll (Figure 7.5). Exposing children to the connection between

science and everyday life serves to increase children’s curiosity about the world around them and hopefully spark lifelong interest in science. We have also received positive feedback from parents, who note that the book also helped them learn about chemistry in the world around them. *The Organic Coloring Book* is accessible for purchase online,<sup>21</sup> although we regularly distribute free copies throughout the world. To make this resource accessible to a broader global population, we have also published a Spanish edition of *The Organic Coloring Book*, entitled *El Libro Para Colorear Orgánico*.<sup>22</sup>



**Figure 7.5.** *The Organic Coloring Book* series and *The O-Chem (Re)Activity Book* are designed to connect organic chemistry to the everyday lives of both children and adults.

The success of *The Organic Coloring Book*, as well as its medicine-themed sequel (*Cheesy Goes to the Doctor*),<sup>23</sup> led us to wonder whether we could develop similar resources to reach adults as well. Indeed, we felt that our motivations for creating the organic coloring book for children could also be extended to adults. As an example, “chemical-free” products are often marketed as desirable despite the impossibility of a product that does not contain chemicals. We ultimately created *The Adult Organic Coloring Book*,<sup>24</sup> highlighting molecules that have relevance to adult life, such as ethanol and creatine, an amino acid used for muscle growth.

Another interactive resource that we felt would be exciting to children is an activity book, which we envisioned would consist of chemistry-themed exercises. Similar to *The Organic Coloring Book*, each of these activities would serve to expose children to chemistry and its connection to daily life. We ultimately developed *The O-Chem (Re)Activity Book*, which is comprised of fun exercises including connect-the-dots, word searches, mazes, and ‘spot the difference,’ each of which highlight chemistry in the world around us. The book is available free of charge online as a downloadable PDF,<sup>25</sup> allowing parents around the world to download the book and enjoy it with their children.

Additionally, we recently launched ChemMatch (ChemMatch.net), an online matching game that includes several chemistry-oriented subjects designed to reach various audiences (Figure 7.6). This includes topics relevant to all audiences such as “Chemistry in Your Life” and “Kids Movies,” as well as topics for high school chemistry students and college general chemistry students including “Elements” and “Polyatomic Ion Charges.” Organic Chemistry specific categories are also included.

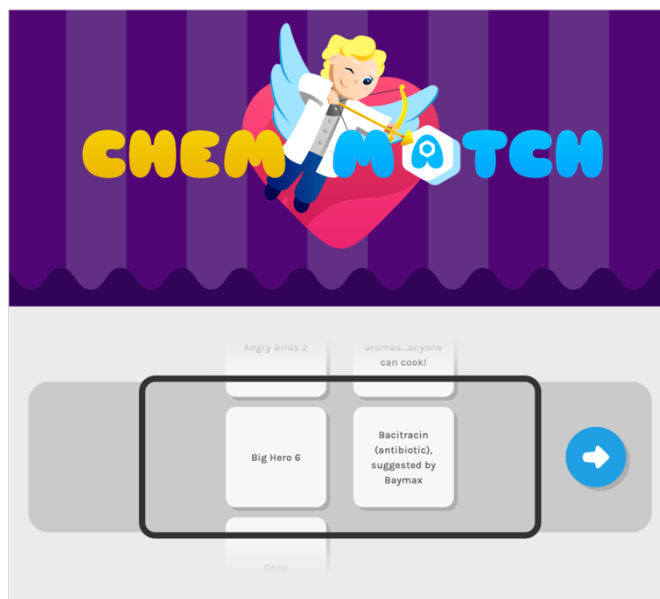


**Figure 7.6.** ChemMatch, an online matching game that serves as an educational resource for children, students, and adults.

In addition to the books and online resources created by our lab, there have been a multitude of chemistry books and activities that connect children with the science found around them.<sup>26</sup> Introducing chemistry to children at a young age can have a lasting impact on the importance of science in their worldview. More broadly, developing resources that reach a wide audience can also help to promote a positive public perception of chemistry among non-scientist adults. We look forward to seeing future efforts in this area.

## 7.6 Global Impact and Innovation in Education

A crucial objective of our efforts in education is reaching audiences across the globe. Accordingly, we have evaluated the usage of our web-based resources in countries worldwide and have been gratified to observe that our online resources have been used all around the world. To illustrate this, Figure 7.7 depicts global usage of QR Chem, R/S Chemistry, and ChemMatch,



which have a combined total of over 90,000 users in 157 countries. These widely accessible resources not only engage chemistry students, but also present a step toward educating the more general population. We hope to continue expanding the reach of these resources around the world.

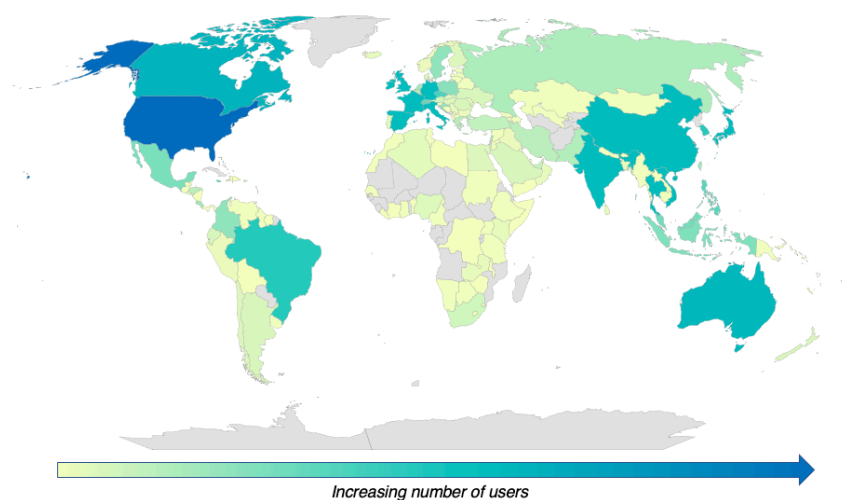


**Figure 7.7.** Map of combined users of QR Chem, R/S Chemistry, and ChemMatch worldwide (data from Google Analytics).

## 7.7 Conclusion

We have developed a multitude of non-traditional chemical education resources, including a smartphone application, several websites, and children's books. These tools transcend classic teaching methods, such as those primarily focused on textbooks and memorization. Instead, we largely rely on internet-based technologies that enable critical thinking and engagement in order to help students learn about and appreciate chemistry. In addition, our educational resources for children and the general population contribute to the widespread societal challenge of improving scientific literacy. Collectively, the resources we have developed so far have positively benefitted hundreds of thousands of people all over the world.

Our goal in writing this chapter is not to simply advertise our educational materials. Instead, we offer our view as active researchers of the potential impact we, as a community of scientists, can make as we think about science education on a global scale. It is incumbent upon *all of us* to contribute to science education worldwide. Such efforts not only benefit our own fields by engaging individuals in chemistry, but more importantly, have the capacity to benefit society in the long-term. We should also prioritize the development of resources that are fun, engaging, promote critical thinking skills, and are accessible to everyone.

Lastly, we offer sentiments regarding “innovation,” a term frequently employed in academia. Although there exists a strong spirit of innovation in scientific research, a comparable sentiment is notably lacking in many research-intensive colleges and universities when discussing chemical education. By choosing to prioritize innovation in chemical education, we stand to improve the student experience, educate the scientific leaders of the future, enhance global education and scientific literacy, and even strengthen the public perception of our fields.

## 7.8 Related Links

BACON: <https://learnbacon.com/>

Backside Attack: <https://apps.apple.com/us/app/backside-attack/id1278956096/>

QR Chem: <https://qrchem.net/>

R/S Chemistry: <https://rschemistry.com/>

ChemMatch: <https://chemmatch.net/>

Organic Coloring Book Series: <https://www.amazon.com/dp/B08NXL4SWP/>

The O-Chem (Re)Activity Book: <https://garg.chem.ucla.edu/ochem-re-activity/>

Element26: <https://www.element26.net/>

## 7.9 Notes and References

- (1) National Research Council. *National Science Education Standards*; The National Academies Press: Washington, D.C., 1996. DOI: 10.17226/4962.
- (2) Scheufele, D. A.; Krause, N. M. Science Audiences, Misinformation, and Fake News. *Proc. Natl. Acad. Sci.* **2019**, *116*, 7662–7669.
- (3) Garg, N. K. Empowering Students to Innovate: Engagement in Organic Chemistry Teaching. *Angew. Chem., Int. Ed.* **2018**, *57*, 15612–15613.
- (4) (a) Handelsman, M. M.; Briggs, W. L.; Sullivan, N.; Towler, A. A Measure of College Student Course Engagement. *J. Educ. Res.* **2005**, *98*, 184–192. (b) Martin, F.; Bolliger, D. U. Engagement Matters: Student Perceptions on the Importance of Engagement Strategies in the Online Learning Environment. *Online Learn. J.* **2018**, *22*, 205–222.
- (5) *Digital 2022: Global Overview Report*. <https://datareportal.com/reports/digital-2022-global-overview-report/> (accessed March 2022).
- (6) (a) Wester, E. R.; Walsh, L. L.; Arango-Caro, S.; Callis-Duehl, K. L. Student Engagement Declines in STEM Undergraduates during COVID-19–Driven Remote Learning. *J. Microbiol. Biol. Educ.* **2021**, *22*, ev22i1.2385. (b) Wu, F.; Teets, T. S. Effects of the COVID-19 Pandemic on Student Engagement in a General Chemistry Course. *J. Chem. Educ.* **2021**, *98*, 3633–3642.
- (7) Shah, T. K.; Garg, N. K. Organic Chemistry Can Sizzle. *Nat. Rev. Chem.* **2017**, *1*, 0020.
- (8) Nobelprize.org: The Official Web Site of the Nobel Prize. All Nobel Prizes in Chemistry. <https://www.nobelprize.org/prizes/lists/all-nobel-prizes-in-chemistry> (accessed February 2022).

- (9) Data obtained from Google Analytics.
- (10) BACON tutorials are available for less than 1 USD each, although full cost waivers are commonly granted.
- (11) *Alchemie*. <https://www.alchem.ie/> (accessed February 2022).
- (12) (a) Fromm, F. On Teaching Stereochemistry. *J. Chem. Educ.* **1945**, *22*, 43. (b) Shine, H. J. Aids in Teaching Stereochemistry: Plastic Sheets for Plane Projection Diagrams. *J. Chem. Educ.* **1957**, *34*, 355. (c) Evans, G. G. Stereochemistry in the Terminal Course. *J. Chem. Educ.* **1963**, *40*, 438–440. (d) Beauchamp, P. S. “Absolutely” Simple Stereochemistry. *J. Chem. Educ.* **1984**, *61*, 666–667. (e) Lyon, G. L. Ph.D. Dissertation, Louisiana State University and Agricultural & Mechanical College, Baton Rouge, LA, USA, 1999; [https://digitalcommons.lsu.edu/gradschool\\_disstheses/7105/](https://digitalcommons.lsu.edu/gradschool_disstheses/7105/) (accessed February 2022). (f) Raupp, D.; Del Pino, J. C.; Prochnow, T. R. Teaching of Stereochemistry in High School: An Approach Based on Vergnaud’s Conceptual Theory. *ESERA Conference*; Dublin City University: Dublin, Ireland, 2017.
- (13) Dang, J.; Lin, B.; Yuan, J.; Schwartz, S. T.; Shah, R. M.; Garg, N. K. Smart Access to 3D Structures. *Nat. Rev. Chem.* **2018**, *2*, 95–96.
- (14) Chari, J. V.; Knapp, R. R.; Boit, T. B.; Garg, N. K. Catalysis in Modern Drug Discovery: Insights from a Graduate Student-Taught Undergraduate Course. *J. Chem. Educ.* **2022**, *99*, 1296–1303.
- (15) QR Chem is currently used in several *Top Hat* online textbooks for General Chemistry and Organic Chemistry.

- (16) Ippoliti, F. M.; Nguyen, M. M.; Reilly, A. J.; Garg, N. K. Gaming Stereochemistry. *Nat. Rev. Chem.* **2022**, Accepted Article. DOI: 10.1038/s41570-022-00395-5.
- (17) (a) Maksimenko, N.; Okolzina, A.; Vlasova, A.; Tracey, C.; Kurushkin, M. Introducing Atomic Structure to First-Year Undergraduate Chemistry Students with an Immersive Virtual Reality Experience. *J. Chem. Educ.* **2021**, *98*, 2104–2108. (b) Dai, R.; Laureanti, J. A.; Kopelevich, M.; Diaconescu, P. L. Developing a Virtual Reality Approach Toward a Better Understanding of Coordination Chemistry and Molecular Orbitals. *J. Chem. Educ.* **2020**, *97*, 3647–3651. (c) Edwards, B. I.; Bielawski, K. S.; Prada, R.; Cheok, A. D. Haptic Virtual Reality and Immersive Learning for Enhanced Organic Chemistry Instruction. *Virtual Reality* **2019**, *23*, 363–373. (d) O’Connor, M.; Deeks, H. M.; Dawn, E.; Metatla, O.; Roudaut, A.; Sutton, M.; Thomas, L. M.; Glowacki, B. R.; Sage, R.; Tew, P.; Wonnacott, M.; Bates, P.; Mulholland, A. J.; Glowacki, D. R. Sampling Molecular Conformations and Dynamics in a Multiuser Virtual Reality Framework. *Sci. Adv.* **2018**, *4*, eaat2731. (e) O’Connor, M. B.; Bennie, S. J.; Deeks, H. M.; Jamieson-Binnie, A.; Jones, A. J.; Shannon, R. J.; Walters, R.; Mitchell, T. J.; Mulholland, A. J.; Glowacki, D. R. Interactive Molecular Dynamics in Virtual Reality from Quantum Chemistry to Drug Binding: An Open-Source Multi-Person Framework. *J. Chem. Phys.* **2019**, *150*, 220901. (f) Merchant, Z.; Goetz, E. T.; Keeney-Kennicutt, W.; Kwok, O. M.; Cifuentes, L.; Davis, T. J. The Learner Characteristics, Features of Desktop 3D Virtual Reality Environments, and College Chemistry Instruction: A Structural Equation Modeling Analysis. *Comput. Educ.* **2012**, *59*, 551–568. (g) Ferrell, J. B.; Campbell, J. P.; McCarthy, D. R.; McKay, K. T.; Hensinger, M.; Srinivasan, R.; Zhao, X.; Wurthmann, A.; Li, J.; Schneebeli, S. T.

- Chemical Exploration with Virtual Reality in Organic Teaching Laboratories. *J. Chem. Educ.* **2019**, *96*, 1961–1966. (h) Fung, F. M.; Choo, W. Y.; Ardisara, A.; Zimmermann, C. D.; Watts, S.; Koscielniak, T.; Blanc, E.; Coumoul, X.; Dumke, R. Applying a Virtual Reality Platform in Environmental Chemistry Education to Conduct a Field Trip to an Overseas Site. *J. Chem. Educ.* **2019**, *96*, 382–386. (i) Bennie, S. J.; Ranaghan, K. E.; Deeks, H.; Goldsmith, H. E.; O'Connor, M. B.; Mulholland, A. J.; Glowacki, D. R. Teaching Enzyme Catalysis Using Interactive Molecular Dynamics in Virtual Reality. *J. Chem. Educ.* **2019**, *96*, 2488–2496. (j) Goddard, T. D.; Brilliant, A. A.; Skillman, T. L.; Vergenz, S.; Tyrwhitt-Drake, J.; Meng, E. C.; Ferrin, T. E. Molecular Visualization on the Holodeck. *J. Mol. Biol.* **2018**, *430*, 3982–3996.
- (18) For a review of VR tools developed for chemical education, see: Fombona-Pascual, A.; Fombona, J.; Vásquez-Cano, E. VR in Chemistry, a Review of Scientific Research on Advanced Atomic/Molecular Visualization. *Chem. Educ. Res. Pract.* **2022**, *23*, 300–312.
- (19) (a) Clemons, T. D.; Fouché, L.; Rummey, C.; Lopez, R. E.; Spagnoli, D. Introducing the First Year Laboratory to Undergraduate Chemistry Students with an Interactive 360° Experience. *J. Chem. Educ.* **2019**, *96*, 1491–1496. (b) Sanii, B. Creating Augmented Reality USDZ Files to Visualize 3D Objects on Student Phones in the Classroom. *J. Chem. Educ.* **2020**, *97*, 253–257. (c) Yang, S.; Mei, B.; Yue, X. Mobile Augmented Reality Assisted Chemical Education: Insights from Elements 4D. *J. Chem. Educ.* **2018**, *95*, 1060–1062.
- (20) *Isomers AR*. <https://www.alchem.ie/isomers-ar/> (accessed February 2022).

- (21) Garg, N. K.; Garg, E.; Garg, K. *The Organic Coloring Book*; 2017. <https://www.amazon.com/gp/product/0692860541>.
- (22) Garg, N. K.; Garg, E.; Garg, K. *El Libro Para Colorear Orgánico*; 2021. <https://www.amazon.com/gp/product/B0991DVNTC>.
- (23) Garg, N. K.; Garg, E.; Garg, K. *Cheesy Goes to the Doctor*; 2020. <https://www.amazon.com/gp/product/B08CWJ8FN7>.
- (24) Garg, N. K.; Dander, J. E.; Darzi, E. R. *The Adult Organic Coloring Book*; 2020. <https://www.amazon.com/gp/product/B08NWQZVWK>.
- (25) *The O-Chem (Re)-Activity Book*. <https://garg.chem.ucla.edu/ochem-re-activity/> (accessed February 2022).
- (26) For examples of children's books that connect children with chemistry in the world around them, see: (a) Sperber, C. *The Organic Chemistry Alphabet Book*; Nanoscale Scientists Publishing LLC, 2019. <https://www.amazon.com/Organic-Chemistry-Alphabet-Book/dp/1732926514>. (b) Barfield, M. *The Element in the Room: Investigating the Atomic Ingredients that Make Up Your Home*; Laurence King Publishing, 2018. <https://www.amazon.com/Element-Room-Investigating-Atomic-Ingredients/dp/1786271788>. (c) Huggins-Cooper, L. *Chemistry for Curious Kids: An Illustrated Introduction to Atoms, Elements, Chemical Reactions, and More!*; Arcturus, 2021. <https://www.amazon.com/Chemistry-Curious-Kids-Illustrated-Introduction/dp/1398802670>. (d) Wynne P. J.; Silver, D. M. *My First Book About Chemistry*; Dover Publications, 2020. <https://www.amazon.com/First-About-Chemistry-Childrens-Science/dp/0486837580>.